TABLE OF CONTENTS

		Page
	ABSTRACT	vii
1	INTRODUCTION	1
2	CUBE-CORNER SPECIFICATIONS	2
3	GEOMETRY OF THE ARRAY	3
4	METHOD OF COMPUTING THE TRANSFER FUNCTION	10
5	SIGNAL-STRENGTH COMPUTATION	12
6	OPTICAL CUBE-CORNER REFLECTIVITY	14
7	ARRAY REFLECTIVITY	25
8	RANGE CORRECTION	50
9	EFFECT OF OPTICAL COHERENCE	77
10	ACCURACY OF THE RESULTS	106
11	INFRARED TRANSFER FUNCTION	139
12	ACKNOWLEDGMENTS	146
13	REFERENCES	147

ILLUSTRATIONS

		Page
1	Geos 3 satellite	3
2	Orientation of optical cube corners	4
3	Displacement of the spacecraft center of gravity from the satellite symmetry axis	5
4	Coordinate system for the optical cube-corner orientation angle θ	5
5	Position and orientation of the infrared cube corner	6
6	Direction of incident beam	14
7	Active reflecting area and average reflectivity in the 25- to 50-μrad annulus of the far-field diffraction pattern for a Geos 3 optical cube corner	17
8	Diffraction-pattern coordinate system	26
9	Contour plots of the gain-function matrices given in Table 7	42
10	Alternate method of cube-corner orientation	27
11	Contour plots of the centroid range-correction matrices given in Table 13	71
12	Sample incoherent and coherent reflected pulse shapes	81
13	Contour plots of the gain-function matrices given in Table 17	116
14	Contour plots of the centroid range-correction matrices given in Table 19	130
15	Active reflection area and average reflectivity in the 25- to 50-μrad annulus of the far-field diffraction pattern for the Geos 3 infrared reflector	141

TABLES

1	Radius and Z position of each row of optical cube corners	4
2	Cube-corner coordinates	7
3	Average reflectivity of a Geos 3 optical cube corner in the 25- to 50-μrad annulus of the far-field diffraction pattern	16
4	Total reflectivity of the Geos 3 optical retroreflector array vs. incidence angle	28
5	Average reflectivity of the Geos 3 optical retroreflector array in the 25- to 50-μrad annulus of the far-field diffraction pattern	29

TABLES (Cont.)

		Page
6	Gain function vs. velocity aberration for the Geos 3 optical retroreflector array	31
7	Sample gain-function matrices	38
8	Centroid range correction for total reflected energy vs. incidence angle	52
9	Average centroid range correction in the 25- to 50-μrad annulus of the far-field pattern vs. incidence angle	54
10	Difference between half-maximum and centroid range correction vs. incidence angle	58
11	Difference between half-area and centroid range correction vs. incidence angle	59
12	Centroid range correction vs. velocity aberration	60
13	Sample centroid range-correction matrices	67
14	Root-mean-square deviation of centroid range correction due to coherent interference vs. incidence angle	78
15	Difference between the average range correction for a set of coherent returns and the range correction for the incoherent return	79
16	Gain and centroid range correction vs. dihedral-angle offset	106
17	Gain-function matrices for various dihedral-angle offsets	108
18	Gain function vs. velocity aberration for various dihedral-angle offsets	112
19	Centroid range-correction matrices for various dihedral-angle offsets	124
20	Centroid range correction vs. velocity aberration for various dihedral-angle offsets	128
21	Half-maximum and half-area range corrections vs. velocity aberration	138
22	Average reflectivity of the infrared cube corner of the 25- to 50-μrad annulus of the far-field diffraction pattern	144

ABSTRACT

This report covers work done under NASA Grant NGR 09-015-002 Supplement No. 57. The transfer function of the retroreflector array carried by the Geos 3 satellite has been computed at three wavelength: 5300, 6943, and 106000 A. The range correction is given for extrapolating laser range measurements to the center of gravity of the satellite. The reflectivity of the array has been computed for estimating laser-echo signal strengths.

OPTICAL AND INFRARED TRANSFER FUNCTION OF THE GEOS 3 RETROREFLECTOR ARRAY

Technical Report
RTOP 161-05-02

1. INTRODUCTION

This is the fourth in a series of reports giving transfer functions for satellites with retroreflector arrays (refs. 1, 2, and 3). Some transfer-function analyses were included in ref. 4. In this report, the analysis of Geos 3 (7502701), which was partially presented in ref. 1, is completed. A special analysis has been done for the infrared cube corner designed for use with lasers operating at $\lambda = 106000$ Å.

Data on the Geos 3 retroreflector array were obtained from the Applied Physics Laboratory of Johns Hopkins University and from Goddard Space Flight Center.

2. CUBE-CORNER SPECIFICATIONS

The cube corners on Geos 3 have hexagonal entrance faces, each with a width of 35 mm across flats. The length from vertex to face is $35/\sqrt{2} = 24.75$ mm. The optical reflectors are made of fused silica, and the reflecting faces are silver coated. The dihedral angles between the back faces are $90° + 2''.0 \pm 0''.5$ in order to compensate for velocity aberration. The infrared cube corner is made of Irtran-2. The reflecting faces are uncoated, and the dihedral angles are not offset from 90°. Diffraction provides the necessary beam spread at a wavelength of 106000 Å.

3. GEOMETRY OF THE ARRAY

The optical retroreflector array consists of 264 cube corners mounted on a 45° conic frustrum, as shown in Figure 1. The infrared cube corner is mounted on the end of a tube facing the earth. The optical cube corners are arranged in three rows with 88 cube corners in each row; their orientation is shown in Figure 2.

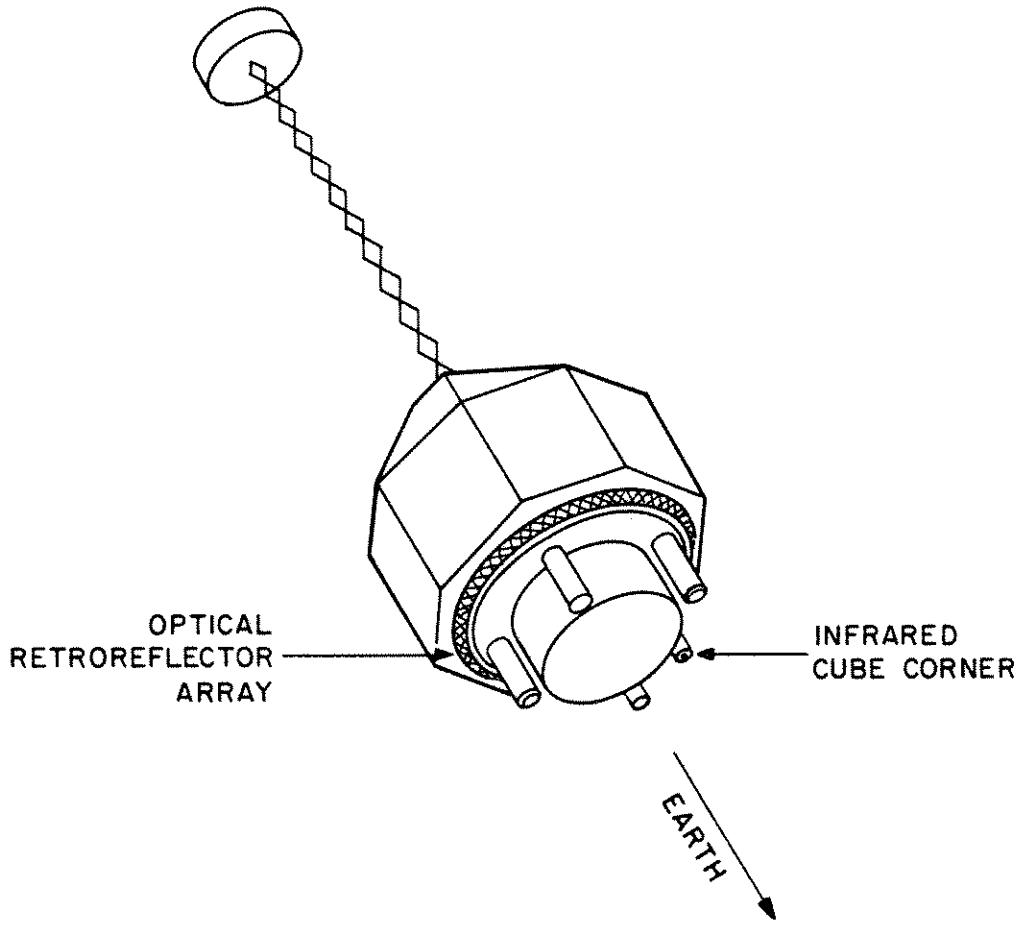

Figure 1. Geos 3 satellite.

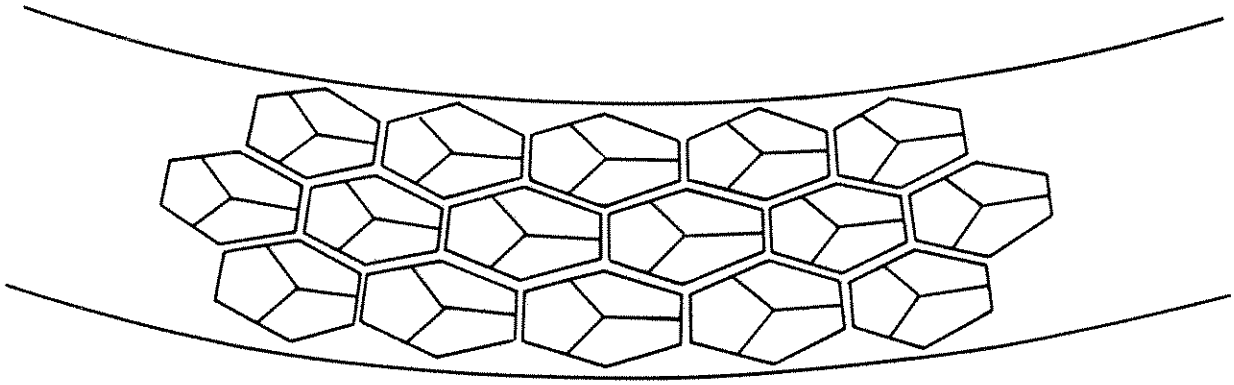

Figure 2. Orientation of optical cube corners.

The coordinate system used to position the cube corners has its origin at the spacecraft orbital center of gravity. The Z axis is parallel to the gravity-gradient boom, with the positive direction away from the spacecraft toward the end mass; the X axis is along the velocity vector, with the positive direction in the direction of flight; and the Y axis is perpendicular to the X and Z axes, with the positive direction chosen to form a right-hand coordinate system. Table 1 lists the radius and Z coordinates of the center of the front face of each row of cube corners.

Table 1. Radius and Z position of each row of optical cube corners.

	Radius		Z	
Row	(inches)	(m)	(inches)	(m)
1	21.390	0.5433	-53.448	-1.3576
2	22.250	0.5652	-52.589	-1.3358
3	23.109	0.5870	-51.730	-1.3139

The spacecraft's center of gravity is not precisely on the symmetry axis of the satellite; the relationship is shown in Figure 3.

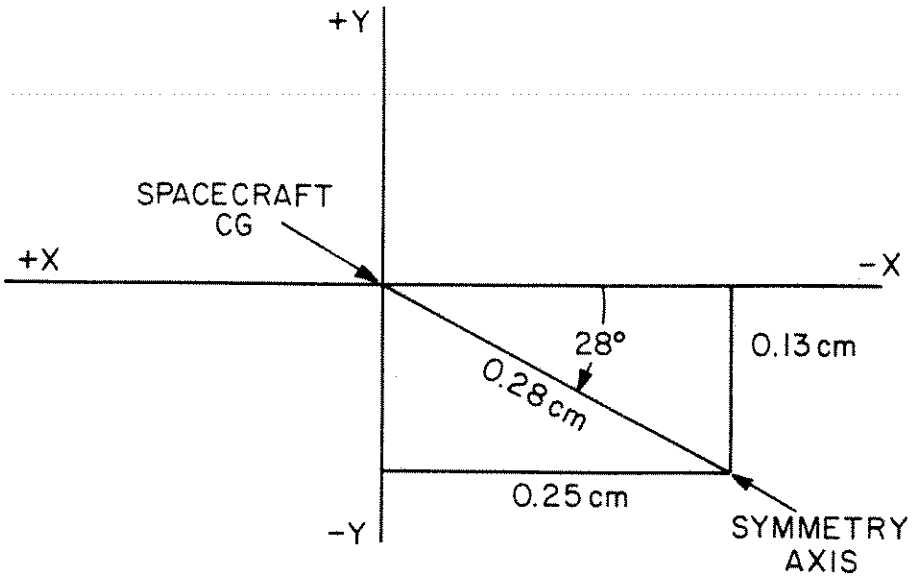

Figure 3. Displacement of the spacecraft center of gravity (CG) from the satellite symmetry axis.

The coordinates of the infrared and the optical cube corners are given in Table 2. The angle θ, in degrees, is measured from the center of the array (the symmetry axis of the satellite), as shown in Figure 4. The X′ and Y′ axes are parallel to the X and Y axes, with the origin at the symmetry axis. The position and orientation of the infrared cube corner are shown in Figure 5; the Z coordinate is -1.7399 m. The front face points toward the earth (the direction of the negative Z axis).

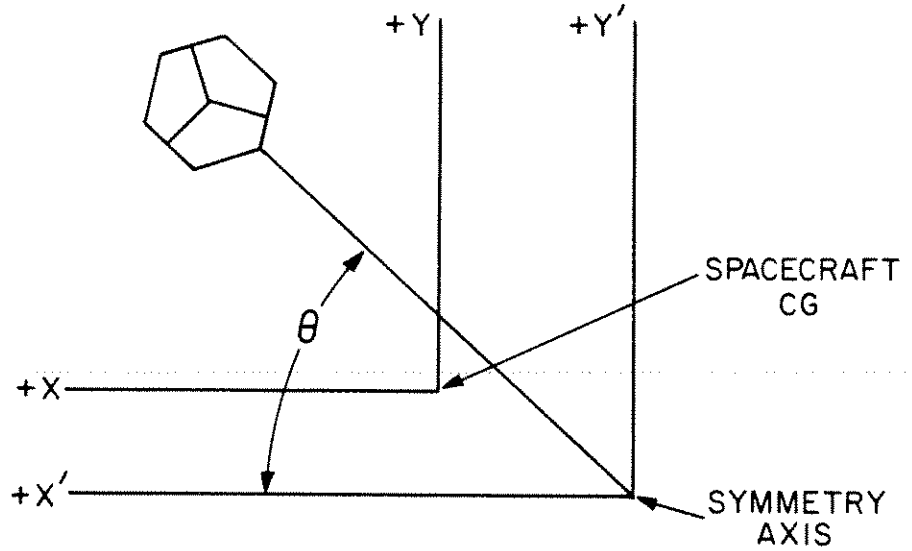

Figure 4. Coordinate system for the optical cube-corner orientation angle θ.

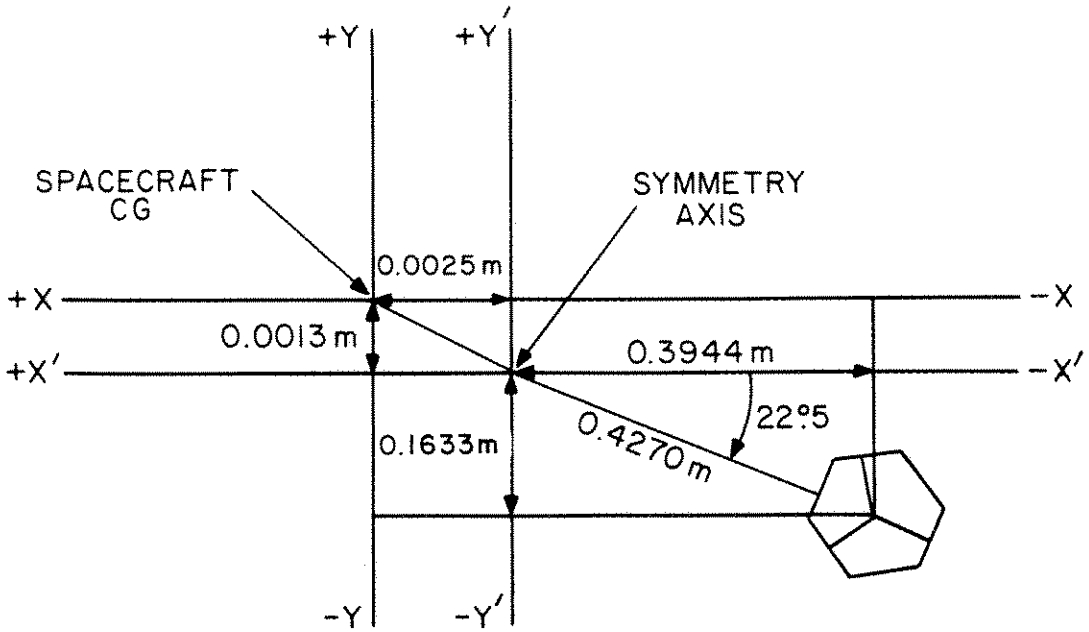

Figure 5. Position and orientation of the infrared cube corner.

Table 2. Cube-corner coordinates.

a: Infrared coordinates (m)

X	Y	Z
-0.3969	-0.1646	-1.7399

b: Optical coordinates (m) and orientation (degrees)

ROW	RETRO	X	Y	Z	THETA
1	1	-.00250	.54201	-1.35758	90.000
1	2	.03626	.54062	-1.35758	85.909
1	3	.07482	.53648	-1.35758	81.818
1	4	.11299	.52959	-1.35758	77.727
1	5	.15057	.52000	-1.35758	73.636
1	6	.18737	.50775	-1.35758	69.545
1	7	.22320	.49291	-1.35758	65.454
1	8	.25788	.47555	-1.35758	61.364
1	9	.29123	.45576	-1.35758	57.273
1	10	.32309	.43364	-1.35758	53.182
1	11	.35329	.40930	-1.35758	49.091
1	12	.38168	.38288	-1.35758	45.000
1	13	.40810	.35449	-1.35758	40.909
1	14	.43244	.32429	-1.35758	36.818
1	15	.45456	.29243	-1.35758	32.727
1	16	.47435	.25908	-1.35758	28.636
1	17	.49171	.22440	-1.35758	24.545
1	18	.50655	.18857	-1.35758	20.454
1	19	.51880	.15177	-1.35758	16.363
1	20	.52839	.11419	-1.35758	12.273
1	21	.53528	.07602	-1.35758	8.182
1	22	.53942	.03746	-1.35758	4.091
1	23	.54081	-.00130	-1.35758	360.000
1	24	.53942	-.04006	-1.35758	355.909
1	25	.53528	-.07862	-1.35758	351.818
1	26	.52839	-.11679	-1.35758	347.727
1	27	.51880	-.15437	-1.35758	343.636
1	28	.50655	-.19117	-1.35758	339.545
1	29	.49171	-.22700	-1.35758	335.454
1	30	.47435	-.26168	-1.35758	331.363
1	31	.45456	-.29503	-1.35758	327.273
1	32	.43244	-.32689	-1.35758	323.182
1	33	.40810	-.35709	-1.35758	319.091
1	34	.38168	-.38548	-1.35758	315.000
1	35	.35329	-.41190	-1.35758	310.909
1	36	.32309	-.43624	-1.35758	306.818
1	37	.29123	-.45836	-1.35758	302.728
1	38	.25788	-.47815	-1.35758	298.637
1	39	.22320	-.49551	-1.35758	294.546
1	40	.18737	-.51035	-1.35758	290.455
1	41	.15057	-.52260	-1.35758	286.364
1	42	.11299	-.53219	-1.35758	282.273
1	43	.07482	-.53908	-1.35758	278.182
1	44	.03626	-.54322	-1.35758	274.091
1	45	-.00250	-.54461	-1.35758	270.000
1	46	-.04126	-.54322	-1.35758	265.909
1	47	-.07982	-.53908	-1.35758	261.818
1	48	-.11799	-.53219	-1.35758	257.727
1	49	-.15557	-.52260	-1.35758	253.636
1	50	-.19237	-.51035	-1.35758	249.546
1	51	-.22820	-.49551	-1.35758	245.455
1	52	-.26288	-.47815	-1.35758	241.364
1	53	-.29623	-.45836	-1.35758	237.273
1	54	-.32809	-.43624	-1.35758	233.182
1	55	-.35829	-.41190	-1.35758	229.091
1	56	-.38668	-.38548	-1.35758	225.000
1	57	-.41310	-.35709	-1.35758	220.909
1	58	-.43744	-.32689	-1.35758	216.818
1	59	-.45956	-.29503	-1.35758	212.727
1	60	-.47935	-.26168	-1.35758	208.636
1	61	-.49671	-.22700	-1.35758	204.545
1	62	-.51155	-.19117	-1.35758	200.455
1	63	-.52380	-.15437	-1.35758	196.364
1	64	-.53339	-.11679	-1.35758	192.273
1	65	-.54028	-.07862	-1.35758	188.182
1	66	-.54442	-.04006	-1.35758	184.091
1	67	-.54581	-.00130	-1.35758	180.000
1	68	-.54442	.03746	-1.35758	175.909
1	69	-.54028	.07602	-1.35758	171.818
1	70	-.53339	.11419	-1.35758	167.727
1	71	-.52380	.15177	-1.35758	163.636
1	72	-.51155	.18857	-1.35758	159.545
1	73	-.49671	.22440	-1.35758	155.454
1	74	-.47935	.25908	-1.35758	151.364
1	75	-.45956	.29243	-1.35758	147.273
1	76	-.43744	.32429	-1.35758	143.182
1	77	-.41310	.35449	-1.35758	139.091
1	78	-.38668	.38288	-1.35758	135.000
1	79	-.35829	.40930	-1.35758	130.909
1	80	-.32809	.43364	-1.35758	126.818
1	81	-.29623	.45576	-1.35758	122.727
1	82	-.26288	.47555	-1.35758	118.636
1	83	-.22820	.49291	-1.35758	114.545
1	84	-.19237	.50775	-1.35758	110.454
1	85	-.15557	.52000	-1.35758	106.363
1	86	-.11799	.52959	-1.35758	102.272
1	87	-.07982	.53648	-1.35758	98.182
1	88	-.04126	.54062	-1.35758	94.091
2	1	.01767	.56349	-1.33576	87.955
2	2	.05791	.56061	-1.33576	83.864
2	3	.09784	.55487	-1.33576	79.773
2	4	.13727	.54629	-1.33576	75.682
2	5	.17597	.53493	-1.33576	71.591
2	6	.21377	.52083	-1.33576	67.500
2	7	.25047	.50407	-1.33576	63.409
2	8	.28588	.48474	-1.33576	59.318
2	9	.31982	.46293	-1.33576	55.227
2	10	.35211	.43875	-1.33576	51.136
2	11	.38260	.41233	-1.33576	47.045
2	12	.41113	.38380	-1.33576	42.954

Table 2. (Cont.)

ROW	RETRO	X	Y	Z	THETA	ROW	RETRO	X	Y	Z	THETA
2	13	.43755	.35331	-1.33576	38.864	2	63	-.55009	-.14107	-1.33576	194.318
2	14	.46173	.32102	-1.33576	34.773	2	64	-.55867	-.10164	-1.33576	190.227
2	15	.48354	.28708	-1.33576	30.682	2	65	-.56441	-.06171	-1.33576	186.136
2	16	.50287	.25167	-1.33576	26.591	2	66	-.56729	-.02147	-1.33576	182.045
2	17	.51963	.21497	-1.33576	22.500	2	67	-.56729	.01887	-1.33576	177.954
2	18	.53373	.17717	-1.33576	18.409	2	68	-.56441	.05911	-1.33576	173.864
2	19	.54509	.13847	-1.33576	14.318	2	69	-.55867	.09904	-1.33576	169.773
2	20	.55367	.09904	-1.33576	10.227	2	70	-.55009	.13847	-1.33576	165.682
2	21	.55941	.05911	-1.33576	6.136	2	71	-.53873	.17717	-1.33576	161.591
2	22	.56229	.01887	-1.33576	2.045	2	72	-.52463	.21497	-1.33576	157.500
2	23	.56229	-.02147	-1.33576	357.954	2	73	-.50787	.25167	-1.33576	153.409
2	24	.55941	-.06171	-1.33576	353.863	2	74	-.48854	.28708	-1.33576	149.318
2	25	.55367	-.10164	-1.33576	349.772	2	75	-.46673	.32102	-1.33576	145.227
2	26	.54509	-.14107	-1.33576	345.682	2	76	-.44255	.35331	-1.33576	141.136
2	27	.53373	-.17977	-1.33576	341.591	2	77	-.41613	.38380	-1.33576	137.045
2	28	.51963	-.21757	-1.33576	337.500	2	78	-.38760	.41233	-1.33576	132.954
2	29	.50287	-.25427	-1.33576	333.409	2	79	-.35711	.43875	-1.33576	128.863
2	30	.48354	-.28968	-1.33576	329.318	2	80	-.32482	.46293	-1.33576	124.773
2	31	.46173	-.32362	-1.33576	325.228	2	81	-.29088	.48474	-1.33576	120.682
2	32	.43755	-.35591	-1.33576	321.137	2	82	-.25547	.50407	-1.33576	116.591
2	33	.41113	-.38640	-1.33576	317.046	2	83	-.21877	.52083	-1.33576	112.500
2	34	.38260	-.41493	-1.33576	312.955	2	84	-.18097	.53493	-1.33576	108.409
2	35	.35211	-.44135	-1.33576	308.864	2	85	-.14227	.54629	-1.33576	104.318
2	36	.31982	-.46553	-1.33576	304.773	2	86	-.10284	.55487	-1.33576	100.227
2	37	.28588	-.48734	-1.33576	300.682	2	87	-.06291	.56061	-1.33576	96.136
2	38	.25047	-.50667	-1.33576	296.591	2	88	-.02267	.56349	-1.33576	92.045
2	39	.21377	-.52343	-1.33576	292.500	3	1	-.00250	.58567	-1.31394	90.000
2	40	.17597	-.53753	-1.33576	288.409	3	2	.03937	.58417	-1.31394	85.909
2	41	.13727	-.54889	-1.33576	284.318	3	3	.08103	.57969	-1.31394	81.818
2	42	.09784	-.55747	-1.33576	280.227	3	4	.12227	.57225	-1.31394	77.727
2	43	.05791	-.56321	-1.33576	276.137	3	5	.16287	.56189	-1.31394	73.636
2	44	.01767	-.56609	-1.33576	272.046	3	6	.20262	.54866	-1.31394	69.545
2	45	-.02267	-.56609	-1.33576	267.955	3	7	.24134	.53263	-1.31394	65.454
2	46	-.06291	-.56321	-1.33576	263.864	3	8	.27880	.51387	-1.31394	61.364
2	47	-.10284	-.55747	-1.33576	259.773	3	9	.31484	.49249	-1.31394	57.273
2	48	-.14227	-.54889	-1.33576	255.682	3	10	.34926	.46859	-1.31394	53.182
2	49	-.18097	-.53753	-1.33576	251.591	3	11	.38188	.44230	-1.31394	49.091
2	50	-.21877	-.52343	-1.33576	247.500	3	12	.41255	.41375	-1.31394	45.000
2	51	-.25547	-.50667	-1.33576	243.409	3	13	.44110	.38308	-1.31394	40.909
2	52	-.29088	-.48734	-1.33576	239.318	3	14	.46739	.35046	-1.31394	36.818
2	53	-.32482	-.46553	-1.33576	235.227	3	15	.49129	.31604	-1.31394	32.727
2	54	-.35711	-.44135	-1.33576	231.136	3	16	.51267	.28000	-1.31394	28.636
2	55	-.38760	-.41493	-1.33576	227.046	3	17	.53143	.24254	-1.31394	24.545
2	56	-.41613	-.38640	-1.33576	222.955	3	18	.54746	.20382	-1.31394	20.454
2	57	-.44255	-.35591	-1.33576	218.864	3	19	.56069	.16407	-1.31394	16.363
2	58	-.46673	-.32362	-1.33576	214.773	3	20	.57105	.12347	-1.31394	12.273
2	59	-.48854	-.28968	-1.33576	210.682	3	21	.57849	.08223	-1.31394	8.182
2	60	-.50787	-.25427	-1.33576	206.591	3	22	.58297	.04057	-1.31394	4.091
2	61	-.52463	-.21757	-1.33576	202.500	3	23	.58447	-.00130	-1.31394	360.000
2	62	-.53873	-.17977	-1.33576	198.409	3	24	.58297	-.04317	-1.31394	355.909

Table 2. (Cont.)

ROW	RETRO	X	Y	Z	THETA
3	25	.57849	-.08483	-1.31394	351.818
3	26	.57105	-.12607	-1.31394	347.727
3	27	.56069	-.16667	-1.31394	343.636
3	28	.54746	-.20642	-1.31394	339.545
3	29	.53143	-.24514	-1.31394	335.454
3	30	.51267	-.28260	-1.31394	331.363
3	31	.49129	-.31864	-1.31394	327.273
3	32	.46739	-.35306	-1.31394	323.182
3	33	.44110	-.38568	-1.31394	319.091
3	34	.41255	-.41635	-1.31394	315.000
3	35	.38188	-.44490	-1.31394	310.909
3	36	.34926	-.47119	-1.31394	306.818
3	37	.31484	-.49509	-1.31394	302.728
3	38	.27880	-.51647	-1.31394	298.637
3	39	.24134	-.53523	-1.31394	294.546
3	40	.20262	-.55126	-1.31394	290.455
3	41	.16287	-.56449	-1.31394	286.364
3	42	.12227	-.57485	-1.31394	282.273
3	43	.08103	-.58229	-1.31394	278.182
3	44	.03937	-.58677	-1.31394	274.091
3	45	-.00250	-.58827	-1.31394	270.000
3	46	-.04437	-.58677	-1.31394	265.909
3	47	-.08603	-.58229	-1.31394	261.818
3	48	-.12727	-.57485	-1.31394	257.727
3	49	-.16787	-.56449	-1.31394	253.636
3	50	-.20762	-.55126	-1.31394	249.546
3	51	-.24634	-.53523	-1.31394	245.455
3	52	-.28380	-.51647	-1.31394	241.364
3	53	-.31984	-.49509	-1.31394	237.273
3	54	-.35426	-.47119	-1.31394	233.182
3	55	-.38688	-.44490	-1.31394	229.091
3	56	-.41755	-.41635	-1.31394	225.000
3	57	-.44610	-.38568	-1.31394	220.909
3	58	-.47239	-.35306	-1.31394	216.818
3	59	-.49629	-.31864	-1.31394	212.727
3	60	-.51767	-.28260	-1.31394	208.636
3	61	-.53643	-.24514	-1.31394	204.545
3	62	-.55246	-.20642	-1.31394	200.455
3	63	-.56569	-.16667	-1.31394	196.364
3	64	-.57605	-.12607	-1.31394	192.273
3	65	-.58349	-.08483	-1.31394	188.182
3	66	-.58797	-.04317	-1.31394	184.091
3	67	-.58947	-.00130	-1.31394	180.000
3	68	-.58797	.04057	-1.31394	175.909
3	69	-.58349	.08223	-1.31394	171.818
3	70	-.57605	.12347	-1.31394	167.727
3	71	-.56569	.16407	-1.31394	163.636
3	72	-.55246	.20382	-1.31394	159.545
3	73	-.53643	.24254	-1.31394	155.454
3	74	-.51767	.28000	-1.31394	151.364
3	75	-.49629	.31604	-1.31394	147.273
3	76	-.47239	.35046	-1.31394	143.182
3	77	-.44610	.38308	-1.31394	139.091
3	78	-.41755	.41375	-1.31394	135.000
3	79	-.38688	.44230	-1.31394	130.909
3	80	-.35426	.46859	-1.31394	126.818
3	81	-.31984	.49249	-1.31394	122.727
3	82	-.28380	.51387	-1.31394	118.636
3	83	-.24634	.53263	-1.31394	114.545
3	84	-.20762	.54866	-1.31394	110.454
3	85	-.16787	.56189	-1.31394	106.363
3	86	-.12727	.57225	-1.31394	102.272
3	87	-.08603	.57969	-1.31394	98.182
3	88	-.04437	.58417	-1.31394	94.091

4. METHOD OF COMPUTING THE TRANSFER FUNCTION

In computing the reflectivity of the Geos 3 retroreflector array, the cube corners have been modeled as isothermal, geometrically perfect reflectors (except for the dihedral-angle offset) with perfect-metal reflecting coatings on the back faces. The primary effect of real metal faces is a decrease in the intensity of the return signal because of the triple metallic reflection. This loss should be added to the constant η of the next section, along with reflection losses at the front face on entering and leaving the cube corners.

Computation of the range correction includes a correction for the optical path length of the ray within the cube corner. The range correction is the difference between the centroid of the actual return signal and the centroid of the return signal that would be received from a point reflector at the center of gravity of the satellite. The correction listed is the one-way correction.

The reflectivities and range corrections presented in all the tables are for the incoherent case; that is, the intensities of the reflections are added without taking into account coherent interference among the reflected signals from the individual cube corners.

The variation of the range correction due to optical coherence has been derived by statistical analysis of a set of coherent returns, which was constructed by assigning random phases to the reflection from each cube corner by means of a pseudo random-number generator. Since the computer time required to compute a coherent return increases as the square of the number of cube corners, the calculations were done with a reduced array obtained by selecting every Nth reflector in each row of cube corners, where N is 2, 4, or 8. Reduced arrays have also been used in diffraction calculations. Except when the calculations have been performed for specific values of velocity aberration, the curves in Figure 7 (Section 6), giving the average reflectivity of the cube corners between velocity aberrations of 25 and 50 μrad, have been used to

compute the strength of the reflection from each cube corner. As the curves for 5300 and 6943 Å are almost the same, the one for 5300 Å is used unless runs have been made for both wavelengths.

Since the array consists of circular rings of cube corners, the reflectivity is independent of azimuth. The slight offset of the center of gravity from the symmetry axis causes a slight variation of the range correction with azimuth, but the effect on the range is zero when averaged over all azimuths. All the computer runs have been done at an azimuth 90° away from the offset, so there is no effect on the range correction.

5. SIGNAL-STRENGTH COMPUTATION

The data contained in the tables presented later can be used to estimate signal strengths for laser ranging by use of the following equation:

$$N = \frac{E}{h\nu} G_T A_S G_S A_R \frac{T^2}{R^4} \eta \quad ,$$

where

N = number of photoelectrons,

E = transmitted energy,

h = Planck's constant,

ν = frequency of laser light,

G_T = "gain" of transmitter,

A_S = active reflecting area of satellite,

G_S = "gain" of satellite array,

A_R = area of receiving telescope,

T = atmospheric-transmission factor,

R = range from station to satellite,

η = constant, which includes the quantum efficiency of the photomultiplier and the optical transmission factors of the transmitter, the satellite, and the receiver.

If the transmitted beam is a uniform spot of solid angle Ω_T, the "gain" function of the transmitter is

$$G_T = \frac{1}{\Omega_T} \quad .$$

The gain functions in this equation do not contain the factor of 4π used in the standard definition of gain. Those given in later sections can be converted to the standard definition by multiplying by 4π. The signal-strength equation above can be converted to the standard definition of gain by adding the factor $1/(4\pi)^2$.

6. OPTICAL CUBE-CORNER REFLECTIVITY

The reflectivity of the Geos 3 optical cube corners is given below as a function of incidence angle. The angle ϕ is measured from the normal to the front face, and the angle θ is the angle to the projection of the incident beam onto the front face; both these angles are shown in Figure 6. In each graph, the upper curve is the total reflectivity and is proportional to the active reflecting area; the lower curve is the average reflectivity in the annulus between 25 and 50 μrad from the center of the reflected beam in the far field, which is approximately that region of the far field observed during laser ranging because of velocity aberration. The curves do not include reflection losses, and all curves are normalized to unity at normal incidence. The active reflecting area at normal incidence is

$$\frac{\sqrt{3}}{2} W^2 = \frac{\sqrt{3}}{2} (3.5 \text{ cm})^2 = 10.6088 \text{ cm}^2$$

for a hexagonal cube corner whose width W = 3.5 cm across flats. If the cube corners had perfect-metal reflecting faces and no dihedral-angle offset, the gain at the center of the far-field pattern would be $G = A/\lambda^2$, where A is the active reflecting area, λ the wavelength of the incident beam, and G the gain as defined in Section 5. (The standard expression for gain in this case is $4\pi A/\lambda^2$.) For the Geos 3 cube corners, the gain at normal incidence in the 25- to 50-μrad annulus for the 5300 and 6943 Å wavelengths is 0.0262 and 0.0394, respectively, times A/λ^2.

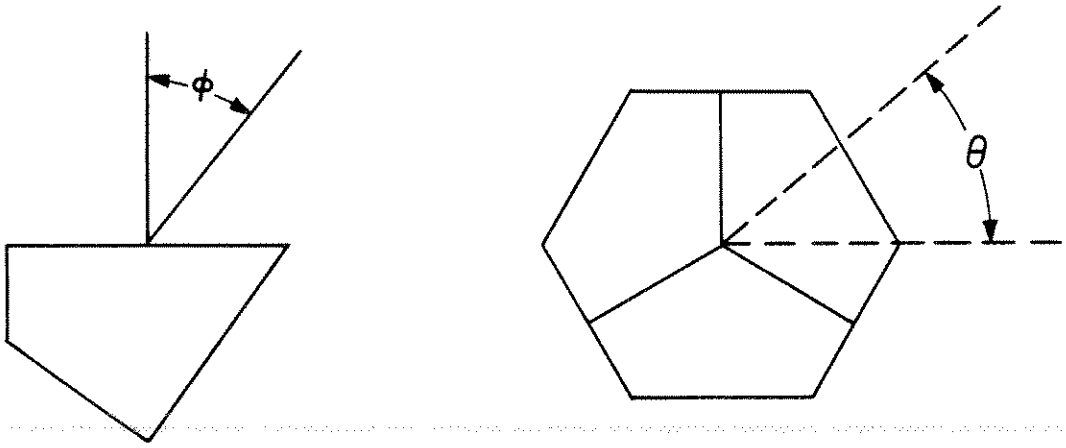

Figure 6. Direction of incident beam.

To convert the normalized reflectivities in the annulus to gain, values from Figure 7 are multiplied by G_{5300} or G_{6943}, where

$$G_{5300} = 0.0262 \frac{A}{\lambda_{5300}^2} = 9.895 \times 10^7$$

and

$$G_{6943} = 0.0394 \frac{A}{\lambda_{6943}^2} = 8.671 \times 10^7 \quad .$$

In all the curves of Figure 7, the reflectivity in the annulus falls off more rapidly with incidence angle than does the total reflectivity, because diffraction spreads the beam as the active reflecting area becomes smaller. The curves for the two different wavelengths are fairly similar, but the difference between the total reflectivity and the reflectivity in the annulus is significant. The latter reflectivity does not go as the square of the active reflecting area for two reasons: The reflectivity is not measured at the center of the far-field pattern, and the reflectors have dihedral-angle offsets designed to spread the beam by an amount equal to the velocity aberration. The data used to plot the reflectivity in the annulus are listed in Table 3. The active reflecting area and the reflectivity in the annulus repeat every 60° in θ. In addition, the values for $30° - \theta$ are equal to those for $30° + \theta$.

Table 3. Average reflectivity of a Geos 3 optical cube corner in the 25- to 50-μrad annulus of the far-field diffraction pattern. The angles θ and φ are defined in Figure 6.

PHI	THETA 0	THETA 10	THETA 20	THETA 30
		a: λ = 5300 Å		
0	1.000000	1.000000	1.000000	1.000000
5	.873459	.866570	.861876	.860404
10	.747223	.734170	.725697	.723136
15	.613009	.598221	.590054	.588197
20	.485628	.474333	.470211	.469748
25	.376493	.366436	.359414	.355880
30	.263542	.256402	.247662	.241249
35	.151124	.155796	.162208	.162041
40	.080963	.089195	.110225	.118907
45	.047715	.050723	.064463	.074054
50	.023934	.022251	.023511	.027179
55	.007978	.005420	.002824	.002481
60	.001145	.000191	0.000000	0.000000
65	0.000000	0.000000	0.000000	0.000000
		b: λ = 6943 Å		
0	1.000000	1.000000	1.000000	1.000000
5	.858437	.850265	.846888	.846205
10	.725605	.713353	.709062	.708398
15	.609522	.593175	.585329	.583179
20	.486866	.469136	.458091	.454153
25	.347309	.336414	.331691	.330076
30	.221709	.222177	.232867	.238484
35	.138974	.145139	.166315	.178464
40	.090526	.092933	.110301	.123062
45	.052331	.051291	.056090	.064462
50	.023348	.020770	.017723	.020024
55	.006598	.004545	.001854	.001396
60	.000711	.000076	0.000000	0.000000
65	0.000000	0.000000	0.000000	0.000000

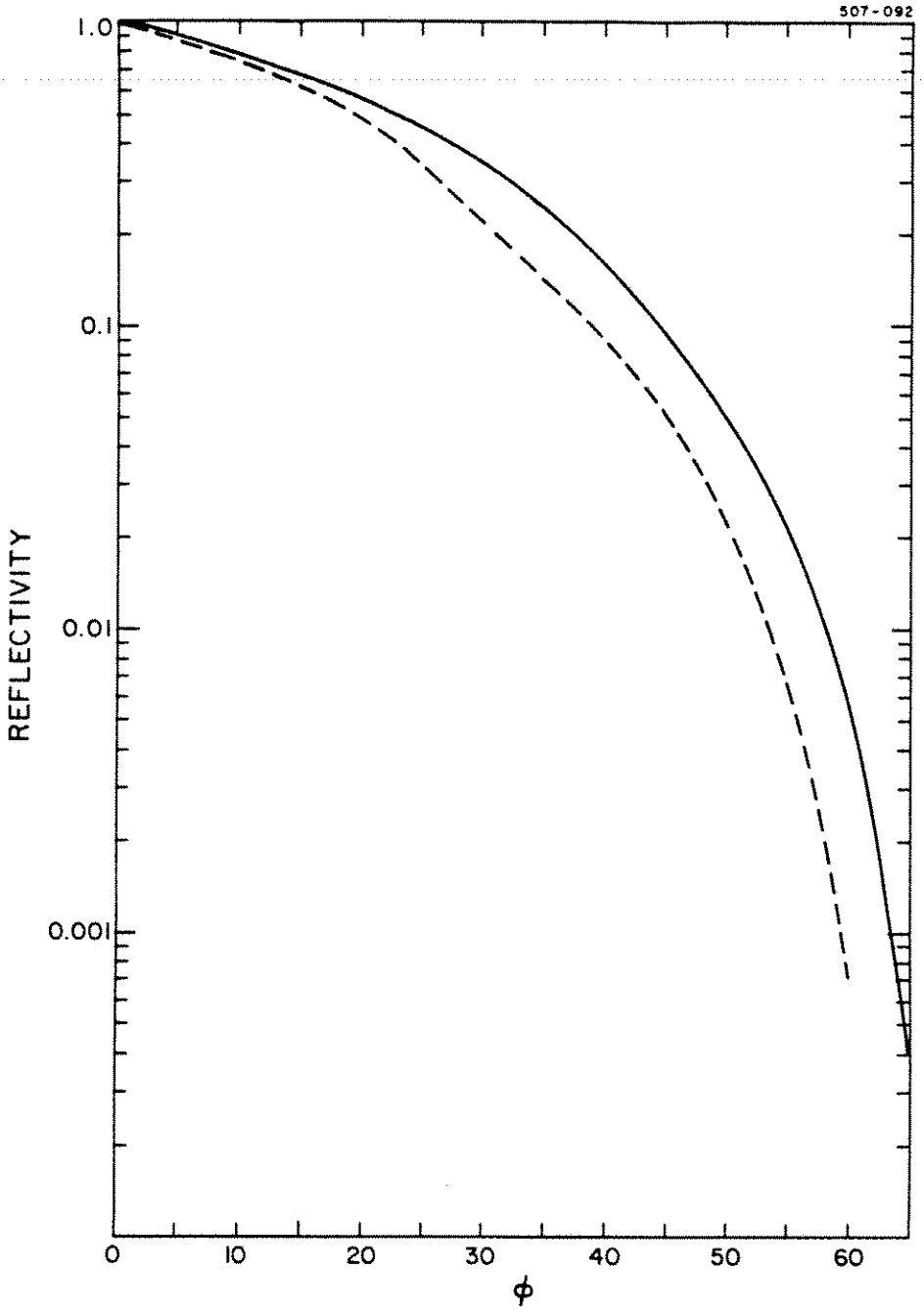

Figure 7. Active reflecting area and average reflectivity in the 25- to 50-μrad annulus of the far-field diffraction pattern for a Geos 3 optical cube corner. The incidence angles θ and ϕ are defined in Figure 6; the index of refraction n and the wavelength λ are listed for each set of curves. The solid curve is the active reflecting area (total reflectivity), and the dashed curve, the reflectivity in the 25- to 50-μrad annulus. a: $\theta = 0°$, $n = 1.455$, $\lambda = 6943$ Å.

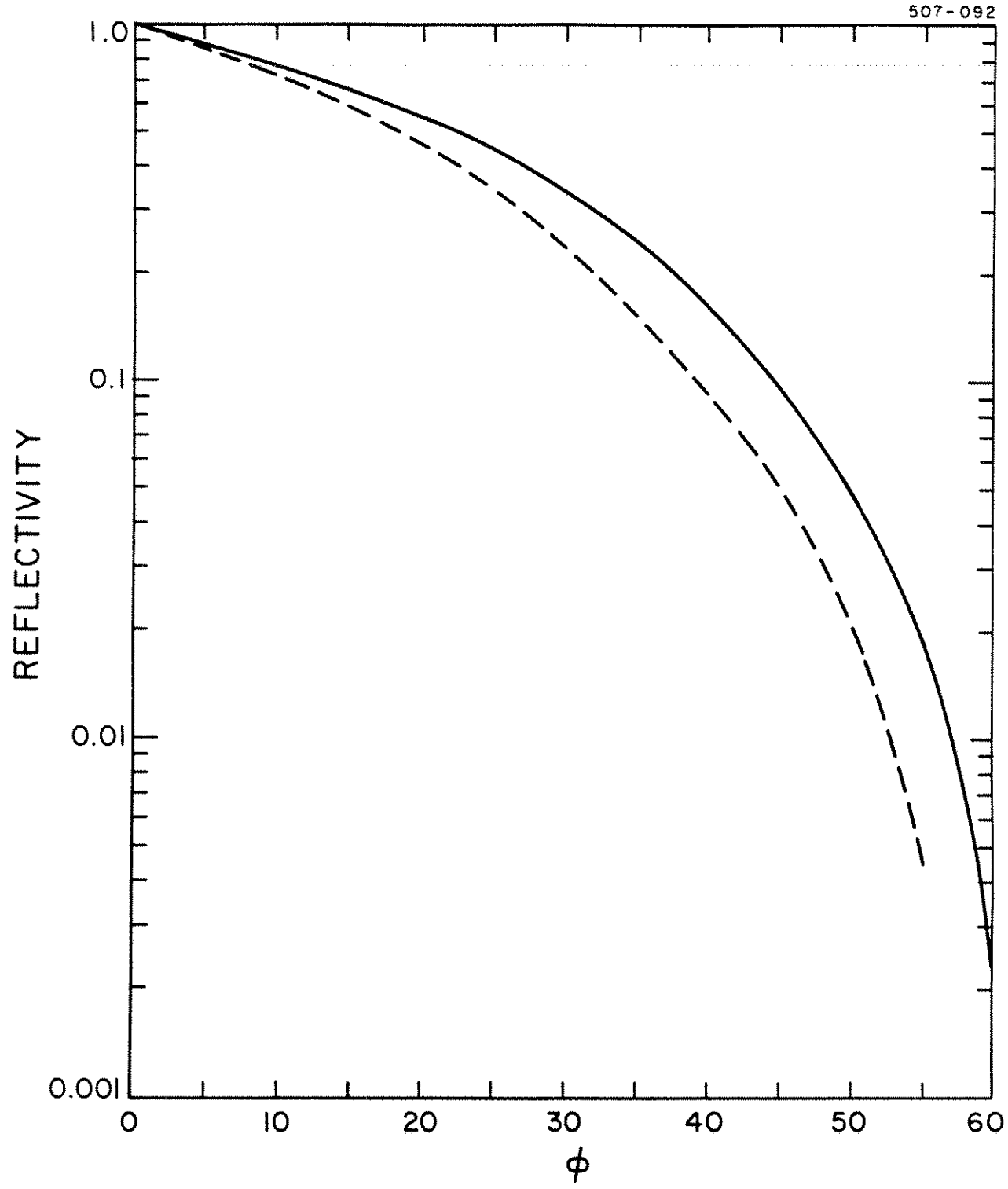

Figure 7b: $\theta = 10°$, $n = 1.455$, $\lambda = 6943$ Å.

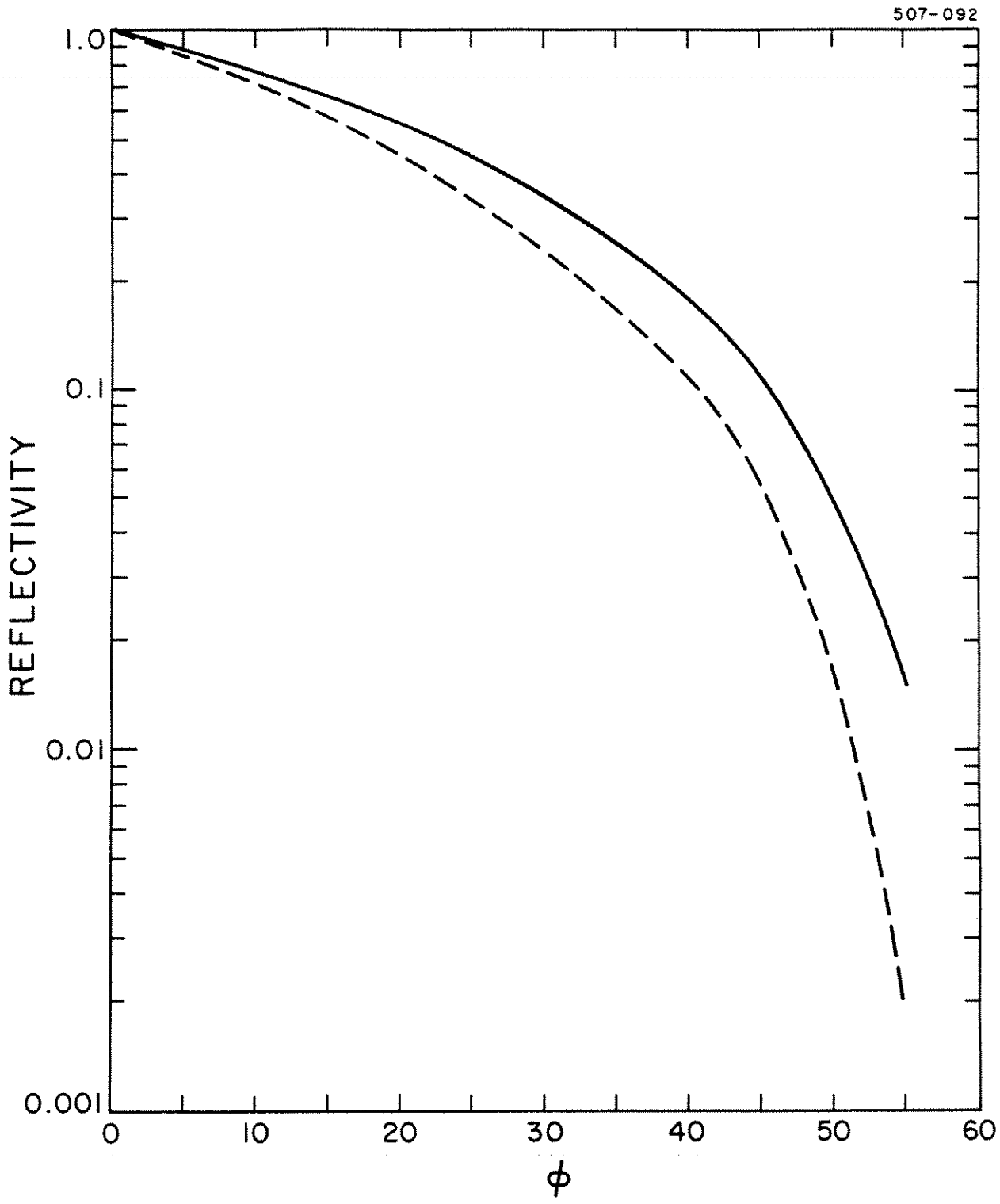

Figure 7c: $\theta = 20°$, $n = 1.455$, $\lambda = 6943$ Å.

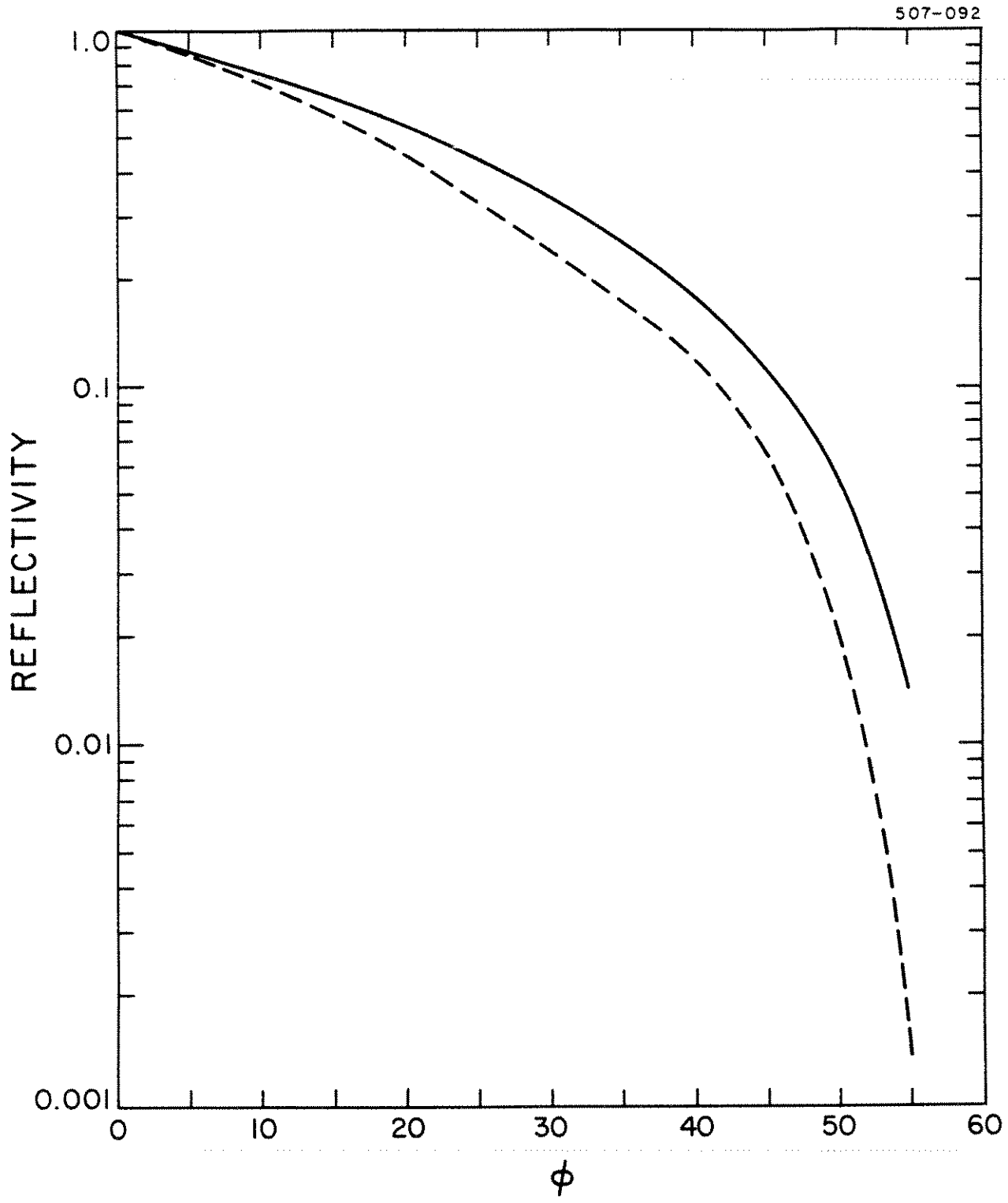

Figure 7d: $\theta = 30°$, $n = 1.455$, $\lambda = 6943$ Å.

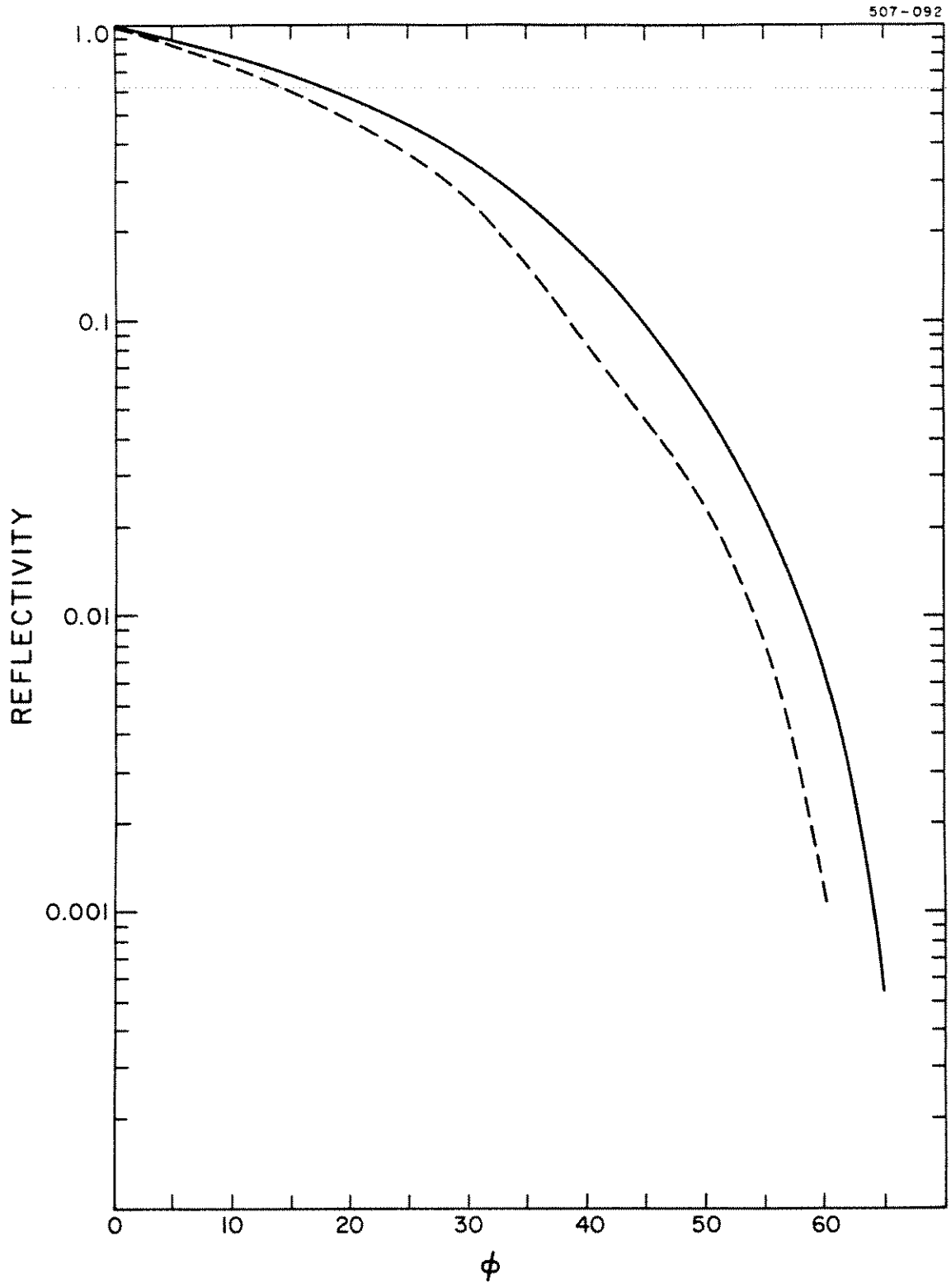

Figure 7e: $\theta = 0°$, $n = 1.461$, $\lambda = 5300$ Å.

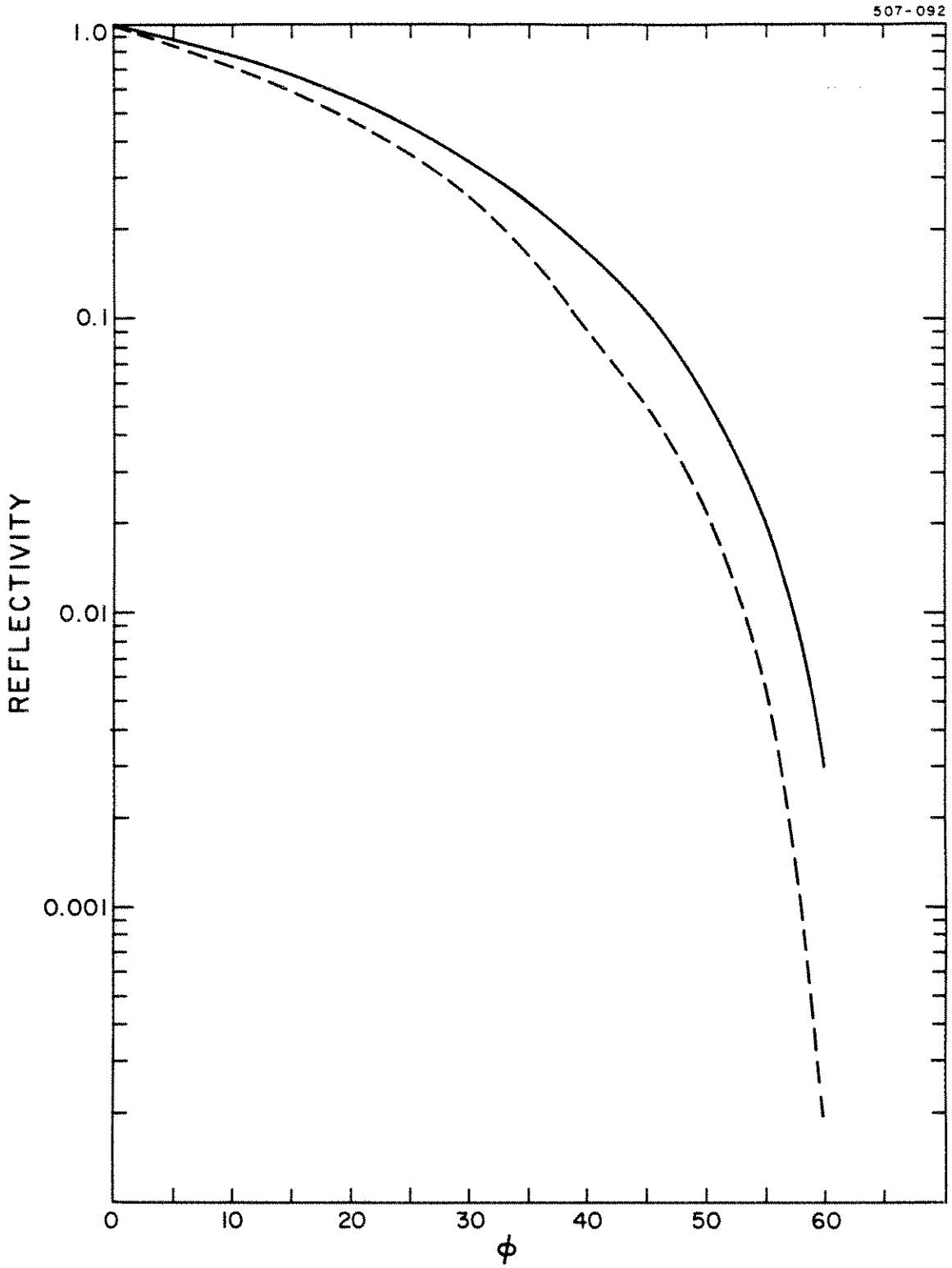

Figure 7f: $\theta = 10°$, $n = 1.461$, $\lambda = 5300$ Å.

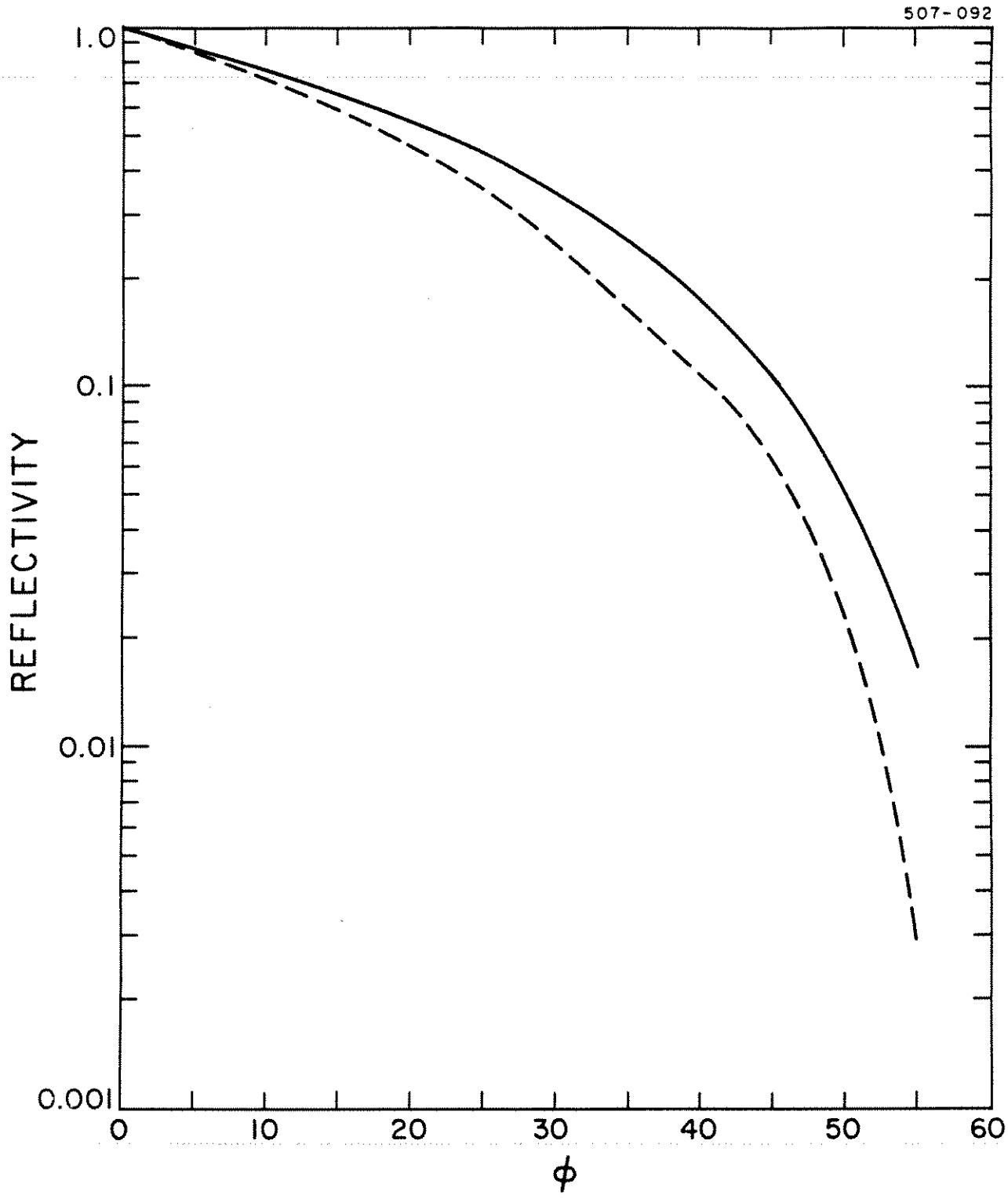

Figure 7g: $\theta = 20°$, $n = 1.461$, $\lambda = 5300$ Å.

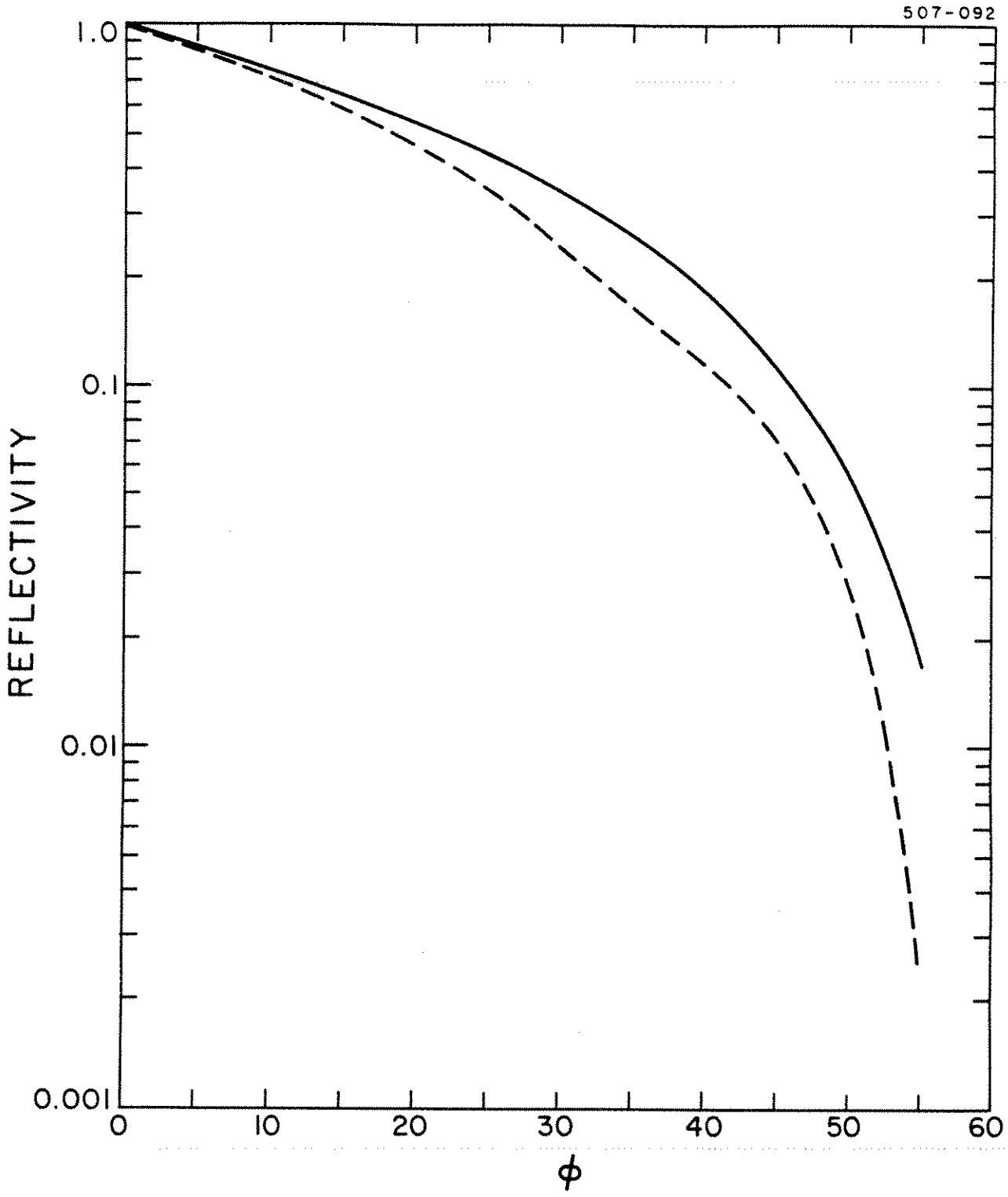

Figure 7h: $\theta = 30°$, $n = 1.461$, $\lambda = 5300$ Å.

7. ARRAY REFLECTIVITY

This section contains information on the reflectivity of the Geos 3 optical retroreflector array.

Tables 4 and 5 were computed by using the cube-corner reflectivity curves of Figure 7. Table 4 gives the total reflectivity N_T, and Table 5, the reflectivity in the annulus N_λ in terms of the equivalent number of cube corners at normal incidence. The area A of one cube corner at normal incidence is 10.6088 cm^2. The total reflected energy, which is proportional to the active reflecting area AN_T, can be measured only under laboratory conditions. From Table 5, estimates of signal strengths for laser ranging can be made by means of the range equation in Section 5. The array cross section $A_S G_S$ is given by $AN_\lambda G_\lambda$, where $G_{5300} = 9.895 \times 10^7$ and $G_{6943} = 8.671 \times 10^7$. To use the gain-function data of Tables 6 and 7 in the range equation, set the cross section $A_S G_S$ equal to $AN_T G$, taking G from the appropriate table.

Table 5 shows that the reflectivity in the 25- to 50-μrad annulus is about the same for both wavelengths, but there is a significant difference between the curves of Tables 4 and 5. For example, at $\phi = 0°$, the total reflectivity is equivalent to about 25 cube corners; however, the reflectivity in the annulus is equivalent to only 12 or 13 cube corners. The maximum reflectivity of the array occurs between 40° and 45° as a result of the 45° tilt of the cube corners with respect to the symmetry axis. The reflectivity at 60° is large compared to previous Geos arrays, with the result that signal strengths are much stronger under the adverse conditions of long range and low elevations above the horizon. Since the satellite is gravity stabilized, the incidence angle ϕ cannot be more than about 60°.

In the computer-plotted graphs to the right of Tables 4 and 5, the reflectivity increases to the right and the incidence angle ϕ increases down the page.

Table 6 shows how the array gain function varies with velocity aberration. The first column is the magnitude of the velocity aberration in microradians, and the

second is the array gain function in units of 10^7. In the computer-plotted graph, the gain function increases to the right and the velocity aberration, down the page. The gain function is the average value around a circle in the far field with radius equal to the velocity aberration. The second part of each table gives the root-mean-square (rms) variation of the gain around the circle. At $\phi = 0°$, the gain has almost perfect circular symmetry, as indicated by the fact that the rms variation is nearly zero. The curves for larger incidence angles, such as $\phi = 45°$, show the effect of the dihedral-angle offset in peaking the intensity in the 25- to 50-μrad annulus.

Some of the gain-function matrices from which the data of Table 6 were computed are given in Table 7. Only the right half of the matrix has been presented, since the diffraction pattern for a cube corner with perfect-metal reflecting faces has the symmetry property $G(\theta_1, \theta_2) = G(-\theta_1, -\theta_2)$. The angles θ_1 and θ_2, in microradians, are defined in Figure 8. The angle θ_2 is in the direction of decreasing ϕ in the plane containing the -Z axis and the direction toward the illuminating laser (the vector $\vec{V}$). The angle θ_1 is normal to the plane in the direction of $-\hat{Z} \times \vec{V}$.

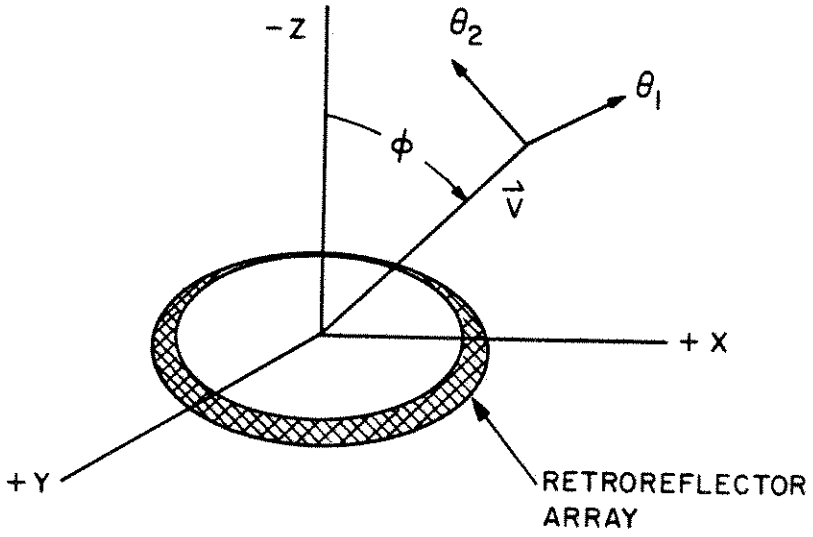

Figure 8. Diffraction-pattern coordinate system.

Figure 9 (p. 42) consists of contour plots of the gain-function matrices given in Table 7. Circles have been drawn with radii of 25 and 50 μrad to mark the minimum and maximum values of velocity aberration. The contour levels plotted are 8, 4, 2, 1, and 0.5×10^{7}. The positions of peaks in the pattern are indicated by asterisks. The contours for $\phi = 0°$ are circles because of the symmetry of the array, while those for larger values of ϕ show an unexpected asymmetry. We had expected to find $G(\theta_1, \theta_2) = G(-\theta_1, \theta_2)$ because the distribution of cube corners in the array is symmetrical in this direction (see Figure 8). The asymmetry is the result of the orientation of the cube corners: From Figure 2 we see that the orientation of a cube corner on the left is not symmetrical with respect to one on the right.

If the cube corners were oriented as shown in Figure 10, the far-field pattern would be symmetrical from left to right. [Note: The packing is obviously not so efficient in Figure 10 as it is in Figure 2.] If the dihedral-angle offset were not present, the asymmetry would disappear, since the direction of the exiting wavefront for each of the six sectors of the cube corner would be the same regardless of the order of the reflections at the back faces. The array transfer function would not be improved by making it symmetrical, however, because the variations in intensity and range correction between different points in the far field would still be about the same.

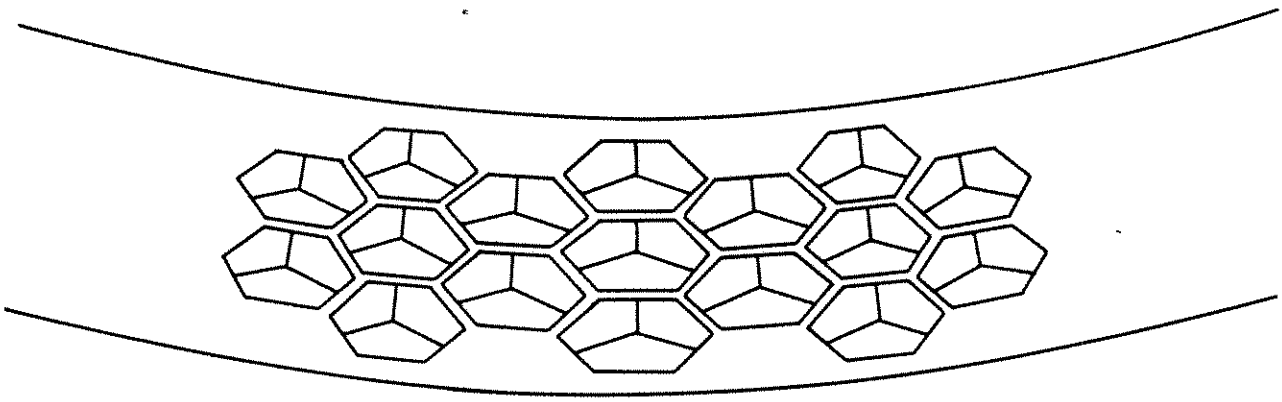

Figure 10. Alternate method of cube-corner orientation.

Table 4. Total reflectivity (active reflecting area) of the Geos 3 optical retroreflector array vs. incidence angle.

PHI (DEG)	REFLECTIVITY
0.0	25.3219
1.0	25.3645
2.0	25.4922
3.0	25.7048
4.0	26.0019
5.0	26.3832
6.0	26.8480
7.0	27.3957
8.0	28.0253
9.0	28.7359
10.0	29.5265
11.0	30.3774
12.0	31.2534
13.0	32.1389
14.0	33.0266
15.0	33.9106
16.0	34.7862
17.0	35.6489
18.0	36.4986
19.0	37.4014
20.0	38.3168
21.0	39.2199
22.0	40.1024
23.0	40.9548
24.0	41.7718
25.0	42.5542
26.0	43.3003
27.0	44.0151
28.0	44.7099
29.0	45.3828
30.0	46.0394
31.0	46.6773
32.0	47.2979
33.0	47.8972
34.0	48.4759
35.0	49.0348
36.0	49.5727
37.0	50.0898
38.0	50.5691
39.0	50.8707
40.0	51.0306
41.0	51.0704
42.0	50.9790
43.0	50.7805
44.0	50.4567
45.0	50.0118
46.0	49.4659
47.0	48.8188
48.0	48.0613
49.0	47.2324
50.0	46.3289
51.0	45.3640
52.0	44.3277
53.0	43.2273
54.0	42.0866
55.0	40.9030

ONE REFLECTOR AT NORMAL INCIDENCE HAS UNIT REFLECTIVITY

PHI (DEG)	REFLECTIVITY
56.0	39.6922
57.0	38.4430
58.0	37.1668
59.0	35.8654
60.0	34.5506
61.0	33.2210
62.0	31.8783
63.0	30.5294
64.0	29.1755
65.0	27.8229
66.0	26.4738
67.0	25.1459
68.0	23.8541
69.0	22.6005
70.0	21.3793
71.0	20.1916
72.0	19.0404
73.0	17.9232
74.0	16.8379
75.0	15.7857
76.0	14.7653
77.0	13.7737
78.0	12.8108
79.0	11.8781
80.0	10.9755
81.0	10.1027
82.0	9.2628
83.0	8.4550
84.0	7.6798
85.0	6.9379
86.0	6.2295
87.0	5.5555
88.0	4.9163
89.0	4.3120
90.0	3.7425
91.0	3.2075
92.0	2.7069
93.0	2.2424
94.0	1.8300
95.0	1.4719
96.0	1.1618
97.0	.9051
98.0	.6922
99.0	.5190
100.0	.3835
101.0	.2789
102.0	.1972
103.0	.1329
104.0	.0867
105.0	.0555
106.0	.0327
107.0	.0178
108.0	.0079
109.0	.0028
110.0	.0006
111.0	.0001

ONE REFLECTOR AT NORMAL INCIDENCE HAS UNIT REFLECTIVITY

Table 5. Average reflectivity of the Geos 3 optical retroreflector array in the 25- to 50-μrad annulus of the far-field diffraction pattern. a: $\lambda = 5300$ Å.

PHI (DEG)	REFLECTIVITY
0.0	12.5966
1.0	12.8215
2.0	13.0345
3.0	13.2356
4.0	13.4248
5.0	13.6020
6.0	14.0430
7.0	14.6349
8.0	15.3530
9.0	16.1393
10.0	16.9381
11.0	17.9411
12.0	19.0581
13.0	20.2037
14.0	21.3457
15.0	22.4211
16.0	23.4786
17.0	24.5371
18.0	25.5926
19.0	26.6455
20.0	27.6897
21.0	28.7051
22.0	29.6262
23.0	30.5322
24.0	31.4339
25.0	32.3358
26.0	33.2677
27.0	34.2080
28.0	35.0859
29.0	35.9273
30.0	36.7416
31.0	37.5435
32.0	38.3311
33.0	39.0926
34.0	39.8415
35.0	40.5836
36.0	41.3034
37.0	41.9966
38.0	42.6427
39.0	43.1059
40.0	43.4326
41.0	43.6205
42.0	43.6604
43.0	43.5997
44.0	43.3630
45.0	42.9896
46.0	42.4823
47.0	41.8602
48.0	41.1219
49.0	40.3021
50.0	39.4056
51.0	38.4444
52.0	37.4072
53.0	36.3102
54.0	35.1854
55.0	34.0247
56.0	32.8375
57.0	31.6278
58.0	30.4000
59.0	29.1506
60.0	27.8940
61.0	26.6296
62.0	25.3382
63.0	24.0273
64.0	22.7034
65.0	21.3837
66.0	20.0970
67.0	18.8160
68.0	17.5627
69.0	16.3471
70.0	15.1700
71.0	14.0570
72.0	13.0052
73.0	12.0208
74.0	11.1036
75.0	10.2482
76.0	9.4432
77.0	8.6856
78.0	7.9663
79.0	7.2966
80.0	6.6751
81.0	6.1288
82.0	5.5822
83.0	5.0335
84.0	4.4966
85.0	3.9920
86.0	3.5545
87.0	3.1232
88.0	2.7006
89.0	2.2995
90.0	1.9339
91.0	1.6116
92.0	1.3160
93.0	1.0529
94.0	.8252
95.0	.6435
96.0	.4992
97.0	.3725
98.0	.2698
99.0	.1865
100.0	.1318
101.0	.1016
102.0	.0729
103.0	.0467
104.0	.0239
105.0	.0096
106.0	.0077
107.0	.0057
108.0	.0037
109.0	.0017

ONE REFLECTOR AT NORMAL INCIDENCE HAS UNIT REFLECTIVITY

ONE REFLECTOR AT NORMAL INCIDENCE HAS UNIT REFLECTIVITY

Table 5b: $\lambda = 6943$ Å.

PHI (DEG)	REFLECTIVITY
0.0	13.8152
1.0	13.9392
2.0	14.0522
3.0	14.1542
4.0	14.2451
5.0	14.3247
6.0	14.5429
7.0	14.8489
8.0	15.2425
9.0	15.7016
10.0	16.1949
11.0	16.9008
12.0	17.7405
13.0	18.6415
14.0	19.5677
15.0	20.4991
16.0	21.5805
17.0	22.7439
18.0	23.9256
19.0	25.1052
20.0	26.2602
21.0	27.4096
22.0	28.4329
23.0	29.4027
24.0	30.3372
25.0	31.2489
26.0	32.1222
27.0	32.9793
28.0	33.7877
29.0	34.5745
30.0	35.3561
31.0	36.1214
32.0	36.8676
33.0	37.5906
34.0	38.3623
35.0	39.1284
36.0	39.8863
37.0	40.6168
38.0	41.2922
39.0	41.7810
40.0	42.1089
41.0	42.2956
42.0	42.3424
43.0	42.3173
44.0	42.1546
45.0	41.8672
46.0	41.4072
47.0	40.8101
48.0	40.0850
49.0	39.2887
50.0	38.4285
51.0	37.5242
52.0	36.5497
53.0	35.5040
54.0	34.4152
55.0	33.2708

ONE REFLECTOR AT NORMAL INCIDENCE HAS UNIT REFLECTIVITY

PHI (DEG)	REFLECTIVITY
56.0	32.0954
57.0	30.8587
58.0	29.5680
59.0	28.2297
60.0	26.8592
61.0	25.4667
62.0	24.0744
63.0	22.6834
64.0	21.3307
65.0	20.0170
66.0	18.7418
67.0	17.5065
68.0	16.3334
69.0	15.2342
70.0	14.2083
71.0	13.2635
72.0	12.3609
73.0	11.4964
74.0	10.6758
75.0	9.9117
76.0	9.2262
77.0	8.5509
78.0	7.8838
79.0	7.2348
80.0	6.6082
81.0	6.0407
82.0	5.4752
83.0	4.9132
84.0	4.3711
85.0	3.8538
86.0	3.3732
87.0	2.9162
88.0	2.4837
89.0	2.0873
90.0	1.7383
91.0	1.4347
92.0	1.1591
93.0	.9166
94.0	.7086
95.0	.5469
96.0	.4261
97.0	.3185
98.0	.2289
99.0	.1543
100.0	.1049
101.0	.0813
102.0	.0583
103.0	.0368
104.0	.0176
105.0	.0055
106.0	.0044
107.0	.0033
108.0	.0021
109.0	.0010

ONE REFLECTOR AT NORMAL INCIDENCE HAS UNIT REFLECTIVITY

Table 6. Gain function vs. velocity aberration for the Geos 3 optical retroreflector array. The average and rms fluctuations are computed around a circle in the far field whose radius is the velocity aberration listed in the first column, in microradians. The gain differs by 4π from the standard definition (see Section 5).

a: PHI 0 DIHEDRAL ANGLE 2.00 WAVELENGTH 5300

AVERAGE GAIN FUNCTION (1.E+7)

0	10.94
5	10.70
10	10.18
15	9.43
20	8.54
25	7.58
30	6.56
35	5.51
40	4.50
45	3.61
50	2.91

R.M.S. FLUCTUATION

0	0.00
5	.02
10	.02
15	.01
20	.01
25	.01
30	.01
35	.01
40	.01
45	.01
50	.01

b: PHI 5 DIHEDRAL ANGLE 2.00 WAVELENGTH 5300

AVERAGE GAIN FUNCTION (1.E+7)

0	9.93
5	9.75
10	9.34
15	8.75
20	8.02
25	7.17
30	6.25
35	5.36
40	4.60
45	3.99
50	3.51

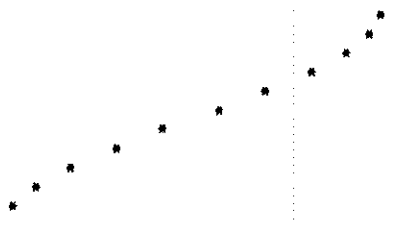

R.M.S. FLUCTUATION

0	0.00
5	.05
10	.17
15	.31
20	.37
25	.34
30	.24
35	.17
40	.22
45	.28
50	.33

c: PHI 10 DIHEDRAL ANGLE 2.00 WAVELENGTH 5300

AVERAGE GAIN FUNCTION (1.E+7)

0	7.71
5	7.63
10	7.43
15	7.14
20	6.75
25	6.31
30	5.96
35	5.73
40	5.52
45	5.16
50	4.60

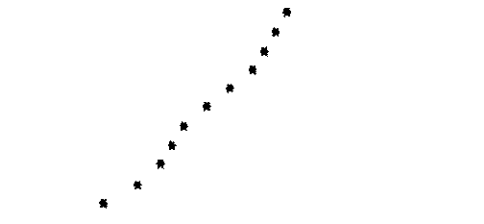

R.M.S. FLUCTUATION

0	0.00
5	.12
10	.45
15	.72
20	.76
25	.58
30	.42
35	.53
40	.71
45	.84
50	.85

d: PHI 15 DIHEDRAL ANGLE 2.00 WAVELENGTH 5300

AVERAGE GAIN FUNCTION (1.E+7)

0	5.60
5	5.52
10	5.50
15	5.67
20	5.97
25	6.33
30	6.70
35	6.95
40	6.79
45	6.12
50	5.13

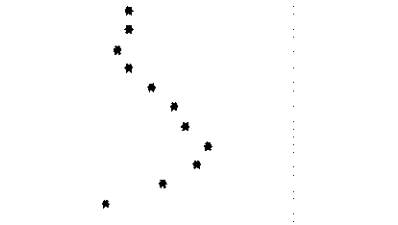

R.M.S. FLUCTUATION

0	0.00
5	.19
10	.63
15	.79
20	.49
25	.52
30	.90
35	1.09
40	1.25
45	1.31
50	1.19

Table 6. (Cont.)

e: PHI 20 DIHEDRAL ANGLE 2.00 WAVELENGTH 5300

AVERAGE GAIN FUNCTION (1.E+7)

0	4.68
5	4.34
10	4.17
15	4.83
20	6.09
25	7.23
30	7.83
35	7.84
40	7.31
45	6.42
50	5.44

R.M.S. FLUCTUATION

0	0.00
5	.25
10	.69
15	.59
20	.62
25	1.51
30	1.67
35	1.37
40	1.45
45	1.46
50	1.30

f: PHI 25 DIHEDRAL ANGLE 2.00 WAVELENGTH 5300

AVERAGE GAIN FUNCTION (1.E+7)

0	4.60
5	3.84
10	3.34
15	4.28
20	6.18
25	7.63
30	8.12
35	8.02
40	7.61
45	6.92
50	5.98

R.M.S. FLUCTUATION

0	0.00
5	.22
10	.50
15	.45
20	1.24
25	1.86
30	1.50
35	1.17
40	1.35
45	1.39
50	1.38

g: PHI 30 DIHEDRAL ANGLE 2.00 WAVELENGTH 5300

AVERAGE GAIN FUNCTION (1.E+7)

0	5.02
5	3.84
10	2.96
15	3.97
20	6.00
25	7.30
30	7.81
35	8.20
40	8.32
45	7.66
50	6.37

R.M.S. FLUCTUATION

0	0.00
5	.22
10	.53
15	.83
20	1.34
25	1.35
30	.94
35	1.28
40	1.61
45	1.60
50	1.47

h: PHI 35 DIHEDRAL ANGLE 2.00 WAVELENGTH 5300

AVERAGE GAIN FUNCTION (1.E+7)

0	5.49
5	3.97
10	2.79
15	3.73
20	5.55
25	6.66
30	7.58
35	8.70
40	8.99
45	8.03
50	6.58

R.M.S. FLUCTUATION

0	0.00
5	.25
10	.71
15	.99
20	.96
25	.76
30	1.20
35	1.90
40	1.93
45	1.58
50	1.42

Table 6. (Cont.)

i: PHI 40 DIHEDRAL ANGLE 2.00 WAVELENGTH 5300

AVERAGE GAIN FUNCTION (1.E+7)

0	5.83
5	4.00
10	2.60
15	3.50
20	5.11
25	6.20
30	7.67
35	9.21
40	9.35
45	8.23
50	6.85

R.M.S. FLUCTUATION

0	0.00
5	.22
10	.72
15	1.02
20	.79
25	.93
30	1.75
35	2.30
40	1.95
45	1.57
50	1.42

j: PHI 45 DIHEDRAL ANGLE 2.00 WAVELENGTH 5300

AVERAGE GAIN FUNCTION (1.E+7)

0	6.71
5	4.30
10	2.33
15	3.25
20	5.18
25	6.29
30	7.62
35	9.25
40	9.57
45	8.41
50	6.87

R.M.S. FLUCTUATION

0	0.00
5	.19
10	.56
15	1.13
20	1.23
25	1.24
30	1.68
35	1.99
40	1.92
45	1.67
50	1.41

k: PHI 50 DIHEDRAL ANGLE 2.00 WAVELENGTH 5300

AVERAGE GAIN FUNCTION (1.E+7)

0	6.16
5	3.96
10	2.17
15	3.24
20	5.44
25	6.70
30	7.71
35	8.97
40	9.33
45	8.39
50	6.88

R.M.S. FLUCTUATION

0	0.00
5	.15
10	.39
15	.90
20	1.37
25	1.56
30	1.81
35	1.96
40	1.90
45	1.84
50	1.59

l: PHI 55 DIHEDRAL ANGLE 2.00 WAVELENGTH 5300

AVERAGE GAIN FUNCTION (1.E+7)

0	5.01
5	3.44
10	2.25
15	3.42
20	5.66
25	7.07
30	7.94
35	8.76
40	8.87
45	8.00
50	6.69

R.M.S. FLUCTUATION

0	0.00
5	.09
10	.24
15	.50
20	1.06
25	1.60
30	1.87
35	2.06
40	2.07
45	1.97
50	1.79

Table 6. (Cont.)

m: PHI 60 DIHEDRAL ANGLE 2.00 WAVELENGTH 5300

AVERAGE GAIN FUNCTION (1.E+7)

0	4.44
5	3.45
10	2.76
15	3.77
20	5.69
25	7.11
30	7.97
35	8.55
40	8.47
45	7.57
50	6.30

R.M.S. FLUCTUATION

0	0.00
5	.07
10	.23
15	.52
20	.82
25	1.34
30	1.81
35	2.09
40	2.21
45	2.12
50	1.89

n: PHI 0 DIHEDRAL ANGLE 2.00 WAVELENGTH 6943

AVERAGE GAIN FUNCTION (1.E+7)

0	10.52
5	10.29
10	9.80
15	9.05
20	8.14
25	7.18
30	6.23
35	5.34
40	4.52
45	3.78
50	3.11

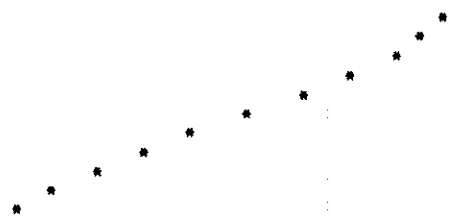

R.M.S. FLUCTUATION

0	0.00
5	.02
10	.02
15	.01
20	.01
25	.01
30	.01
35	.01
40	.00
45	.00
50	.00

o: PHI 5 DIHEDRAL ANGLE 2.00 WAVELENGTH 6943

AVERAGE GAIN FUNCTION (1.E+7)

0	10.49
5	10.25
10	9.71
15	8.92
20	8.01
25	7.05
30	6.12
35	5.24
40	4.43
45	3.70
50	3.07

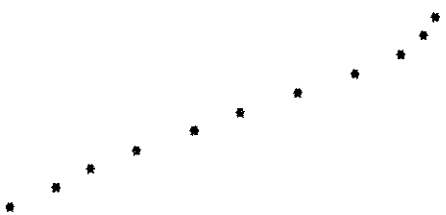

R.M.S. FLUCTUATION

0	0.00
5	.03
10	.08
15	.16
20	.25
25	.32
30	.35
35	.33
40	.26
45	.17
50	.11

p: PHI 10 DIHEDRAL ANGLE 2.00 WAVELENGTH 6943

AVERAGE GAIN FUNCTION (1.E+7)

0	10.14
5	9.87
10	9.31
15	8.54
20	7.68
25	6.81
30	5.96
35	5.15
40	4.44
45	3.85
50	3.37

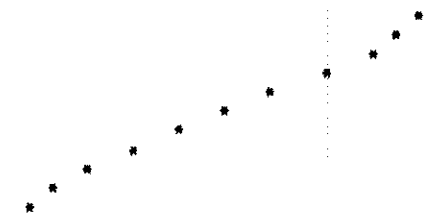

R.M.S. FLUCTUATION

0	0.00
5	.08
10	.31
15	.61
20	.87
25	1.01
30	.96
35	.78
40	.55
45	.39
50	.38

Table 6. (Cont.)

q: PHI 15 DIHEDRAL ANGLE 2.00 WAVELENGTH 6943

AVERAGE GAIN FUNCTION (1.E+7)

0	10.16
5	9.77
10	9.01
15	8.12
20	7.33
25	6.69
30	6.13
35	5.60
40	5.09
45	4.62
50	4.14

R.M.S. FLUCTUATION

0	0.00
5	.16
10	.59
15	1.10
20	1.44
25	1.44
30	1.13
35	.77
40	.67
45	.74
50	.79

r: PHI 20 DIHEDRAL ANGLE 2.00 WAVELENGTH 6943

AVERAGE GAIN FUNCTION (1.E+7)

0	11.28
5	10.51
10	9.14
15	7.77
20	6.96
25	6.72
30	6.69
35	6.52
40	6.08
45	5.43
50	4.65

R.M.S. FLUCTUATION

0	0.00
5	.21
10	.75
15	1.33
20	1.60
25	1.38
30	.92
35	.92
40	1.14
45	1.13
50	1.03

s: PHI 25 DIHEDRAL ANGLE 2.00 WAVELENGTH 6943

AVERAGE GAIN FUNCTION (1.E+7)

0	12.07
5	10.92
10	8.94
15	7.19
20	6.55
25	6.85
30	7.29
35	7.27
40	6.65
45	5.72
50	4.75

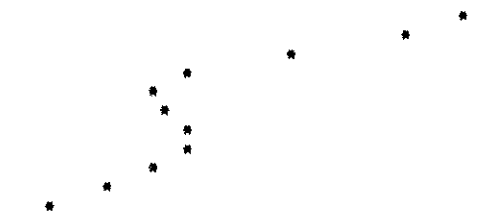

R.M.S. FLUCTUATION

0	0.00
5	.22
10	.69
15	1.15
20	1.26
25	1.00
30	.98
35	1.32
40	1.37
45	1.18
50	1.06

t: PHI 30 DIHEDRAL ANGLE 2.00 WAVELENGTH 6943

AVERAGE GAIN FUNCTION (1.E+7)

0	12.12
5	10.67
10	8.32
15	6.55
20	6.35
25	7.21
30	7.87
35	7.65
40	6.76
45	5.75
50	4.91

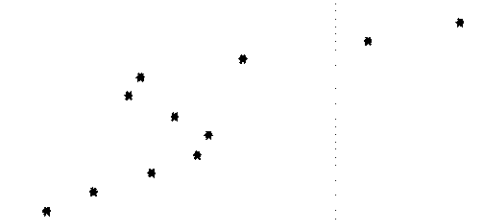

R.M.S. FLUCTUATION

0	0.00
5	.21
10	.55
15	.84
20	.90
25	1.00
30	1.32
35	1.47
40	1.31
45	1.10
50	1.00

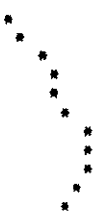

Table 6. (Cont.)

u: PHI 35 DIHEDRAL ANGLE 2.00 WAVELENGTH 6943

AVERAGE GAIN FUNCTION (1.E+7)

0	11.32
5	9.73
10	7.33
15	5.93
20	6.39
25	7.66
30	8.23
35	7.71
40	6.75
45	5.97
50	5.35

R.M.S. FLUCTUATION

0	0.00
5	.21
10	.55
15	.97
20	1.30
25	1.47
30	1.48
35	1.34
40	1.15
45	1.09
50	1.11

v: PHI 40 DIHEDRAL ANGLE 2.00 WAVELENGTH 6943

AVERAGE GAIN FUNCTION (1.E+7)

0	10.45
5	8.74
10	6.36
15	5.42
20	6.48
25	8.00
30	8.38
35	7.70
40	6.91
45	6.41
50	5.78

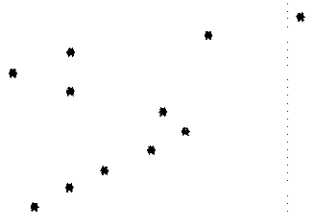

R.M.S. FLUCTUATION

0	0.00
5	.20
10	.64
15	1.33
20	1.88
25	1.90
30	1.50
35	1.21
40	1.24
45	1.41
50	1.37

w: PHI 45 DIHEDRAL ANGLE 2.00 WAVELENGTH 6943

AVERAGE GAIN FUNCTION (1.E+7)

0	11.15
5	9.11
10	6.26
15	5.06
20	6.26
25	8.04
30	8.56
35	7.85
40	7.00
45	6.48
50	5.87

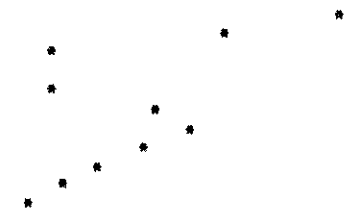

R.M.S. FLUCTUATION

0	0.00
5	.19
10	.41
15	1.05
20	1.73
25	1.95
30	1.62
35	1.26
40	1.32
45	1.44
50	1.30

x: PHI 50 DIHEDRAL ANGLE 2.00 WAVELENGTH 6943

AVERAGE GAIN FUNCTION (1.E+7)

0	11.30
5	9.33
10	6.49
15	5.12
20	6.11
25	7.90
30	8.63
35	8.03
40	7.04
45	6.29
50	5.63

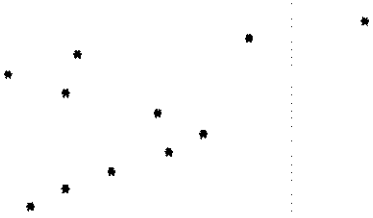

R.M.S. FLUCTUATION

0	0.00
5	.17
10	.22
15	.52
20	.98
25	1.38
30	1.47
35	1.30
40	1.25
45	1.32
50	1.24

Table 6. (Cont.)

y: PHI 55 DIHEDRAL ANGLE 2.00 WAVELENGTH 6943

AVERAGE GAIN FUNCTION (1.E+7)

0	11.24
5	9.58
10	7.06
15	5.59
20	6.10
25	7.56
30	8.37
35	8.01
40	7.06
45	6.15
50	5.35

R.M.S. FLUCTUATION

0	0.00
5	.14
10	.17
15	.32
20	.35
25	.47
30	.87
35	1.15
40	1.19
45	1.18
50	1.17

z: PHI 60 DIHEDRAL ANGLE 2.00 WAVELENGTH 6943

AVERAGE GAIN FUNCTION (1.E+7)

0	11.36
5	10.05
10	7.94
15	6.42
20	6.33
25	7.14
30	7.74
35	7.57
40	6.85
45	6.00
50	5.16

R.M.S. FLUCTUATION

0	0.00
5	.12
10	.26
15	.65
20	1.04
25	1.12
30	.89
35	.87
40	1.07
45	1.13
50	1.09

Table 7. Sample gain-function matrices. The angles θ_1 and θ_2, in microradians, are defined in Figure 8. Only half the matrix is presented since $G(\theta_1, \theta_2) = G(-\theta_1, -\theta_2)$.

a: PHI 0 DIHEDRAL ANGLE 2.00 WAVELENGTH 5300

θ_2	GAIN FUNCTION (1.E+7)										
50	2.90	2.87	2.78	2.66	2.50	2.34	2.18	2.03	1.90	1.78	1.66
45	3.60	3.56	3.43	3.23	2.99	2.73	2.48	2.26	2.07	1.91	1.78
40	4.50	4.44	4.27	3.99	3.65	3.27	2.90	2.56	2.29	2.07	1.90
35	5.52	5.45	5.23	4.89	4.44	3.94	3.43	2.96	2.56	2.26	2.03
30	6.58	6.49	6.24	5.83	5.30	4.69	4.05	3.43	2.90	2.48	2.18
25	7.60	7.50	7.21	6.75	6.15	5.45	4.69	3.94	3.27	2.73	2.34
20	8.56	8.45	8.12	7.60	6.93	6.15	5.30	4.44	3.65	2.99	2.50
15	9.46	9.32	8.93	8.34	7.60	6.75	5.83	4.89	3.99	3.23	2.66
10	10.22	10.05	9.60	8.93	8.12	7.21	6.24	5.23	4.27	3.43	2.78
5	10.75	10.57	10.05	9.32	8.45	7.50	6.49	5.45	4.44	3.56	2.87
0	10.94	10.75	10.22	9.46	8.56	7.60	6.58	5.52	4.50	3.60	2.90
-5	10.75	10.57	10.05	9.32	8.45	7.50	6.49	5.45	4.44	3.56	2.87
-10	10.22	10.05	9.60	8.93	8.12	7.21	6.24	5.23	4.27	3.43	2.78
-15	9.46	9.32	8.93	8.34	7.60	6.75	5.83	4.89	3.99	3.23	2.66
-20	8.56	8.45	8.12	7.60	6.93	6.15	5.30	4.44	3.65	2.99	2.50
-25	7.60	7.50	7.21	6.75	6.15	5.45	4.69	3.94	3.27	2.73	2.34
-30	6.58	6.49	6.24	5.83	5.30	4.69	4.05	3.43	2.90	2.48	2.18
-35	5.52	5.45	5.23	4.89	4.44	3.94	3.43	2.96	2.56	2.26	2.03
-40	4.50	4.44	4.27	3.99	3.65	3.27	2.90	2.56	2.29	2.07	1.90
-45	3.60	3.56	3.43	3.23	2.99	2.73	2.48	2.26	2.07	1.91	1.78
-50	2.90	2.87	2.78	2.66	2.50	2.34	2.18	2.03	1.90	1.78	1.66
	0	5	10	15	20	25	30	35	40	45	50 θ_1

b: PHI 25 DIHEDRAL ANGLE 2.00 WAVELENGTH 5300

θ_2	GAIN FUNCTION (1.E+7)										
50	6.54	6.95	7.18	7.20	7.05	6.79	6.36	5.68	4.74	3.72	2.81
45	7.41	7.95	8.27	8.35	8.23	7.98	7.58	6.92	5.94	4.78	3.62
40	7.77	8.32	8.67	8.84	8.83	8.64	8.24	7.58	6.65	5.52	4.29
35	8.58	8.88	9.04	9.20	9.28	9.15	8.68	7.69	6.90	5.83	4.68
30	9.79	9.62	9.53	9.66	9.82	9.73	9.20	8.20	7.00	5.88	4.82
25	9.76	9.30	9.31	9.69	10.03	10.05	9.60	8.58	7.21	5.93	4.87
20	7.40	7.21	7.81	8.73	9.34	9.52	9.39	8.75	7.53	6.16	4.99
15	4.25	4.68	5.83	7.12	7.84	8.10	8.44	8.55	7.86	6.58	5.28
10	2.93	3.66	4.62	5.63	6.13	6.36	7.16	8.14	8.16	7.12	5.70
5	3.81	4.09	4.15	4.53	4.76	4.99	6.15	7.78	8.37	7.53	6.05
0	4.60	4.08	3.49	3.69	4.04	4.41	5.72	7.56	8.29	7.52	6.07
-5	3.81	2.98	2.73	3.53	4.27	4.73	5.86	7.34	7.78	6.94	5.63
-10	2.93	2.63	3.39	4.82	5.59	5.72	6.25	6.98	6.88	5.95	4.89
-15	4.25	4.77	6.12	7.29	7.33	6.73	6.50	6.42	5.81	4.89	4.13
-20	7.40	8.27	9.17	9.22	8.23	7.05	6.33	5.71	4.82	4.03	3.51
-25	9.76	10.25	10.15	9.16	7.71	6.56	5.81	4.99	4.07	3.43	3.04
-30	9.79	9.62	8.82	7.60	6.52	5.67	5.29	4.46	3.59	3.05	2.67
-35	8.58	7.96	7.08	6.28	5.84	5.56	5.01	4.13	3.32	2.79	2.36
-40	7.77	7.06	6.41	6.02	5.84	5.50	4.76	3.83	3.06	2.53	2.05
-45	7.41	6.81	6.32	6.01	5.67	5.06	4.17	3.30	2.65	2.14	1.69
-50	6.54	6.06	5.62	5.22	4.69	3.97	3.18	2.54	2.05	1.64	1.28
	0	5	10	15	20	25	30	35	40	45	50 θ_1

Table 7. (Cont.)

c: PHI 45 DIHEDRAL ANGLE 2.00 WAVELENGTH 5300

GAIN FUNCTION (1.E+7)

θ_2	0	5	10	15	20	25	30	35	40	45	50
50	7.25	7.87	8.31	8.48	8.24	7.57	6.43	4.98	3.58	2.56	1.92
45	9.69	10.40	10.80	10.74	10.20	9.34	8.16	6.57	4.80	3.39	2.50
40	11.40	12.23	12.87	12.82	11.78	10.31	8.98	7.55	5.82	4.24	3.13
35	10.23	11.54	13.30	14.26	13.37	11.31	9.51	8.11	6.55	5.02	3.83
30	7.56	9.19	11.70	13.61	13.42	11.59	9.83	8.50	7.04	5.55	4.38
25	6.73	7.94	9.58	10.88	10.87	9.96	9.23	8.58	7.35	5.82	4.59
20	6.90	7.45	7.88	7.93	7.46	7.18	7.67	8.14	7.54	6.13	4.75
15	4.87	5.23	5.54	5.54	5.06	4.93	5.98	7.35	7.58	6.57	5.16
10	2.90	2.91	2.88	3.42	3.79	4.05	5.23	6.69	7.47	6.78	5.58
5	4.72	3.56	1.73	2.05	3.50	4.64	5.99	7.34	7.45	6.56	5.66
0	6.71	4.57	1.53	1.73	4.03	5.95	7.40	8.23	7.62	6.35	5.63
-5	4.72	3.00	1.19	2.25	4.78	6.66	7.99	8.66	7.97	6.68	5.90
-10	2.90	2.26	2.24	3.64	5.28	6.45	7.72	8.75	8.56	7.46	6.33
-15	4.87	4.59	4.73	5.21	5.62	6.31	7.76	9.13	9.17	7.96	6.37
-20	6.90	6.37	6.12	6.19	6.41	7.12	8.48	9.52	9.16	7.66	5.94
-25	6.73	6.19	6.52	7.38	7.98	8.32	8.84	9.06	8.22	6.72	5.30
-30	7.56	7.21	8.01	9.02	9.05	8.36	7.94	7.64	6.77	5.56	4.51
-35	10.23	9.73	9.75	9.47	8.31	6.96	6.37	6.11	5.37	4.37	3.49
-40	11.40	10.53	9.50	8.13	6.58	5.52	5.21	4.92	4.11	3.13	2.36
-45	9.69	8.72	7.54	6.26	5.19	4.57	4.23	3.66	2.76	1.94	1.40
-50	7.25	6.50	5.63	4.75	3.97	3.36	2.79	2.14	1.49	1.02	.75

θ_1

d: PHI 60 DIHEDRAL ANGLE 2.00 WAVELENGTH 5300

GAIN FUNCTION (1.E+7)

θ_2	0	5	10	15	20	25	30	35	40	45	50
50	6.30	7.18	7.69	7.77	7.33	6.43	5.28	3.95	2.62	1.59	.99
45	6.63	7.73	8.70	9.22	8.99	8.04	6.66	5.04	3.44	2.16	1.34
40	6.79	8.07	9.59	10.71	10.81	9.83	8.10	6.07	4.20	2.77	1.79
35	7.18	8.64	10.41	11.74	11.96	10.96	9.01	6.66	4.63	3.22	2.23
30	7.69	9.29	10.86	11.73	11.63	10.64	8.86	6.61	4.63	3.35	2.48
25	7.31	8.98	10.27	10.54	9.88	8.89	7.68	6.06	4.38	3.24	2.54
20	5.33	6.91	8.33	8.62	7.72	6.72	6.15	5.44	4.28	3.26	2.66
15	2.98	4.09	5.69	6.63	6.16	5.26	5.15	5.32	4.80	3.86	3.19
10	2.34	2.58	3.63	5.08	5.47	5.01	5.24	6.08	6.12	5.23	4.29
5	3.56	2.94	2.84	4.23	5.46	5.70	6.36	7.65	8.04	7.07	5.75
0	4.44	3.59	2.87	4.13	5.91	6.86	7.98	9.52	9.97	8.83	7.15
-5	3.56	3.15	3.02	4.62	6.72	8.10	9.50	11.00	11.27	9.97	8.14
-10	2.34	2.37	3.22	5.33	7.58	9.14	10.50	11.61	11.54	10.24	8.52
-15	2.98	2.77	3.76	5.83	8.06	9.72	10.84	11.34	10.90	9.72	8.26
-20	5.33	4.41	4.61	6.01	8.02	9.69	10.52	10.48	9.78	8.73	7.44
-25	7.31	5.94	5.42	6.10	7.67	9.09	9.61	9.32	8.59	7.55	6.25
-30	7.69	6.47	5.90	6.22	7.21	8.06	8.29	8.02	7.39	6.31	4.93
-35	7.18	6.28	5.90	6.05	6.51	6.79	6.77	6.60	6.10	5.03	3.70
-40	6.79	5.90	5.39	5.29	5.41	5.40	5.28	5.14	4.70	3.74	2.65
-45	6.63	5.49	4.54	4.11	4.08	4.05	3.93	3.76	3.34	2.57	1.81
-50	6.30	5.06	3.82	3.11	2.90	2.84	2.73	2.57	2.21	1.66	1.17

θ_1

Table 7. (Cont.)

e: PHI 0 DIHEDRAL ANGLE 2.00 WAVELENGTH 6943

GAIN FUNCTION (1.E+7)

θ_2	0	5	10	15	20	25	30	35	40	45	50
50	3.11	3.08	2.99	2.84	2.65	2.43	2.18	1.93	1.68	1.46	1.26
45	3.78	3.74	3.63	3.45	3.21	2.93	2.63	2.31	2.00	1.71	1.46
40	4.52	4.47	4.33	4.11	3.82	3.48	3.11	2.73	2.36	2.00	1.68
35	5.34	5.28	5.10	4.83	4.47	4.07	3.63	3.18	2.73	2.31	1.93
30	6.24	6.16	5.94	5.60	5.16	4.67	4.15	3.63	3.11	2.63	2.18
25	7.19	7.10	6.82	6.40	5.87	5.28	4.67	4.07	3.48	2.93	2.43
20	8.16	8.05	7.71	7.19	6.56	5.87	5.16	4.47	3.82	3.21	2.65
15	9.08	8.94	8.54	7.93	7.19	6.40	5.60	4.83	4.11	3.45	2.84
10	9.84	9.68	9.22	8.54	7.71	6.82	5.94	5.10	4.33	3.63	2.99
5	10.34	10.17	9.68	8.94	8.05	7.10	6.16	5.28	4.47	3.74	3.08
0	10.52	10.34	9.84	9.08	8.16	7.19	6.24	5.34	4.52	3.78	3.11
-5	10.34	10.17	9.68	8.94	8.05	7.10	6.16	5.28	4.47	3.74	3.08
-10	9.84	9.68	9.22	8.54	7.71	6.82	5.94	5.10	4.33	3.63	2.99
-15	9.08	8.94	8.54	7.93	7.19	6.40	5.60	4.83	4.11	3.45	2.84
-20	8.16	8.05	7.71	7.19	6.56	5.87	5.16	4.47	3.82	3.21	2.65
-25	7.19	7.10	6.82	6.40	5.87	5.28	4.67	4.07	3.48	2.93	2.43
-30	6.24	6.16	5.94	5.60	5.16	4.67	4.15	3.63	3.11	2.63	2.18
-35	5.34	5.28	5.10	4.83	4.47	4.07	3.63	3.18	2.73	2.31	1.93
-40	4.52	4.47	4.33	4.11	3.82	3.48	3.11	2.73	2.36	2.00	1.68
-45	3.78	3.74	3.63	3.45	3.21	2.93	2.63	2.31	2.00	1.71	1.46
-50	3.11	3.08	2.99	2.84	2.65	2.43	2.18	1.93	1.68	1.46	1.26
	0	5	10	15	20	25	30	35	40	45	50 θ_1

f: PHI 25 DIHEDRAL ANGLE 2.00 WAVELENGTH 6943

GAIN FUNCTION (1.E+7)

θ_2	0	5	10	15	20	25	30	35	40	45	50
50	4.36	4.48	4.56	4.61	4.64	4.60	4.46	4.18	3.78	3.27	2.72
45	5.77	5.81	5.81	5.82	5.80	5.69	5.45	5.06	4.51	3.83	3.11
40	7.14	7.11	7.13	7.18	7.17	6.99	6.63	6.08	5.37	4.50	3.58
35	7.72	7.72	7.93	8.22	8.37	8.22	7.74	7.04	6.18	5.17	4.08
30	7.12	7.32	7.90	8.60	9.08	9.05	8.51	7.69	6.73	5.67	4.52
25	5.88	6.38	7.33	8.42	9.20	9.32	8.77	7.66	6.88	5.89	4.79
20	5.19	5.95	7.00	8.14	9.00	9.14	8.54	7.57	6.63	5.79	4.86
15	6.07	6.83	7.51	8.20	8.74	8.72	8.00	6.98	6.11	5.47	4.79
10	8.44	8.86	8.72	8.55	8.50	8.17	7.33	6.27	5.50	5.06	4.63
5	10.98	10.81	9.73	8.69	8.10	7.54	6.65	5.63	4.95	4.68	4.44
0	12.07	11.29	9.58	8.13	7.37	6.85	6.06	5.13	4.55	4.38	4.23
-5	10.98	9.84	8.11	6.90	6.49	6.27	5.68	4.87	4.32	4.16	4.01
-10	8.44	7.31	6.15	5.69	5.89	6.04	5.61	4.64	4.26	4.00	3.76
-15	6.07	5.30	4.94	5.30	6.00	6.29	5.83	4.98	4.29	3.88	3.50
-20	5.19	4.88	5.19	6.00	6.75	6.83	6.13	5.12	4.29	3.73	3.21
-25	5.88	5.93	6.49	7.23	7.59	7.20	6.19	5.05	4.15	3.49	2.88
-30	7.12	7.32	7.74	8.03	7.80	6.96	5.77	4.65	3.79	3.13	2.51
-35	7.72	7.86	7.95	7.74	7.06	6.02	4.90	3.98	3.28	2.69	2.12
-40	7.14	7.14	6.94	6.42	5.62	4.69	3.87	3.24	2.74	2.26	1.76
-45	5.77	5.63	5.29	4.75	4.09	3.47	2.99	2.63	2.29	1.90	1.49
-50	4.36	4.14	3.81	3.40	3.00	2.68	2.45	2.24	1.98	1.64	1.29
	0	5	10	15	20	25	30	35	40	45	50 θ_1

Table 7. (Cont.)

g: PHI 45 DIHEDRAL ANGLE 2.00 WAVELENGTH 6943

GAIN FUNCTION (1.E+7)

θ_2	0	5	10	15	20	25	30	35	40	45	50
50	5.31	5.79	6.50	7.15	7.33	6.78	5.68	4.46	3.45	2.72	2.12
45	5.59	6.26	7.36	8.51	9.13	8.75	7.46	5.83	4.40	3.36	2.58
40	6.32	7.02	8.11	9.31	10.04	9.80	8.55	6.82	5.21	3.97	3.03
35	8.28	8.80	9.39	9.97	10.21	9.74	8.53	6.96	5.51	4.33	3.36
30	10.54	10.82	10.88	10.70	10.19	9.20	7.84	6.44	5.28	4.37	3.56
25	10.89	11.13	11.14	10.83	10.06	8.77	7.20	5.81	4.86	4.25	3.68
20	8.67	9.02	9.35	9.56	9.33	8.39	6.90	5.49	4.62	4.21	3.86
15	6.28	6.54	6.76	7.26	7.79	7.69	6.75	5.54	4.77	4.50	4.25
10	6.69	6.39	5.45	5.23	5.98	6.72	6.60	5.90	5.38	5.20	4.89
5	9.50	8.35	5.73	4.16	4.60	5.88	6.56	6.47	6.25	6.11	5.61
0	11.15	9.42	5.89	3.62	3.92	5.53	6.70	7.00	6.96	6.79	6.10
-5	9.50	7.86	4.92	3.31	4.01	5.75	6.91	7.18	7.09	6.86	6.12
-10	6.69	5.64	4.20	3.89	5.01	6.40	7.01	6.86	6.57	6.29	5.67
-15	6.28	5.78	5.47	5.84	6.65	7.12	6.85	6.19	5.71	5.46	5.04
-20	8.67	8.34	8.17	8.16	8.03	7.45	6.46	5.52	4.99	4.77	4.47
-25	10.89	10.45	9.88	9.23	8.39	7.31	6.14	5.19	4.65	4.36	4.02
-30	10.54	10.00	9.33	8.64	7.94	7.09	6.12	5.23	4.57	4.07	3.55
-35	8.28	7.84	7.56	7.49	7.42	7.04	6.24	5.24	4.33	3.61	2.96
-40	6.32	6.06	6.25	6.73	7.06	6.82	5.92	4.72	3.67	2.89	2.28
-45	5.59	5.45	5.75	6.21	6.38	5.90	4.83	3.64	2.71	2.10	1.66
-50	5.31	5.15	5.23	5.30	5.05	4.34	3.35	2.44	1.85	1.50	1.22
	0	5	10	15	20	25	30	35	40	45	50 θ_1

h: PHI 60 DIHEDRAL ANGLE 2.00 WAVELENGTH 6943

GAIN FUNCTION (1.E+7)

θ_2	0	5	10	15	20	25	30	35	40	45	50
50	4.76	5.13	5.56	5.94	6.07	5.79	5.11	4.14	3.09	2.12	1.38
45	6.26	6.66	6.98	7.14	7.01	6.51	5.67	4.60	3.44	2.36	1.51
40	7.59	8.02	8.21	8.09	7.61	6.81	5.79	4.68	3.55	2.49	1.62
35	8.05	8.52	8.72	8.52	7.85	6.80	5.60	4.47	3.46	2.54	1.76
30	7.27	7.79	8.21	8.31	7.81	6.74	5.42	4.23	3.34	2.64	2.00
25	5.75	6.24	6.98	7.62	7.67	6.88	5.55	4.29	3.44	2.91	2.42
20	4.75	5.06	5.83	6.87	7.55	7.28	6.14	4.81	3.90	3.44	3.05
15	5.40	5.30	5.57	6.48	7.53	7.83	7.04	5.75	4.75	4.25	3.87
10	7.67	7.08	6.38	6.57	7.58	8.32	7.99	6.87	5.81	5.21	4.77
5	10.24	9.27	7.61	6.93	7.65	8.65	8.73	7.86	6.84	6.16	5.62
0	11.36	10.33	8.30	7.19	7.70	8.81	9.15	8.51	7.59	6.90	6.27
-5	10.24	9.51	7.90	7.10	7.72	8.84	9.25	8.75	7.94	7.28	6.60
-10	7.67	7.40	6.74	6.74	7.69	8.76	9.08	8.61	7.91	7.29	6.57
-15	5.40	5.46	5.66	6.39	7.54	8.47	8.65	8.20	7.58	6.97	6.19
-20	4.75	4.85	5.34	6.22	7.24	7.92	8.00	7.61	7.05	6.40	5.56
-25	5.75	5.60	5.77	6.22	6.76	7.13	7.16	6.88	6.38	5.69	4.80
-30	7.27	6.79	6.40	6.17	6.14	6.22	6.24	6.05	5.59	4.88	4.01
-35	8.05	7.37	6.60	5.92	5.50	5.37	5.34	5.16	4.71	4.03	3.26
-40	7.59	6.94	6.15	5.40	4.90	4.67	4.53	4.26	3.79	3.18	2.58
-45	6.26	5.77	5.22	4.70	4.33	4.08	3.82	3.43	2.91	2.41	1.97
-50	4.76	4.45	4.16	3.92	3.72	3.51	3.18	2.70	2.18	1.75	1.46
	0	5	10	15	20	25	30	35	40	45	50 θ_1

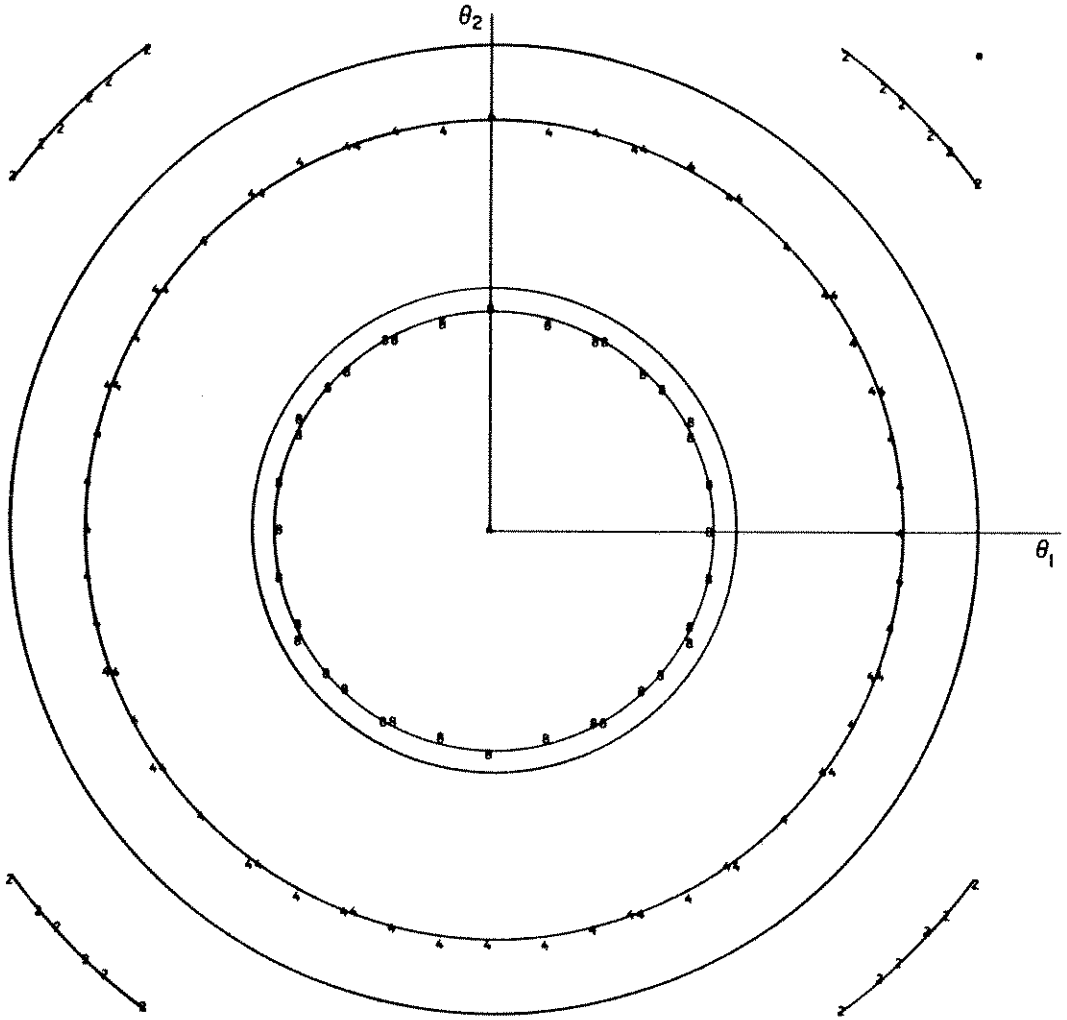

Figure 9. Contour plots of the gain-function matrices given in Table 7. Circles 25 and 50 μrad in radius are shown to mark the minimum and maximum values of the velocity aberration. The numbers are the gain function in units of 10^7. The incidence angle ϕ, the dihedral-angle offset δ, and the wavelength λ are given for each figure. a: $\phi = 0°$, $\delta = 2''.0$, $\lambda = 5300$ Å.

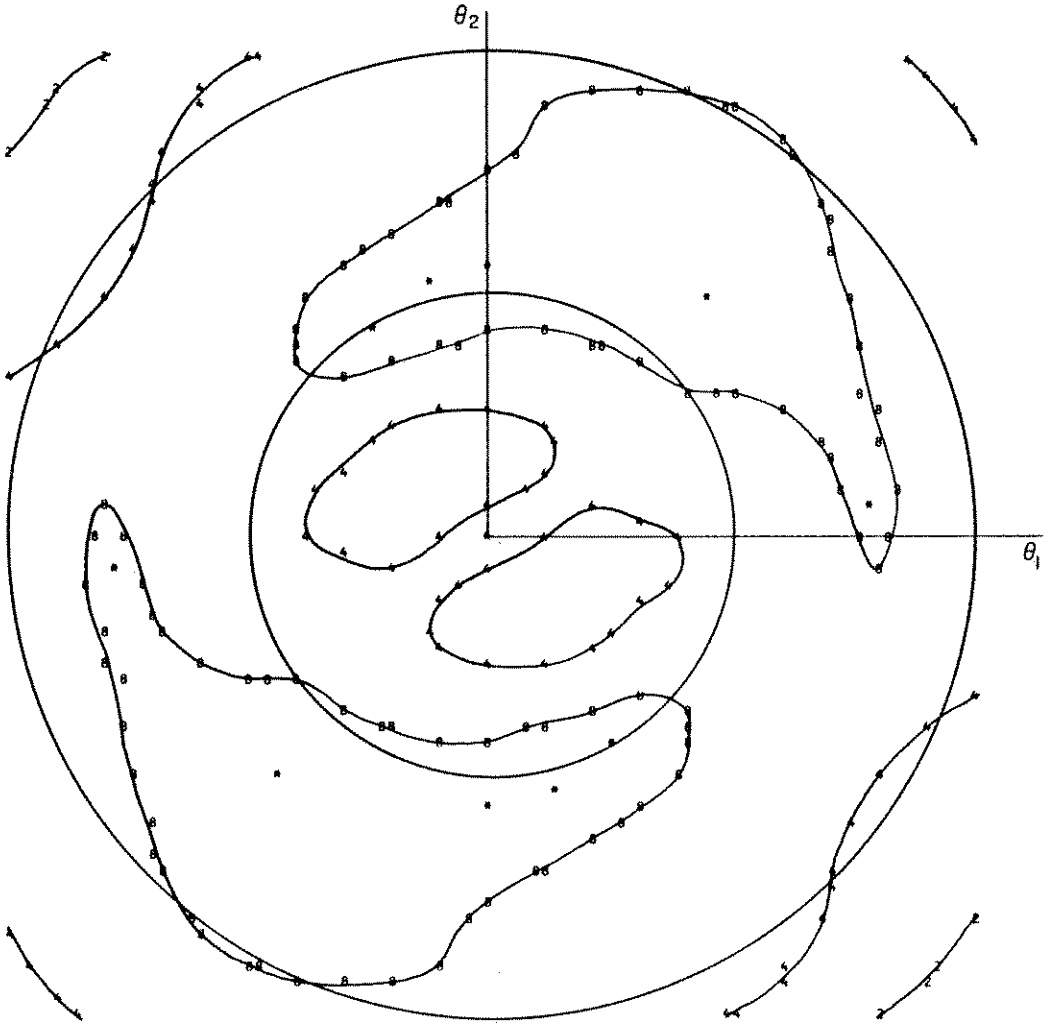

Figure 9b: $\phi = 25°$, $\delta = 2''.0$, $\lambda = 5300$ Å.

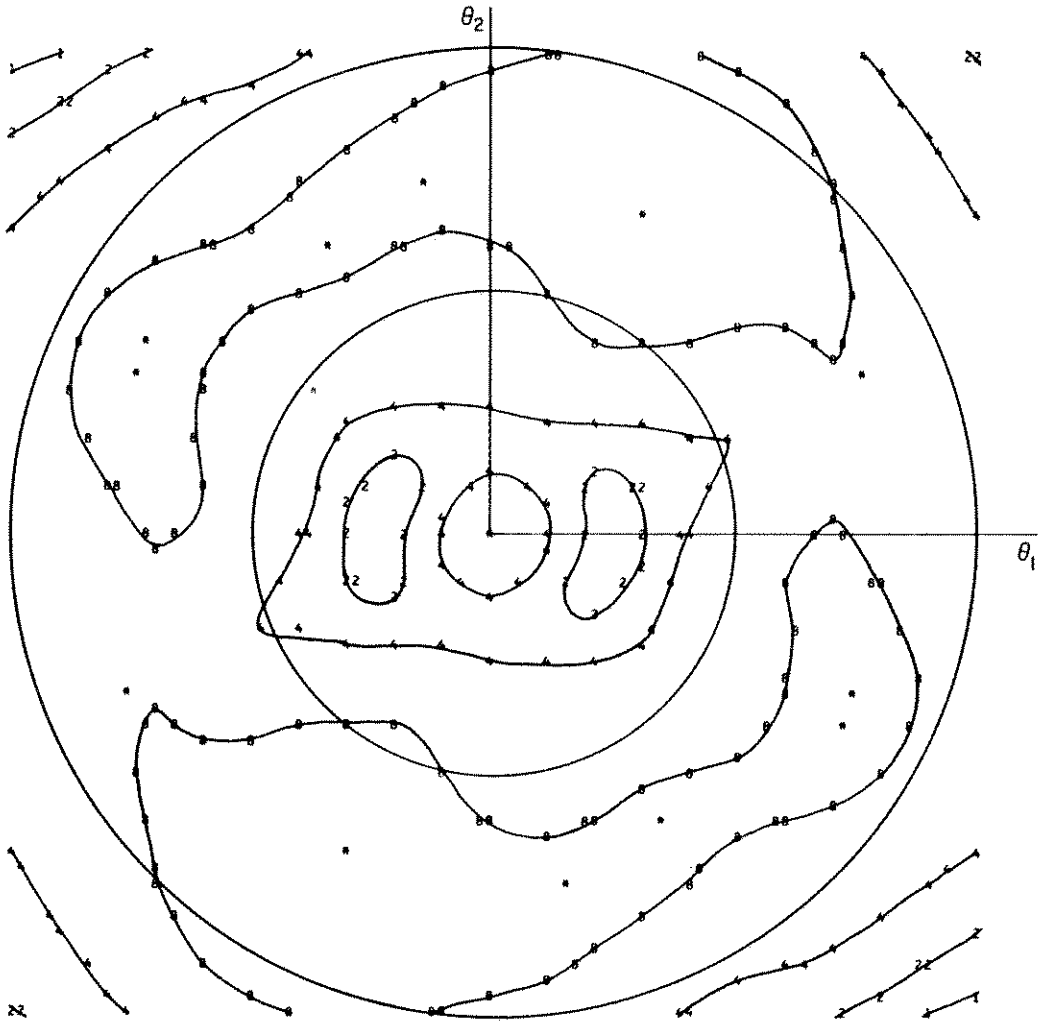

Figure 9c: $\phi = 45°$, $\delta = 2''.0$, $\lambda = 5300$ Å.

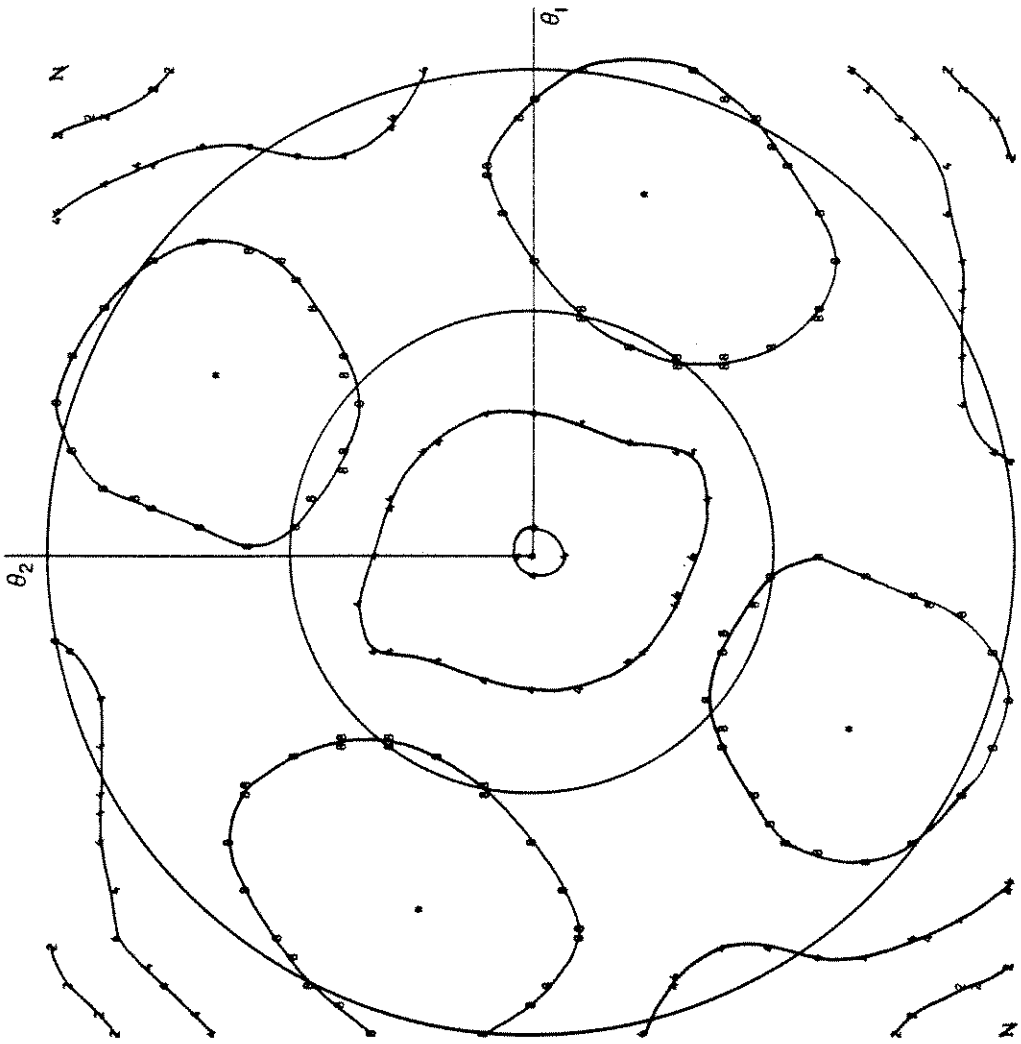

Figure 9d: $\phi = 60°$, $\delta = 2\overset{m}{.}0$, $\lambda = 5300$ Å.

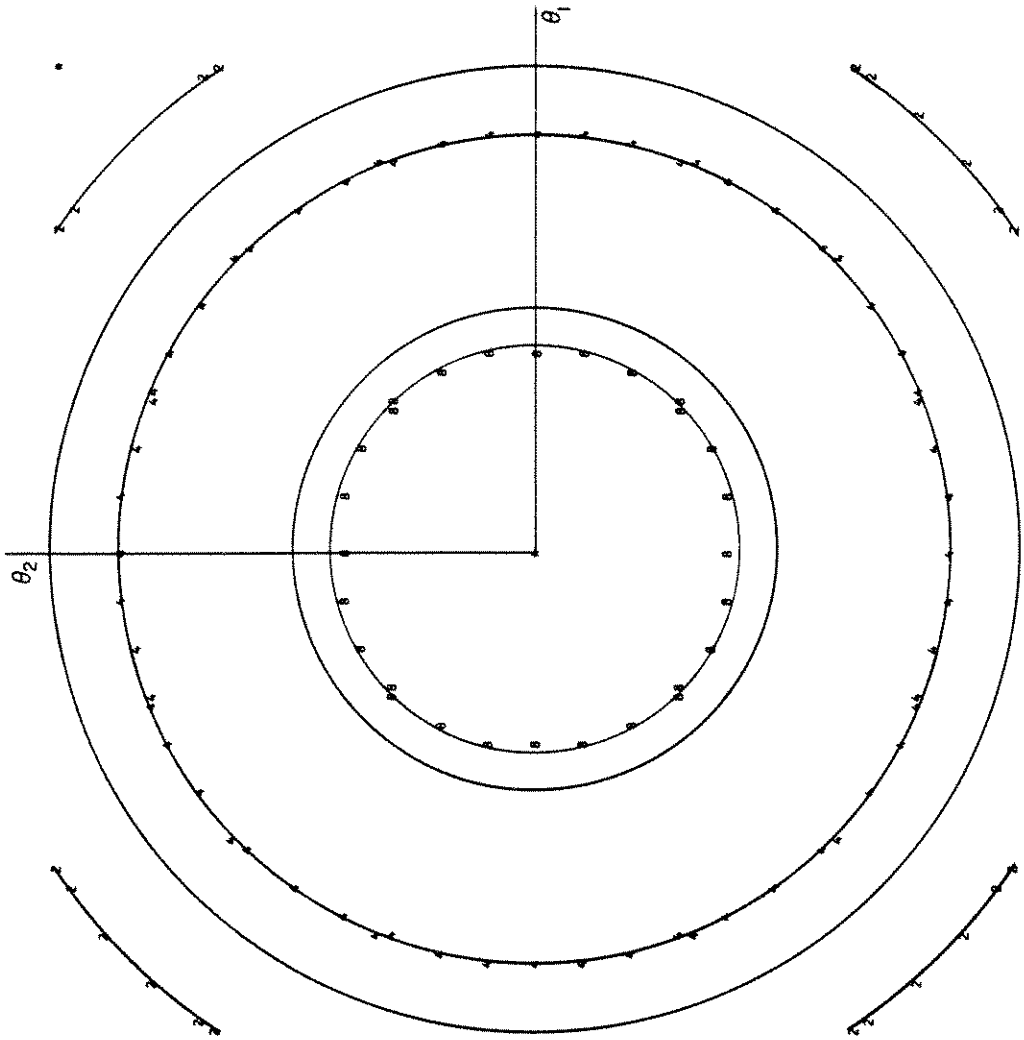

Figure 9e: $\phi = 0°$, $\delta = 2'.0$, $\lambda = 6943$ Å.

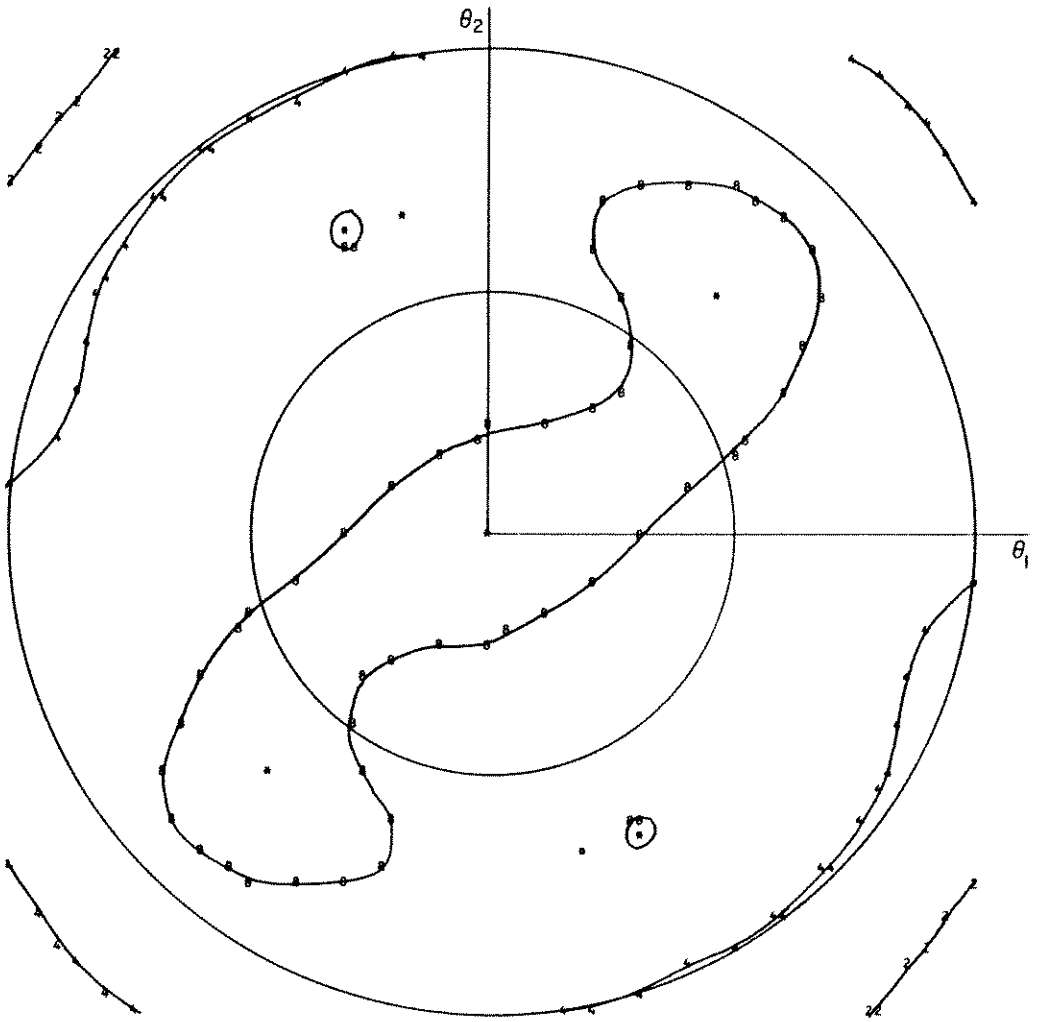

Figure 9f: $\phi = 25°$, $\delta = 2''.0$, $\lambda = 6943$ Å.

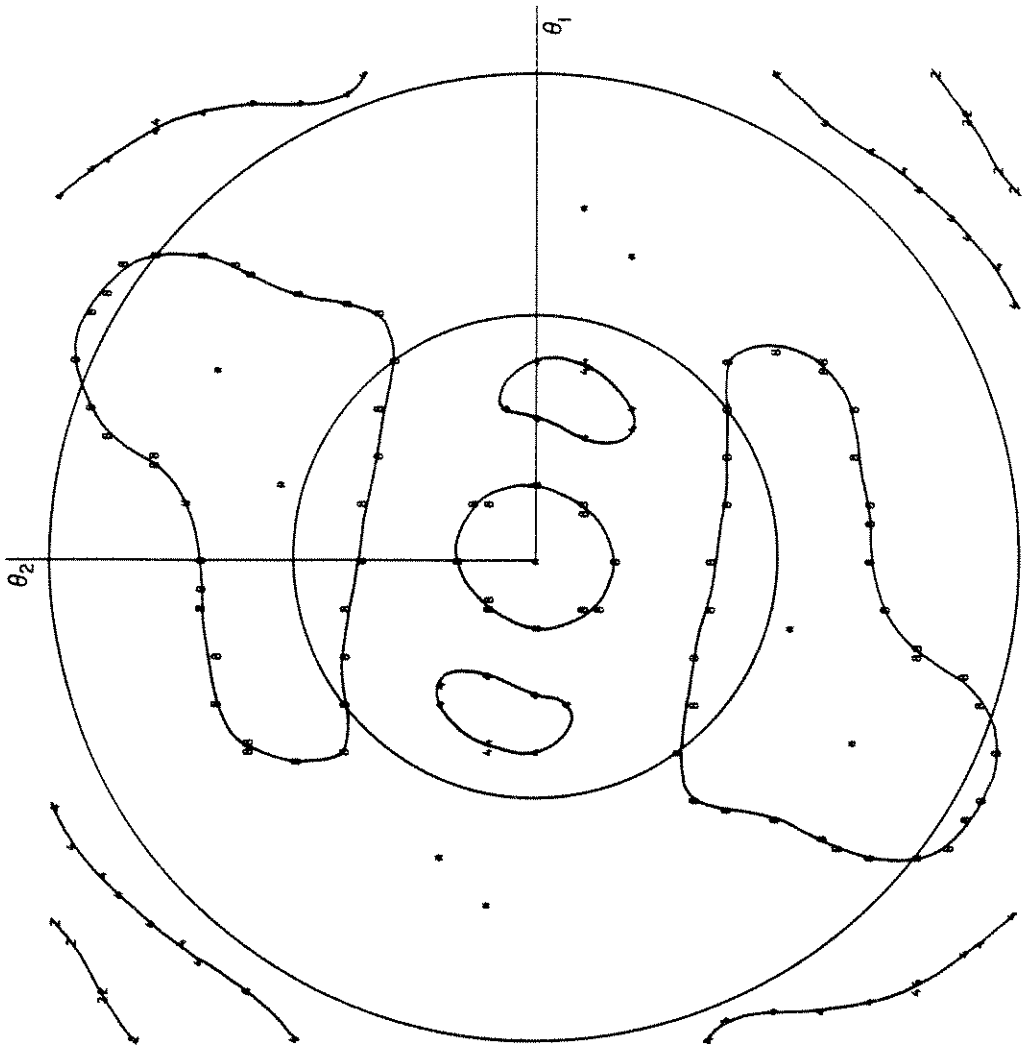

Figure 9g: $\phi = 45°$, $\delta = 2''.0$, $\lambda = 6943$ Å.

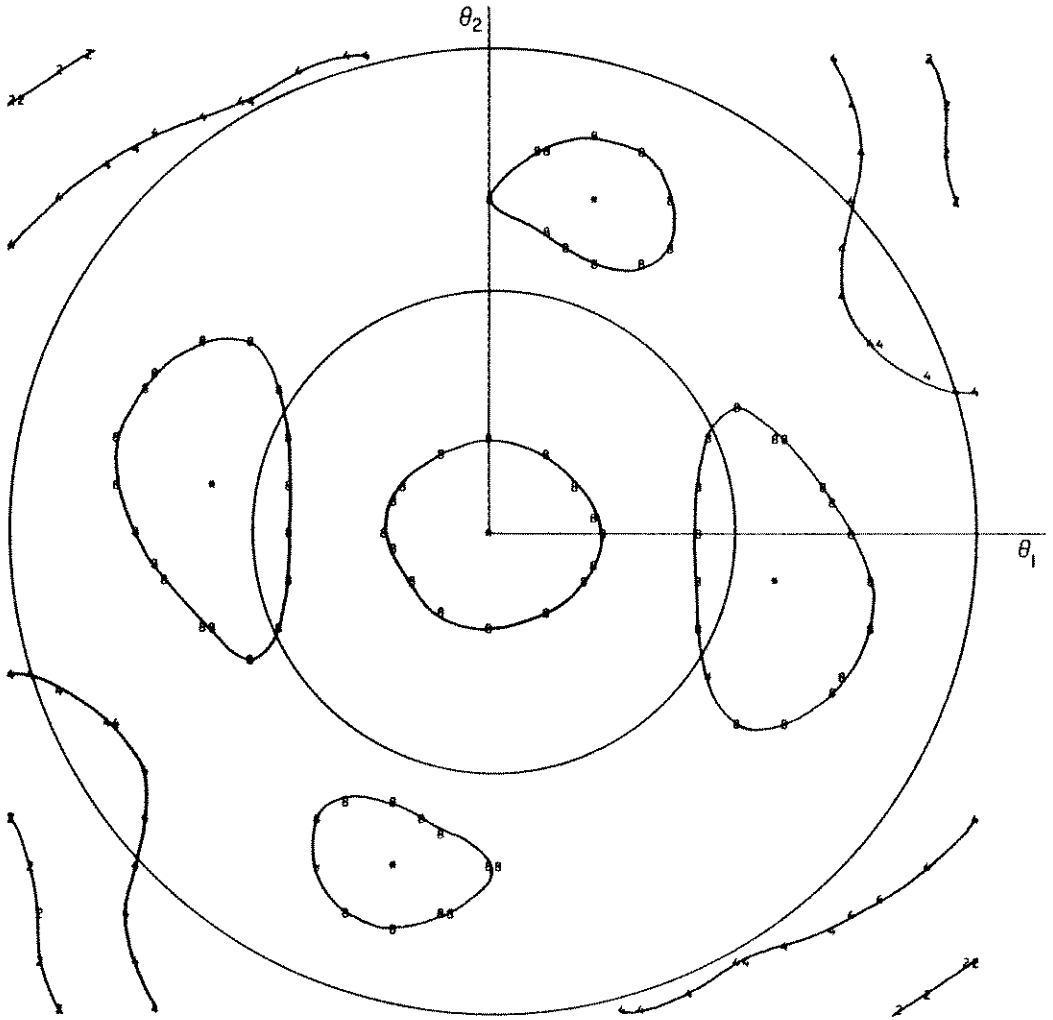

Figure 9h: $\phi = 60°$, $\delta = 2\overset{\circ}{.}0$, $\lambda = 6943$ Å.

8. RANGE CORRECTION

Range corrections corresponding to the reflectivity data from Section 7 are given here; the data have been computed under the same conditions and are presented in the same format. The range correction is the difference between the centroid of the actual return pulse and the centroid of the pulse that would be received from a point reflector at the center of gravity of the satellite. In addition to the data on the centroid of the return, some information is presented on the half-maximum and half-area points of the return signal.

The data in this section have been computed for the incoherent case; the effect of coherent interference is discussed in Section 9. Note that the half-maximum and half-area data are not necessarily the average of the coherent cases.

Tables 8 and 9 were computed from the reflectivity curves of Figure 7. Table 8 gives the centroid of the total reflected signal, a quantity that can be measured only in the laboratory, where it is possible to collect the total reflected energy. Table 9 shows the average range correction in the annulus determined by the velocity aberration; the curves for the two wavelengths 5300 and 6943 Å are nearly identical, the maximum difference being about 1 mm. The difference in the curves between Table 8 and Table 9 is larger, with a maximum difference of about 1 cm. The range correction is plotted against the incidence angle ϕ out to the largest angle at which the array is reflective. Only angles up to about 60° can actually be observed, as the satellite is gravity stabilized. The computer graph to the right of each page is plotted with the incidence angle increasing down the page and the range correction increasing to the right at a scale of 1 cm per horizontal print position. The horizontal origin of the graph has been displaced on each page to try to keep the points from going off scale.

The difference between the range correction for a half-maximum detection system and the range correction for a centroid detection system is shown in Table 10. The correction from this table, added to that from Table 9, yields the total range correction for this type of pulse detection. The largest values in the table are for the

shortest transmitted pulses. In Table 11, the difference between the range correction for a half-area detection system and that for a centroid detection system is given. The difference is largest for a 0.2-nsec pulse and is zero to within the accuracy of the computation for a 20-nsec pulse.

Table 12 shows how the range correction varies with velocity aberration. The format is the same as that of Table 6 for the gain function. The computer graphs on the right are plotted at a scale of 1 cm per horizontal print position. The horizontal origin of the range correction has been adjusted to keep the maximum in the same position on each page, while that for the rms fluctuation has not been adjusted. For $\phi = 0°$, the range correction is constant throughout the whole far-field pattern. At other incidence angles, such as $\phi = 45°$, variations with velocity aberration are larger. Fortunately, the largest variations occur around 10 μrad, which is not an observable value of velocity aberration. The variations in the 25- to 50-μrad range are under 2 cm.

Some of the range-correction matrices from which the data of Table 12 were computed are given in Table 13, where the format is the same as that of the gain matrices (Table 7). The angles θ_1 and θ_2 are defined in Figure 8. The average range correction in the 25- to 50-μrad annulus obtained from these matrices agrees with the range corrections of Table 9, which were computed with the reflectivity curve of Figure 7 to within 1 mm for $\lambda = 6943$ Å and 1.5 mm for $\lambda = 5300$ Å.

Figure 11 consists of 1-cm-interval contour plots of the range-correction matrices in Table 13. No plots are given for $\phi = 0°$, since the range correction is constant for this case. For other values of ϕ, the range correction is asymmetric from left to right, just as the gain function was. As discussed in Section 7, the asymmetry is due to the method of orienting the cube corners.

Table 8. Centroid range correction for total reflected energy vs. incidence angle. (This quantity can be observed only under laboratory conditions, where it is possible to collect all the reflected energy.)

PHI (DEG)	RANGE CORRECTION (METERS)
0.0	1.3043
1.0	1.3046
2.0	1.3057
3.0	1.3074
4.0	1.3098
5.0	1.3126
6.0	1.3160
7.0	1.3198
8.0	1.3238
9.0	1.3281
10.0	1.3324
11.0	1.3368
12.0	1.3410
13.0	1.3450
14.0	1.3489
15.0	1.3524
16.0	1.3557
17.0	1.3586
18.0	1.3612
19.0	1.3629
20.0	1.3639
21.0	1.3645
22.0	1.3646
23.0	1.3643
24.0	1.3637
25.0	1.3627
26.0	1.3614
27.0	1.3597
28.0	1.3576
29.0	1.3550
30.0	1.3520
31.0	1.3486
32.0	1.3448
33.0	1.3405
34.0	1.3359
35.0	1.3308
36.0	1.3253
37.0	1.3194
38.0	1.3131
39.0	1.3064
40.0	1.2993
41.0	1.2917
42.0	1.2837
43.0	1.2752
44.0	1.2663
45.0	1.2569
46.0	1.2471
47.0	1.2369
48.0	1.2262
49.0	1.2152
50.0	1.2038
51.0	1.1920
52.0	1.1799
53.0	1.1675
54.0	1.1547
55.0	1.1416

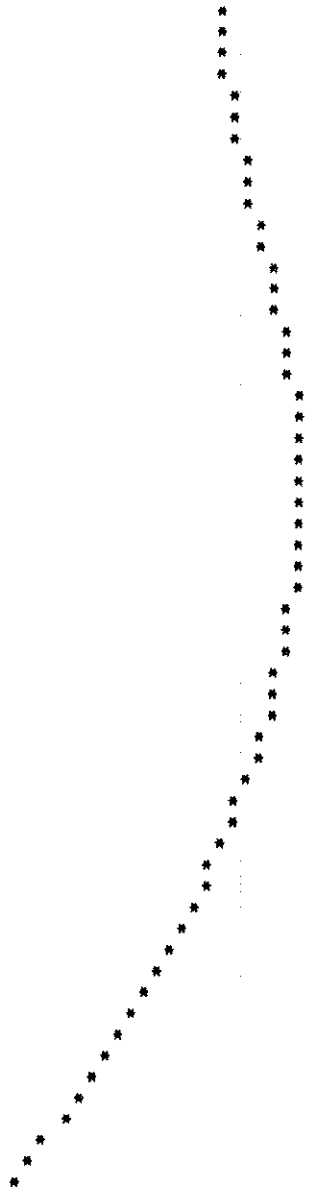

Table 8. (Cont.)

PHI(DEG)	RANGE CORRECTION (METERS)
56.0	1.1281
57.0	1.1143
58.0	1.1002
59.0	1.0857
60.0	1.0710
61.0	1.0560
62.0	1.0407
63.0	1.0252
64.0	1.0094
65.0	.9933
66.0	.9771
67.0	.9606
68.0	.9438
69.0	.9266
70.0	.9091
71.0	.8913
72.0	.8732
73.0	.8548
74.0	.8361
75.0	.8170
76.0	.7977
77.0	.7781
78.0	.7583
79.0	.7382
80.0	.7178
81.0	.6973
82.0	.6765
83.0	.6555
84.0	.6343
85.0	.6130
86.0	.5916
87.0	.5700
88.0	.5484
89.0	.5268
90.0	.5053
91.0	.4839
92.0	.4629
93.0	.4424
94.0	.4216
95.0	.4002
96.0	.3788
97.0	.3568
98.0	.3343
99.0	.3122
100.0	.2892
101.0	.2651
102.0	.2415
103.0	.2187
104.0	.1952
105.0	.1694
106.0	.1430
107.0	.1185
108.0	.0984
109.0	.0840
110.0	.0740
111.0	.0491

Table 9. Average centroid range correction in the 25- to 50-μrad annulus of the far-field pattern vs. incidence angle. a: $\lambda = 5300$ Å.

PHI (DEG)	RANGE CORRECTION (METERS)
0.0	1.3041
1.0	1.3045
2.0	1.3056
3.0	1.3074
4.0	1.3099
5.0	1.3131
6.0	1.3173
7.0	1.3221
8.0	1.3271
9.0	1.3322
10.0	1.3374
11.0	1.3426
12.0	1.3474
13.0	1.3519
14.0	1.3560
15.0	1.3598
16.0	1.3629
17.0	1.3655
18.0	1.3675
19.0	1.3690
20.0	1.3700
21.0	1.3706
22.0	1.3710
23.0	1.3711
24.0	1.3708
25.0	1.3700
26.0	1.3688
27.0	1.3672
28.0	1.3653
29.0	1.3630
30.0	1.3603
31.0	1.3571
32.0	1.3535
33.0	1.3495
34.0	1.3451
35.0	1.3401
36.0	1.3347
37.0	1.3289
38.0	1.3227
39.0	1.3162
40.0	1.3092
41.0	1.3016
42.0	1.2936
43.0	1.2851
44.0	1.2762
45.0	1.2669
46.0	1.2571
47.0	1.2468
48.0	1.2361
49.0	1.2249
50.0	1.2134
51.0	1.2014
52.0	1.1891
53.0	1.1764
54.0	1.1633
55.0	1.1499

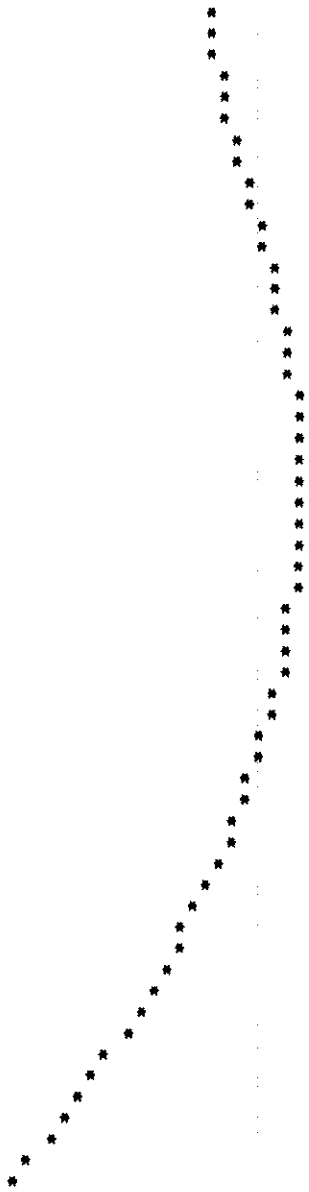

Table 9a. (Cont.)

PHI(DEG)	RANGE CORRECTION (METERS)
56.0	1.1362
57.0	1.1221
58.0	1.1077
59.0	1.0931
60.0	1.0782
61.0	1.0631
62.0	1.0477
63.0	1.0322
64.0	1.0164
65.0	1.0004
66.0	.9841
67.0	.9677
68.0	.9509
69.0	.9338
70.0	.9164
71.0	.8985
72.0	.8801
73.0	.8614
74.0	.8424
75.0	.8230
76.0	.8034
77.0	.7833
78.0	.7629
79.0	.7421
80.0	.7213
81.0	.7005
82.0	.6796
83.0	.6585
84.0	.6370
85.0	.6155
86.0	.5943
87.0	.5731
88.0	.5518
89.0	.5306
90.0	.5090
91.0	.4876
92.0	.4661
93.0	.4444
94.0	.4229
95.0	.4008
96.0	.3790
97.0	.3571
98.0	.3338
99.0	.3110
100.0	.2869
101.0	.2636
102.0	.2407
103.0	.2170
104.0	.1943
105.0	.1688
106.0	.1440
107.0	.1191
108.0	.0944
109.0	.0704

Table 9b: $\lambda = 6943$ Å.

PHI (DEG)	RANGE CORRECTION (METERS)
0.0	1.3043
1.0	1.3047
2.0	1.3059
3.0	1.3080
4.0	1.3108
5.0	1.3145
6.0	1.3186
7.0	1.3231
8.0	1.3279
9.0	1.3328
10.0	1.3380
11.0	1.3431
12.0	1.3478
13.0	1.3523
14.0	1.3563
15.0	1.3599
16.0	1.3630
17.0	1.3656
18.0	1.3676
19.0	1.3691
20.0	1.3701
21.0	1.3707
22.0	1.3713
23.0	1.3716
24.0	1.3715
25.0	1.3709
26.0	1.3699
27.0	1.3684
28.0	1.3666
29.0	1.3643
30.0	1.3616
31.0	1.3585
32.0	1.3549
33.0	1.3508
34.0	1.3462
35.0	1.3411
36.0	1.3356
37.0	1.3297
38.0	1.3235
39.0	1.3168
40.0	1.3097
41.0	1.3022
42.0	1.2942
43.0	1.2858
44.0	1.2769
45.0	1.2676
46.0	1.2577
47.0	1.2473
48.0	1.2365
49.0	1.2253
50.0	1.2137
51.0	1.2017
52.0	1.1894
53.0	1.1767
54.0	1.1637
55.0	1.1504

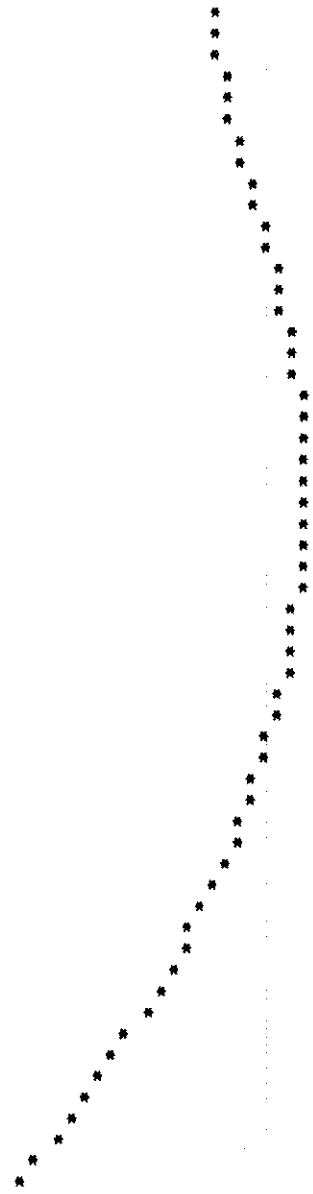

Table 9b. (Cont.)

PHI(DEG)	RANGE CORRECTION (METERS)
56.0	1.1368
57.0	1.1229
58.0	1.1088
59.0	1.0943
60.0	1.0796
61.0	1.0646
62.0	1.0494
63.0	1.0338
64.0	1.0180
65.0	1.0019
66.0	.9854
67.0	.9686
68.0	.9515
69.0	.9340
70.0	.9161
71.0	.8979
72.0	.8792
73.0	.8602
74.0	.8410
75.0	.8215
76.0	.8021
77.0	.7823
78.0	.7623
79.0	.7419
80.0	.7214
81.0	.7011
82.0	.6805
83.0	.6599
84.0	.6390
85.0	.6179
86.0	.5969
87.0	.5758
88.0	.5546
89.0	.5334
90.0	.5119
91.0	.4906
92.0	.4690
93.0	.4472
94.0	.4254
95.0	.4030
96.0	.3811
97.0	.3590
98.0	.3356
99.0	.3125
100.0	.2879
101.0	.2644
102.0	.2411
103.0	.2174
104.0	.1948
105.0	.1694
106.0	.1446
107.0	.1197
108.0	.0949
109.0	.0707

Table 10. Difference between half-maximum and centroid range correction vs. incidence angle. The half-maximum range correction is the sum of Tables 9 and 10.

.2 NANOSECOND PULSE

PHI (DEG)	1/2 MAX. CORRECTION (METERS)
0.0	.0177
2.0	.0198
4.0	.0325
6.0	.0407
8.0	.0443
10.0	.0450
20.0	.0427
30.0	.0395
40.0	.0361
50.0	.0369
60.0	.0393
70.0	.0355
80.0	.0351
90.0	.0292
100.0	.0248

5 NANOSECOND PULSE

PHI (DEG)	1/2 MAX. CORRECTION (METERS)
0.0	.0006
10.0	.0051
20.0	.0059
30.0	.0062
40.0	.0059
50.0	.0063
60.0	.0061
70.0	.0046
80.0	.0035
90.0	.0020
100.0	.0010

20 NANOSECOND PULSE

PHI (DEG)	1/2 MAX. CORRECTION (METERS)
0.0	.0001
10.0	.0012
20.0	.0014
30.0	.0014
40.0	.0014
50.0	.0015
60.0	.0014
70.0	.0011
80.0	.0008
90.0	.0005
100.0	.0002

Table 11. Difference between half-area and centroid range correction vs. incidence angle. The half-area range correction is the sum of Tables 9 and 11.

.2 NANOSECOND PULSE

PHI (DEG)	1/2 AREA CORRECTION (METERS)
0.0	0.0000
2.0	.0003
4.0	.0026
6.0	.0076
8.0	.0118
10.0	.0137
20.0	.0172
30.0	.0182
40.0	.0181
50.0	.0191
60.0	.0180
70.0	.0135
80.0	.0090
90.0	.0035
100.0	0.0000

5 NANOSECOND PULSE

PHI (DEG)	1/2 AREA CORRECTION (METERS)
0.0	0.0000
10.0	.0002
20.0	.0004
30.0	.0005
40.0	.0005
50.0	.0005
60.0	.0005
70.0	.0003
80.0	.0001
90.0	.0001
100.0	0.0000

20 NANOSECOND PULSE

PHI (DEG)	1/2 AREA CORRECTION (METERS)
0.0	0.0000
10.0	-.0001
20.0	-.0001
30.0	-.0001
40.0	-.0001
50.0	-.0001
60.0	-.0001
70.0	-.0001
80.0	-.0001
90.0	-.0001
100.0	-.0001

Table 12. Centroid range correction vs. velocity aberration. The average and rms fluctuations are computed around a circle in the far field whose radius is the velocity aberration listed, in microradians, in the first column.

a: PHI 0 DIHEDRAL ANGLE 2.00 WAVELENGTH 5300

AVERAGE RANGE CORRECTION (METERS)

0	1.3041
5	1.3041
10	1.3041
15	1.3041
20	1.3041
25	1.3041
30	1.3041
35	1.3041
40	1.3041
45	1.3041
50	1.3041

R.M.S. FLUCTUATION

0	0.0000
5	.0000
10	.0000
15	.0000
20	.0000
25	.0000
30	.0000
35	.0000
40	.0000
45	.0000
50	.0000

b: PHI 5 DIHEDRAL ANGLE 2.00 WAVELENGTH 5300

AVERAGE RANGE CORRECTION (METERS)

0	1.3125
5	1.3126
10	1.3128
15	1.3131
20	1.3132
25	1.3131
30	1.3127
35	1.3123
40	1.3123
45	1.3131
50	1.3143

R.M.S. FLUCTUATION

0	0.0000
5	.0002
10	.0010
15	.0021
20	.0033
25	.0044
30	.0050
35	.0052
40	.0051
45	.0046
50	.0042

c: PHI 10 DIHEDRAL ANGLE 2.00 WAVELENGTH 5300

AVERAGE RANGE CORRECTION (METERS)

0	1.3342
5	1.3345
10	1.3350
15	1.3352
20	1.3349
25	1.3346
30	1.3351
35	1.3367
40	1.3386
45	1.3399
50	1.3400

R.M.S. FLUCTUATION

0	0.0000
5	.0007
10	.0030
15	.0059
20	.0084
25	.0097
30	.0101
35	.0098
40	.0094
45	.0091
50	.0093

d: PHI 15 DIHEDRAL ANGLE 2.00 WAVELENGTH 5300

AVERAGE RANGE CORRECTION (METERS)

0	1.3557
5	1.3561
10	1.3565
15	1.3564
20	1.3565
25	1.3573
30	1.3593
35	1.3617
40	1.3630
45	1.3625
50	1.3605

R.M.S. FLUCTUATION

0	0.0000
5	.0014
10	.0054
15	.0092
20	.0107
25	.0107
30	.0107
35	.0108
40	.0108
45	.0112
50	.0122

Table 12. (Cont.)

e: PHI 20 DIHEDRAL ANGLE 2.00 WAVELENGTH 5300

AVERAGE RANGE CORRECTION (METERS)

0	1.3614
5	1.3609
10	1.3606
15	1.3631
20	1.3664
25	1.3685
30	1.3707
35	1.3727
40	1.3730
45	1.3716
50	1.3694

R.M.S. FLUCTUATION

0	0.0000
5	.0020
10	.0081
15	.0117
20	.0114
25	.0109
30	.0117
35	.0126
40	.0128
45	.0129
50	.0130

f: PHI 25 DIHEDRAL ANGLE 2.00 WAVELENGTH 5300

AVERAGE RANGE CORRECTION (METERS)

0	1.3576
5	1.3517
10	1.3464
15	1.3557
20	1.3650
25	1.3687
30	1.3703
35	1.3709
40	1.3712
45	1.3712
50	1.3707

R.M.S. FLUCTUATION

0	0.0000
5	.0025
10	.0091
15	.0107
20	.0100
25	.0099
30	.0118
35	.0137
40	.0134
45	.0114
50	.0099

g: PHI 30 DIHEDRAL ANGLE 2.00 WAVELENGTH 5300

AVERAGE RANGE CORRECTION (METERS)

0	1.3451
5	1.3316
10	1.3154
15	1.3333
20	1.3514
25	1.3573
30	1.3587
35	1.3600
40	1.3619
45	1.3628
50	1.3622

R.M.S. FLUCTUATION

0	0.0000
5	.0031
10	.0068
15	.0051
20	.0074
25	.0080
30	.0101
35	.0114
40	.0102
45	.0083
50	.0073

h: PHI 35 DIHEDRAL ANGLE 2.00 WAVELENGTH 5300

AVERAGE RANGE CORRECTION (METERS)

0	1.3227
5	1.3030
10	1.2722
15	1.2986
20	1.3249
25	1.3328
30	1.3364
35	1.3407
40	1.3437
45	1.3436
50	1.3418

R.M.S. FLUCTUATION

0	0.0000
5	.0033
10	.0130
15	.0039
20	.0067
25	.0071
30	.0072
35	.0070
40	.0064
45	.0063
50	.0064

Table 12. (Cont.)

i: PHI 40 DIHEDRAL ANGLE 2.00 WAVELENGTH 5300

AVERAGE RANGE CORRECTION (METERS)

0	1.2926
5	1.2694
10	1.2275
15	1.2585
20	1.2871
25	1.2962
30	1.3037
35	1.3105
40	1.3132
45	1.3126
50	1.3115

R.M.S. FLUCTUATION

0	0.0000
5	.0032
10	.0172
15	.0049
20	.0076
25	.0072
30	.0059
35	.0050
40	.0051
45	.0055
50	.0055

j: PHI 45 DIHEDRAL ANGLE 2.00 WAVELENGTH 5300

AVERAGE RANGE CORRECTION (METERS)

0	1.2570
5	1.2347
10	1.1811
15	1.2113
20	1.2424
25	1.2509
30	1.2599
35	1.2683
40	1.2708
45	1.2699
50	1.2694

R.M.S. FLUCTUATION

0	0.0000
5	.0031
10	.0138
15	.0076
20	.0082
25	.0082
30	.0066
35	.0051
40	.0052
45	.0056
50	.0060

k: PHI 50 DIHEDRAL ANGLE 2.00 WAVELENGTH 5300

AVERAGE RANGE CORRECTION (METERS)

0	1.2048
5	1.1853
10	1.1417
15	1.1694
20	1.1937
25	1.1992
30	1.2058
35	1.2141
40	1.2173
45	1.2163
50	1.2149

R.M.S. FLUCTUATION

0	0.0000
5	.0026
10	.0076
15	.0053
20	.0082
25	.0086
30	.0083
35	.0066
40	.0057
45	.0060
50	.0066

l: PHI 55 DIHEDRAL ANGLE 2.00 WAVELENGTH 5300

AVERAGE RANGE CORRECTION (METERS)

0	1.1412
5	1.1249
10	1.0985
15	1.1196
20	1.1365
25	1.1398
30	1.1430
35	1.1490
40	1.1530
45	1.1532
50	1.1512

R.M.S. FLUCTUATION

0	0.0000
5	.0028
10	.0065
15	.0069
20	.0082
25	.0088
30	.0095
35	.0086
40	.0068
45	.0068
50	.0080

Table 12. (Cont.)

m: PHI 60 DIHEDRAL ANGLE 2.00 WAVELENGTH 5300

AVERAGE RANGE CORRECTION (METERS)

0	1.0682
5	1.0562
10	1.0425
15	1.0553
20	1.0690
25	1.0728
30	1.0737
35	1.0759
40	1.0785
45	1.0796
50	1.0788

R.M.S. FLUCTUATION

0	0.0000
5	.0028
10	.0070
15	.0088
20	.0082
25	.0084
30	.0094
35	.0097
40	.0088
45	.0084
50	.0101

n: PHI 0 DIHEDRAL ANGLE 2.00 WAVELENGTH 6943

AVERAGE RANGE CORRECTION (METERS)

0	1.3043
5	1.3043
10	1.3043
15	1.3043
20	1.3043
25	1.3043
30	1.3043
35	1.3043
40	1.3043
45	1.3043
50	1.3043

R.M.S. FLUCTUATION

0	0.0000
5	.0000
10	.0000
15	.0000
20	.0000
25	.0000
30	.0000
35	.0000
40	.0000
45	.0000
50	.0000

o: PHI 5 DIHEDRAL ANGLE 2.00 WAVELENGTH 6943

AVERAGE RANGE CORRECTION (METERS)

0	1.3174
5	1.3173
10	1.3171
15	1.3167
20	1.3164
25	1.3159
30	1.3155
35	1.3149
40	1.3141
45	1.3132
50	1.3123

R.M.S. FLUCTUATION

0	0.0000
5	.0000
10	.0002
15	.0004
20	.0009
25	.0015
30	.0022
35	.0030
40	.0037
45	.0041
50	.0043

p: PHI 10 DIHEDRAL ANGLE 2.00 WAVELENGTH 6943

AVERAGE RANGE CORRECTION (METERS)

0	1.3437
5	1.3436
10	1.3434
15	1.3431
20	1.3425
25	1.3417
30	1.3404
35	1.3389
40	1.3376
45	1.3367
50	1.3363

R.M.S. FLUCTUATION

0	0.0000
5	.0001
10	.0006
15	.0015
20	.0028
25	.0044
30	.0059
35	.0071
40	.0076
45	.0076
50	.0076

Table 12. (Cont.)

q: PHI 15 DIHEDRAL ANGLE 2.00 WAVELENGTH 6943

AVERAGE RANGE CORRECTION (METERS)

0	1.3655
5	1.3654
10	1.3652
15	1.3648
20	1.3639
25	1.3625
30	1.3612
35	1.3603
40	1.3600
45	1.3602
50	1.3608

R.M.S. FLUCTUATION

0	0.0000
5	.0002
10	.0011
15	.0027
20	.0052
25	.0075
30	.0088
35	.0087
40	.0081
45	.0077
50	.0077

r: PHI 20 DIHEDRAL ANGLE 2.00 WAVELENGTH 6943

AVERAGE RANGE CORRECTION (METERS)

0	1.3746
5	1.3742
10	1.3733
15	1.3720
20	1.3707
25	1.3702
30	1.3705
35	1.3707
40	1.3709
45	1.3713
50	1.3715

R.M.S. FLUCTUATION

0	0.0000
5	.0003
10	.0013
15	.0037
20	.0075
25	.0101
30	.0102
35	.0091
40	.0082
45	.0082
50	.0086

s: PHI 25 DIHEDRAL ANGLE 2.00 WAVELENGTH 6943

AVERAGE RANGE CORRECTION (METERS)

0	1.3723
5	1.3709
10	1.3679
15	1.3647
20	1.3647
25	1.3683
30	1.3714
35	1.3724
40	1.3721
45	1.3713
50	1.3701

R.M.S. FLUCTUATION

0	0.0000
5	.0004
10	.0018
15	.0050
20	.0085
25	.0095
30	.0088
35	.0078
40	.0076
45	.0087
50	.0100

t: PHI 30 DIHEDRAL ANGLE 2.00 WAVELENGTH 6943

AVERAGE RANGE CORRECTION (METERS)

0	1.3585
5	1.3556
10	1.3493
15	1.3442
20	1.3485
25	1.3573
30	1.3627
35	1.3640
40	1.3630
45	1.3613
50	1.3600

R.M.S. FLUCTUATION

0	0.0000
5	.0005
10	.0022
15	.0053
20	.0067
25	.0067
30	.0060
35	.0055
40	.0061
45	.0078
50	.0086

Table 12. (Cont.)

u: PHI 35 DIHEDRAL ANGLE 2.00 WAVELENGTH 6943

AVERAGE RANGE CORRECTION (METERS)

0	1.3335
5	1.3287
10	1.3185
15	1.3129
20	1.3233
25	1.3362
30	1.3423
35	1.3432
40	1.3421
45	1.3414
50	1.3417

R.M.S. FLUCTUATION

0	0.0000
5	.0007
10	.0023
15	.0039
20	.0026
25	.0040
30	.0045
35	.0043
40	.0049
45	.0059
50	.0062

v: PHI 40 DIHEDRAL ANGLE 2.00 WAVELENGTH 6943

AVERAGE RANGE CORRECTION (METERS)

0	1.2980
5	1.2914
10	1.2777
15	1.2732
20	1.2903
25	1.3051
30	1.3102
35	1.3104
40	1.3101
45	1.3110
50	1.3122

R.M.S. FLUCTUATION

0	0.0000
5	.0008
10	.0027
15	.0073
20	.0025
25	.0032
30	.0047
35	.0048
40	.0054
45	.0065
50	.0066

w: PHI 45 DIHEDRAL ANGLE 2.00 WAVELENGTH 6943

AVERAGE RANGE CORRECTION (METERS)

0	1.2561
5	1.2492
10	1.2342
15	1.2295
20	1.2486
25	1.2633
30	1.2672
35	1.2666
40	1.2666
45	1.2688
50	1.2704

R.M.S. FLUCTUATION

0	0.0000
5	.0007
10	.0014
15	.0063
20	.0031
25	.0044
30	.0060
35	.0064
40	.0072
45	.0080
50	.0078

x: PHI 50 DIHEDRAL ANGLE 2.00 WAVELENGTH 6943

AVERAGE RANGE CORRECTION (METERS)

0	1.2042
5	1.1986
10	1.1867
15	1.1834
20	1.1992
25	1.2115
30	1.2144
35	1.2130
40	1.2120
45	1.2137
50	1.2160

R.M.S. FLUCTUATION

0	0.0000
5	.0007
10	.0013
15	.0029
20	.0039
25	.0056
30	.0065
35	.0071
40	.0080
45	.0088
50	.0089

Table 12. (Cont.)

y: PHI 55 DIHEDRAL ANGLE 2.00 WAVELENGTH 6943

AVERAGE RANGE CORRECTION (METERS)

0	1.1451	*
5	1.1411	*
10	1.1330	*
15	1.1296	*
20	1.1393	*
25	1.1490	*
30	1.1522	*
35	1.1510	*
40	1.1489	*
45	1.1485	*
50	1.1498	*

R.M.S. FLUCTUATION

0	0.0000	*
5	.0008	*
10	.0025	*
15	.0051	*
20	.0063	*
25	.0063	*
30	.0064	*
35	.0071	*
40	.0085	*
45	.0099	*
50	.0104	*

z: PHI 60 DIHEDRAL ANGLE 2.00 WAVELENGTH 6943

AVERAGE RANGE CORRECTION (METERS)

0	1.0785	*
5	1.0759	*
10	1.0702	*
15	1.0659	*
20	1.0692	*
25	1.0764	*
30	1.0807	*
35	1.0811	*
40	1.0793	*
45	1.0773	*
50	1.0764	*

R.M.S. FLUCTUATION

0	0.0000	*
5	.0007	*
10	.0028	*
15	.0063	*
20	.0086	*
25	.0077	*
30	.0066	*
35	.0069	*
40	.0084	*
45	.0102	*
50	.0116	*

Table 13. Sample centroid range-correction matrices. The angles θ_1 and θ_2, in microradians, are defined in Figure 8. Only half the matrix is presented since the value for (θ_1, θ_2) equals that for $(-\theta_1, -\theta_2)$.

a: PHI 0 DIHEDRAL ANGLE 2.00 WAVELENGTH 5300

θ_2	RANGE CORRECTION (METERS)										
50	1.304	1.304	1.304	1.304	1.304	1.304	1.304	1.304	1.304	1.304	1.304
45	1.304	1.304	1.304	1.304	1.304	1.304	1.304	1.304	1.304	1.304	1.304
40	1.304	1.304	1.304	1.304	1.304	1.304	1.304	1.304	1.304	1.304	1.304
35	1.304	1.304	1.304	1.304	1.304	1.304	1.304	1.304	1.304	1.304	1.304
30	1.304	1.304	1.304	1.304	1.304	1.304	1.304	1.304	1.304	1.304	1.304
25	1.304	1.304	1.304	1.304	1.304	1.304	1.304	1.304	1.304	1.304	1.304
20	1.304	1.304	1.304	1.304	1.304	1.304	1.304	1.304	1.304	1.304	1.304
15	1.304	1.304	1.304	1.304	1.304	1.304	1.304	1.304	1.304	1.304	1.304
10	1.304	1.304	1.304	1.304	1.304	1.304	1.304	1.304	1.304	1.304	1.304
5	1.304	1.304	1.304	1.304	1.304	1.304	1.304	1.304	1.304	1.304	1.304
0	1.304	1.304	1.304	1.304	1.304	1.304	1.304	1.304	1.304	1.304	1.304
-5	1.304	1.304	1.304	1.304	1.304	1.304	1.304	1.304	1.304	1.304	1.304
-10	1.304	1.304	1.304	1.304	1.304	1.304	1.304	1.304	1.304	1.304	1.304
-15	1.304	1.304	1.304	1.304	1.304	1.304	1.304	1.304	1.304	1.304	1.304
-20	1.304	1.304	1.304	1.304	1.304	1.304	1.304	1.304	1.304	1.304	1.304
-25	1.304	1.304	1.304	1.304	1.304	1.304	1.304	1.304	1.304	1.304	1.304
-30	1.304	1.304	1.304	1.304	1.304	1.304	1.304	1.304	1.304	1.304	1.304
-35	1.304	1.304	1.304	1.304	1.304	1.304	1.304	1.304	1.304	1.304	1.304
-40	1.304	1.304	1.304	1.304	1.304	1.304	1.304	1.304	1.304	1.304	1.304
-45	1.304	1.304	1.304	1.304	1.304	1.304	1.304	1.304	1.304	1.304	1.304
-50	1.304	1.304	1.304	1.304	1.304	1.304	1.304	1.304	1.304	1.304	1.304
	0	5	10	15	20	25	30	35	40	45	50 θ_1

b: PHI 25 DIHEDRAL ANGLE 2.00 WAVELENGTH 5300

θ_2	RANGE CORRECTION (METERS)										
50	1.362	1.362	1.362	1.362	1.363	1.364	1.367	1.368	1.369	1.369	1.368
45	1.360	1.360	1.360	1.361	1.363	1.365	1.368	1.371	1.373	1.373	1.372
40	1.357	1.357	1.358	1.359	1.362	1.366	1.370	1.373	1.376	1.377	1.377
35	1.357	1.355	1.356	1.358	1.362	1.367	1.371	1.375	1.377	1.380	1.381
30	1.357	1.355	1.355	1.358	1.364	1.370	1.374	1.377	1.379	1.382	1.384
25	1.356	1.353	1.355	1.360	1.367	1.373	1.377	1.380	1.382	1.384	1.385
20	1.350	1.349	1.355	1.364	1.371	1.377	1.382	1.385	1.386	1.386	1.386
15	1.337	1.343	1.356	1.368	1.375	1.381	1.386	1.390	1.391	1.390	1.388
10	1.333	1.345	1.359	1.371	1.379	1.384	1.390	1.394	1.395	1.393	1.389
5	1.351	1.355	1.360	1.371	1.379	1.384	1.391	1.396	1.396	1.393	1.389
0	1.358	1.355	1.356	1.368	1.377	1.382	1.389	1.394	1.394	1.390	1.386
-5	1.351	1.343	1.348	1.367	1.376	1.379	1.384	1.389	1.389	1.385	1.380
-10	1.333	1.331	1.352	1.369	1.374	1.375	1.379	1.382	1.381	1.377	1.373
-15	1.337	1.347	1.361	1.369	1.371	1.370	1.373	1.375	1.373	1.369	1.367
-20	1.350	1.357	1.364	1.367	1.367	1.366	1.368	1.369	1.366	1.363	1.362
-25	1.356	1.360	1.363	1.364	1.363	1.363	1.365	1.364	1.361	1.359	1.360
-30	1.357	1.360	1.360	1.359	1.359	1.362	1.364	1.363	1.359	1.358	1.357
-35	1.357	1.357	1.357	1.357	1.360	1.364	1.365	1.362	1.358	1.356	1.353
-40	1.357	1.357	1.358	1.360	1.364	1.367	1.367	1.363	1.358	1.355	1.350
-45	1.360	1.360	1.361	1.364	1.368	1.369	1.367	1.363	1.358	1.355	1.349
-50	1.362	1.363	1.365	1.367	1.369	1.369	1.367	1.363	1.359	1.355	1.350
	0	5	10	15	20	25	30	35	40	45	50 θ_1

Table 13. (Cont.)

c: PHI 45 DIHEDRAL ANGLE 2.00 WAVELENGTH 5300

RANGE CORRECTION (METERS)

θ_2	0	5	10	15	20	25	30	35	40	45	50
50	1.270	1.267	1.266	1.264	1.263	1.262	1.258	1.250	1.239	1.228	1.222
45	1.269	1.267	1.265	1.263	1.262	1.261	1.260	1.255	1.246	1.237	1.231
40	1.268	1.266	1.264	1.262	1.260	1.258	1.258	1.256	1.252	1.246	1.242
35	1.262	1.262	1.264	1.265	1.263	1.260	1.257	1.257	1.256	1.254	1.253
30	1.250	1.254	1.261	1.265	1.266	1.263	1.261	1.261	1.261	1.260	1.260
25	1.240	1.245	1.253	1.259	1.261	1.261	1.264	1.267	1.268	1.266	1.265
20	1.239	1.241	1.244	1.247	1.249	1.254	1.264	1.272	1.274	1.272	1.267
15	1.223	1.225	1.231	1.236	1.238	1.245	1.263	1.274	1.277	1.274	1.269
10	1.192	1.189	1.196	1.223	1.238	1.248	1.264	1.275	1.277	1.274	1.270
5	1.239	1.221	1.162	1.206	1.250	1.262	1.270	1.276	1.276	1.273	1.271
0	1.257	1.242	1.166	1.207	1.260	1.268	1.272	1.275	1.274	1.271	1.272
-5	1.239	1.218	1.139	1.227	1.260	1.265	1.268	1.272	1.272	1.271	1.273
-10	1.192	1.180	1.199	1.242	1.256	1.258	1.264	1.270	1.272	1.272	1.273
-15	1.223	1.226	1.237	1.248	1.253	1.258	1.266	1.273	1.275	1.273	1.271
-20	1.239	1.241	1.246	1.254	1.261	1.267	1.274	1.277	1.276	1.273	1.268
-25	1.240	1.243	1.253	1.266	1.273	1.276	1.277	1.278	1.275	1.270	1.266
-30	1.250	1.255	1.265	1.274	1.277	1.276	1.276	1.275	1.273	1.269	1.266
-35	1.262	1.266	1.271	1.275	1.275	1.273	1.273	1.274	1.273	1.270	1.267
-40	1.268	1.270	1.272	1.273	1.273	1.273	1.276	1.278	1.276	1.271	1.266
-45	1.269	1.271	1.273	1.274	1.276	1.279	1.281	1.280	1.276	1.268	1.262
-50	1.270	1.272	1.275	1.278	1.280	1.282	1.281	1.276	1.268	1.259	1.254
	0	5	10	15	20	25	30	35	40	45	50 θ_1

d: PHI 60 DIHEDRAL ANGLE 2.00 WAVELENGTH 5300

RANGE CORRECTION (METERS)

θ_2	0	5	10	15	20	25	30	35	40	45	50
50	1.074	1.073	1.072	1.072	1.072	1.072	1.072	1.069	1.060	1.046	1.031
45	1.069	1.069	1.071	1.073	1.075	1.075	1.074	1.070	1.063	1.053	1.041
40	1.062	1.065	1.070	1.075	1.078	1.078	1.076	1.072	1.065	1.058	1.051
35	1.059	1.065	1.072	1.076	1.078	1.079	1.077	1.072	1.066	1.060	1.056
30	1.062	1.070	1.075	1.078	1.078	1.077	1.076	1.072	1.065	1.060	1.057
25	1.066	1.074	1.079	1.078	1.075	1.073	1.073	1.071	1.065	1.058	1.056
20	1.062	1.072	1.077	1.077	1.071	1.067	1.068	1.070	1.066	1.060	1.056
15	1.043	1.056	1.067	1.071	1.068	1.063	1.066	1.072	1.072	1.067	1.062
10	1.035	1.031	1.047	1.064	1.068	1.066	1.070	1.078	1.080	1.077	1.071
5	1.059	1.042	1.036	1.061	1.072	1.074	1.079	1.086	1.087	1.083	1.078
0	1.068	1.058	1.046	1.066	1.078	1.082	1.086	1.091	1.091	1.087	1.083
-5	1.059	1.056	1.055	1.073	1.083	1.086	1.090	1.093	1.093	1.090	1.086
-10	1.035	1.040	1.057	1.075	1.083	1.066	1.090	1.092	1.093	1.091	1.088
-15	1.043	1.041	1.057	1.073	1.080	1.084	1.087	1.090	1.091	1.091	1.090
-20	1.062	1.054	1.057	1.068	1.077	1.081	1.084	1.087	1.090	1.091	1.091
-25	1.066	1.058	1.057	1.066	1.075	1.080	1.083	1.086	1.089	1.092	1.092
-30	1.062	1.057	1.060	1.069	1.078	1.083	1.085	1.088	1.090	1.092	1.092
-35	1.059	1.059	1.065	1.075	1.084	1.088	1.090	1.091	1.093	1.094	1.093
-40	1.062	1.065	1.071	1.080	1.088	1.092	1.093	1.095	1.096	1.095	1.094
-45	1.069	1.071	1.075	1.081	1.088	1.092	1.094	1.096	1.097	1.096	1.094
-50	1.074	1.074	1.074	1.078	1.083	1.087	1.090	1.094	1.096	1.096	1.093
	0	5	10	15	20	25	30	35	40	45	50 θ_1

Table 13. (Cont.)

e: PHI 0 DIHEDRAL ANGLE 2.00 WAVELENGTH 6943

RANGE CORRECTION (METERS)

θ_2	0	5	10	15	20	25	30	35	40	45	50
50	1.304	1.304	1.304	1.304	1.304	1.304	1.304	1.304	1.304	1.304	1.304
45	1.304	1.304	1.304	1.304	1.304	1.304	1.304	1.304	1.304	1.304	1.304
40	1.304	1.304	1.304	1.304	1.304	1.304	1.304	1.304	1.304	1.304	1.304
35	1.304	1.304	1.304	1.304	1.304	1.304	1.304	1.304	1.304	1.304	1.304
30	1.304	1.304	1.304	1.304	1.304	1.304	1.304	1.304	1.304	1.304	1.304
25	1.304	1.304	1.304	1.304	1.304	1.304	1.304	1.304	1.304	1.304	1.304
20	1.304	1.304	1.304	1.304	1.304	1.304	1.304	1.304	1.304	1.304	1.304
15	1.304	1.304	1.304	1.304	1.304	1.304	1.304	1.304	1.304	1.304	1.304
10	1.304	1.304	1.304	1.304	1.304	1.304	1.304	1.304	1.304	1.304	1.304
5	1.304	1.304	1.304	1.304	1.304	1.304	1.304	1.304	1.304	1.304	1.304
0	1.304	1.304	1.304	1.304	1.304	1.304	1.304	1.304	1.304	1.304	1.304
-5	1.304	1.304	1.304	1.304	1.304	1.304	1.304	1.304	1.304	1.304	1.304
-10	1.304	1.304	1.304	1.304	1.304	1.304	1.304	1.304	1.304	1.304	1.304
-15	1.304	1.304	1.304	1.304	1.304	1.304	1.304	1.304	1.304	1.304	1.304
-20	1.304	1.304	1.304	1.304	1.304	1.304	1.304	1.304	1.304	1.304	1.304
-25	1.304	1.304	1.304	1.304	1.304	1.304	1.304	1.304	1.304	1.304	1.304
-30	1.304	1.304	1.304	1.304	1.304	1.304	1.304	1.304	1.304	1.304	1.304
-35	1.304	1.304	1.304	1.304	1.304	1.304	1.304	1.304	1.304	1.304	1.304
-40	1.304	1.304	1.304	1.304	1.304	1.304	1.304	1.304	1.304	1.304	1.304
-45	1.304	1.304	1.304	1.304	1.304	1.304	1.304	1.304	1.304	1.304	1.304
-50	1.304	1.304	1.304	1.304	1.304	1.304	1.304	1.304	1.304	1.304	1.304
	0	5	10	15	20	25	30	35	40	45	50 θ_1

f: PHI 25 DIHEDRAL ANGLE 2.00 WAVELENGTH 6943

RANGE CORRECTION (METERS)

θ_2	0	5	10	15	20	25	30	35	40	45	50
50	1.361	1.360	1.359	1.361	1.363	1.365	1.368	1.370	1.370	1.371	1.370
45	1.361	1.360	1.360	1.362	1.364	1.367	1.369	1.371	1.372	1.372	1.370
40	1.361	1.360	1.361	1.364	1.367	1.369	1.371	1.373	1.374	1.373	1.371
35	1.359	1.359	1.361	1.365	1.369	1.372	1.374	1.376	1.376	1.376	1.374
30	1.356	1.357	1.362	1.367	1.372	1.376	1.377	1.378	1.379	1.379	1.377
25	1.351	1.355	1.362	1.370	1.375	1.379	1.380	1.381	1.382	1.382	1.381
20	1.351	1.357	1.365	1.372	1.378	1.381	1.383	1.383	1.384	1.385	1.384
15	1.359	1.363	1.368	1.373	1.379	1.382	1.383	1.364	1.385	1.387	1.387
10	1.367	1.369	1.370	1.373	1.377	1.381	1.382	1.383	1.385	1.387	1.389
5	1.371	1.371	1.370	1.371	1.375	1.379	1.380	1.381	1.383	1.386	1.388
0	1.372	1.371	1.369	1.369	1.372	1.377	1.379	1.379	1.380	1.384	1.386
-5	1.371	1.369	1.366	1.366	1.371	1.376	1.378	1.377	1.377	1.380	1.382
-10	1.367	1.364	1.361	1.364	1.371	1.377	1.377	1.376	1.375	1.376	1.377
-15	1.359	1.355	1.355	1.363	1.372	1.377	1.377	1.374	1.372	1.372	1.371
-20	1.351	1.349	1.355	1.365	1.372	1.375	1.374	1.371	1.368	1.367	1.365
-25	1.351	1.353	1.359	1.367	1.371	1.373	1.371	1.368	1.365	1.363	1.359
-30	1.356	1.358	1.363	1.367	1.370	1.370	1.367	1.364	1.362	1.359	1.355
-35	1.359	1.362	1.365	1.367	1.368	1.366	1.364	1.361	1.359	1.357	1.352
-40	1.361	1.363	1.365	1.366	1.365	1.363	1.361	1.360	1.359	1.357	1.352
-45	1.361	1.363	1.364	1.364	1.362	1.361	1.360	1.361	1.361	1.358	1.353
-50	1.361	1.362	1.362	1.362	1.361	1.361	1.362	1.364	1.364	1.361	1.355
	0	5	10	15	20	25	30	35	40	45	50 θ_1

Table 13. (Cont.)

g: PHI 45 DIHEDRAL ANGLE 2.00 WAVELENGTH 6943

RANGE CORRECTION (METERS)

θ_2	0	5	10	15	20	25	30	35	40	45	50
50	1.266	1.266	1.267	1.269	1.270	1.268	1.263	1.257	1.250	1.243	1.237
45	1.263	1.264	1.267	1.271	1.273	1.272	1.269	1.262	1.254	1.247	1.240
40	1.260	1.261	1.265	1.269	1.272	1.272	1.270	1.264	1.258	1.251	1.244
35	1.261	1.262	1.264	1.266	1.268	1.268	1.266	1.262	1.258	1.253	1.249
30	1.264	1.263	1.263	1.263	1.263	1.262	1.260	1.257	1.255	1.254	1.253
25	1.262	1.262	1.262	1.262	1.261	1.258	1.255	1.251	1.251	1.254	1.257
20	1.253	1.253	1.255	1.258	1.260	1.259	1.256	1.252	1.252	1.257	1.262
15	1.236	1.237	1.241	1.250	1.258	1.262	1.261	1.259	1.260	1.265	1.269
10	1.236	1.233	1.227	1.235	1.253	1.265	1.269	1.269	1.271	1.275	1.277
5	1.251	1.245	1.230	1.223	1.247	1.268	1.276	1.277	1.279	1.281	1.282
0	1.256	1.251	1.233	1.218	1.246	1.271	1.279	1.281	1.282	1.283	1.283
-5	1.251	1.245	1.228	1.220	1.252	1.274	1.279	1.280	1.279	1.280	1.280
-10	1.236	1.231	1.224	1.237	1.262	1.274	1.276	1.275	1.274	1.274	1.275
-15	1.236	1.237	1.243	1.256	1.267	1.272	1.271	1.268	1.267	1.268	1.269
-20	1.253	1.255	1.259	1.264	1.268	1.268	1.266	1.263	1.262	1.265	1.267
-25	1.262	1.263	1.264	1.266	1.267	1.267	1.265	1.264	1.264	1.267	1.267
-30	1.264	1.264	1.265	1.266	1.268	1.270	1.270	1.270	1.270	1.270	1.269
-35	1.261	1.262	1.264	1.269	1.273	1.276	1.277	1.276	1.274	1.271	1.268
-40	1.260	1.262	1.267	1.273	1.279	1.281	1.281	1.278	1.274	1.269	1.264
-45	1.263	1.265	1.271	1.277	1.281	1.282	1.280	1.275	1.270	1.264	1.260
-50	1.266	1.269	1.273	1.276	1.278	1.278	1.275	1.269	1.264	1.261	1.258

θ_1

h: PHI 60 DIHEDRAL ANGLE 2.00 WAVELENGTH 6943

RANGE CORRECTION (METERS)

θ_2	0	5	10	15	20	25	30	35	40	45	50
50	1.059	1.062	1.066	1.074	1.078	1.081	1.081	1.080	1.076	1.068	1.055
45	1.065	1.068	1.073	1.077	1.080	1.081	1.080	1.078	1.074	1.066	1.053
40	1.070	1.074	1.077	1.080	1.081	1.080	1.078	1.075	1.071	1.063	1.050
35	1.073	1.076	1.080	1.082	1.082	1.079	1.075	1.070	1.065	1.059	1.049
30	1.073	1.075	1.079	1.081	1.081	1.077	1.071	1.065	1.060	1.056	1.050
25	1.067	1.069	1.072	1.076	1.078	1.076	1.070	1.063	1.058	1.057	1.055
20	1.059	1.057	1.062	1.069	1.074	1.075	1.072	1.065	1.061	1.061	1.063
15	1.061	1.055	1.055	1.063	1.072	1.076	1.075	1.071	1.067	1.068	1.070
10	1.070	1.064	1.058	1.062	1.071	1.078	1.079	1.076	1.074	1.075	1.077
5	1.077	1.072	1.066	1.065	1.074	1.081	1.083	1.081	1.080	1.081	1.082
0	1.078	1.076	1.071	1.070	1.077	1.084	1.086	1.085	1.084	1.085	1.086
-5	1.077	1.076	1.073	1.074	1.081	1.087	1.089	1.089	1.088	1.089	1.090
-10	1.070	1.072	1.073	1.078	1.085	1.090	1.092	1.091	1.091	1.091	1.091
-15	1.061	1.066	1.072	1.080	1.087	1.092	1.093	1.092	1.092	1.092	1.092
-20	1.059	1.065	1.073	1.081	1.088	1.092	1.093	1.092	1.091	1.091	1.092
-25	1.067	1.069	1.075	1.081	1.087	1.090	1.091	1.090	1.090	1.090	1.090
-30	1.073	1.072	1.075	1.080	1.084	1.088	1.089	1.089	1.089	1.088	1.089
-35	1.073	1.072	1.073	1.076	1.081	1.065	1.088	1.089	1.088	1.087	1.087
-40	1.070	1.068	1.069	1.072	1.078	1.084	1.088	1.090	1.089	1.088	1.087
-45	1.065	1.063	1.064	1.069	1.076	1.084	1.090	1.092	1.092	1.090	1.087
-50	1.059	1.058	1.061	1.067	1.076	1.085	1.092	1.095	1.094	1.092	1.088

θ_1

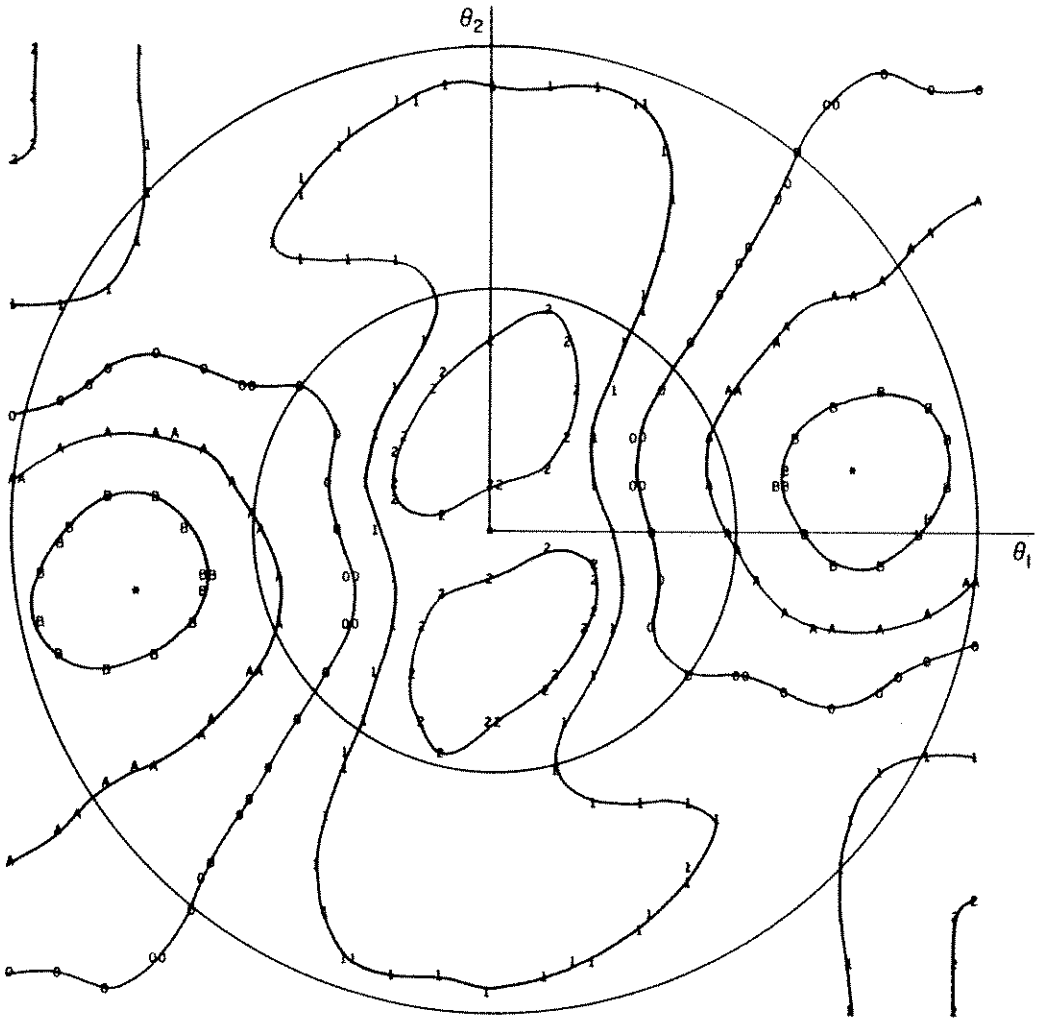

Figure 11. Contour plots of the centroid range-correction matrices given in Table 13. Circles of radius 25 and 50 μrad are shown to mark the minimum and maximum values of the velocity aberration. On the plots, the symbol B indicates that the range correction minus the average range correction in the 25- to 50-μrad annulus is equal to +2 cm; A equals +1 cm; 0 equals 0 cm; and 1 through 8 equal −1 through −8 cm. a: $\phi = 25°$, $\delta = 2\overset{\circ}{.}0$, $\lambda = 5300$ Å.

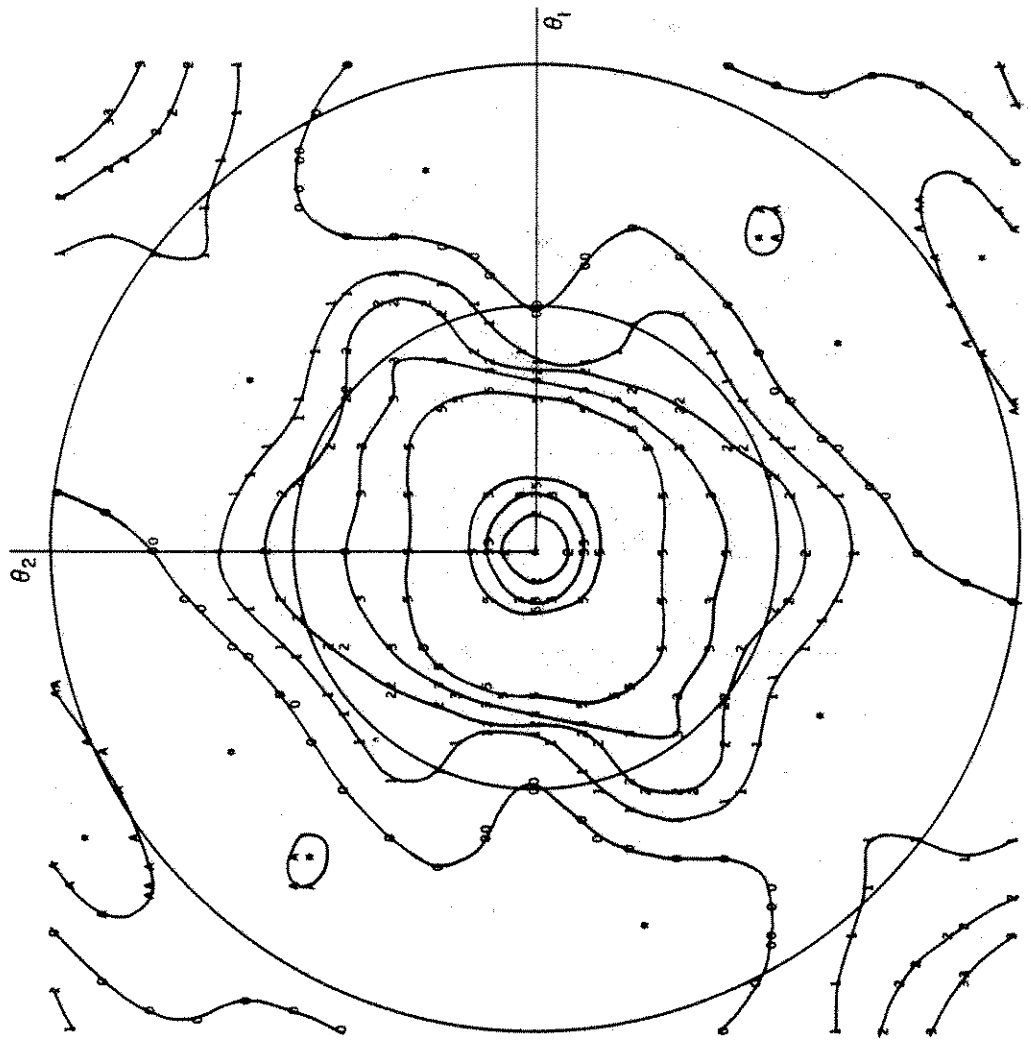

Figure 11b: $\phi = 45°$, $\delta = 2''.0$, $\lambda = 5300$ Å.

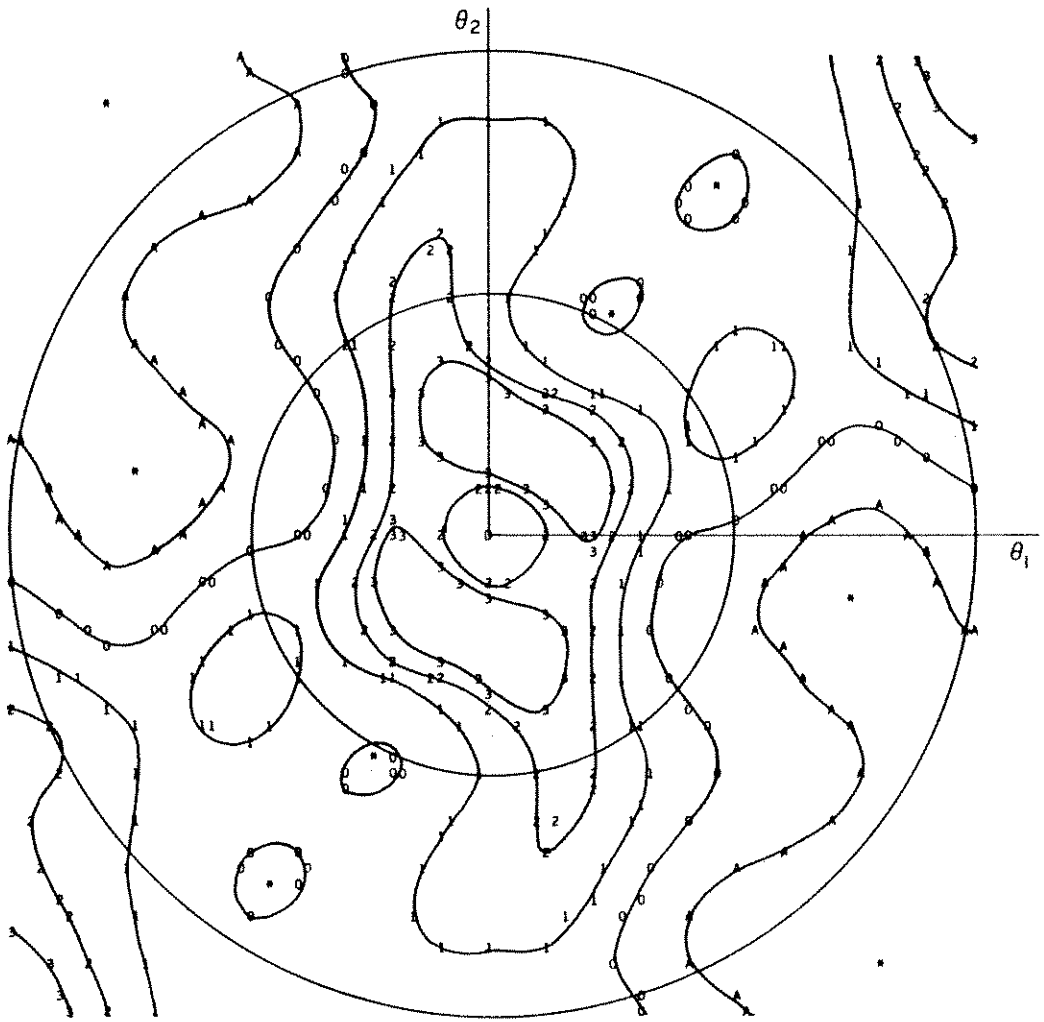

Figure 11c: $\phi = 60°$, $\delta = 2\farcs0$, $\lambda = 5300$ Å.

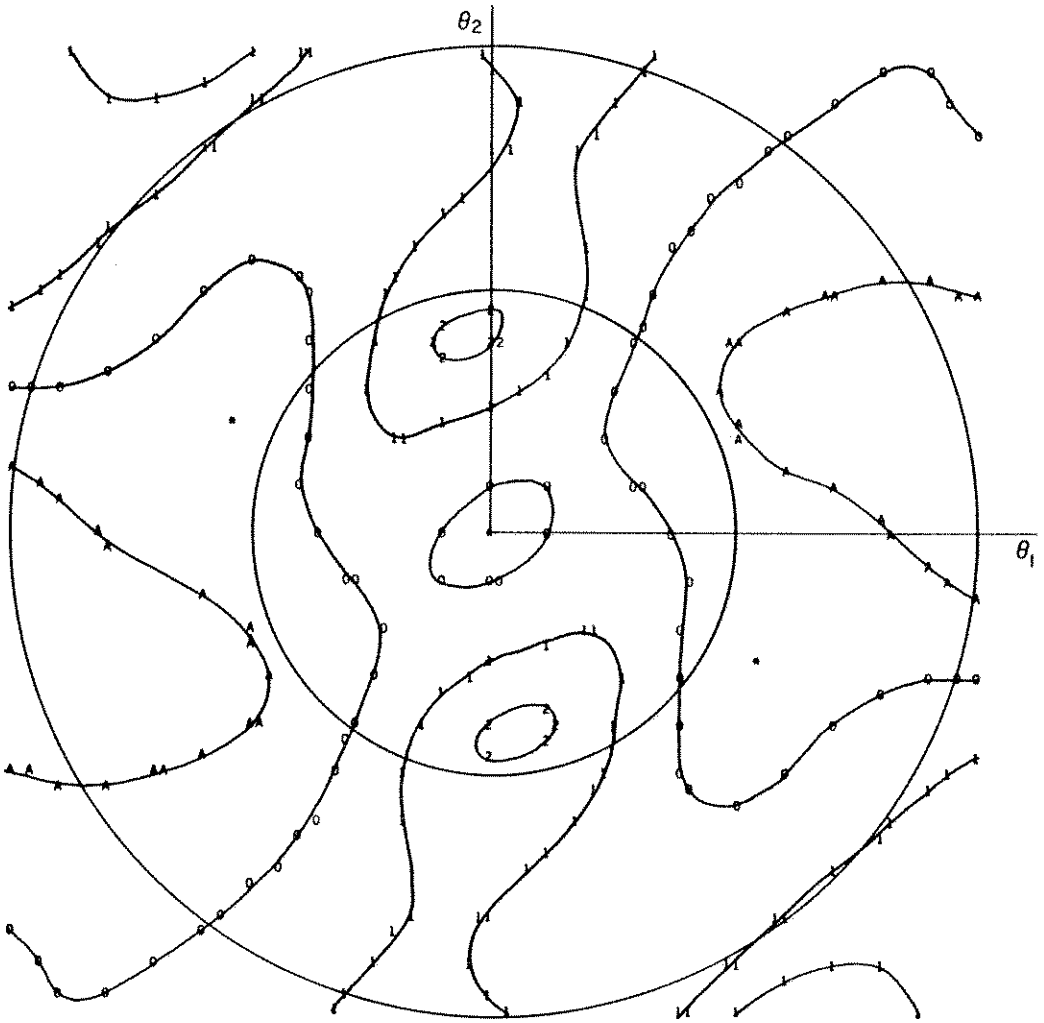

Figure 11d: $\phi = 25°$, $\delta = 2\overset{''}{.}0$, $\lambda = 6943$ Å.

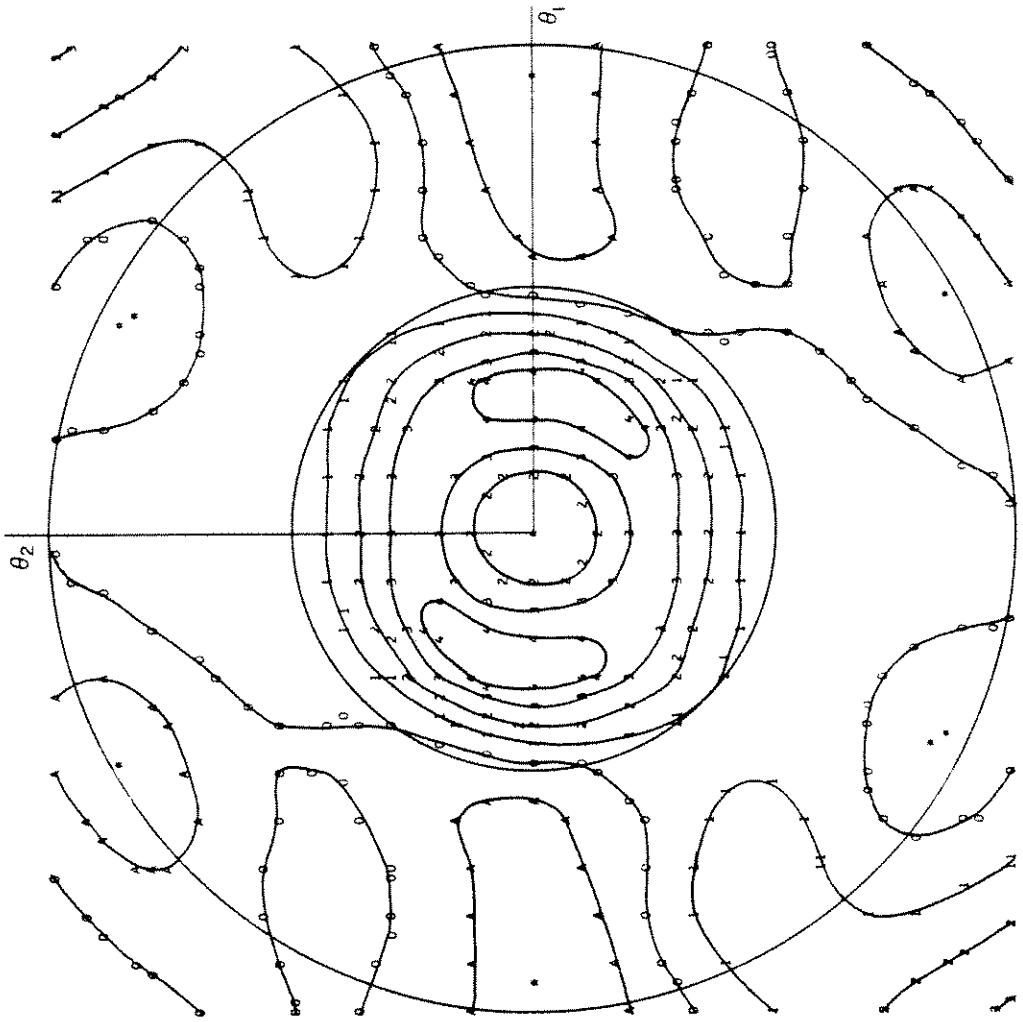

Figure 11e: $\phi = 45°$, $\delta = 2''.0$, $\lambda = 6943$ Å.

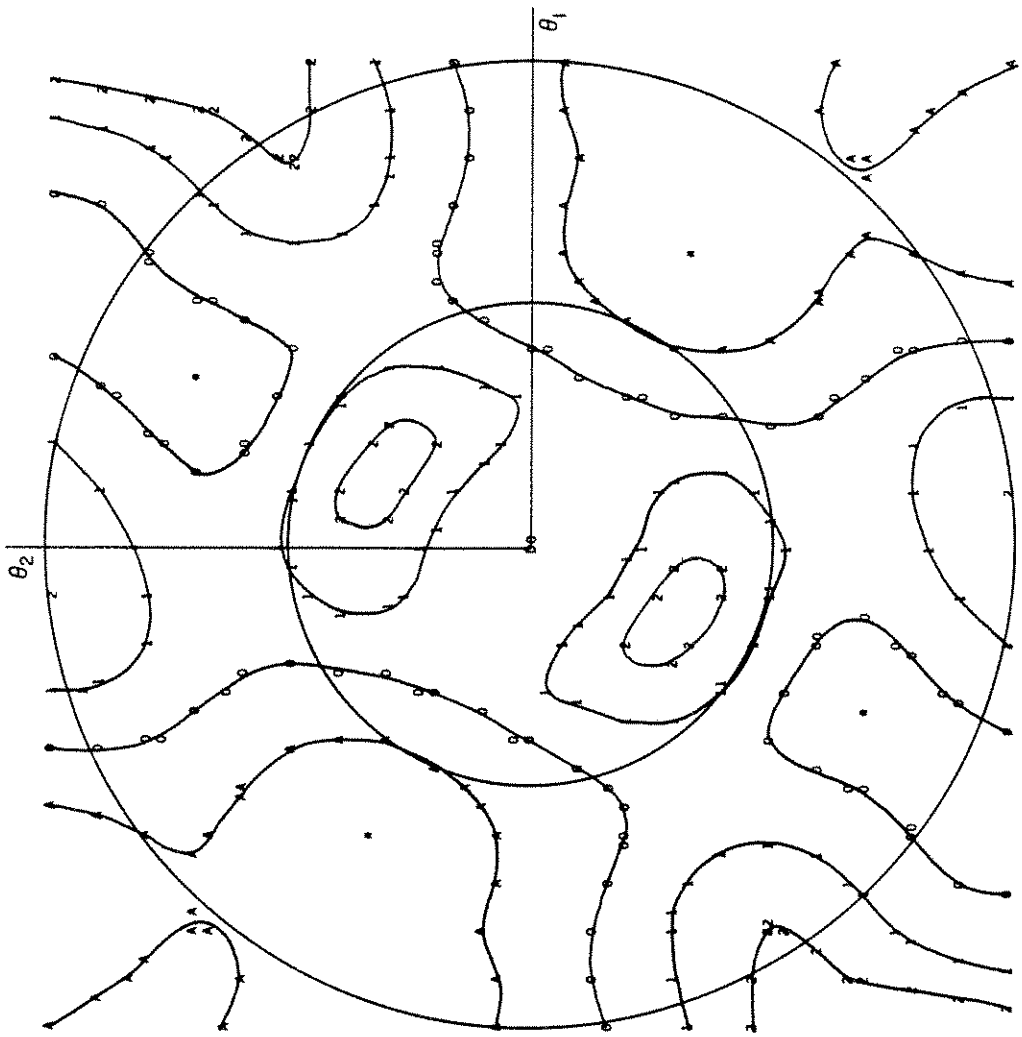

Figure 11f: $\phi = 60°$, $\delta = 2\overset{''}{.}0$, $\lambda = 6943$ Å.

9. EFFECT OF OPTICAL COHERENCE

Because of coherent interference between the reflections from individual cube corners, the strength and shape of the laser echo from the Geos 3 array vary from pulse to pulse. This section contains data on the variations of the range correction due to coherent interference. A special set of calculations has been done to investigate the relationship between the incoherent range correction and the average of the coherent range corrections for different types of detection methods and different transmitted pulse lengths. Some sample pulse shapes are presented for both the coherent and the incoherent case.

Table 14 lists the coherent variation of the centroid range correction as a function of the incidence angle ϕ. Each value is the rms variation of a set of 100 coherent returns. In Table 14a, each return has equal weight, while in Table 14b, each return is weighted by the ratio of the strength of the return to the strength of an incoherent return. This type of weighting reduces the rms deviation because of the fact that weaker pulses tend to have larger variations in centroid than do stronger pulses. In general, the fluctuation of the range correction decreases as the pulse length decreases. Since each rms deviation is computed from a limited number of coherent returns, the results should be considered as only an indication of the magnitude of the effect.

The range corrections given in Section 8 are all for the incoherent case. In the mathematical model used to calculate the transfer function, the incoherent centroid range correction is equal to the average of the coherent centroid range corrections when each pulse is weighted by its intensity. It is not obvious from the model what to expect for different weightings or for detection methods other than centroid detection. A series of computer runs has been done with a large number of coherent returns to see how big the differences are for Geos 3, and the results are presented in Table 15. The runs were made at an incidence angle of 45° with respect to the symmetry axis of the satellite. The table lists the coherent average minus the incoherent value (Δ), the standard deviation of an individual pulse (σ), the number of coherent returns in the

Table 14. Root-mean-square deviation of centroid range correction due to coherent interference vs. incidence angle. a: All pulses have equal weight. b: Each pulse is weighted by the ratio of the strength of the pulse to the strength of an average (or incoherent) pulse.

a: Equal weighting

.2 NS. EQUAL WEIGHTING

PHI (DEG)	R.M.S. DEVIATION OF RANGE CORRECTION (METERS)
0.0	.0094
10.0	.0202
20.0	.0190
30.0	.0189
40.0	.0198
50.0	.0189
60.0	.0192

5. NS. EQUAL WEIGHTING

PHI (DEG)	R.M.S. DEVIATION OF RANGE CORRECTION (METERS)
0.0	.0259
10.0	.0636
20.0	.0666
30.0	.0718
40.0	.0588
50.0	.0719
60.0	.0479

20 NS. EQUAL WEIGHTING

PHI (DEG)	R.M.S. DEVIATION OF RANGE CORRECTION (METERS)
0.0	.0268
10.0	.0528
20.0	.0609
30.0	.0861
40.0	.0676
50.0	.0631
60.0	.0790

b: Weighted by signal strength

.2 NS. WEIGHTED

PHI (DEG)	R.M.S. DEVIATION OF RANGE CORRECTION (METERS)
0.0	.0086
10.0	.0187
20.0	.0181
30.0	.0166
40.0	.0181
50.0	.0159
60.0	.0169

5. NS. WEIGHTED

PHI (DEG)	R.M.S. DEVIATION OF RANGE CORRECTION (METERS)
0.0	.0104
10.0	.0364
20.0	.0354
30.0	.0434
40.0	.0294
50.0	.0414
60.0	.0365

20. NS. WEIGHTED

PHI (DEG)	R.M.S. DEVIATION OF RANGE CORRECTION (METERS)
0.0	.0121
10.0	.0330
20.0	.0324
30.0	.0415
40.0	.0390
50.0	.0325
60.0	.0414

Table 15. Difference between the average range correction for a set of coherent returns and the range correction for the incoherent return. The pulse length is in nanoseconds; Δ, σ, and σ_m are in millimeters.

Pulse length	Δ	σ	N	σ_m	Δ/σ_m	Pulse length	Δ	σ	N	σ_m	Δ/σ_m
	a: Centroid, equal weighting						b: Centroid, weighted by signal strength				
0.2	-8.15	20.95	1000	0.66	-12.3	0.2	-0.68	17.51	1000	0.55	-1.2
1.0	-9.56	35.89	1000	1.14	-8.4	1.0	-0.76	25.34	1000	0.80	-0.9
2.0	-7.64	47.57	1000	1.50	-5.1	2.0	-0.68	32.80	1000	1.04	-0.7
3.0	-4.67	58.46	1000	1.85	-2.5	3.0	+0.83	34.19	1000	1.08	+0.8
5.0	-2.34	70.06	1000	2.22	-1.1	5.0	+0.99	38.26	1000	1.21	+0.8
5.0	0.45	65.23	1000	2.06	+0.2	5.0	+0.80	36.59	1000	1.16	+0.7
	c: Half-maximum, equal weighting						d: Half-maximum, weighted by signal strength				
0.2	-5.94	13.53	300	0.78	-7.6	0.2	-4.25	10.39	300	0.60	-7.1
5.0	-4.20	67.75	1096	2.05	-2.1	5.0	-2.44	33.59	1096	1.01	-2.4
20.0	-2.97	94.43	1100	2.85	-1.0	20.0	-2.37	36.62	1100	1.10	-2.1
	e: Half-area, equal weighting						f: Half-area, weighted by signal strength				
0.2	-10.32	22.80	300	1.32	-7.8	0.2	-3.99	18.59	300	1.07	-3.7
5.0	-2.87	68.32	1096	2.06	-1.4	5.0	+0.17	36.35	1096	1.10	0.2
20.0	-2.53	92.28	1100	2.78	-0.9	20.0	-1.76	37.46	1100	1.13	-1.6

sample (N), the standard deviation of the average ($\sigma_m = \sigma/\sqrt{N}$), and the ratio of the difference Δ to the standard deviation of the mean (σ_m). The last column is a measure of the statistical significance of Δ. In Table 15a, a statistically significant difference occurs between the coherent average and the incoherent value of the centroid range correction for short transmitted pulses; this difference decreases as the pulse length increases. The two runs for 5.0 nsec indicate no statistically significant difference. Table 15b shows the same set of coherent returns weighted by signal strength. For all pulse lengths, the bias in the coherent average is removed, in agreement with what should be expected from the model. In Table 15c, for half-maximum detection, the magnitude of the bias is smaller; this bias is not removed when the returns are weighted by signal strength (Table 15d). For half-area detection (Tables 15e and 15f), weighting seems to be somewhat more helpful but the bias still remains. The size of the bias in all cases is on the order of 1 cm or less. The data in Table 15 are probably typical of incidence angles from 10° to 60° or 70°. At $\phi = 0°$, the distribution of reflectors along the line of sight is symmetrical, so there is no mechanism for producing a bias.

Sample pulse shapes for $\phi = 0°$ and 45° are shown in Figure 12. In each case, the incoherent return is given first, followed by one or more coherent returns. When the transmitted pulse is much longer than the array, as is the case for 20 and 5 nsec, the reflection has nearly the same gaussian shape as the incident pulse does. Only one coherent return is given in each case for these pulse lengths. The returns for 0.2 nsec tend to be irregularly shaped. Effects such as differences between the range correction for different types of detection systems and differences between the incoherent range correction and the average of the coherent range corrections seem to be associated with the pulse distortion that occurs when the pulse length is comparable to, or less than, the size of the array.

The position, in meters, listed in the first column of Figure 12 is measured with respect to the center of the pulse that would be received from a point reflector at the center of gravity of the satellite. The intensity in the second column is in normalized units such that the area under the curve is equal to the signal strength in equivalent number of cube corners at normal incidence.

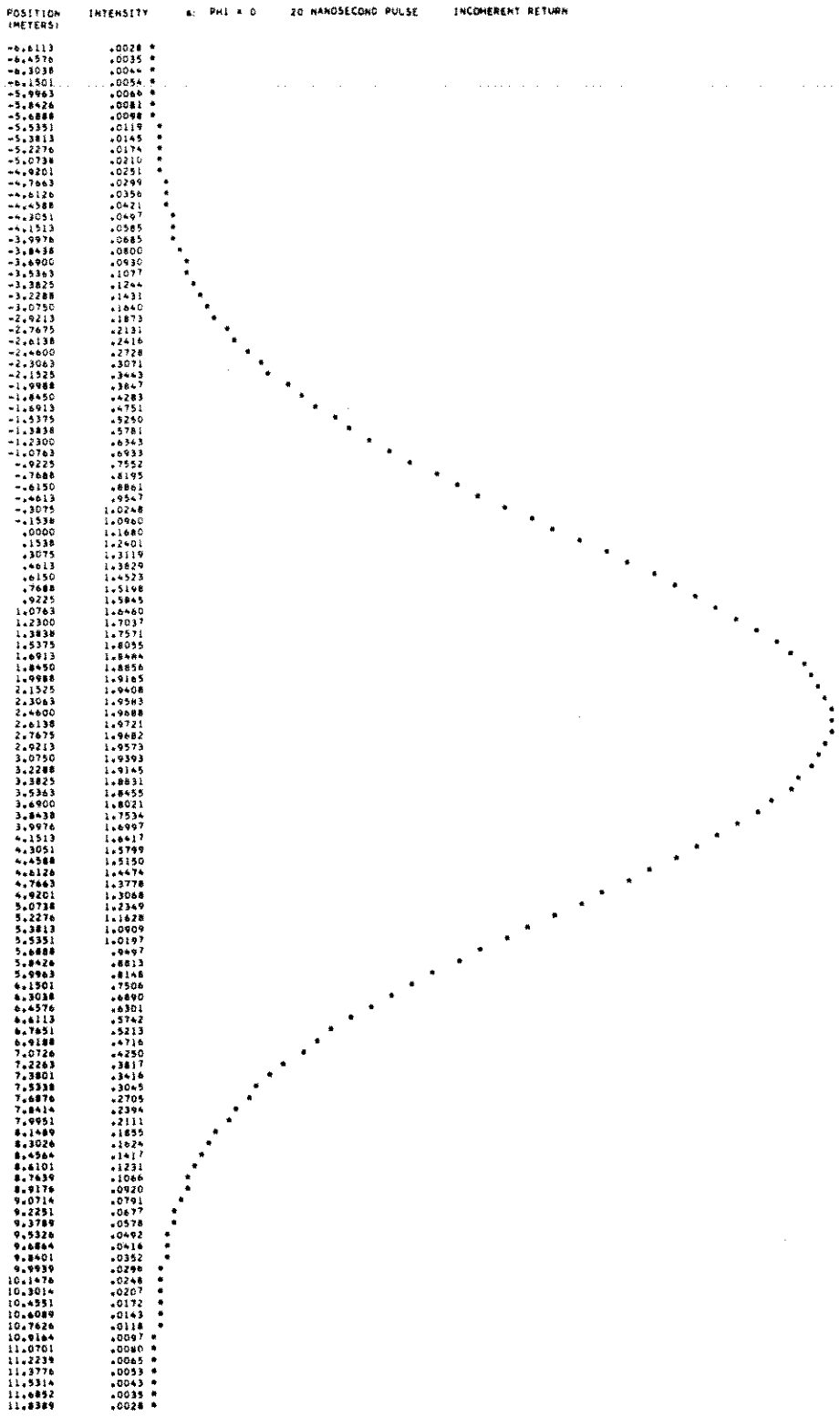

Figure 12. Sample incoherent and coherent reflected pulse shapes. The intensity is plotted vs. the distance along the line of sight.

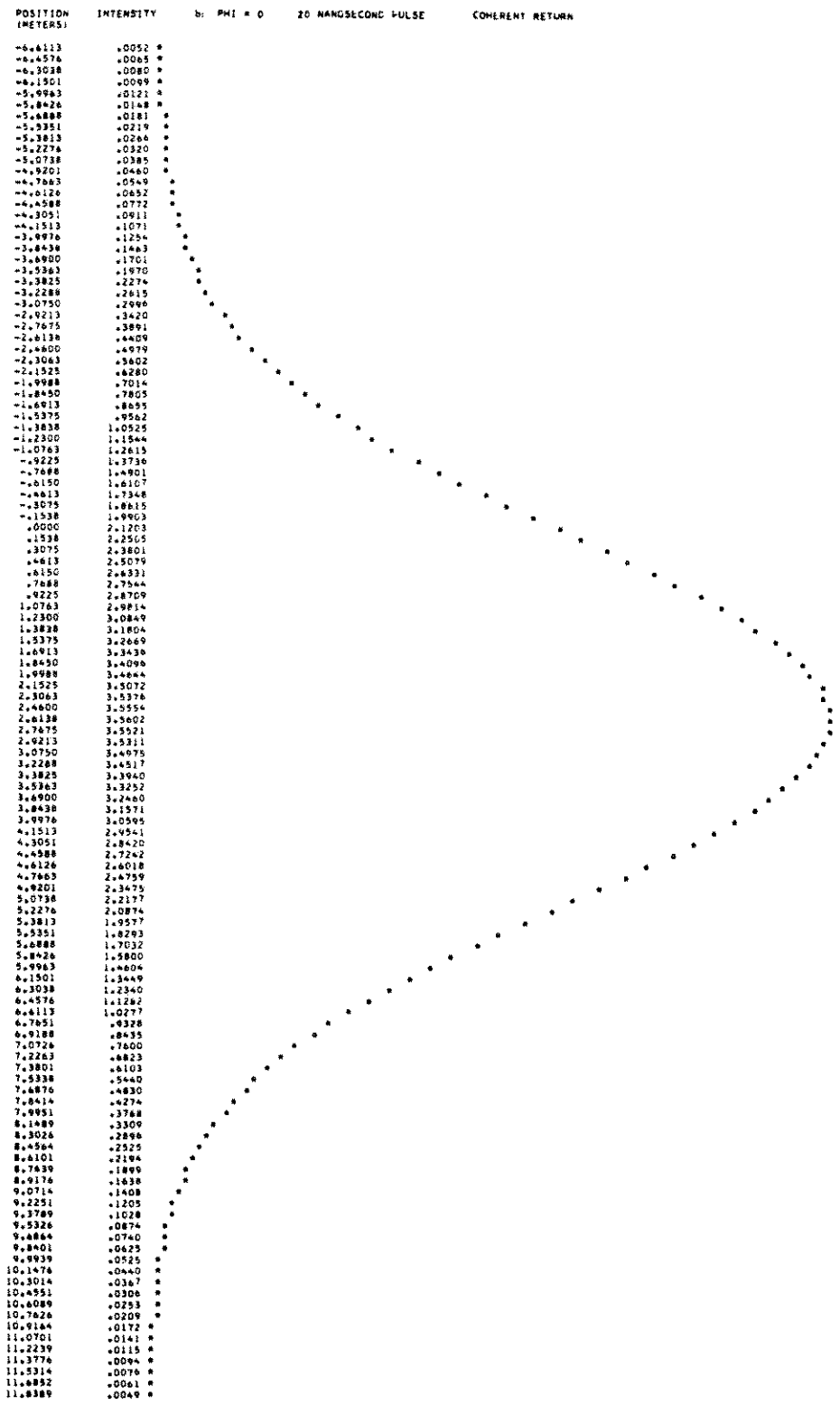

Figure 12. (Cont.)

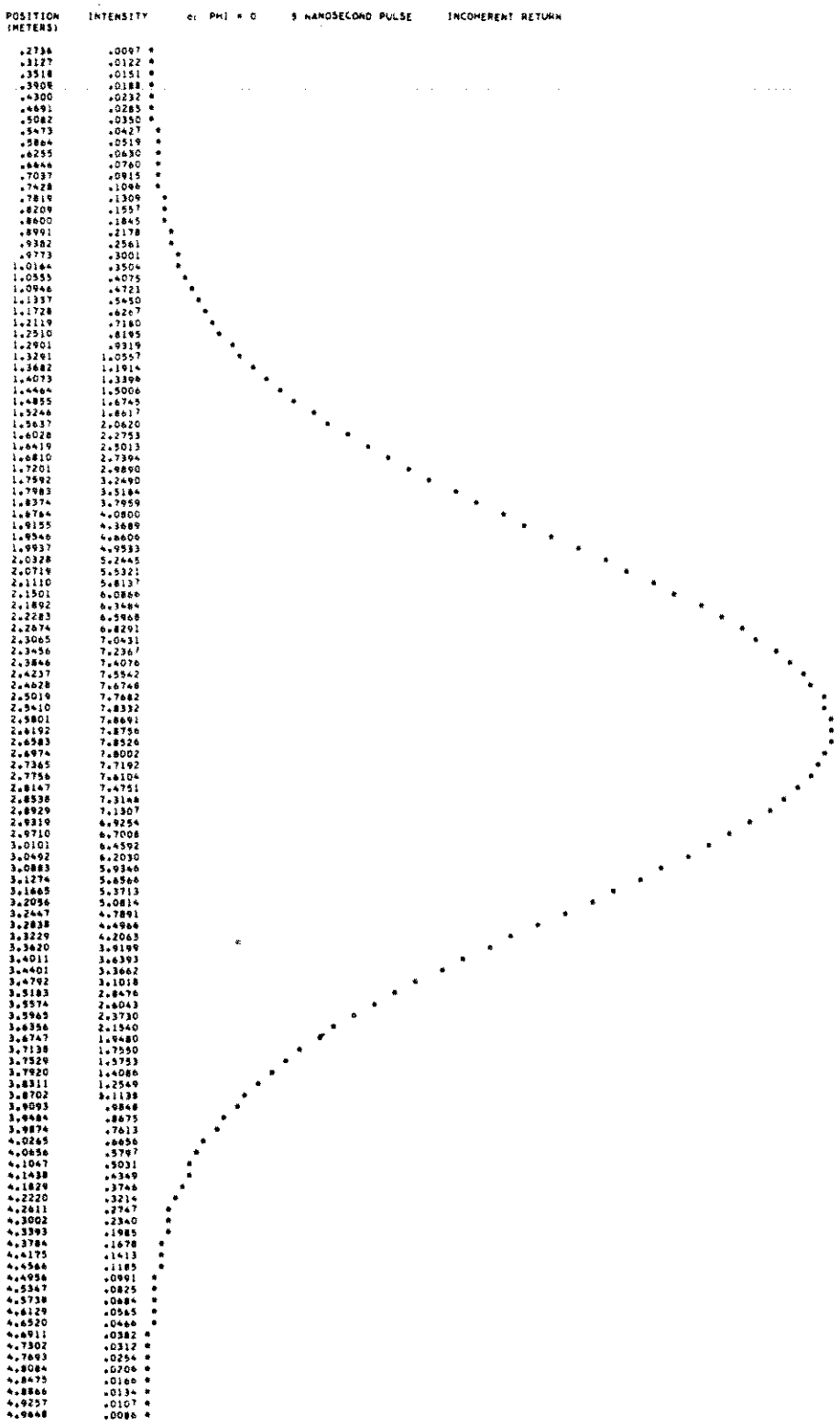

Figure 12. (Cont.)

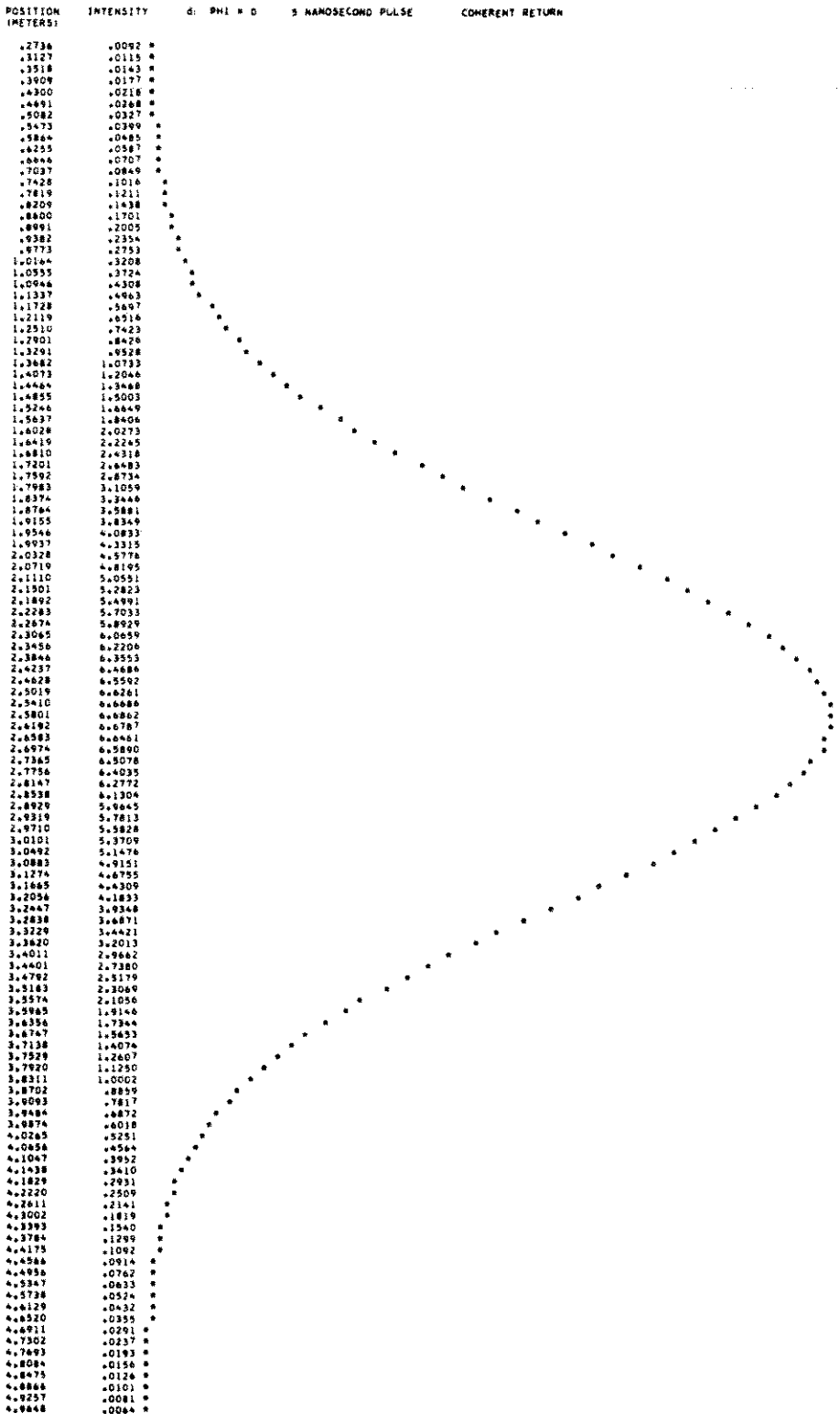

Figure 12. (Cont.)

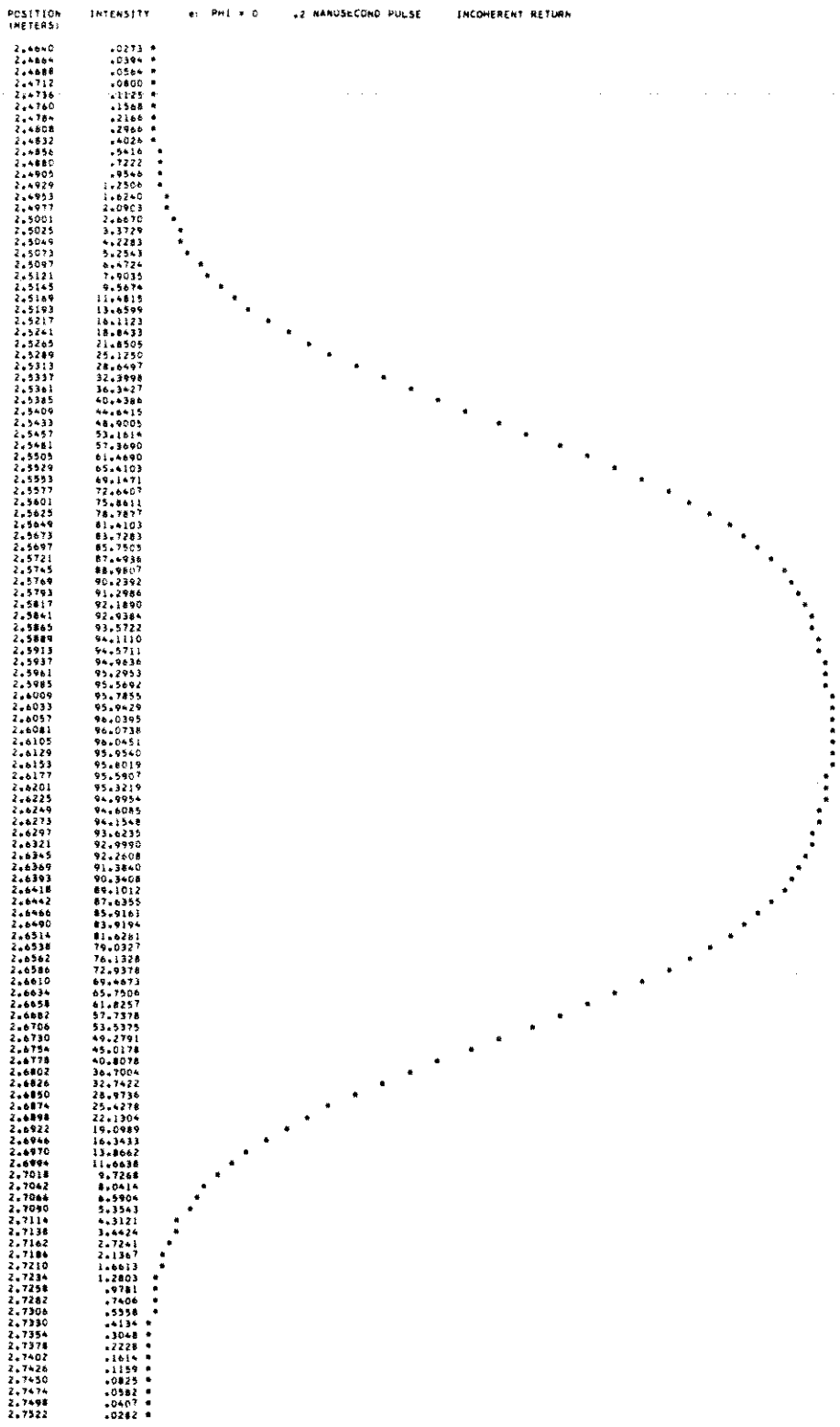

Figure 12. (Cont.)

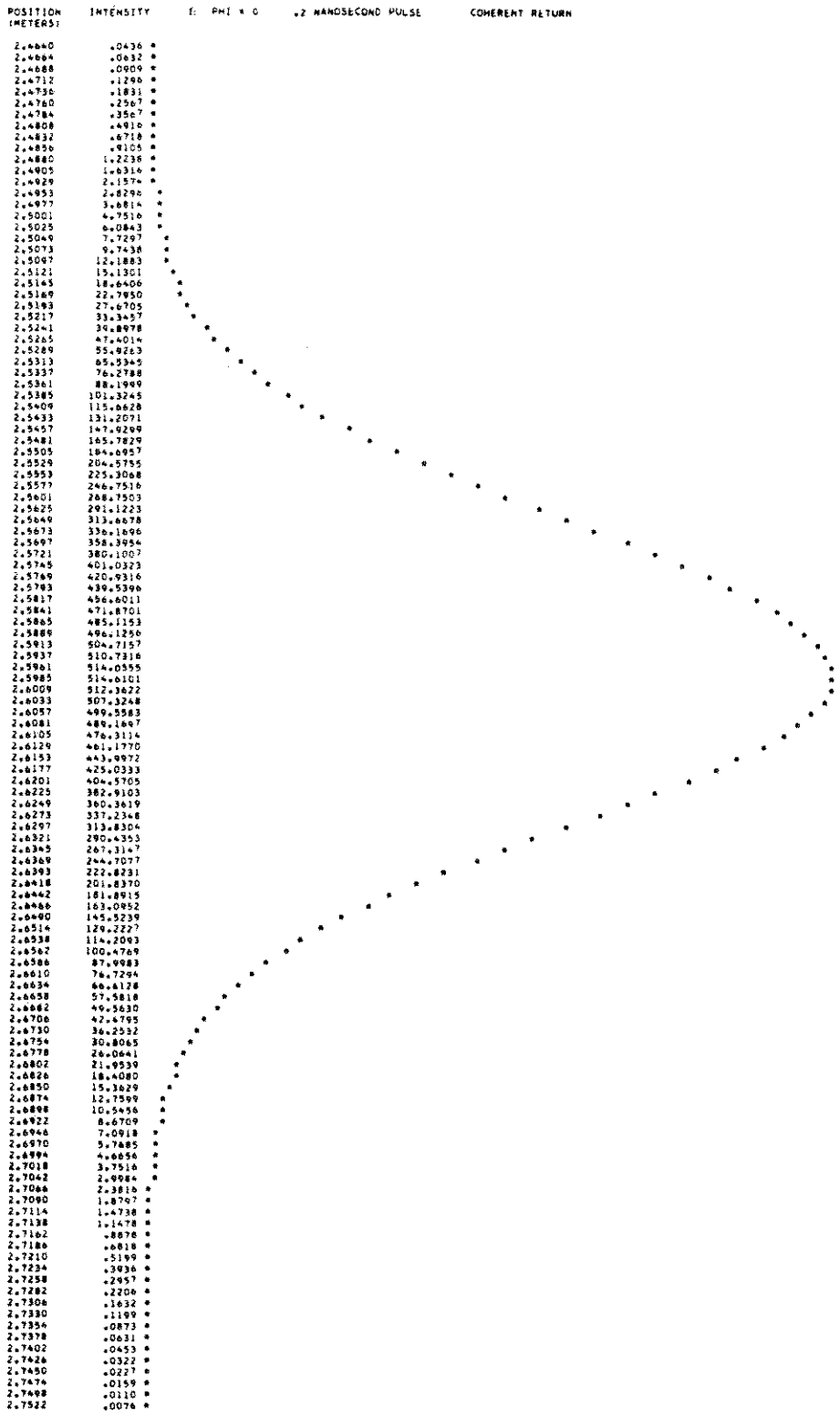

Figure 12. (Cont.)

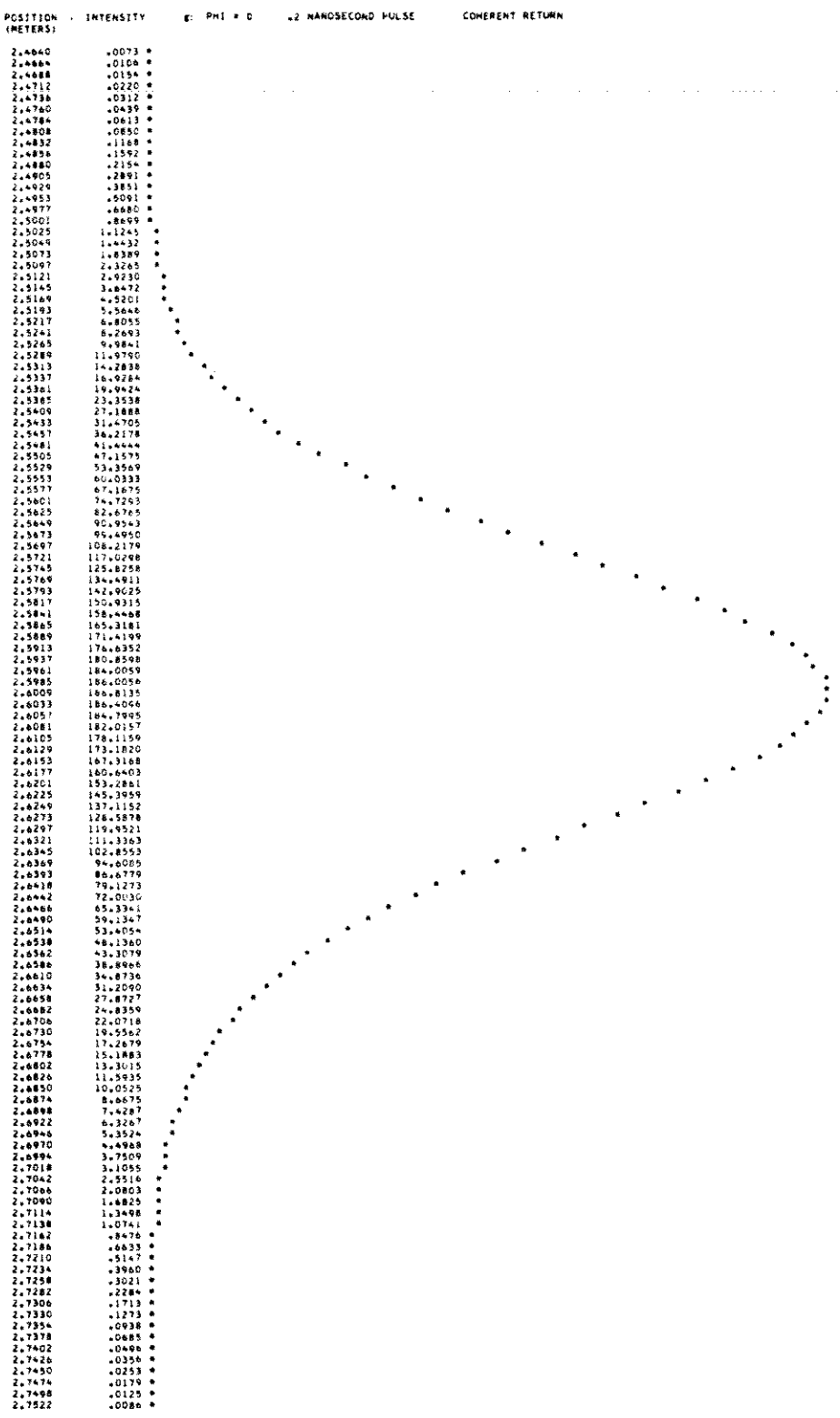

Figure 12. (Cont.)

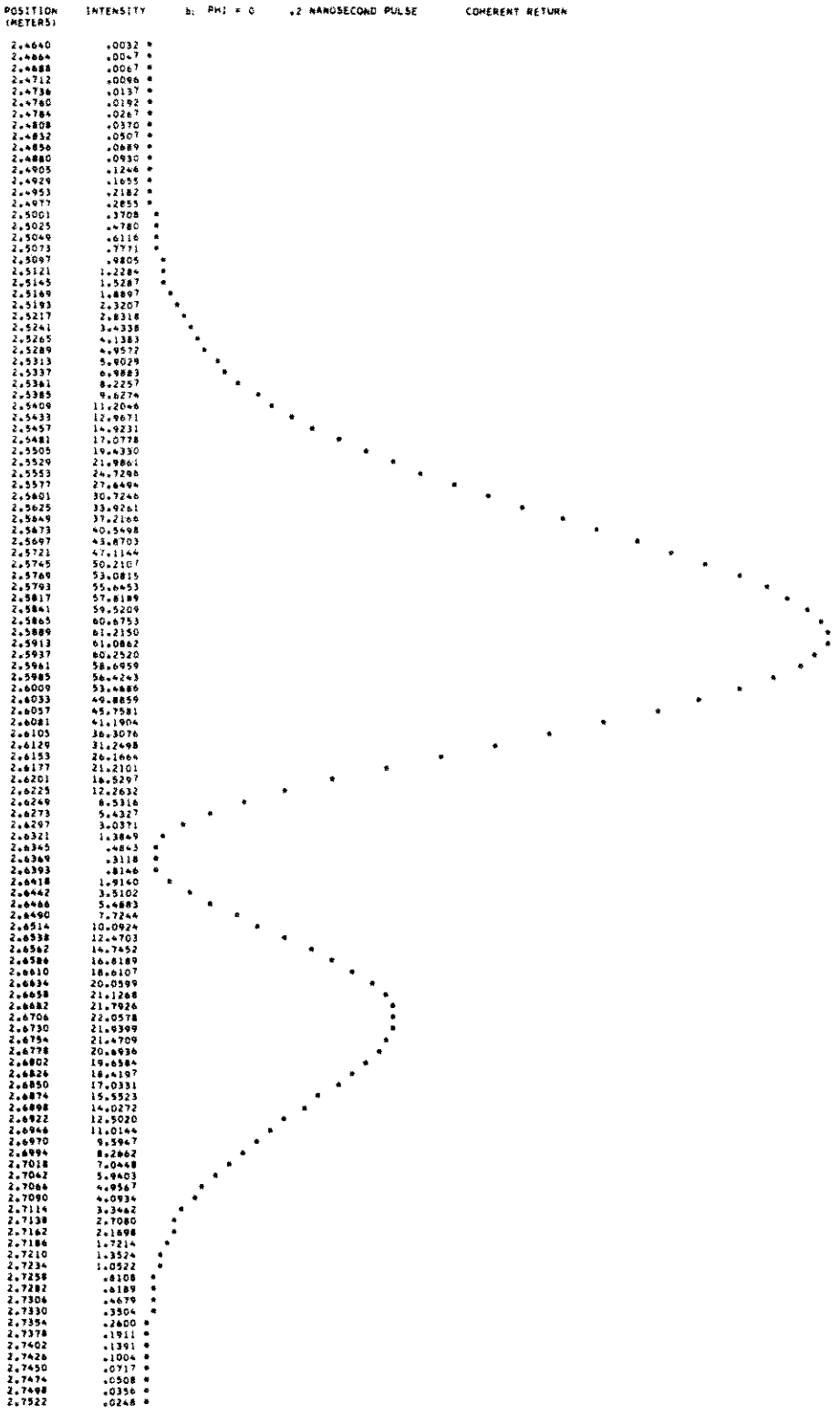

Figure 12. (Cont.)

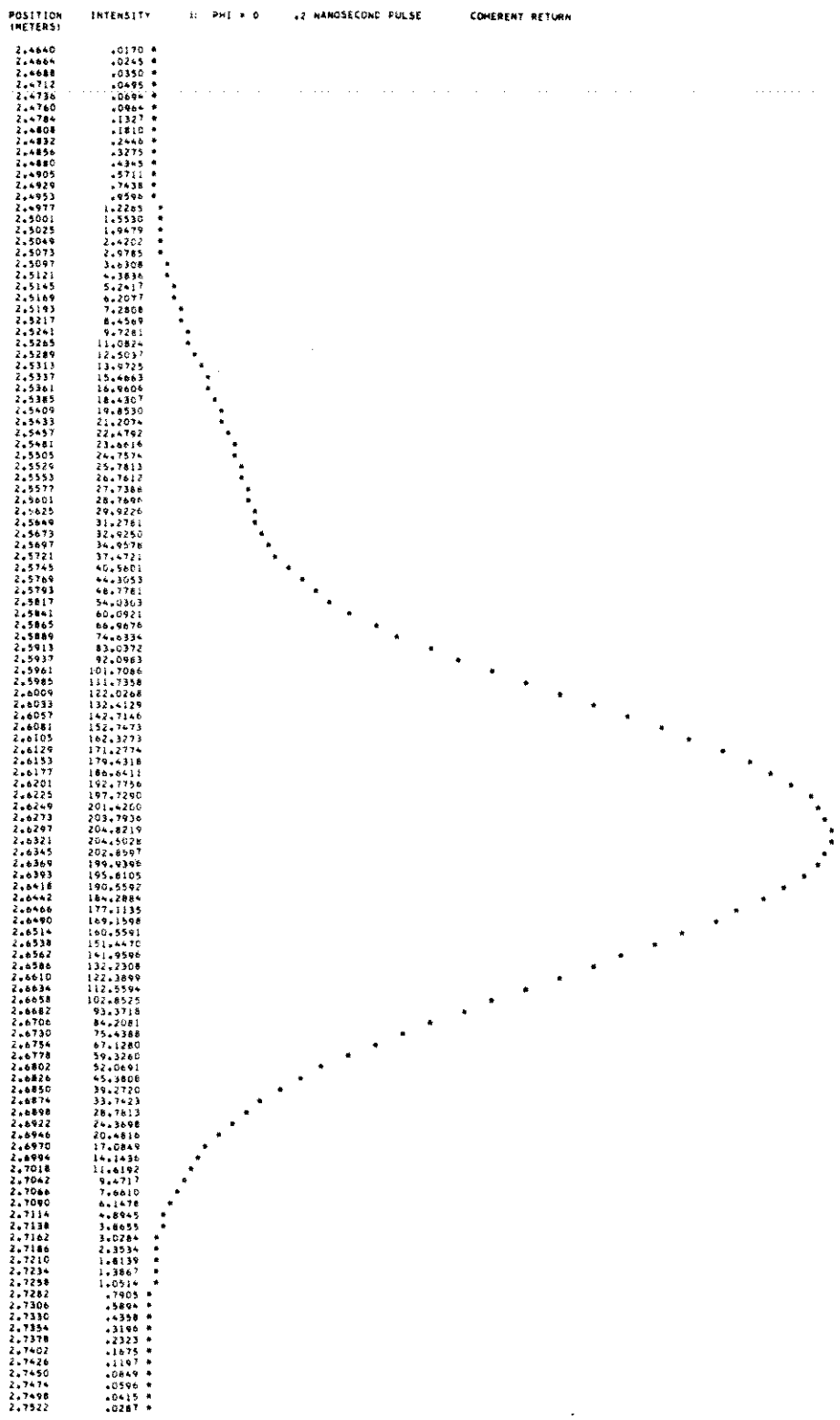

Figure 12. (Cont.)

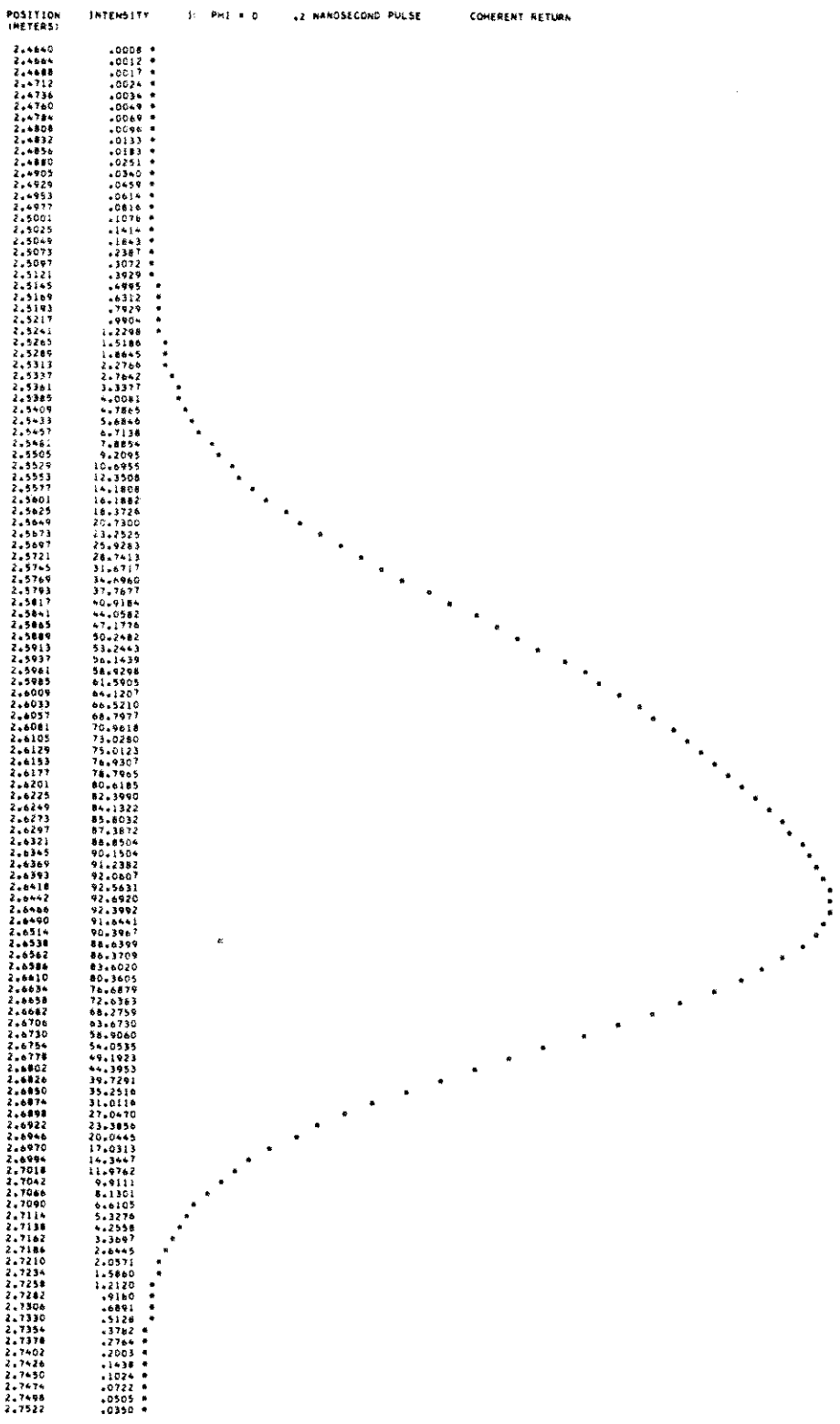

Figure 12. (Cont.)

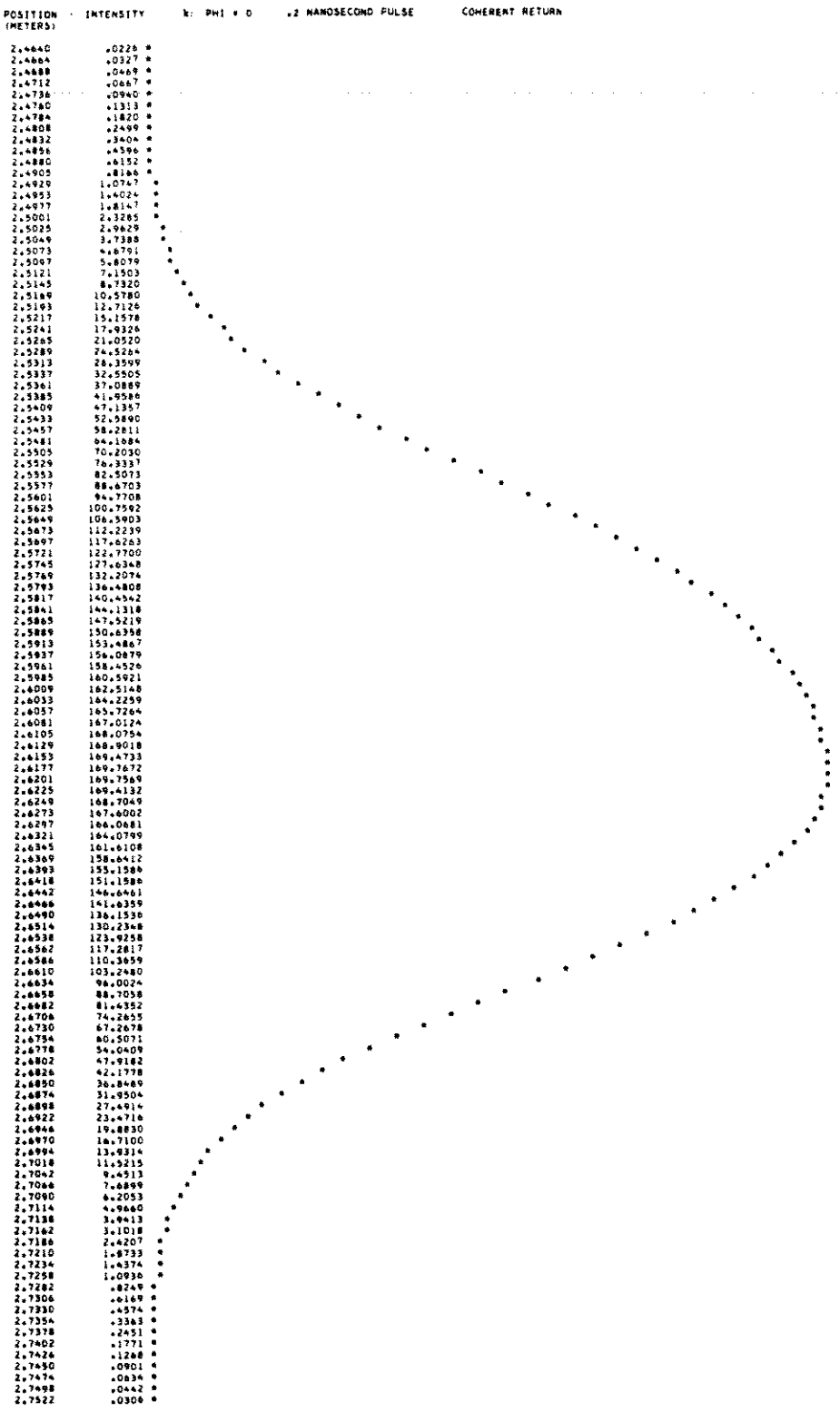

Figure 12. (Cont.)

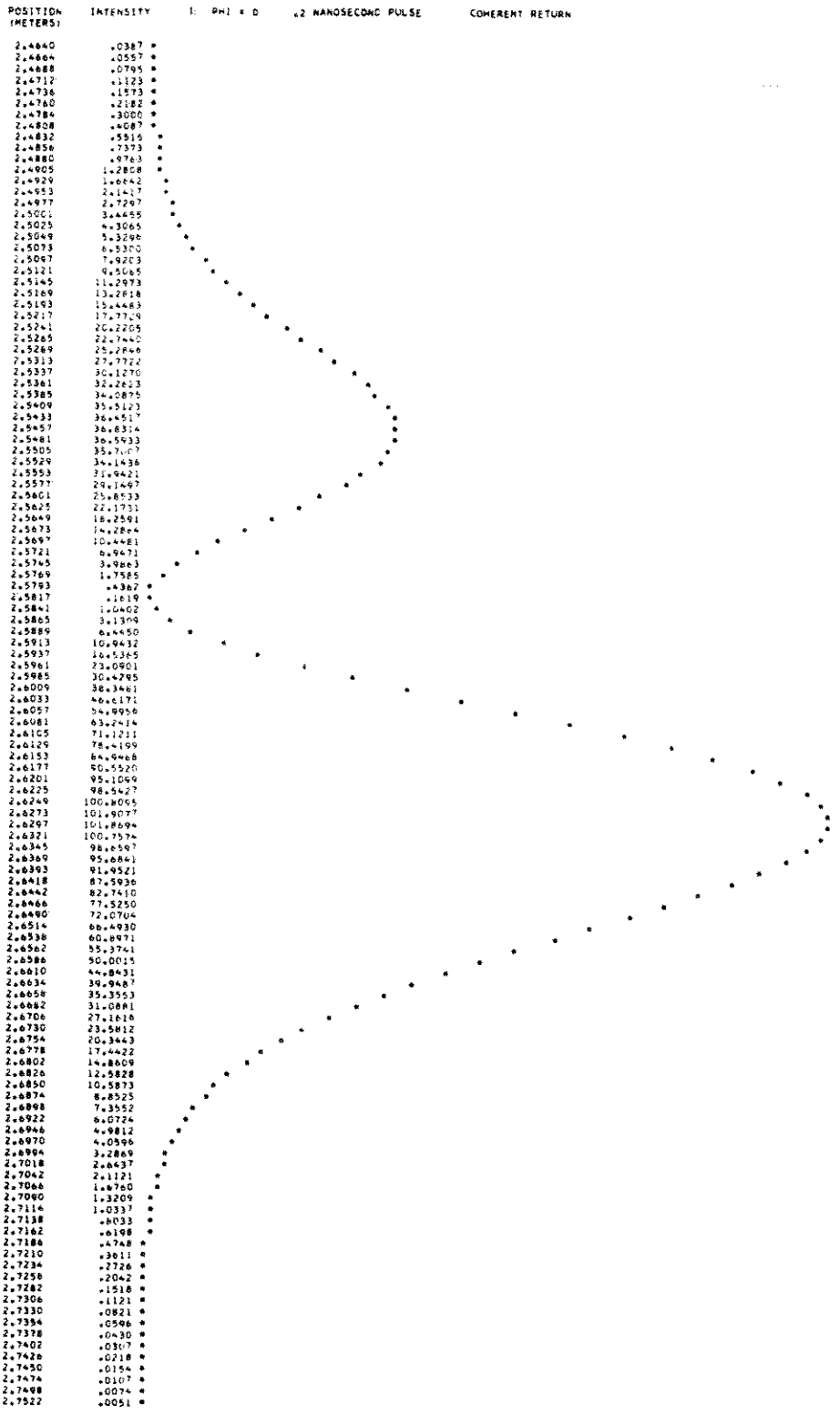

Figure 12. (Cont.)

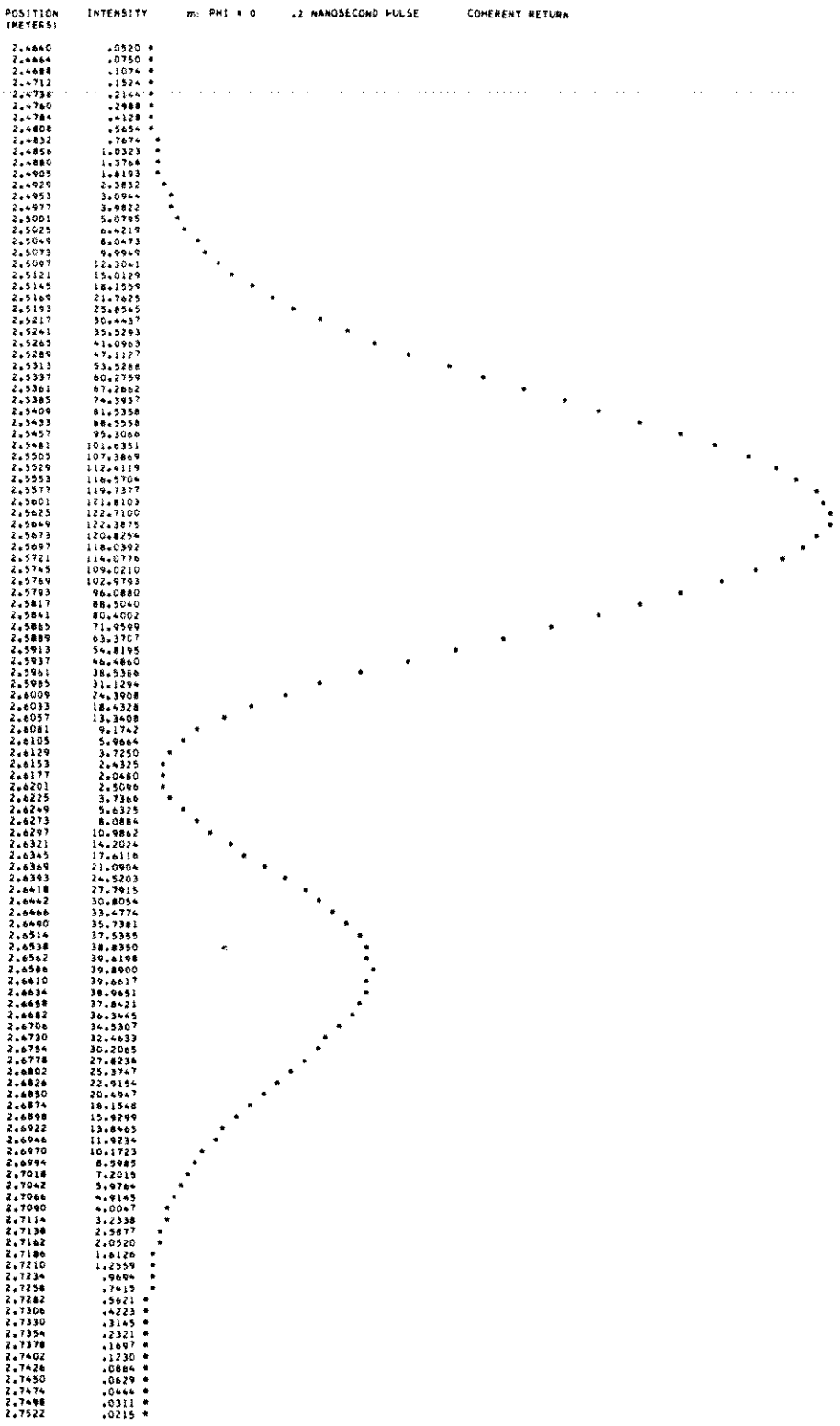

Figure 12. (Cont.)

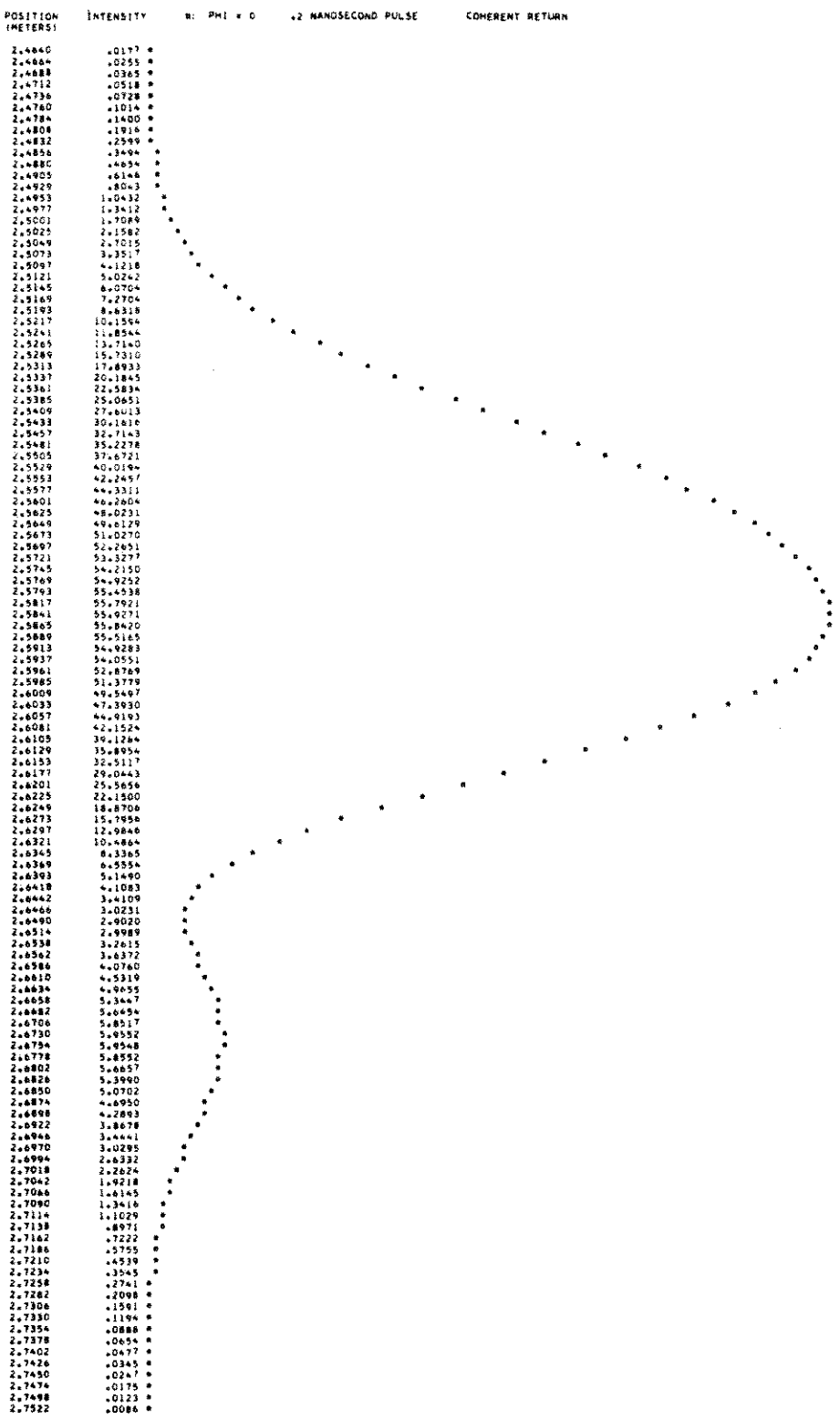

Figure 12. (Cont.)

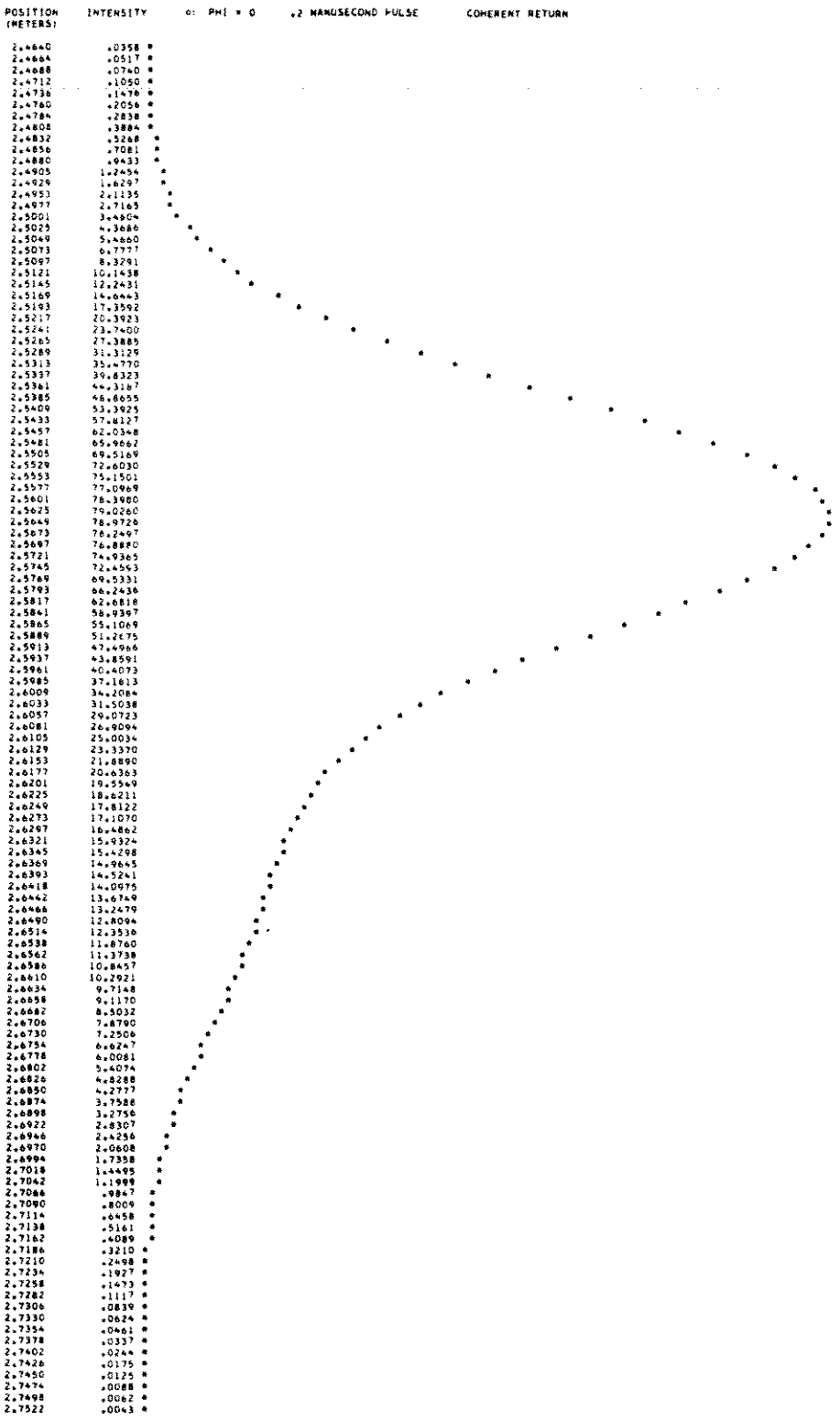

Figure 12. (Cont.)

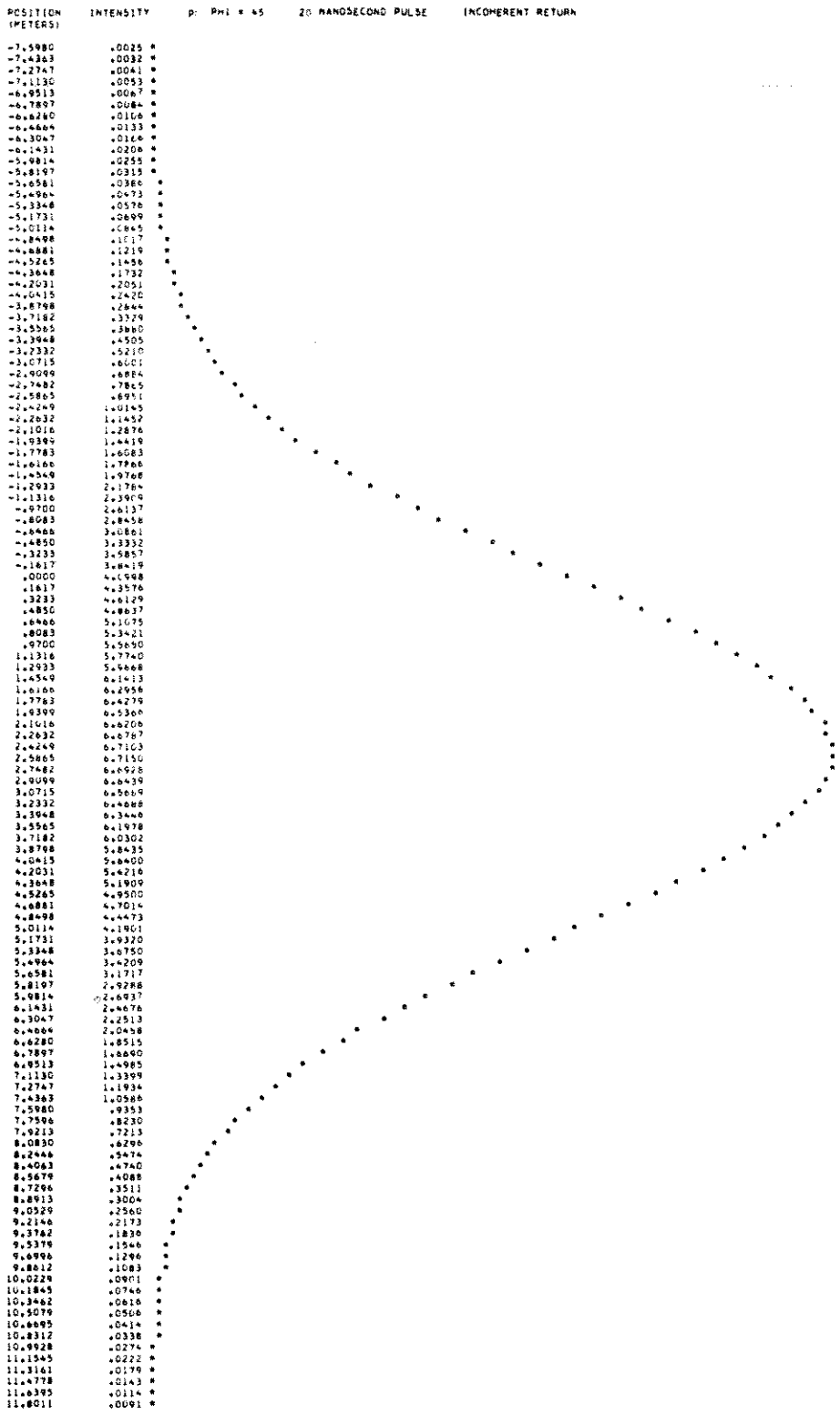

Figure 12. (Cont.)

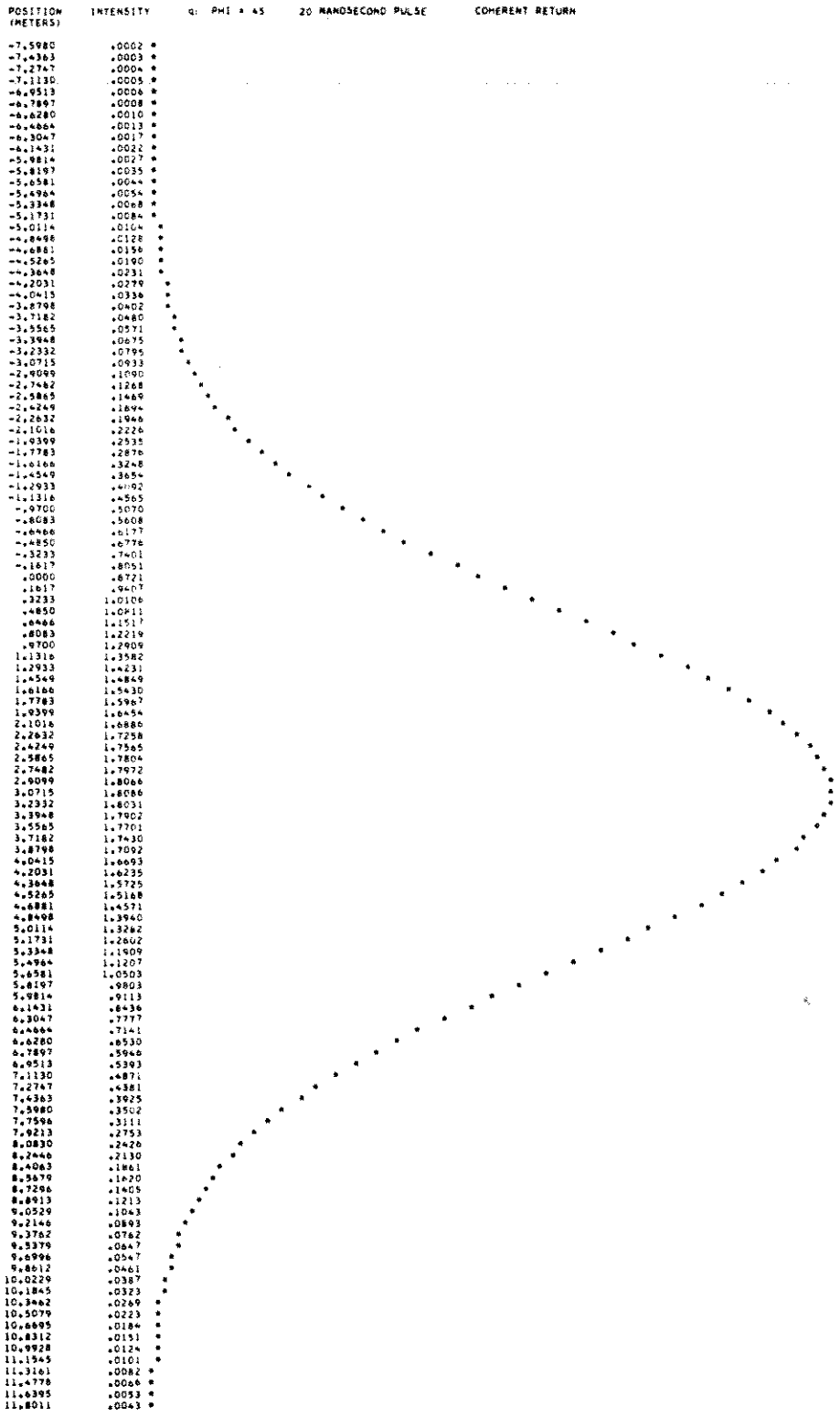

Figure 12. (Cont.)

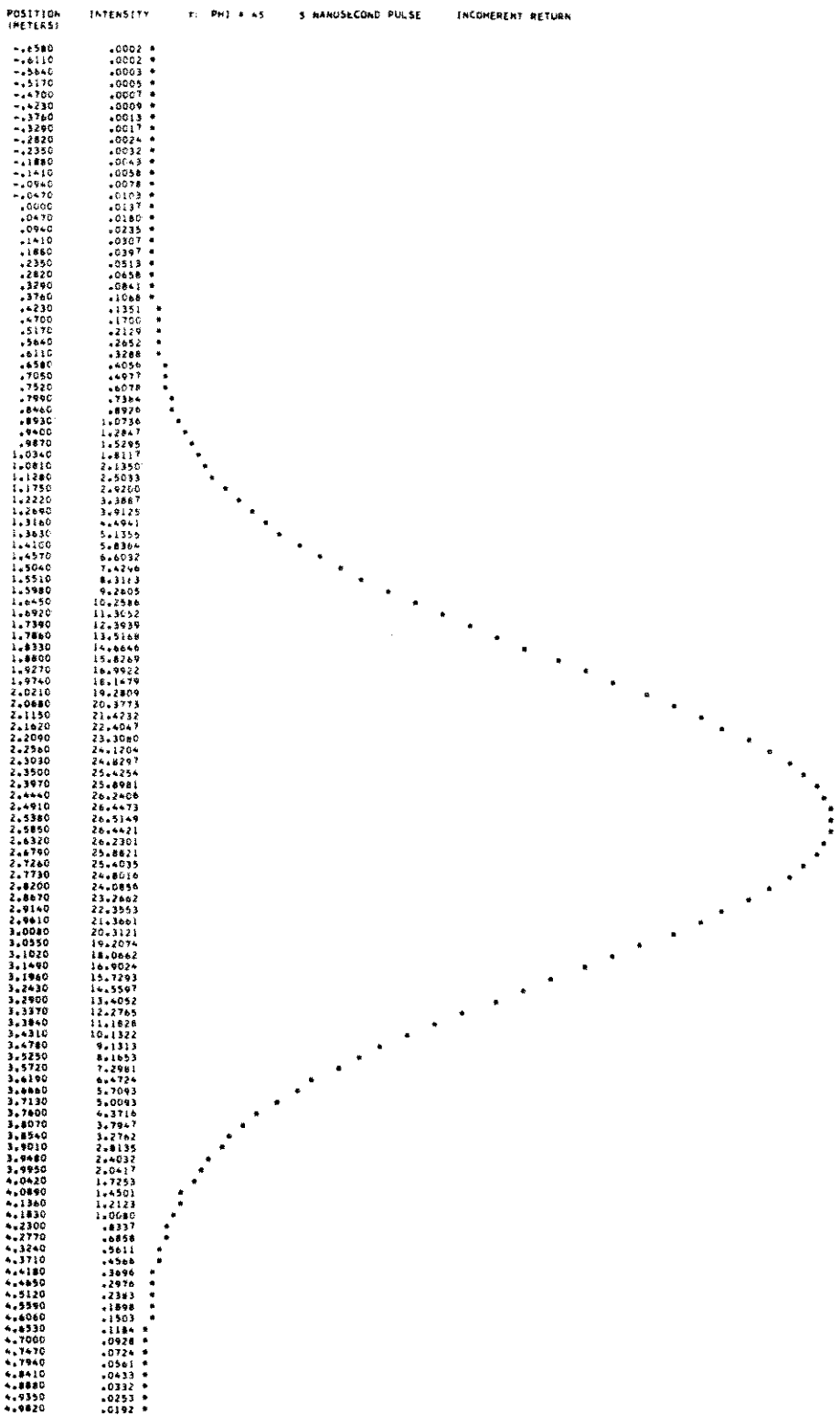

Figure 12. (Cont.)

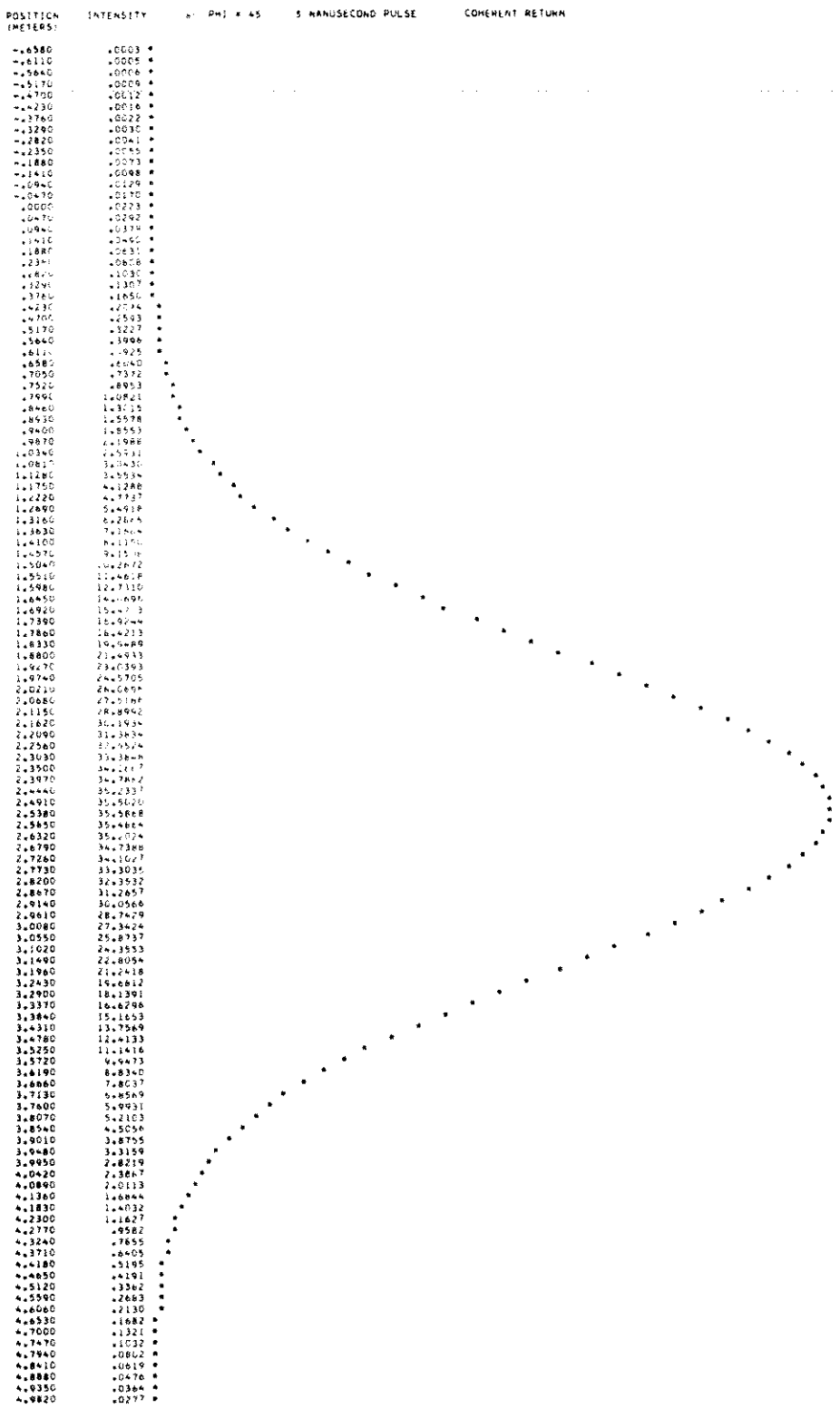

Figure 12. (Cont.)

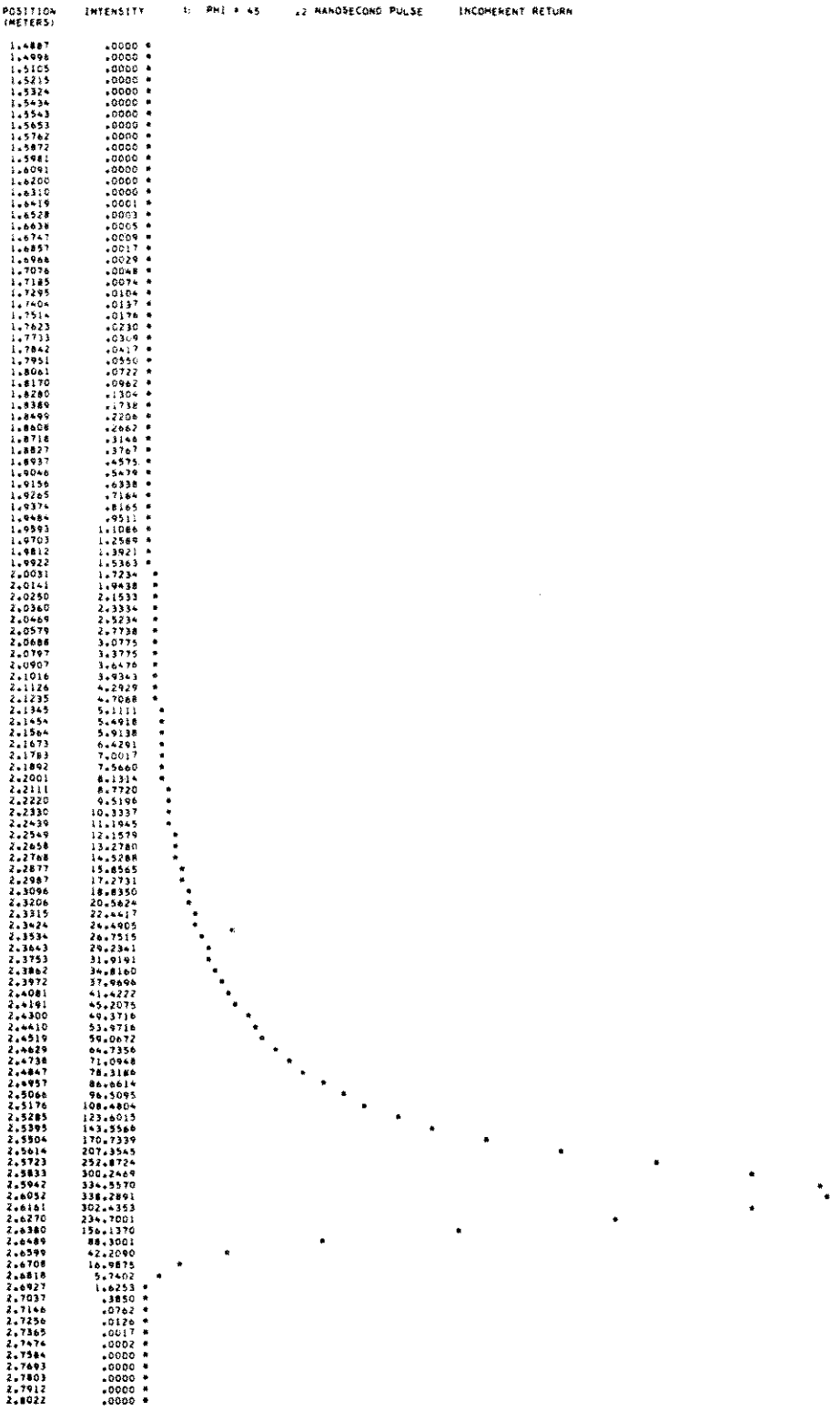

Figure 12. (Cont.)

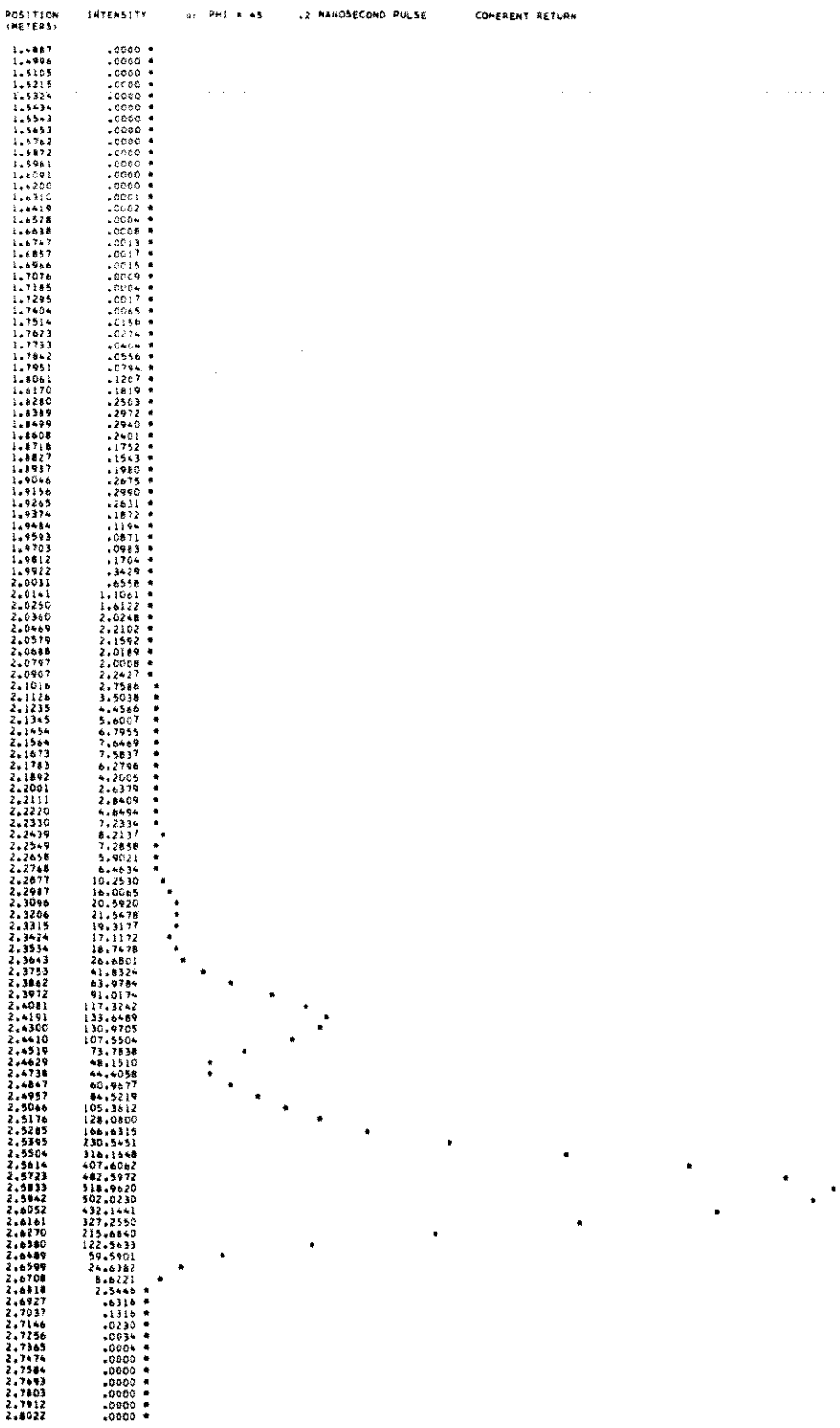

Figure 12. (Cont.)

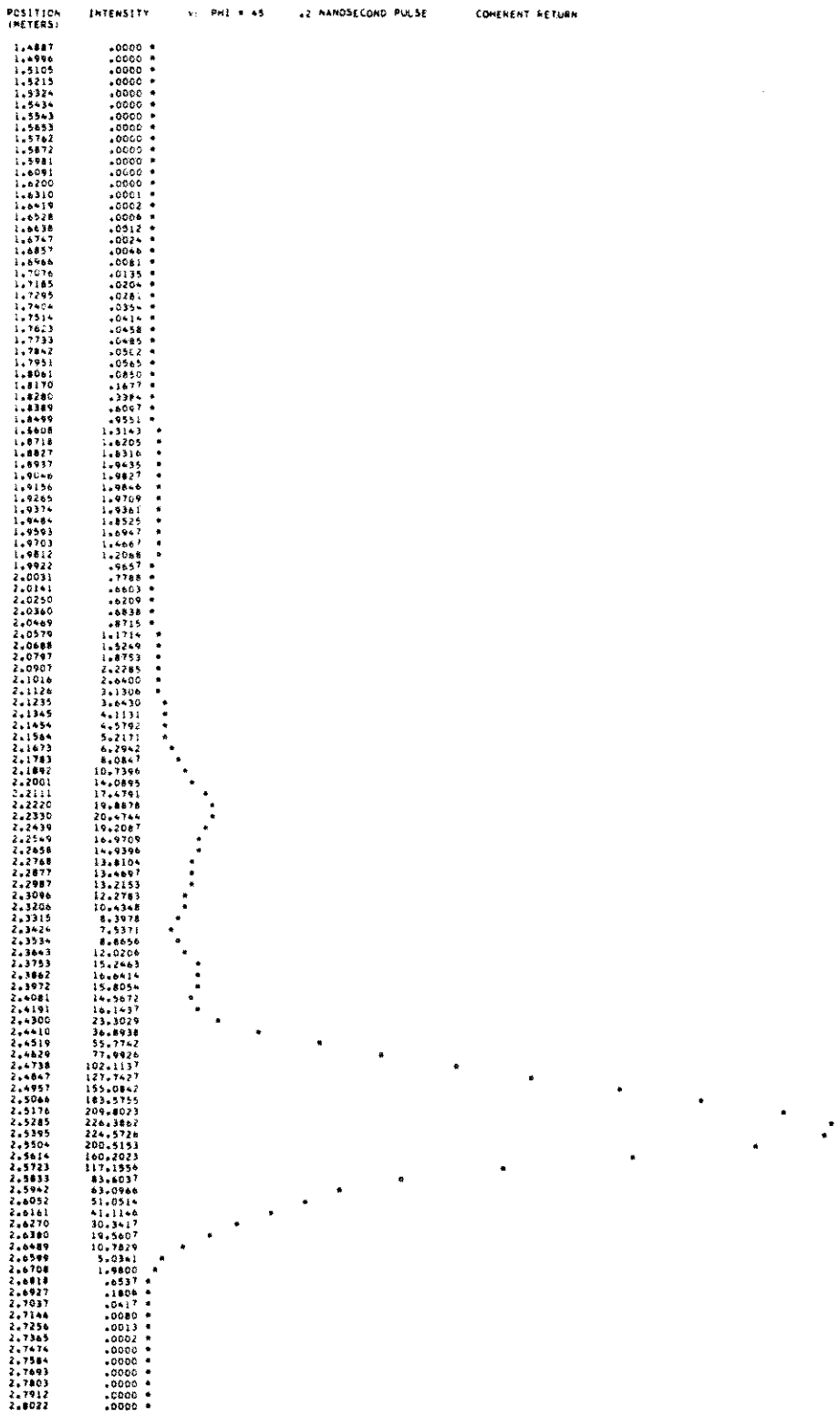

Figure 12. (Cont.)

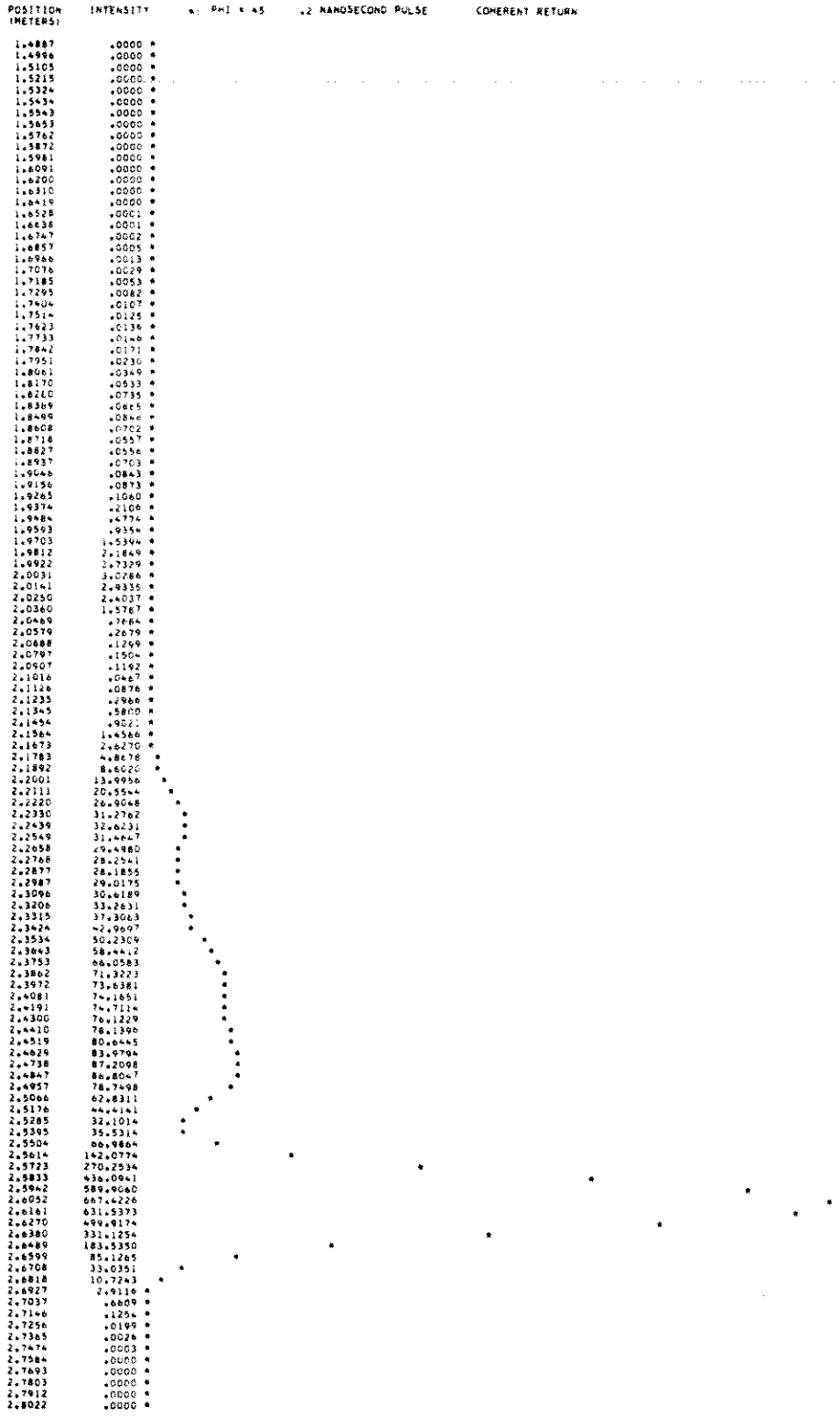

Figure 12. (Cont.)

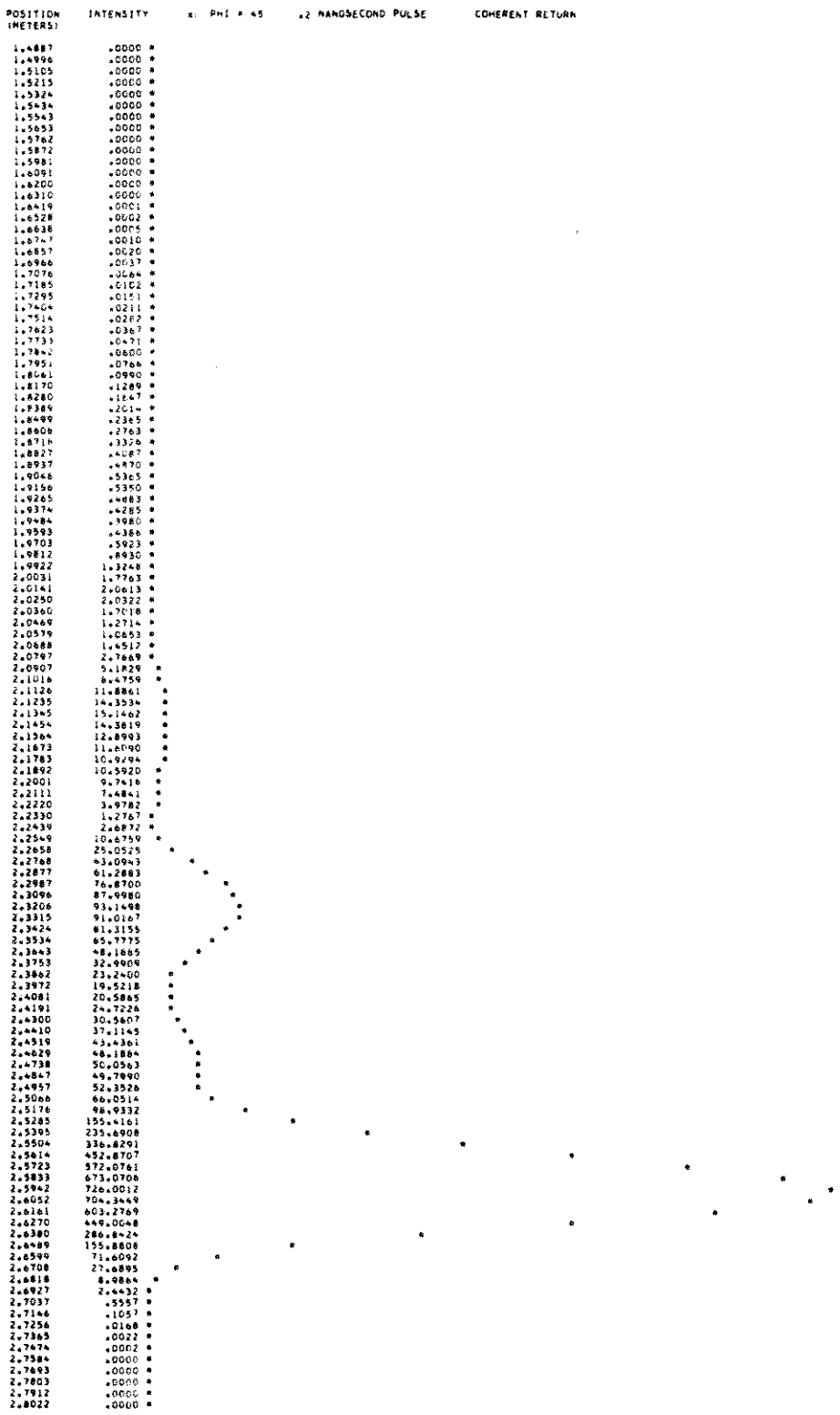

Figure 12. (Cont.)

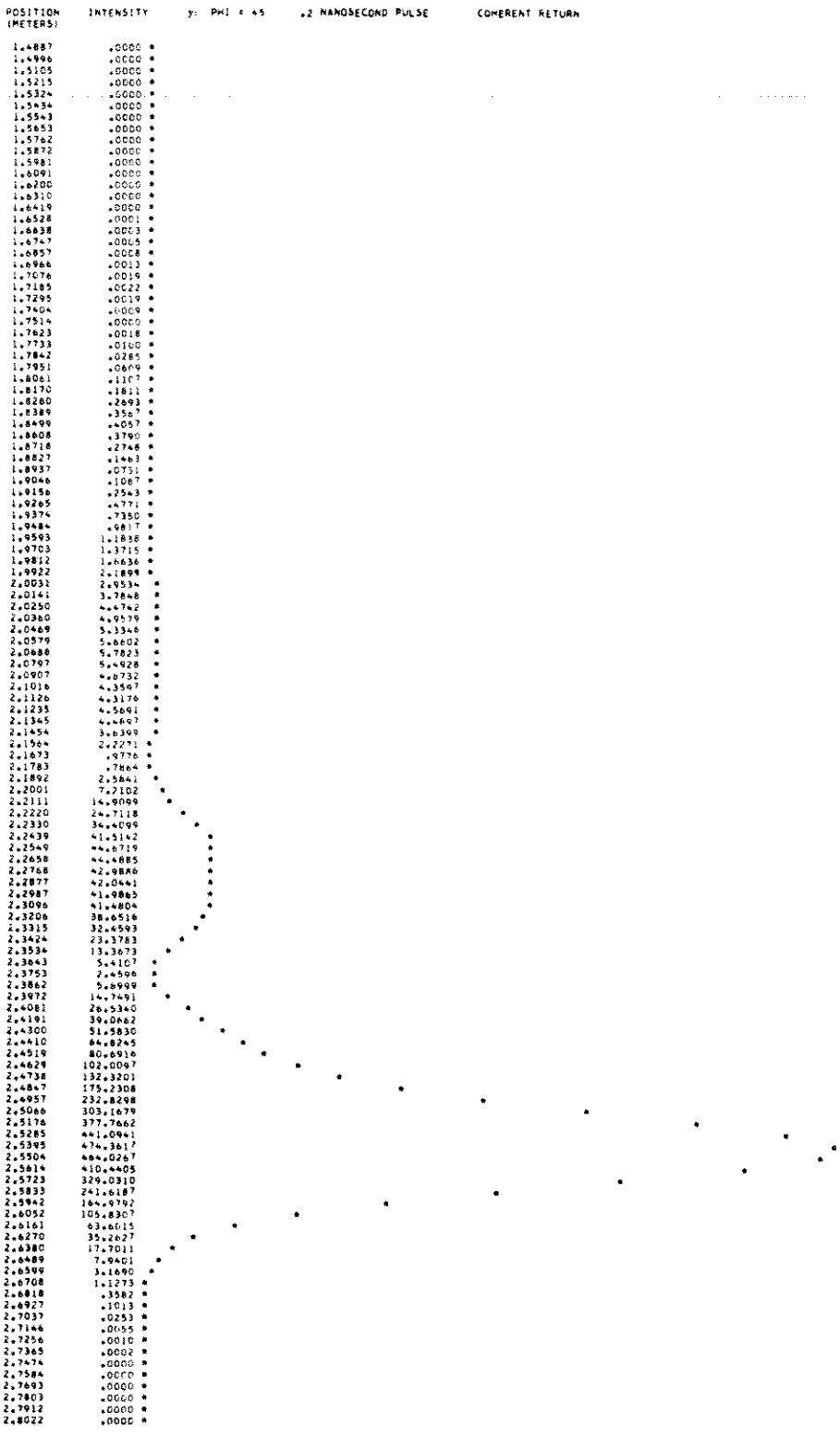

Figure 12. (Cont.)

10. ACCURACY OF THE RESULTS

The cube-corner specifications give a tolerance on the cube-corner dihedral-angle offset of 0".5. In addition, manufacturing errors, material inhomogeneities, or thermal gradients could cause deviations from the perfect optical performance computed by the transfer-function model used in this report. In order to estimate what the effect of these imperfections might be, we have made a set of runs in which the dihedral-angle offset has been varied from 1".5 to 2".5. In addition to computing full gain and centroid range-correction matrices, the half-maximum and half-area range correction has been calculated at a few values of θ_1 and θ_2.

Table 16 lists the average gain and centroid range correction in the 25- to 50-μrad annulus as a function of dihedral-angle offset. The difference from the nominal 2".0 values is listed in the columns headed Δ_{gain} and Δ_{range}. In the last two rows, instead of having all the offsets the same, we have used an equal mixture of the dihedral-angle offsets. This is an attempt to simulate the fact that the actual cube corners have some distribution of offsets within the given tolerance (the last entry would not actually be allowed by the specifications, since it includes 3".0 offsets). The computations were done for a 45° angle of incidence on the satellite; this angle shows fairly pronounced variations of the range correction with velocity aberration (see Table 12j) and thus probably represents a suitable worst-case situation.

Table 16. Gain and centroid range correction vs. dihedral-angle offset. The incidence angle is 45°; Δ_{gain} and Δ_{range} are the differences between the gain or range and the value for 2".0.

λ (Å)	δ	Gain ($\times 10^7$)	Δ_{gain} ($\times 10^7$)	Centroid range correction (m)	Δ_{range} (m)
5300	1".5	8.8817	+0.4571	1.2659	-0.0012
5300	2.0	8.4246	0	1.2671	0
5300	2.5	4.9797	-3.4449	1.2556	-0.0115
6943	1.5	7.5060	+0.2621	1.2660	-0.0016
6943	2.0	7.2439	0	1.2676	0
6943	2.5	5.1599	-2.0840	1.2628	-0.0048
5300	1.5, 2.0, 2.5	7.5191	-0.9055	1.2661	-0.0010
5300	2.0, 2.5, 3.0	5.3068	-3.1178	1.2637	-0.0034

Tables 17 to 20 and Figures 13 and 14 give the complete details for the cases summarized in Table 16. In Table 18, the shift of the energy distribution from small to large values of velocity aberration as the dihedral-angle offset increases can be seen. Figure 13 illustrates the shift in more detail. The largest deviation of the centroid range correction between 25 and 50 μrad occurs in Table 20c for $\delta = 2\overset{''}{.}5$ and $\lambda = 5300$ Å. At 25 μrad, the average centroid range correction is 1.2089 m, which is 5.8 cm less than the nominal centroid range correction of 1.2671 m. Figure 14c shows that deviations of 8 cm occur at some spots; this is, of course, an extremely unlikely situation. The variation of the range correction within the far-field pattern is reduced when a mixture of offsets is used. For example, the deviation of the average centroid range correction at 25 μrad for $\lambda = 5300$ Å is reduced from 1.6 cm for $\delta = 2\overset{''}{.}0$ (Table 20b) to 0.5 cm for a mixture of dihedral angles whose average is $2\overset{''}{.}0$ (Table 20g). The corresponding maximum centroid range deviation is reduced from almost 3 cm (Figure 14b) to a little over 1 cm (Figure 14g). Considering that it is unlikely that all the dihedral-angle offsets are $2\overset{''}{.}5$ and that some mixture of angles is certainly present, the maximum systematic error in the range correction is probably something between the values of 3 and 1 cm in Figures 14b and 14g.

To estimate the uncertainty in the range correction for other pulse-detection methods, we have performed computations for selected points in the far field and for two different dihedral-angle offsets. The data in Table 21 were computed for $\lambda = 5300$ Å, $\phi = 45°$, and a 0.2-nsec incident pulse. By using the reflectivity curve for $\lambda = 5300$ Å in Figure 7, the total range corrections for the three pulse-detection methods are as follows:

centroid	=	1.2669 m
half-maximum	=	1.3030 m
half-area	=	1.2855 m .

The columns headed Δ give the difference between each value and the nominal values above.

Table 17. Gain-function matrices for various dihedral-angle offsets. The angles θ_1 and θ_2, in microradians, are defined in Figure 8. Only half the matrix is presented since $G(\theta_1, \theta_2) = G(-\theta_1, -\theta_2)$.

a: PHI 45 DIHEDRAL ANGLE 1.50 WAVELENGTH 5300

θ_2	GAIN FUNCTION (1.E+7)										
50	2.80	3.13	3.43	3.55	3.37	2.92	2.32	1.69	1.20	.93	.80
45	5.65	6.12	6.46	6.33	5.60	4.60	3.65	2.75	1.91	1.32	1.02
40	8.37	9.27	10.37	10.63	9.32	7.12	5.21	3.86	2.74	1.86	1.34
35	9.36	10.95	13.44	15.02	13.91	10.66	7.40	5.18	3.64	2.49	1.77
30	11.24	12.89	15.36	17.19	16.40	13.06	9.29	6.49	4.50	3.03	2.13
25	16.47	17.30	17.81	17.65	15.89	12.73	9.57	7.13	5.12	3.45	2.34
20	19.52	19.92	19.46	17.83	14.81	11.29	8.68	7.07	5.57	3.93	2.62
15	15.01	15.81	16.54	16.40	14.17	10.65	8.12	7.10	6.15	4.63	3.12
10	10.92	10.99	11.08	12.55	12.88	10.78	8.72	8.03	7.16	5.36	3.56
5	15.63	12.89	8.48	8.77	11.17	11.33	10.40	9.92	8.49	5.84	3.64
0	20.28	15.32	7.75	6.92	10.41	12.12	12.03	11.52	9.42	6.05	3.56
-5	15.63	11.55	6.57	7.37	11.02	12.42	12.09	11.39	9.28	6.07	3.69
-10	10.92	9.25	8.53	10.49	12.26	11.69	10.49	9.75	8.29	5.92	3.89
-15	15.01	14.30	14.14	14.07	12.72	10.34	8.69	8.08	7.16	5.48	3.77
-20	19.52	18.35	16.73	14.72	12.13	9.56	7.95	7.12	6.11	4.65	3.22
-25	16.47	15.29	14.18	13.26	11.81	9.70	7.74	6.28	4.90	3.55	2.50
-30	11.24	10.74	11.37	12.16	11.47	9.12	6.60	4.81	3.49	2.46	1.83
-35	9.36	9.22	10.08	10.54	9.23	6.64	4.42	3.15	2.29	1.62	1.24
-40	8.37	8.03	7.92	7.23	5.61	3.77	2.61	2.04	1.52	1.03	.77
-45	5.65	5.20	4.65	3.85	2.89	2.11	1.68	1.34	.93	.60	.46
-50	2.80	2.50	2.21	1.88	1.53	1.21	.94	.67	.45	.34	.31
	0	5	10	15	20	25	30	35	40	45	50 θ_1

b: PHI 45 DIHEDRAL ANGLE 2.00 WAVELENGTH 5300

θ_2	GAIN FUNCTION (1.E+7)										
50	7.25	7.87	8.31	8.48	8.24	7.57	6.43	4.98	3.58	2.56	1.92
45	9.69	10.40	10.80	10.74	10.20	9.34	8.16	6.57	4.80	3.39	2.50
40	11.40	12.23	12.87	12.82	11.78	10.31	8.98	7.55	5.82	4.24	3.13
35	10.23	11.54	13.30	14.26	13.37	11.31	9.51	8.11	6.55	5.02	3.83
30	7.56	9.19	11.70	13.61	13.42	11.59	9.83	8.50	7.04	5.55	4.38
25	6.73	7.94	9.58	10.88	10.87	9.96	9.23	8.58	7.35	5.82	4.59
20	6.90	7.45	7.88	7.93	7.46	7.18	7.67	8.14	7.54	6.13	4.75
15	4.87	5.23	5.54	5.54	5.06	4.93	5.98	7.35	7.58	6.57	5.16
10	2.90	2.91	2.88	3.42	3.79	4.05	5.23	6.89	7.47	6.78	5.58
5	4.72	3.56	1.73	2.05	3.50	4.64	5.99	7.34	7.45	6.56	5.66
0	6.71	4.57	1.53	1.73	4.03	5.95	7.40	8.23	7.62	6.35	5.63
-5	4.72	3.00	1.19	2.25	4.78	6.66	7.99	8.66	7.97	6.68	5.90
-10	2.90	2.26	2.24	3.64	5.28	6.45	7.72	8.75	8.56	7.46	6.33
-15	4.87	4.59	4.73	5.21	5.62	6.31	7.76	9.13	9.17	7.96	6.37
-20	6.90	6.37	6.12	6.19	6.41	7.12	8.48	9.52	9.16	7.66	5.94
-25	6.73	6.19	6.52	7.38	7.98	8.32	8.84	9.06	8.22	6.72	5.30
-30	7.56	7.21	8.01	9.02	9.05	8.36	7.94	7.64	6.77	5.56	4.51
-35	10.23	9.73	9.75	9.47	8.31	6.96	6.37	6.11	5.37	4.37	3.49
-40	11.40	10.53	9.50	8.13	6.58	5.52	5.21	4.92	4.11	3.13	2.36
-45	9.69	8.72	7.54	6.26	5.19	4.57	4.23	3.66	2.76	1.94	1.40
-50	7.25	6.50	5.63	4.75	3.97	3.36	2.79	2.14	1.49	1.02	.75
	0	5	10	15	20	25	30	35	40	45	50 θ_1

Table 17. (Cont.)

c: PHI 45 DIHEDRAL ANGLE 2.50 WAVELENGTH 5300

GAIN FUNCTION: (1.E+7)

θ_2	0	5	10	15	20	25	30	35	40	45	50
50	9.08	9.57	9.69	9.64	9.50	9.20	8.51	7.36	6.11	5.10	4.24
45	8.45	9.01	9.23	9.26	9.23	9.15	8.77	7.86	6.69	5.73	4.93
40	7.72	8.13	8.24	8.12	7.88	7.61	7.89	7.64	6.97	6.26	5.53
35	5.70	6.14	6.60	6.81	6.52	6.26	6.58	7.00	6.99	6.73	6.19
30	2.98	3.58	4.50	5.21	5.18	5.02	5.55	6.37	6.79	6.89	6.65
25	1.65	2.11	2.73	3.27	3.42	3.76	4.81	5.93	6.42	6.52	6.47
20	1.74	1.86	1.84	1.76	1.79	2.52	4.07	5.49	5.99	5.92	5.78
15	1.50	1.50	1.31	1.04	.93	1.57	3.11	4.69	5.43	5.44	5.20
10	1.31	1.21	.87	.72	.70	1.06	2.20	3.66	4.62	4.98	4.96
5	2.58	2.00	.93	.66	.93	1.28	2.02	3.00	3.76	4.38	4.88
0	3.62	2.60	1.02	.78	1.43	1.98	2.46	2.93	3.32	4.03	5.01
-5	2.58	1.70	.69	.89	1.73	2.35	2.84	3.28	3.69	4.46	5.48
-10	1.31	.92	.69	1.06	1.67	2.30	3.20	4.19	4.92	5.55	6.09
-15	1.50	1.30	1.17	1.25	1.60	2.52	4.10	5.62	6.41	6.61	6.55
-20	1.74	1.47	1.30	1.45	2.02	3.32	5.27	6.86	7.39	7.24	6.96
-25	1.65	1.39	1.55	2.15	2.95	4.17	5.90	7.26	7.65	7.56	7.35
-30	2.98	2.73	2.92	3.34	3.71	4.41	5.78	7.03	7.50	7.53	7.27
-35	5.70	5.21	4.72	4.24	3.91	4.29	5.53	6.67	7.04	6.91	6.41
-40	7.72	6.88	5.74	4.65	4.09	4.46	5.47	6.17	6.13	5.71	5.06
-45	8.45	7.46	6.18	5.04	4.48	4.64	5.06	5.13	4.76	4.27	3.71
-50	9.08	8.10	6.77	5.47	4.58	4.17	3.98	3.69	3.32	2.96	2.54
	0	5	10	15	20	25	30	35	40	45	50 θ_1

d: PHI 45 DIHEDRAL ANGLE 1.50 WAVELENGTH 6943

GAIN FUNCTION: (1.E+7)

θ_2	0	5	10	15	20	25	30	35	40	45	50
50	2.66	2.98	3.53	4.10	4.34	4.02	3.22	2.31	1.62	1.21	.97
45	3.52	3.92	4.61	5.41	5.92	5.72	4.79	3.54	2.46	1.75	1.32
40	5.88	6.16	6.50	6.92	7.19	6.89	5.91	4.54	3.26	2.32	1.70
35	10.09	10.11	9.74	9.23	8.61	7.72	6.46	5.03	3.73	2.74	2.01
30	14.10	13.99	13.22	12.03	10.56	8.65	7.02	5.32	3.94	2.95	2.22
25	15.02	15.08	14.65	13.77	12.36	10.37	8.03	5.83	4.18	3.11	2.40
20	13.19	13.44	13.47	13.38	12.88	11.47	9.15	6.60	4.59	3.39	2.66
15	13.29	13.15	12.31	11.87	11.93	11.46	9.74	7.26	5.12	3.84	3.10
10	19.23	17.83	14.15	11.30	10.53	10.54	9.60	7.60	5.66	4.46	3.70
5	28.27	25.24	18.08	11.93	9.50	9.43	9.12	7.73	6.15	5.12	4.31
0	32.69	28.69	19.77	12.01	8.76	8.67	8.75	7.77	6.47	5.54	4.68
-5	28.27	24.57	16.91	10.55	8.22	8.50	8.66	7.70	6.41	5.47	4.61
-10	19.23	16.79	12.33	9.10	8.45	8.96	8.71	7.38	5.90	4.90	4.11
-15	13.29	12.12	10.46	9.60	9.69	9.63	8.53	6.69	5.05	4.05	3.39
-20	13.19	12.62	11.97	11.46	10.87	9.68	7.78	5.70	4.13	3.25	2.73
-25	15.02	14.45	13.47	12.19	10.60	8.68	6.59	4.74	3.45	2.71	2.26
-30	14.10	13.42	12.12	10.51	8.82	7.13	5.51	4.11	3.07	2.38	1.91
-35	10.09	9.51	8.58	7.61	6.75	5.86	4.83	3.73	2.77	2.05	1.54
-40	5.88	5.58	5.36	5.31	5.30	4.99	4.22	3.18	2.23	1.56	1.13
-45	3.52	3.44	3.65	4.03	4.26	4.01	3.23	2.26	1.47	1.00	.74
-50	2.66	2.63	2.83	3.06	3.07	2.67	1.97	1.26	.81	.60	.50
	0	5	10	15	20	25	30	35	40	45	50 θ_1

Table 17. (Cont.)

e: PHI 45 DIHEDRAL ANGLE 2.00 WAVELENGTH 6943

GAIN FUNCTION (1.E+7)

θ_2	0	5	10	15	20	25	30	35	40	45	50
50	5.31	5.79	6.50	7.15	7.33	6.78	5.68	4.46	3.45	2.72	2.12
45	5.59	6.26	7.36	8.51	9.13	8.75	7.46	5.63	4.40	3.36	2.58
40	6.32	7.02	8.11	9.31	10.04	9.80	8.55	6.82	5.21	3.97	3.03
35	8.28	8.80	9.39	9.97	10.21	9.74	8.53	6.96	5.51	4.33	3.36
30	10.54	10.82	10.88	10.70	10.19	9.20	7.84	6.44	5.28	4.37	3.56
25	10.89	11.13	11.14	10.83	10.06	8.77	7.20	5.81	4.86	4.25	3.68
20	8.67	9.02	9.35	9.56	9.33	8.39	6.90	5.49	4.62	4.21	3.86
15	6.28	6.54	6.76	7.26	7.79	7.69	6.75	5.54	4.77	4.50	4.25
10	6.69	6.39	5.45	5.23	5.98	6.72	6.60	5.90	5.38	5.20	4.89
5	9.50	8.35	5.73	4.16	4.60	5.88	6.56	6.47	6.25	6.11	5.61
0	11.15	9.42	5.89	3.62	3.92	5.53	6.70	7.00	6.96	6.79	6.10
-5	9.50	7.86	4.92	3.31	4.01	5.75	6.91	7.18	7.09	6.86	6.12
-10	6.69	5.64	4.20	3.89	5.01	6.40	7.01	6.86	6.57	6.29	5.67
-15	6.28	5.78	5.47	5.84	6.65	7.12	6.85	6.19	5.71	5.46	5.04
-20	8.67	8.34	8.17	8.16	8.03	7.45	6.46	5.52	4.99	4.77	4.47
-25	10.89	10.45	9.88	9.23	8.39	7.31	6.14	5.19	4.65	4.36	4.02
-30	10.54	10.00	9.33	8.64	7.94	7.09	6.12	5.23	4.57	4.07	3.55
-35	8.28	7.84	7.56	7.49	7.42	7.04	6.24	5.24	4.33	3.61	2.96
-40	6.32	6.06	6.25	6.73	7.06	6.82	5.92	4.72	3.67	2.89	2.28
-45	5.59	5.45	5.75	6.21	6.38	5.90	4.83	3.64	2.71	2.10	1.66
-50	5.31	5.15	5.23	5.30	5.05	4.34	3.35	2.44	1.85	1.50	1.22
	0	5	10	15	20	25	30	35	40	45	50 θ_1

f: PHI 45 DIHEDRAL ANGLE 2.50 WAVELENGTH 6943

GAIN FUNCTION (1.E+7)

θ_2	0	5	10	15	20	25	30	35	40	45	50
50	6.66	7.12	7.67	8.11	8.14	7.64	6.76	5.84	5.07	4.36	3.61
45	6.01	6.65	7.59	8.53	8.99	8.64	7.64	6.47	5.49	4.71	3.95
40	5.06	5.79	6.93	8.16	8.94	8.85	7.98	6.81	5.81	5.00	4.23
35	4.79	5.43	6.34	7.33	8.00	7.99	7.36	6.51	5.77	5.13	4.43
30	5.19	5.60	6.06	6.49	6.68	6.49	6.03	5.59	5.30	5.03	4.54
25	5.10	5.35	5.54	5.61	5.46	5.06	4.63	4.46	4.58	4.72	4.55
20	3.83	4.03	4.25	4.39	4.33	4.00	3.62	3.55	3.90	4.36	4.51
15	2.38	2.52	2.65	2.91	3.19	3.23	3.08	3.11	3.56	4.18	4.50
10	2.36	2.22	1.77	1.72	2.18	2.71	2.98	3.23	3.76	4.38	4.64
5	3.69	3.11	1.81	1.13	1.57	2.51	3.26	3.61	4.41	4.91	4.93
0	4.52	3.63	1.87	.90	1.39	2.64	3.73	4.49	5.10	5.44	5.21
-5	3.69	2.85	1.43	.85	1.61	2.97	4.10	4.85	5.40	5.66	5.35
-10	2.36	1.84	1.21	1.30	2.23	3.38	4.20	4.76	5.25	5.55	5.38
-15	2.38	2.15	2.08	2.46	3.14	3.74	4.11	4.46	4.96	5.39	5.41
-20	3.83	3.66	3.63	3.78	3.96	4.03	4.07	4.34	4.88	5.38	5.47
-25	5.10	4.84	4.64	4.53	4.45	4.35	4.34	4.59	5.07	5.46	5.42
-30	5.19	4.86	4.69	4.72	4.84	4.91	4.93	5.05	5.26	5.37	5.11
-35	4.79	4.50	4.59	4.99	5.43	5.61	5.47	5.26	5.11	4.92	4.50
-40	5.06	4.83	5.08	5.60	6.00	5.94	5.46	4.90	4.50	4.19	3.76
-45	6.01	5.78	5.87	6.07	6.03	5.55	4.78	4.10	3.69	3.43	3.08
-50	6.66	6.35	6.12	5.84	5.34	4.60	3.83	3.28	3.02	2.83	2.51
	0	5	10	15	20	25	30	35	40	45	50 θ_1

Table 17. (Cont.)

g: PHI 45 DIHEDRAL ANGLE 1.50 / 2.00 / 2.50 WAVELENGTH 5300

GAIN FUNCTION (1.E+7)

θ_2	0	5	10	15	20	25	30	35	40	45	50
50	6.18	6.83	7.19	7.23	6.95	6.40	5.58	4.53	3.48	2.66	2.11
45	7.69	8.41	8.83	8.77	8.25	7.50	6.65	5.53	4.23	3.18	2.51
40	8.90	9.85	10.73	10.85	9.85	8.36	7.16	6.09	4.85	3.71	2.92
35	8.18	9.61	11.60	12.74	11.82	9.57	7.65	6.42	5.30	4.26	3.47
30	7.07	8.60	10.93	12.67	12.25	10.09	8.02	6.70	5.62	4.68	4.00
25	8.35	9.23	10.29	10.96	10.37	8.87	7.62	6.80	5.86	4.89	4.23
20	9.68	10.01	10.03	9.48	8.23	7.02	6.68	6.70	6.15	5.13	4.28
15	7.21	7.63	8.11	8.14	7.16	5.98	5.94	6.63	6.58	5.59	4.46
10	4.66	4.72	4.98	6.06	6.45	5.63	5.93	6.89	7.06	6.01	4.69
5	7.13	5.61	3.45	4.18	5.90	6.36	6.76	7.62	7.43	6.04	4.73
0	9.76	7.00	3.13	3.47	5.97	7.18	7.69	8.17	7.45	5.83	4.70
-5	7.13	4.97	2.70	3.96	6.46	7.39	7.61	7.85	7.16	5.79	4.91
-10	4.66	3.94	4.01	5.64	6.87	6.76	6.72	7.16	6.98	6.09	5.25
-15	7.21	6.96	7.13	7.38	6.94	6.23	6.38	7.09	7.14	6.35	5.32
-20	9.68	9.09	8.47	7.90	7.24	6.84	7.13	7.54	7.19	6.17	5.07
-25	8.35	7.72	7.68	8.13	8.33	8.09	7.84	7.50	6.68	5.61	4.71
-30	7.07	6.73	7.56	8.76	8.98	8.12	7.20	6.54	5.75	4.92	4.26
-35	8.18	7.76	8.14	8.40	7.66	6.39	5.62	5.30	4.82	4.18	3.57
-40	8.90	8.14	7.47	6.57	5.41	4.56	4.40	4.37	3.94	3.29	2.68
-45	7.69	6.78	5.77	4.74	3.94	3.61	3.58	3.38	2.85	2.27	1.81
-50	6.18	5.35	4.48	3.70	3.13	2.79	2.50	2.12	1.70	1.37	1.12
	0	5	10	15	20	25	30	35	40	45	50 θ_1

h: PHI 45 DIHEDRAL ANGLE 2.00 / 2.50 / 3.00 WAVELENGTH 5300

GAIN FUNCTION (1.E+7)

θ_2	0	5	10	15	20	25	30	35	40	45	50
50	7.16	7.72	8.00	8.06	7.95	7.60	6.90	5.87	4.83	4.12	3.63
45	7.24	7.80	8.07	8.10	7.96	7.73	7.27	6.38	5.34	4.63	4.18
40	7.26	7.77	8.10	8.08	7.63	7.16	6.89	6.43	5.69	5.07	4.61
35	5.85	6.59	7.59	8.15	7.66	6.76	6.35	6.21	5.85	5.45	5.04
30	3.62	4.58	6.15	7.36	7.24	6.37	5.97	6.00	5.85	5.63	5.37
25	2.75	3.45	4.52	5.41	5.49	5.23	5.45	5.81	5.72	5.47	5.31
20	3.00	3.25	3.48	3.55	3.42	3.67	4.61	5.47	5.53	5.17	4.92
15	2.28	2.42	2.50	2.42	2.19	2.47	3.65	4.90	5.27	4.96	4.59
10	1.51	1.49	1.41	1.60	1.72	2.00	3.06	4.39	4.93	4.74	4.41
5	2.82	2.13	1.03	1.11	1.75	2.32	3.29	4.35	4.64	4.40	4.28
0	4.07	2.80	.98	1.01	2.11	3.00	3.88	4.58	4.51	4.23	4.37
-5	2.82	1.78	.68	1.17	2.35	3.19	4.00	4.68	4.74	4.63	4.84
-10	1.51	1.11	1.02	1.64	2.31	2.88	3.87	4.98	5.47	5.49	5.41
-15	2.28	2.11	2.10	2.23	2.38	2.96	4.33	5.76	6.35	6.16	5.72
-20	3.00	2.74	2.65	2.80	3.12	3.93	5.32	6.51	6.74	6.32	5.83
-25	2.75	2.54	2.95	3.78	4.45	5.05	5.91	6.57	6.54	6.20	5.94
-30	3.62	3.49	4.12	4.96	5.25	5.25	5.65	6.13	6.18	6.03	5.85
-35	5.85	5.51	5.46	5.33	4.90	4.69	5.19	5.80	5.88	5.64	5.27
-40	7.26	6.59	5.77	4.93	4.32	4.40	5.06	5.52	5.34	4.86	4.34
-45	7.24	6.41	5.43	4.58	4.18	4.34	4.70	4.70	4.29	3.81	3.38
-50	7.16	6.33	5.36	4.49	3.95	3.74	3.60	3.35	3.03	2.78	2.52
	0	5	10	15	20	25	30	35	40	45	50 θ_1

Table 18. Gain function vs. velocity aberration for various dihedral-angle offsets. The average and rms deviations are computed around a circle in the far field whose radius is the velocity aberration listed, in microradians, in the first column.

a: PHI 45 DIHEDRAL ANGLE 1.50 WAVELENGTH 5300

AVERAGE GAIN FUNCTION (1.E+7)

0	20.28
5	14.66
10	9.63
15	11.08
20	14.57
25	14.38
30	12.29
35	10.90
40	9.11
45	6.31
50	3.84

R.M.S. FLUCTUATION

0	0.00
5	.45
10	1.36
15	2.92
20	3.31
25	2.36
30	2.18
35	2.38
40	1.90
45	1.17
50	.87

b: PHI 45 DIHEDRAL ANGLE 2.00 WAVELENGTH 5300

AVERAGE GAIN FUNCTION (1.E+7)

0	6.71
5	4.30
10	2.33
15	3.25
20	5.18
25	6.29
30	7.62
35	9.25
40	9.57
45	8.41
50	6.87

R.M.S. FLUCTUATION

0	0.00
5	.19
10	.56
15	1.13
20	1.23
25	1.24
30	1.68
35	1.99
40	1.92
45	1.67
50	1.41

Table 18. (Cont.)

c: PHI 45 DIHEDRAL ANGLE 2.50 WAVELENGTH 5300

AVERAGE GAIN FUNCTION (1.E+7)

0	3.62
5	2.40
10	1.16
15	1.02
20	1.33
25	1.67
30	2.68
35	4.26
40	5.52
45	6.30
50	6.83

R.M.S. FLUCTUATION

0	0.00
5	.10
10	.15
15	.28
20	.31
25	.41
30	.56
35	.94
40	1.33
45	1.48
50	1.56

d: PHI 45 DIHEDRAL ANGLE 1.50 WAVELENGTH 6943

AVERAGE GAIN FUNCTION (1.E+7)

0	32.69
5	27.53
10	19.20
15	12.76
20	10.98
25	11.65
30	11.36
35	9.26
40	6.77
45	5.06
50	3.98

R.M.S. FLUCTUATION

0	0.00
5	.47
10	.45
15	.83
20	1.72
25	2.26
30	1.91
35	1.14
40	.86
45	.96
50	.90

Table 18. (Cont.)

e: PHI 45 DIHEDRAL ANGLE 2.00 WAVELENGTH 6943

AVERAGE GAIN FUNCTION (1.E+7)

0	11.15
5	9.11
10	6.26
15	5.06
20	6.26
25	8.04
30	8.56
35	7.85
40	7.00
45	6.48
50	5.87

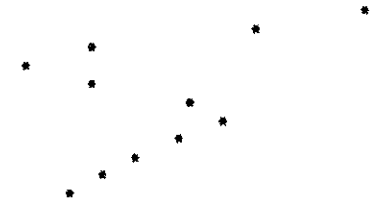

R.M.S. FLUCTUATION

0	0.00
5	.19
10	.41
15	1.05
20	1.73
25	1.95
30	1.62
35	1.26
40	1.32
45	1.44
50	1.30

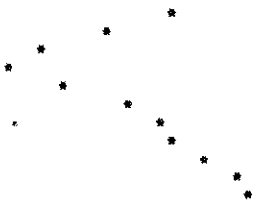

f: PHI 45 DIHEDRAL ANGLE 2.50 WAVELENGTH 6943

AVERAGE GAIN FUNCTION (1.E+7)

0	4.52
5	3.48
10	2.10
15	1.68
20	2.54
25	3.71
30	4.36
35	4.69
40	5.19
45	5.79
50	5.98

R.M.S. FLUCTUATION

0	0.00
5	.10
10	.23
15	.56
20	.88
25	.96
30	.87
35	.94
40	1.16
45	1.29
50	1.24

Table 18. (Cont.)

g: PHI 45 DIHEDRAL ANGLE 1.50 2.00 2.50 WAVELENGTH 5300

AVERAGE GAIN FUNCTION (1.E+7)

0	9.76
5	6.62
10	4.08
15	5.32
20	7.49
25	7.78
30	7.74
35	8.37
40	8.22
45	6.96
50	5.67

R.M.S. FLUCTUATION

0	0.00
5	.23
10	.64
15	1.33
20	1.42
25	1.15
30	1.47
35	1.72
40	1.53
45	1.28
50	1.16

h: PHI 45 DIHEDRAL ANGLE 2.00 2.50 3.00 WAVELENGTH 5300

AVERAGE GAIN FUNCTION (1.E+7)

0	4.07
5	2.60
10	1.29
15	1.57
20	2.34
25	2.85
30	3.86
35	5.25
40	5.94
45	5.94
50	5.88

R.M.S. FLUCTUATION

0	0.00
5	.12
10	.24
15	.47
20	.48
25	.54
30	.81
35	.98
40	1.08
45	1.15
50	1.18

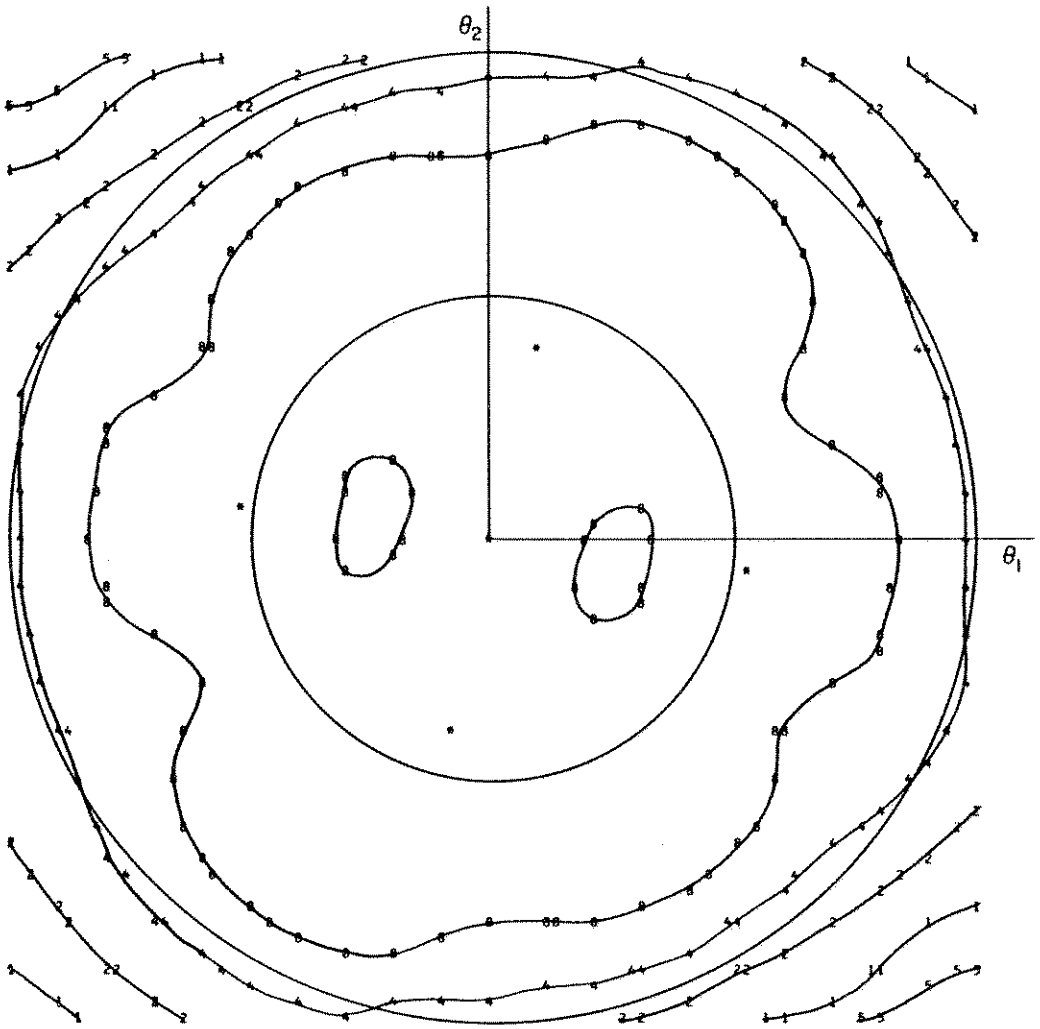

Figure 13. Contour plots of the gain-function matrices given in Table 17. Circles of radius 25 and 50 μrad are shown to mark the minimum and maximum values of velocity aberration. The numbers are the gain function in units of 10^7. The contour levels are plotted at 8, 4, 2, 1, and 0.5×10^7. a: $\phi = 45°$, $\delta = 1\overset{\circ}{.}5$, $\lambda = 5300$ Å.

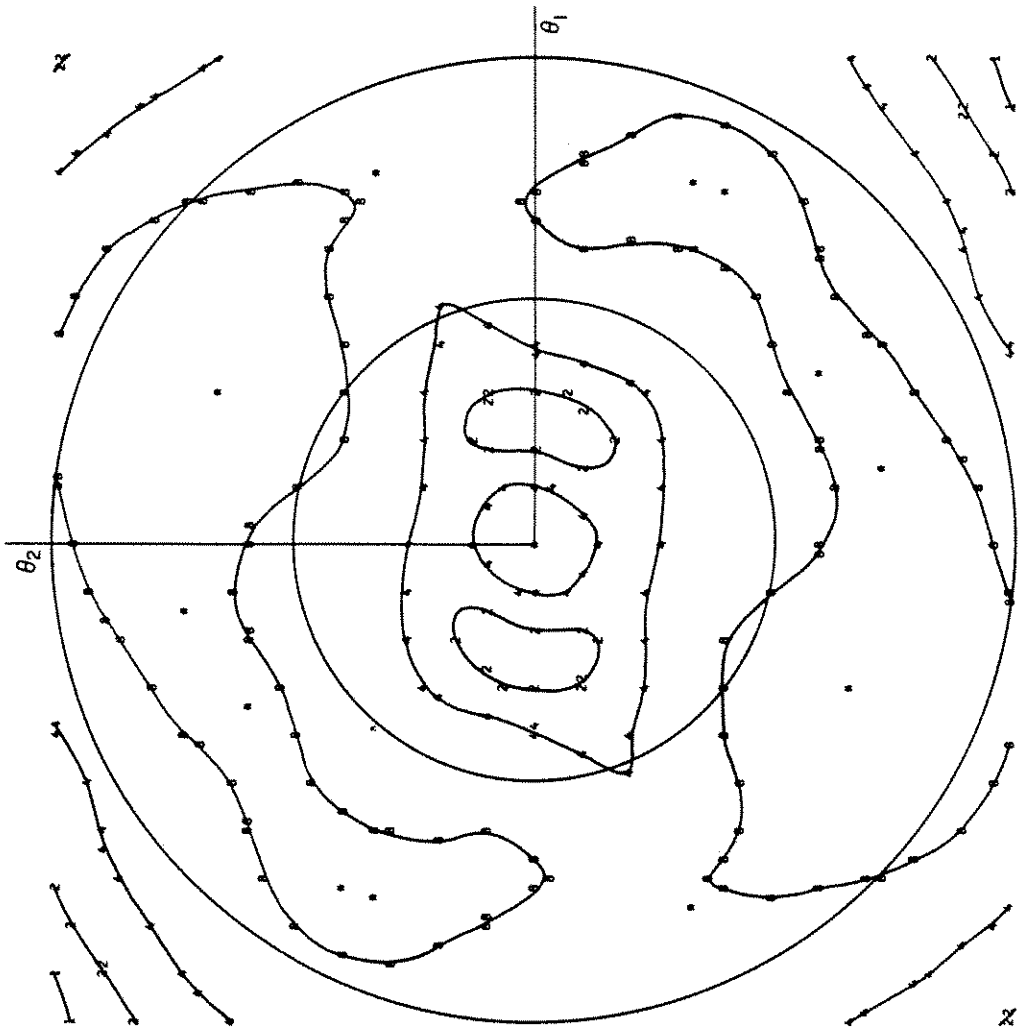

Figure 13b: $\phi = 45°$, $\delta = 2\overset{''}{.}0$, $\lambda = 5300$ Å.

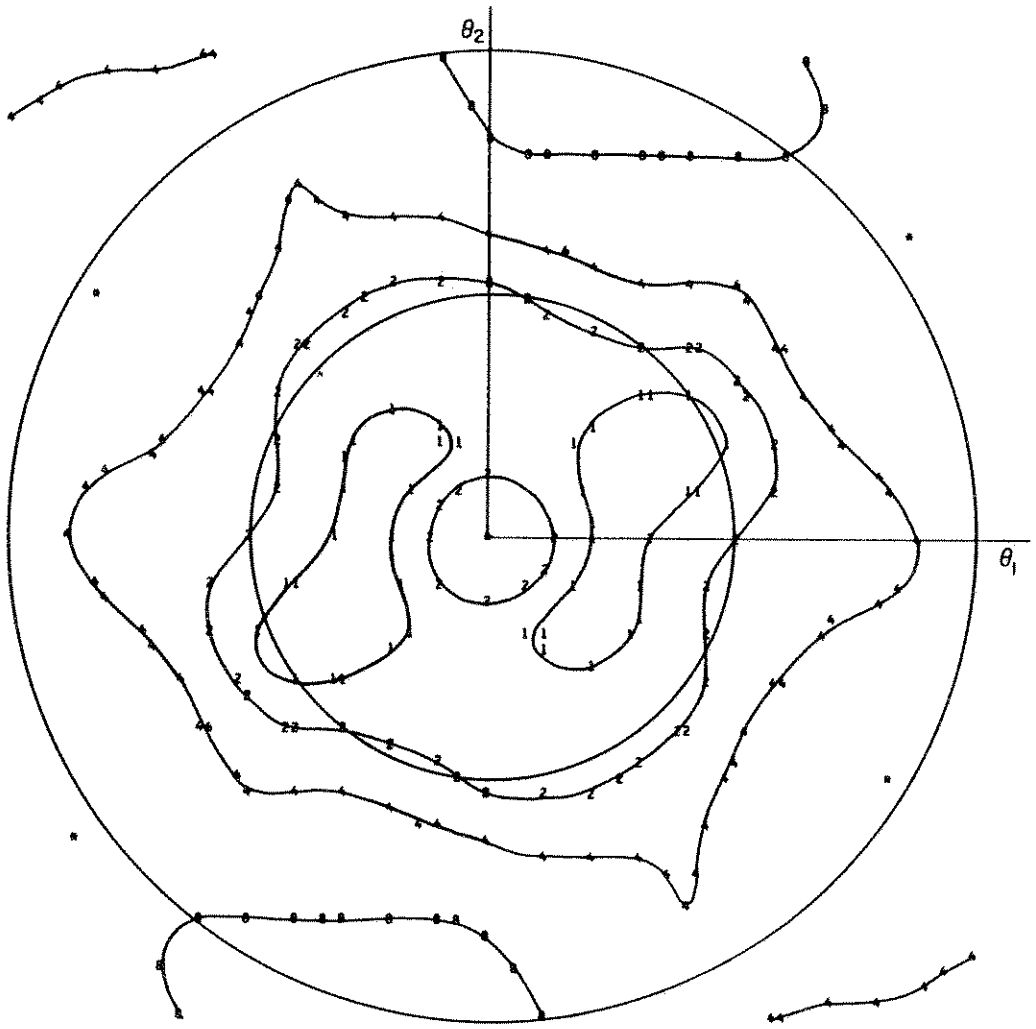

Figure 13c: $\phi = 45°$, $\delta = 2''.5$, $\lambda = 5300$ Å.

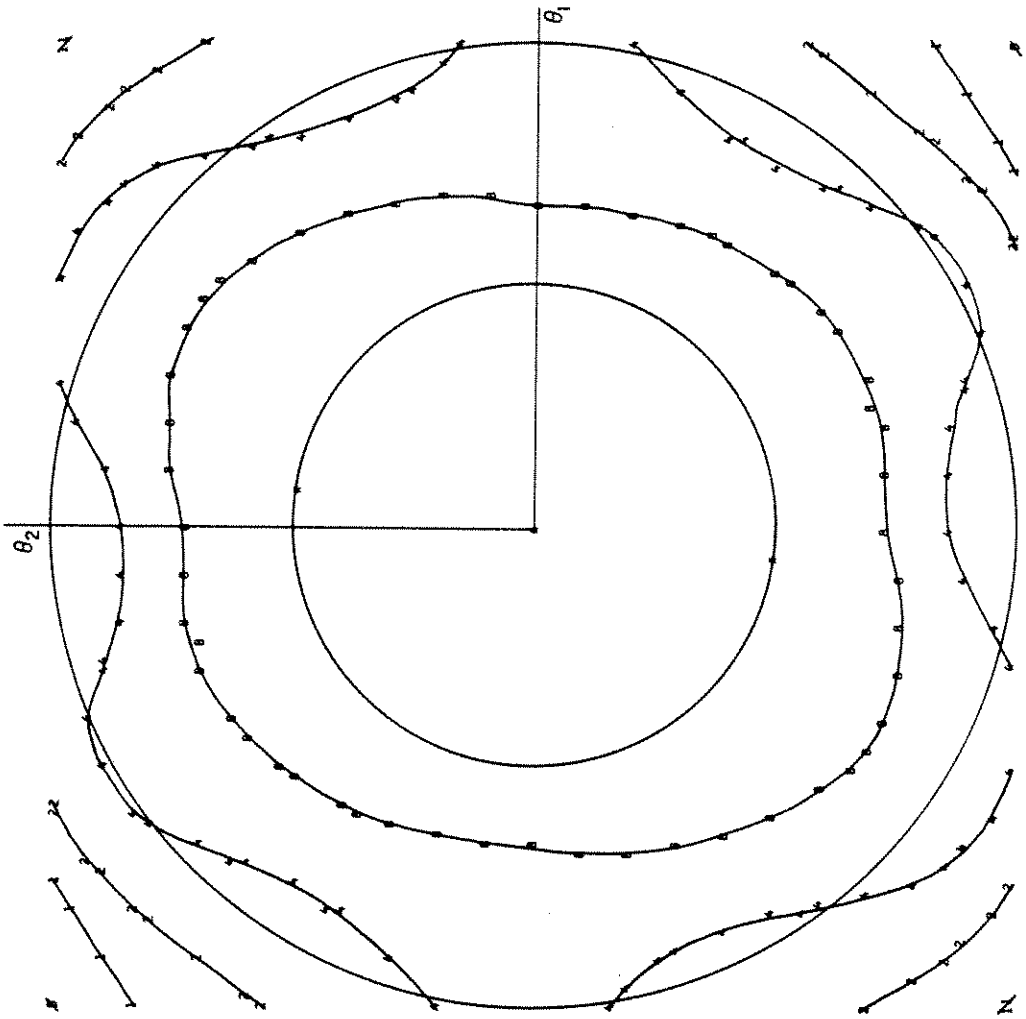

Figure 13d: $\phi = 45°$, $\delta = 1''.5$, $\lambda = 6943$ Å.

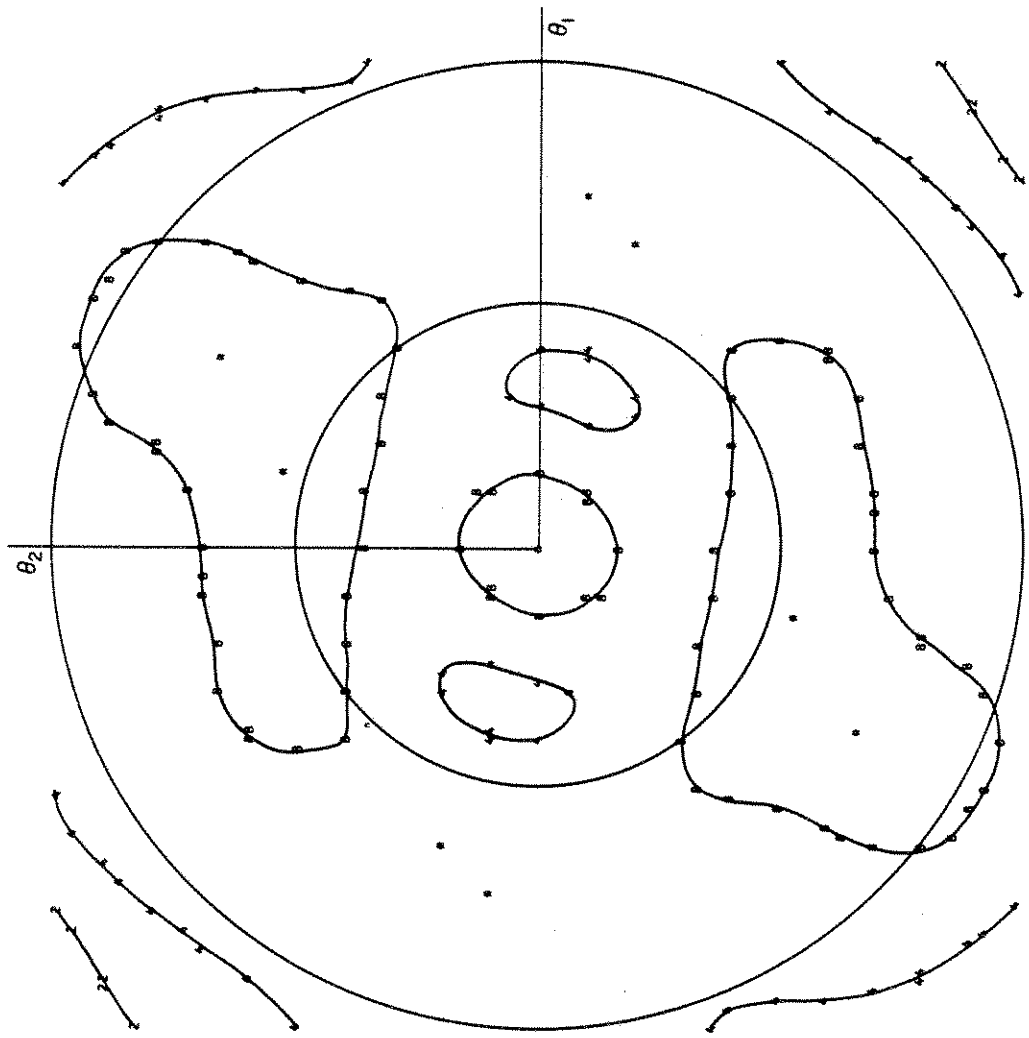

Figure 13e: $\phi = 45°$, $\delta = 2''.0$, $\lambda = 6943$ Å.

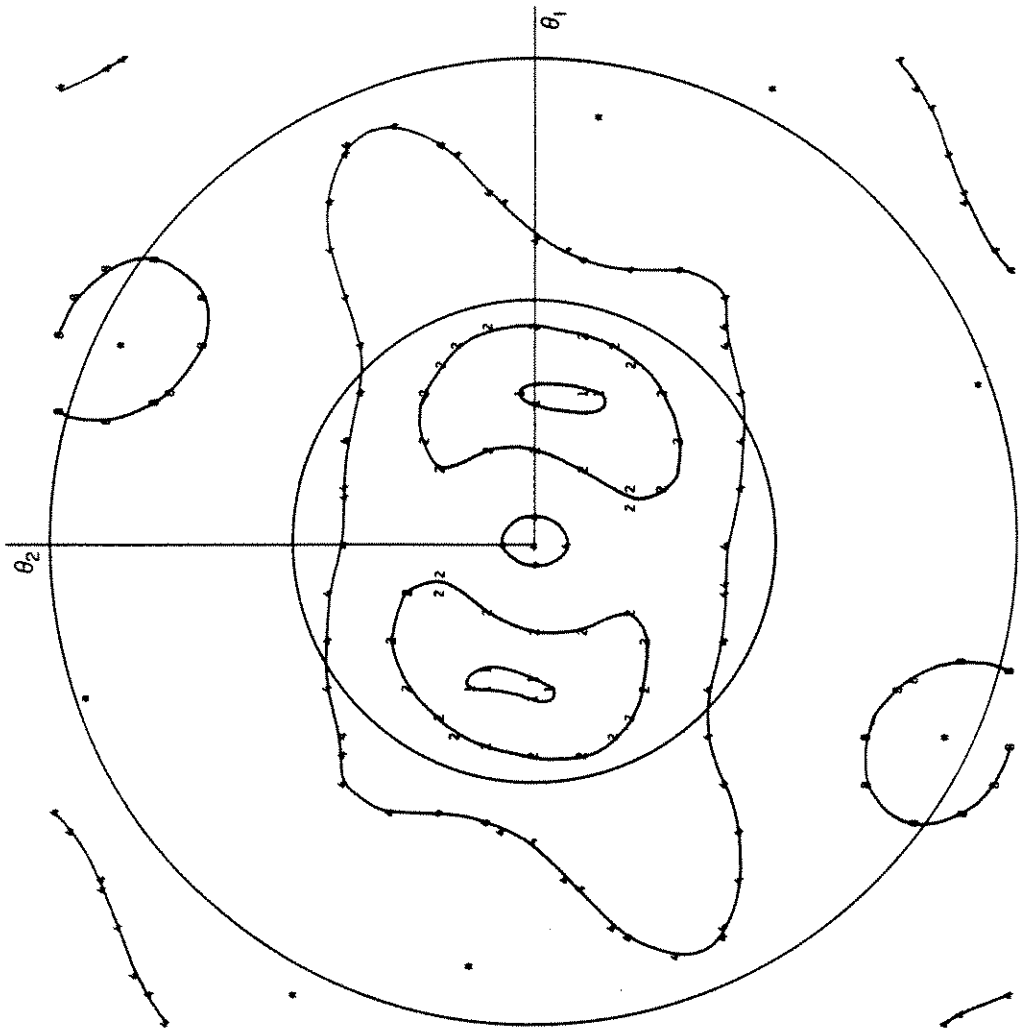

Figure 13f: $\phi = 45°$, $\delta = 2'.5$, $\lambda = 6943$ Å.

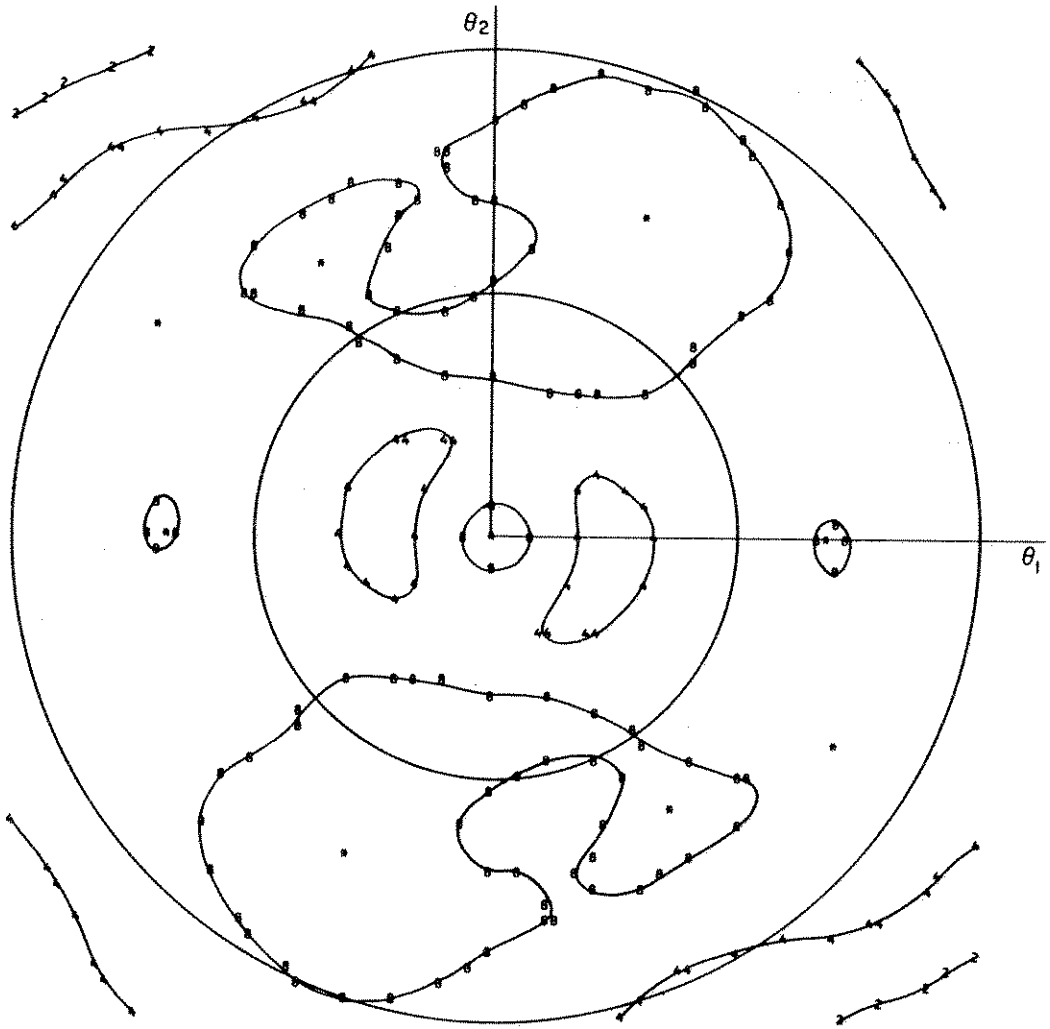

Figure 13g: $\phi = 45°$, $\delta = 1''.5$, $2''.0$, $2''.5$, $\lambda = 5300$ Å.

Table 19. (Cont.)

c: PHI 45 DIHEDRAL ANGLE 2.50 WAVELENGTH 5300

RANGE CORRECTION (METERS)

θ_2	0	5	10	15	20	25	30	35	40	45	50
50	1.271	1.267	1.263	1.261	1.259	1.259	1.257	1.255	1.251	1.250	1.250
45	1.267	1.264	1.260	1.257	1.257	1.258	1.258	1.257	1.255	1.255	1.257
40	1.263	1.259	1.254	1.251	1.250	1.252	1.257	1.260	1.261	1.263	1.265
35	1.255	1.251	1.248	1.247	1.245	1.246	1.254	1.262	1.267	1.271	1.274
30	1.230	1.233	1.239	1.245	1.245	1.246	1.256	1.266	1.273	1.277	1.279
25	1.195	1.208	1.222	1.233	1.238	1.247	1.262	1.273	1.277	1.280	1.281
20	1.207	1.207	1.204	1.203	1.212	1.243	1.268	1.278	1.279	1.279	1.278
15	1.202	1.198	1.187	1.171	1.172	1.230	1.266	1.276	1.276	1.273	1.272
10	1.202	1.190	1.161	1.153	1.161	1.207	1.251	1.265	1.267	1.267	1.267
5	1.251	1.238	1.184	1.159	1.197	1.215	1.237	1.252	1.257	1.261	1.266
0	1.264	1.254	1.202	1.181	1.224	1.232	1.238	1.245	1.250	1.259	1.269
-5	1.251	1.235	1.164	1.192	1.229	1.233	1.239	1.247	1.255	1.265	1.273
-10	1.202	1.177	1.154	1.201	1.222	1.231	1.246	1.259	1.267	1.272	1.275
-15	1.202	1.197	1.196	1.205	1.219	1.243	1.262	1.271	1.274	1.274	1.274
-20	1.207	1.200	1.197	1.212	1.236	1.258	1.271	1.275	1.275	1.274	1.274
-25	1.195	1.189	1.209	1.237	1.252	1.263	1.271	1.274	1.274	1.274	1.275
-30	1.230	1.233	1.243	1.252	1.256	1.261	1.268	1.273	1.274	1.276	1.277
-35	1.255	1.257	1.258	1.257	1.256	1.261	1.270	1.275	1.277	1.278	1.278
-40	1.263	1.265	1.264	1.263	1.264	1.270	1.277	1.279	1.279	1.279	1.277
-45	1.267	1.270	1.270	1.271	1.274	1.278	1.281	1.281	1.279	1.278	1.277
-50	1.271	1.273	1.275	1.276	1.277	1.279	1.279	1.278	1.277	1.277	1.277
	0	5	10	15	20	25	30	35	40	45	50 θ_1

d: PHI 45 DIHEDRAL ANGLE 1.50 WAVELENGTH 6943

RANGE CORRECTION (METERS)

θ_2	0	5	10	15	20	25	30	35	40	45	50
50	1.261	1.263	1.266	1.270	1.271	1.269	1.263	1.251	1.235	1.221	1.212
45	1.260	1.261	1.266	1.271	1.273	1.273	1.269	1.259	1.245	1.230	1.218
40	1.264	1.264	1.265	1.268	1.270	1.270	1.267	1.260	1.249	1.236	1.224
35	1.269	1.269	1.267	1.266	1.265	1.264	1.261	1.255	1.246	1.237	1.228
30	1.272	1.271	1.269	1.267	1.264	1.260	1.255	1.248	1.240	1.234	1.229
25	1.270	1.269	1.268	1.267	1.265	1.261	1.255	1.246	1.238	1.233	1.231
20	1.261	1.261	1.262	1.264	1.266	1.265	1.261	1.252	1.243	1.238	1.239
15	1.254	1.253	1.253	1.257	1.263	1.267	1.266	1.261	1.253	1.250	1.252
10	1.259	1.257	1.251	1.249	1.257	1.267	1.270	1.269	1.265	1.264	1.266
5	1.266	1.264	1.255	1.246	1.251	1.265	1.273	1.275	1.274	1.275	1.276
0	1.269	1.266	1.258	1.247	1.249	1.266	1.276	1.279	1.279	1.279	1.280
-5	1.266	1.264	1.256	1.246	1.252	1.269	1.278	1.279	1.278	1.277	1.277
-10	1.259	1.257	1.251	1.249	1.261	1.273	1.278	1.276	1.272	1.270	1.270
-15	1.254	1.254	1.254	1.260	1.269	1.275	1.275	1.270	1.263	1.259	1.259
-20	1.261	1.263	1.265	1.269	1.272	1.272	1.269	1.262	1.253	1.249	1.250
-25	1.270	1.270	1.270	1.271	1.270	1.268	1.263	1.256	1.249	1.246	1.246
-30	1.272	1.272	1.270	1.269	1.267	1.265	1.262	1.258	1.253	1.250	1.248
-35	1.269	1.269	1.268	1.267	1.268	1.269	1.269	1.266	1.261	1.255	1.248
-40	1.264	1.264	1.266	1.269	1.274	1.276	1.276	1.272	1.264	1.253	1.243
-45	1.260	1.262	1.268	1.274	1.279	1.281	1.278	1.270	1.258	1.243	1.232
-50	1.261	1.264	1.270	1.276	1.278	1.278	1.272	1.259	1.240	1.228	1.224
	0	5	10	15	20	25	30	35	40	45	50 θ_1

Table 19. (Cont.)

e: PHI 45 DIHEDRAL ANGLE 2.00 WAVELENGTH 6943

RANGE CORRECTION (METERS)

θ_2	0	5	10	15	20	25	30	35	40	45	50
50	1.266	1.266	1.267	1.269	1.270	1.268	1.263	1.257	1.250	1.243	1.237
45	1.263	1.264	1.267	1.271	1.273	1.272	1.269	1.262	1.254	1.247	1.240
40	1.260	1.261	1.265	1.269	1.272	1.272	1.270	1.264	1.258	1.251	1.244
35	1.261	1.262	1.264	1.266	1.268	1.268	1.266	1.262	1.258	1.253	1.249
30	1.264	1.263	1.263	1.263	1.263	1.262	1.260	1.257	1.255	1.254	1.253
25	1.262	1.262	1.262	1.262	1.261	1.258	1.255	1.251	1.251	1.254	1.257
20	1.253	1.253	1.255	1.258	1.260	1.259	1.256	1.252	1.252	1.257	1.262
15	1.236	1.237	1.241	1.250	1.258	1.262	1.261	1.259	1.260	1.265	1.269
10	1.236	1.233	1.227	1.235	1.253	1.265	1.269	1.269	1.271	1.275	1.277
5	1.251	1.245	1.230	1.223	1.247	1.268	1.276	1.277	1.279	1.281	1.282
0	1.256	1.251	1.233	1.218	1.246	1.271	1.279	1.281	1.282	1.283	1.283
-5	1.251	1.245	1.228	1.220	1.252	1.274	1.279	1.280	1.279	1.280	1.280
-10	1.236	1.231	1.224	1.237	1.262	1.274	1.276	1.275	1.274	1.274	1.275
-15	1.236	1.237	1.243	1.256	1.267	1.272	1.271	1.268	1.267	1.268	1.269
-20	1.253	1.255	1.259	1.264	1.268	1.268	1.266	1.263	1.262	1.265	1.267
-25	1.262	1.263	1.264	1.266	1.267	1.267	1.265	1.264	1.264	1.267	1.267
-30	1.264	1.264	1.265	1.266	1.268	1.270	1.270	1.270	1.270	1.270	1.269
-35	1.261	1.262	1.264	1.269	1.273	1.276	1.277	1.276	1.274	1.271	1.268
-40	1.260	1.262	1.267	1.273	1.279	1.281	1.281	1.278	1.274	1.269	1.264
-45	1.263	1.265	1.271	1.277	1.281	1.282	1.280	1.275	1.270	1.264	1.260
-50	1.266	1.269	1.273	1.276	1.278	1.278	1.275	1.269	1.264	1.261	1.258
	0	5	10	15	20	25	30	35	40	45	50 θ_1

f: PHI 45 DIHEDRAL ANGLE 2.50 WAVELENGTH 6943

RANGE CORRECTION (METERS)

θ_2	0	5	10	15	20	25	30	35	40	45	50
50	1.267	1.266	1.266	1.266	1.265	1.264	1.261	1.258	1.257	1.255	1.253
45	1.262	1.262	1.264	1.267	1.268	1.267	1.264	1.261	1.258	1.257	1.255
40	1.254	1.256	1.261	1.265	1.268	1.268	1.266	1.263	1.261	1.259	1.258
35	1.248	1.250	1.256	1.261	1.265	1.266	1.265	1.264	1.263	1.263	1.263
30	1.248	1.249	1.252	1.255	1.258	1.259	1.260	1.261	1.264	1.267	1.268
25	1.246	1.246	1.247	1.249	1.250	1.250	1.251	1.256	1.263	1.269	1.272
20	1.233	1.234	1.237	1.242	1.244	1.245	1.245	1.252	1.262	1.271	1.275
15	1.205	1.207	1.213	1.226	1.239	1.245	1.248	1.254	1.265	1.273	1.277
10	1.213	1.205	1.188	1.197	1.230	1.249	1.257	1.263	1.270	1.276	1.278
5	1.245	1.235	1.201	1.169	1.222	1.256	1.267	1.271	1.275	1.279	1.279
0	1.254	1.246	1.211	1.155	1.224	1.262	1.271	1.274	1.276	1.278	1.278
-5	1.245	1.235	1.192	1.157	1.235	1.264	1.270	1.271	1.273	1.275	1.276
-10	1.213	1.199	1.171	1.200	1.247	1.263	1.266	1.266	1.269	1.272	1.273
-15	1.205	1.205	1.214	1.236	1.253	1.259	1.260	1.262	1.266	1.270	1.273
-20	1.233	1.235	1.241	1.249	1.255	1.258	1.259	1.262	1.267	1.272	1.274
-25	1.246	1.247	1.249	1.253	1.258	1.261	1.264	1.268	1.273	1.276	1.276
-30	1.248	1.248	1.251	1.257	1.264	1.269	1.272	1.275	1.277	1.278	1.277
-35	1.248	1.249	1.256	1.264	1.272	1.276	1.278	1.278	1.278	1.277	1.275
-40	1.254	1.257	1.264	1.271	1.277	1.279	1.279	1.277	1.276	1.275	1.273
-45	1.262	1.265	1.270	1.274	1.277	1.278	1.276	1.274	1.274	1.273	1.273
-50	1.267	1.269	1.272	1.274	1.275	1.275	1.273	1.273	1.274	1.275	1.274
	0	5	10	15	20	25	30	35	40	45	50 θ_1

Table 19. (Cont.)

g: PHI 45 DIHEDRAL ANGLE 1.50 / 2.00 / 2.50 WAVELENGTH 5300

RANGE CORRECTION (METERS)

θ_2	0	5	10	15	20	25	30	35	40	45	50
50	1.266	1.264	1.262	1.261	1.259	1.258	1.255	1.250	1.242	1.236	1.233
45	1.265	1.263	1.261	1.259	1.257	1.256	1.255	1.252	1.246	1.239	1.238
40	1.264	1.263	1.262	1.261	1.259	1.255	1.253	1.252	1.249	1.245	1.244
35	1.259	1.260	1.264	1.267	1.265	1.259	1.254	1.253	1.252	1.252	1.253
30	1.252	1.256	1.263	1.268	1.267	1.263	1.258	1.257	1.257	1.258	1.260
25	1.255	1.256	1.259	1.262	1.262	1.260	1.259	1.262	1.263	1.264	1.264
20	1.258	1.257	1.257	1.256	1.253	1.251	1.257	1.265	1.268	1.267	1.266
15	1.245	1.246	1.250	1.254	1.252	1.249	1.256	1.267	1.271	1.269	1.265
10	1.221	1.220	1.230	1.251	1.259	1.258	1.262	1.270	1.273	1.270	1.265
5	1.247	1.234	1.211	1.243	1.267	1.270	1.272	1.276	1.276	1.271	1.266
0	1.260	1.248	1.210	1.241	1.271	1.275	1.275	1.277	1.276	1.270	1.267
-5	1.247	1.233	1.206	1.252	1.272	1.273	1.271	1.273	1.272	1.269	1.268
-10	1.221	1.218	1.236	1.263	1.270	1.266	1.265	1.268	1.269	1.268	1.267
-15	1.245	1.249	1.258	1.266	1.267	1.263	1.265	1.269	1.270	1.268	1.265
-20	1.258	1.259	1.262	1.266	1.268	1.270	1.272	1.274	1.272	1.267	1.263
-25	1.255	1.256	1.262	1.270	1.275	1.277	1.276	1.275	1.271	1.266	1.263
-30	1.252	1.255	1.266	1.275	1.279	1.278	1.275	1.273	1.270	1.267	1.266
-35	1.259	1.262	1.270	1.275	1.276	1.274	1.272	1.272	1.271	1.270	1.268
-40	1.264	1.266	1.269	1.271	1.270	1.270	1.272	1.274	1.273	1.271	1.269
-45	1.265	1.266	1.268	1.269	1.270	1.273	1.276	1.276	1.273	1.270	1.267
-50	1.266	1.267	1.269	1.271	1.274	1.276	1.276	1.272	1.268	1.266	1.266

θ_1

h: PHI 45 DIHEDRAL ANGLE 2.00 / 2.50 / 3.00 WAVELENGTH 5300

RANGE CORRECTION (METERS)

θ_2	0	5	10	15	20	25	30	35	40	45	50
50	1.267	1.264	1.261	1.259	1.258	1.257	1.255	1.251	1.247	1.246	1.249
45	1.266	1.263	1.259	1.257	1.256	1.257	1.257	1.255	1.252	1.252	1.256
40	1.265	1.261	1.258	1.255	1.253	1.253	1.256	1.258	1.258	1.259	1.263
35	1.258	1.256	1.257	1.258	1.256	1.253	1.255	1.260	1.263	1.266	1.269
30	1.241	1.246	1.255	1.261	1.261	1.258	1.259	1.264	1.268	1.271	1.274
25	1.227	1.235	1.247	1.255	1.257	1.258	1.264	1.270	1.273	1.274	1.275
20	1.233	1.233	1.236	1.239	1.241	1.251	1.266	1.275	1.276	1.275	1.273
15	1.217	1.217	1.220	1.223	1.222	1.238	1.262	1.274	1.275	1.273	1.270
10	1.191	1.184	1.184	1.209	1.222	1.235	1.258	1.270	1.272	1.269	1.267
5	1.246	1.228	1.167	1.195	1.236	1.249	1.261	1.269	1.269	1.267	1.267
0	1.263	1.249	1.179	1.199	1.248	1.257	1.264	1.269	1.268	1.266	1.269
-5	1.246	1.225	1.140	1.215	1.250	1.255	1.260	1.266	1.268	1.269	1.271
-10	1.191	1.173	1.185	1.233	1.246	1.248	1.258	1.267	1.270	1.271	1.272
-15	1.217	1.221	1.233	1.244	1.247	1.254	1.266	1.273	1.274	1.272	1.271
-20	1.233	1.234	1.242	1.253	1.261	1.268	1.274	1.276	1.274	1.271	1.270
-25	1.227	1.231	1.250	1.266	1.273	1.274	1.275	1.275	1.272	1.270	1.271
-30	1.241	1.248	1.263	1.272	1.275	1.273	1.273	1.273	1.272	1.272	1.273
-35	1.258	1.263	1.268	1.272	1.271	1.270	1.272	1.275	1.275	1.275	1.274
-40	1.265	1.267	1.269	1.270	1.270	1.273	1.276	1.278	1.277	1.276	1.274
-45	1.266	1.268	1.270	1.271	1.274	1.277	1.279	1.279	1.277	1.276	1.274
-50	1.267	1.269	1.271	1.273	1.275	1.277	1.277	1.276	1.275	1.276	1.276

θ_1

Table 20. Centroid range correction vs. velocity aberration for various dihedral-angle offsets. The average and rms deviations are computed around a circle in the far field whose radius is the velocity aberration listed, in microradians, in the first column.

a: PHI 45 DIHEDRAL ANGLE 1.50 WAVELENGTH 5300

AVERAGE RANGE CORRECTION (METERS)

0	1.2561
5	1.2447
10	1.2298
15	1.2476
20	1.2645
25	1.2668
30	1.2661
35	1.2685
40	1.2694
45	1.2649
50	1.2577

R.M.S. FLUCTUATION

0	0.0000
5	.0012
10	.0048
15	.0032
20	.0048
25	.0061
30	.0069
35	.0081
40	.0076
45	.0068
50	.0078

b: PHI 45 DIHEDRAL ANGLE 2.00 WAVELENGTH 5300

AVERAGE RANGE CORRECTION (METERS)

0	1.2570
5	1.2347
10	1.1811
15	1.2113
20	1.2425
25	1.2509
30	1.2599
35	1.2683
40	1.2708
45	1.2699
50	1.2694

R.M.S. FLUCTUATION

0	0.0000
5	.0031
10	.0138
15	.0076
20	.0082
25	.0082
30	.0066
35	.0052
40	.0052
45	.0056
50	.0060

c: PHI 45 DIHEDRAL ANGLE 2.50 WAVELENGTH 5300

AVERAGE RANGE CORRECTION (METERS)

0	1.2643
5	1.2479
10	1.1950
15	1.1811
20	1.1986
25	1.2089
30	1.2362
35	1.2544
40	1.2612
45	1.2658
50	1.2699

R.M.S. FLUCTUATION

0	0.0000
5	.0024
10	.0058
15	.0134
20	.0180
25	.0157
30	.0060
35	.0077
40	.0090
45	.0079
50	.0068

d: PHI 45 DIHEDRAL ANGLE 1.50 WAVELENGTH 6943

AVERAGE RANGE CORRECTION (METERS)

0	1.2687
5	1.2655
10	1.2580
15	1.2510
20	1.2561
25	1.2665
30	1.2708
35	1.2690
40	1.2651
45	1.2631
50	1.2631

R.M.S. FLUCTUATION

0	0.0000
5	.0003
10	.0006
15	.0027
20	.0041
25	.0025
30	.0034
35	.0047
40	.0062
45	.0097
50	.0127

Table 20. (Cont.)

e: PHI 45 DIHEDRAL ANGLE 2.00 WAVELENGTH 6943

AVERAGE RANGE CORRECTION (METERS)

0	1.2561
5	1.2492
10	1.2342
15	1.2295
20	1.2486
25	1.2633
30	1.2672
35	1.2666
40	1.2666
45	1.2688
50	1.2704

R.M.S. FLUCTUATION

0	0.0000
5	.0007
10	.0014
15	.0063
20	.0031
25	.0045
30	.0060
35	.0064
40	.0072
45	.0080
50	.0078

f: PHI 45 DIHEDRAL ANGLE 2.50 WAVELENGTH 6943

AVERAGE RANGE CORRECTION (METERS)

0	1.2544
5	1.2426
10	1.2085
15	1.1872
20	1.2244
25	1.2480
30	1.2546
35	1.2578
40	1.2634
45	1.2691
50	1.2717

R.M.S. FLUCTUATION

0	0.0000
5	.0015
10	.0031
15	.0175
20	.0061
25	.0071
30	.0079
35	.0077
40	.0068
45	.0058
50	.0052

g: PHI 45 DIHEDRAL ANGLE 1.50 / 2.00 / 2.50 WAVELENGTH 5300

AVERAGE RANGE CORRECTION (METERS)

0	1.2598
5	1.2437
10	1.2184
15	1.2415
20	1.2603
25	1.2620
30	1.2629
35	1.2674
40	1.2688
45	1.2666
50	1.2651

R.M.S. FLUCTUATION

0	0.0000
5	.0019
10	.0053
15	.0033
20	.0060
25	.0067
30	.0073
35	.0066
40	.0056
45	.0055
50	.0057

h: PHI 45 DIHEDRAL ANGLE 2.00 / 2.50 / 3.00 WAVELENGTH 5300

AVERAGE RANGE CORRECTION (METERS)

0	1.2625
5	1.2414
10	1.1831
15	1.2029
20	1.2332
25	1.2418
30	1.2545
35	1.2650
40	1.2675
45	1.2673
50	1.2682

R.M.S. FLUCTUATION

0	0.0000
5	.0031
10	.0100
15	.0088
20	.0091
25	.0098
30	.0078
35	.0057
40	.0062
45	.0066
50	.0063

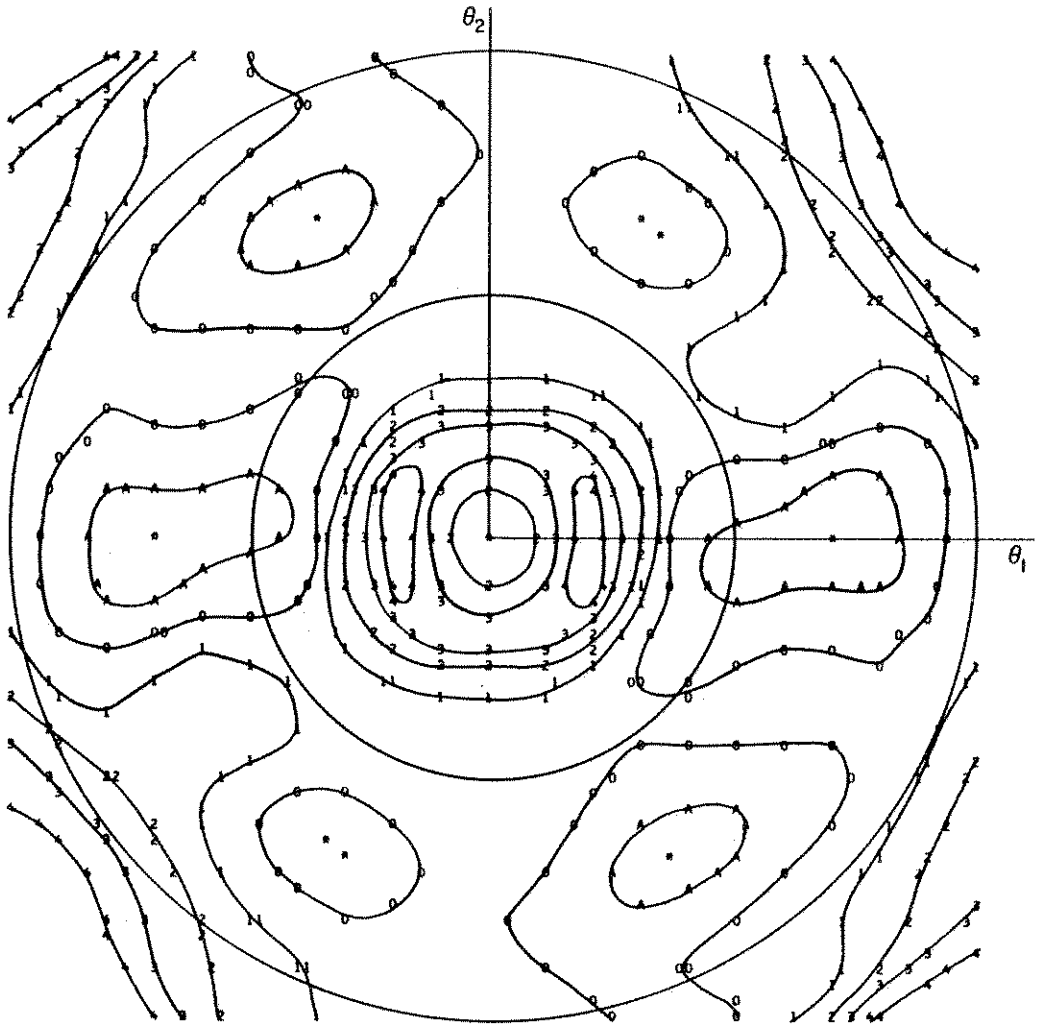

Figure 14. Contour plots of the centroid range-correction matrices given in Table 19. Circles of radius 25 and 50 μrad are shown to mark the minimum and maximum values of the velocity aberration. The symbol B represents a centroid range correction minus the average centroid range correction in the 25- to 50-μrad annulus equal to +2 cm; A equals +1 cm; 0 equals 0 cm; and 1 through 8 equal -1 through -8 cm. a: $\phi = 45°$, $\delta = 1\overset{\circ}{.}5$, $\lambda = 5300$ Å.

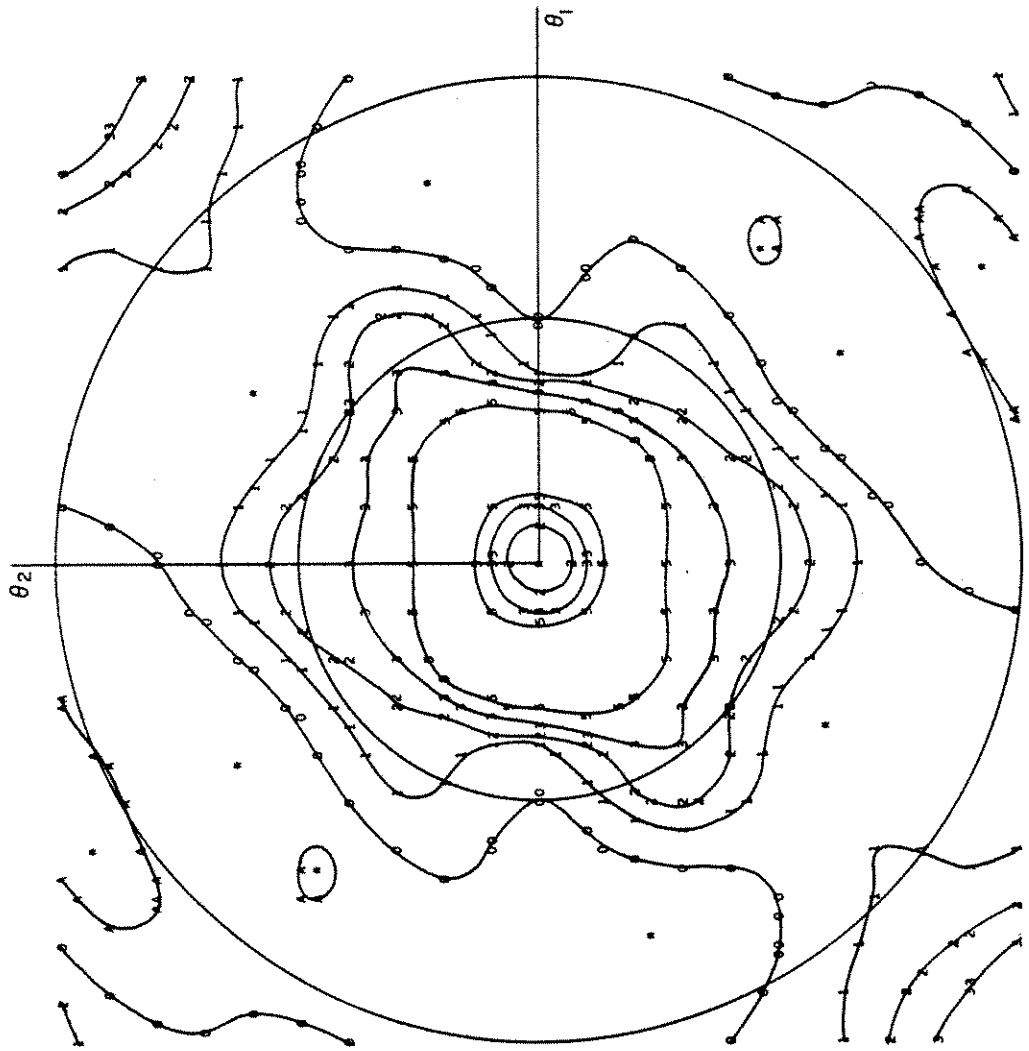

Figure 14b: $\phi = 45°$, $\delta = 2\overset{''}{.}0$, $\lambda = 5300$ Å.

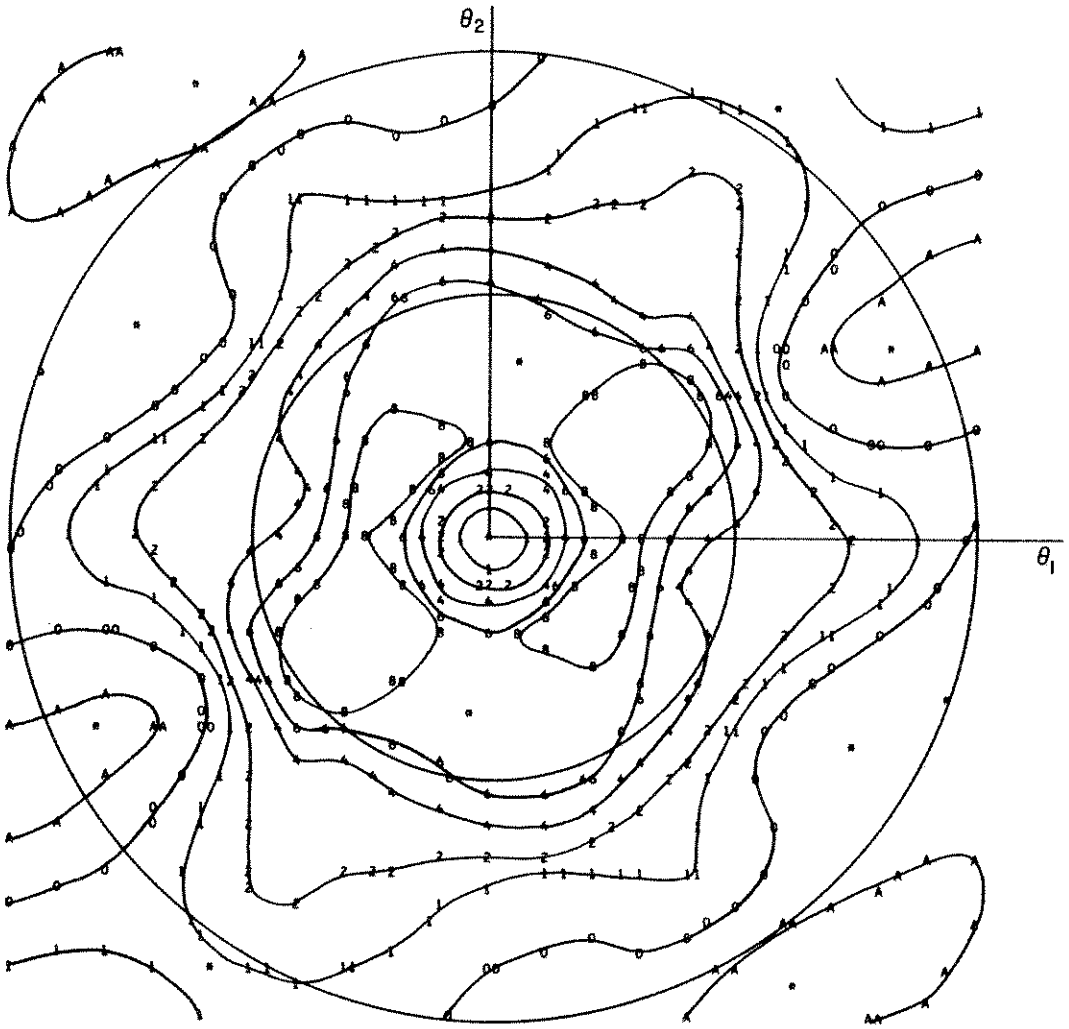

Figure 14c: $\phi = 45°$, $\delta = 2\overset{''}{.}5$, $\lambda = 5300$ Å.

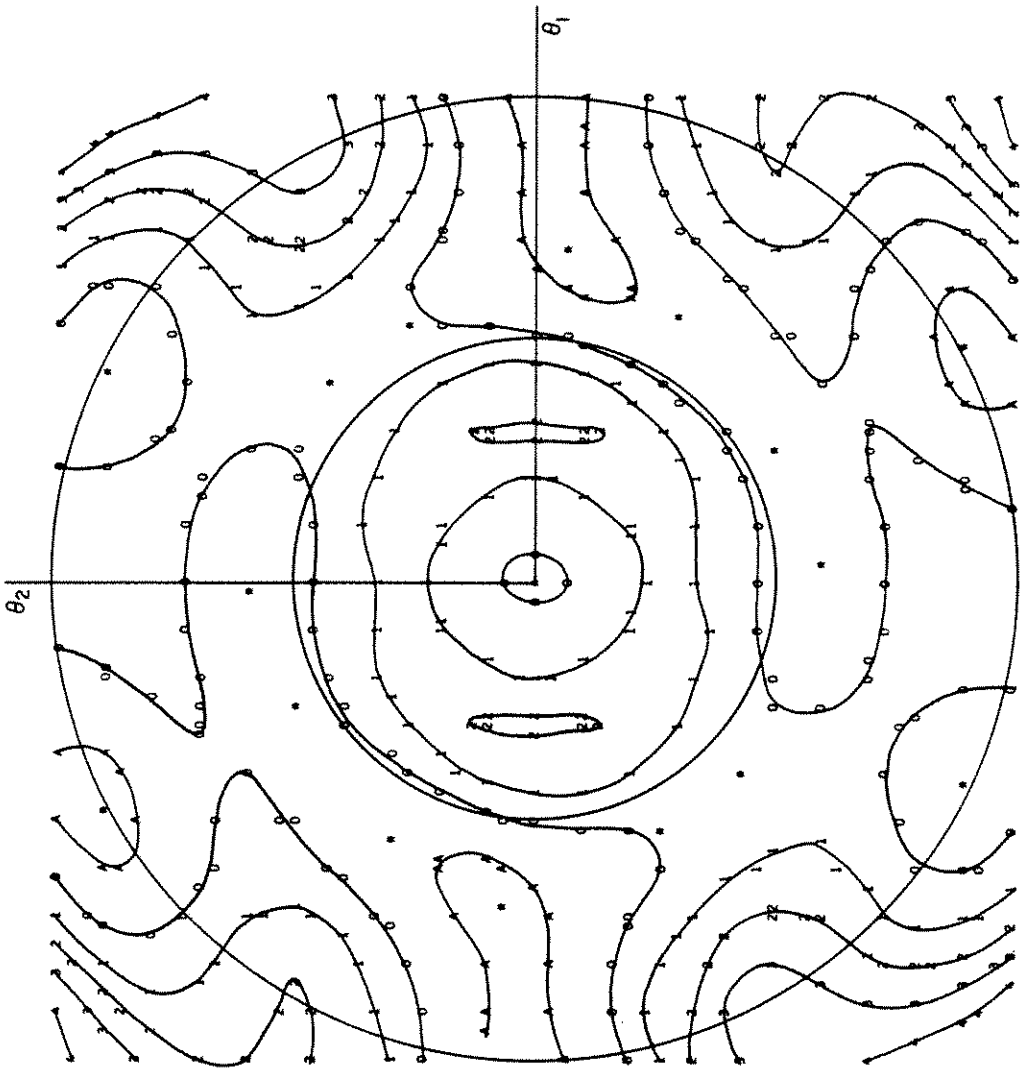

Figure 14d: $\phi = 45°$, $\delta = 1''.5$, $\lambda = 6943$ Å.

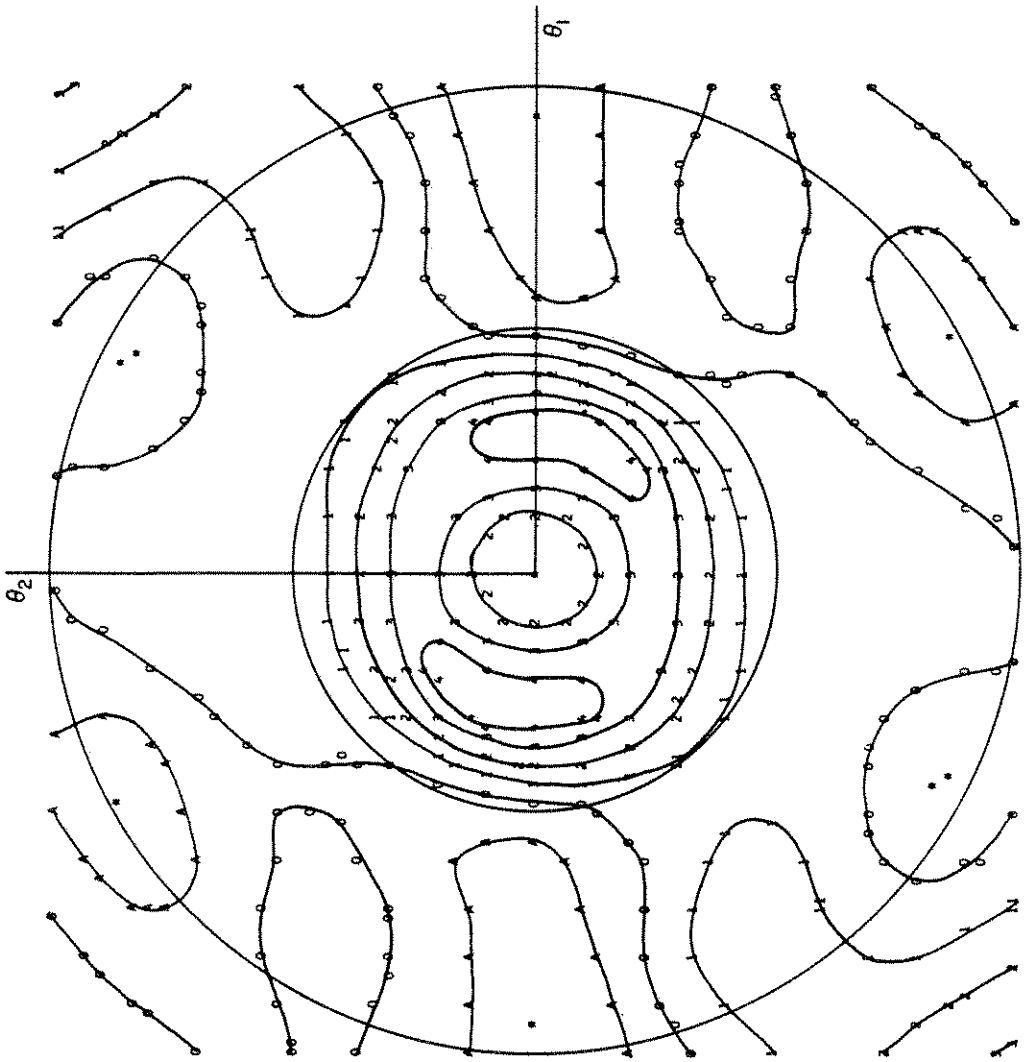

Figure 14e: $\phi = 45°$, $\delta = 2''.0$, $\lambda = 6943$ Å.

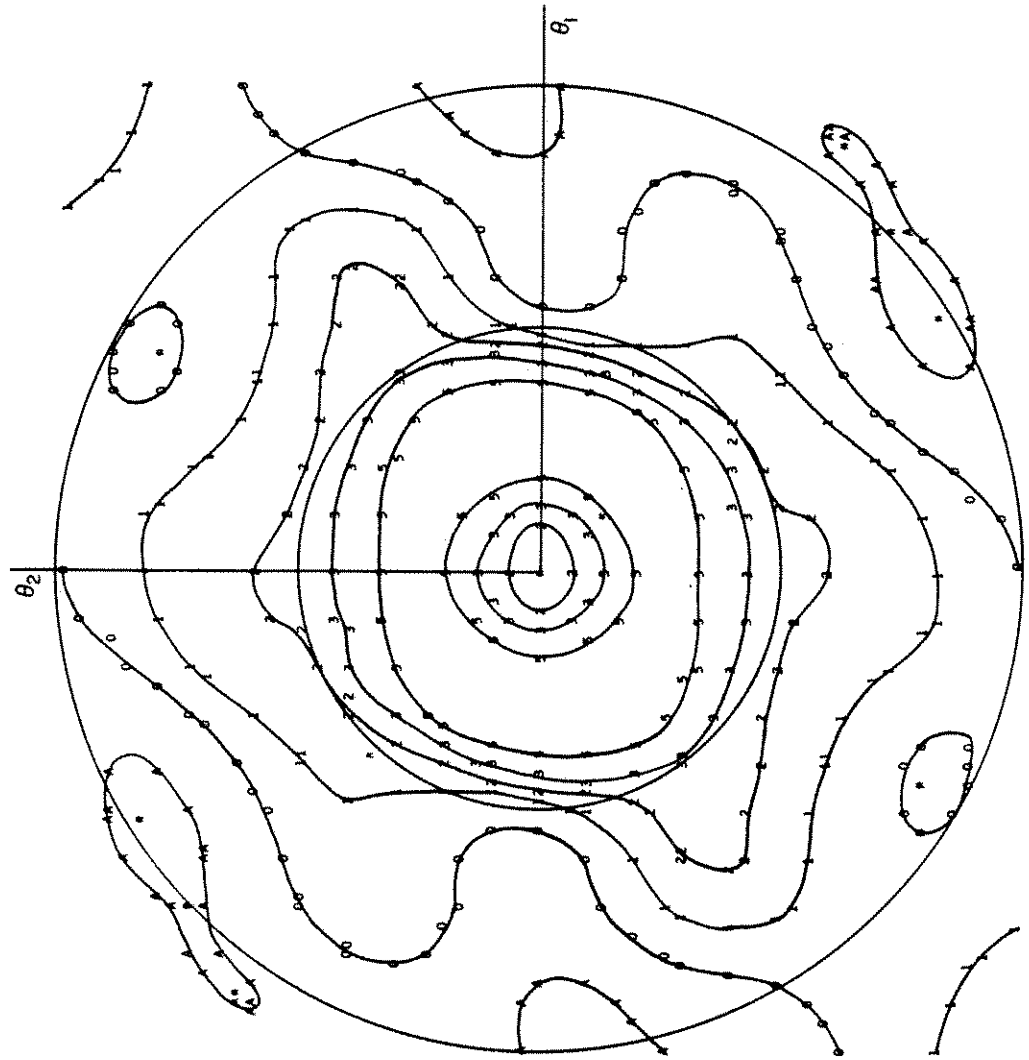

Figure 14f: $\phi = 45°$, $\delta = 2''.5$, $\lambda = 6943$ Å.

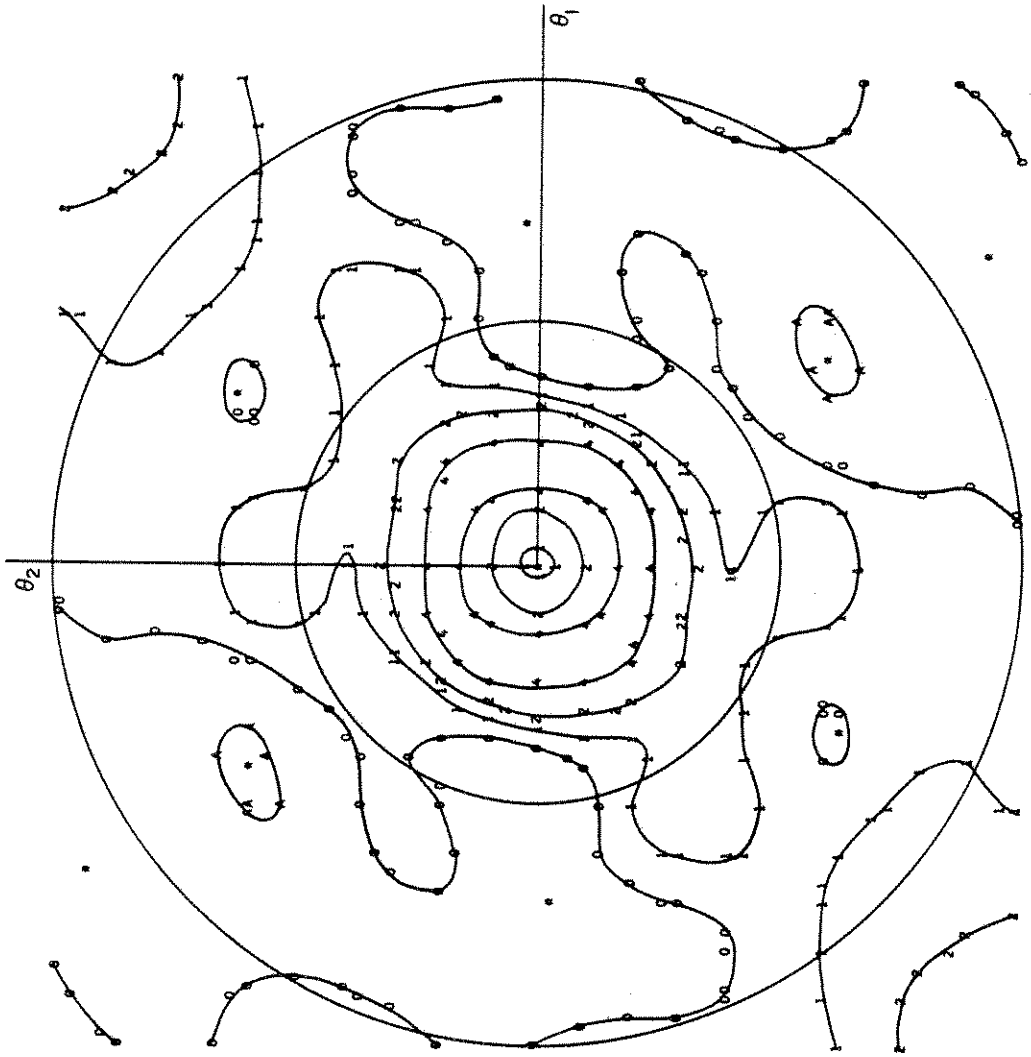

Figure 14g: $\phi = 45°$, $\delta = 1''.5$, $2''.0$, $2''.5$, $\lambda = 5300$ Å.

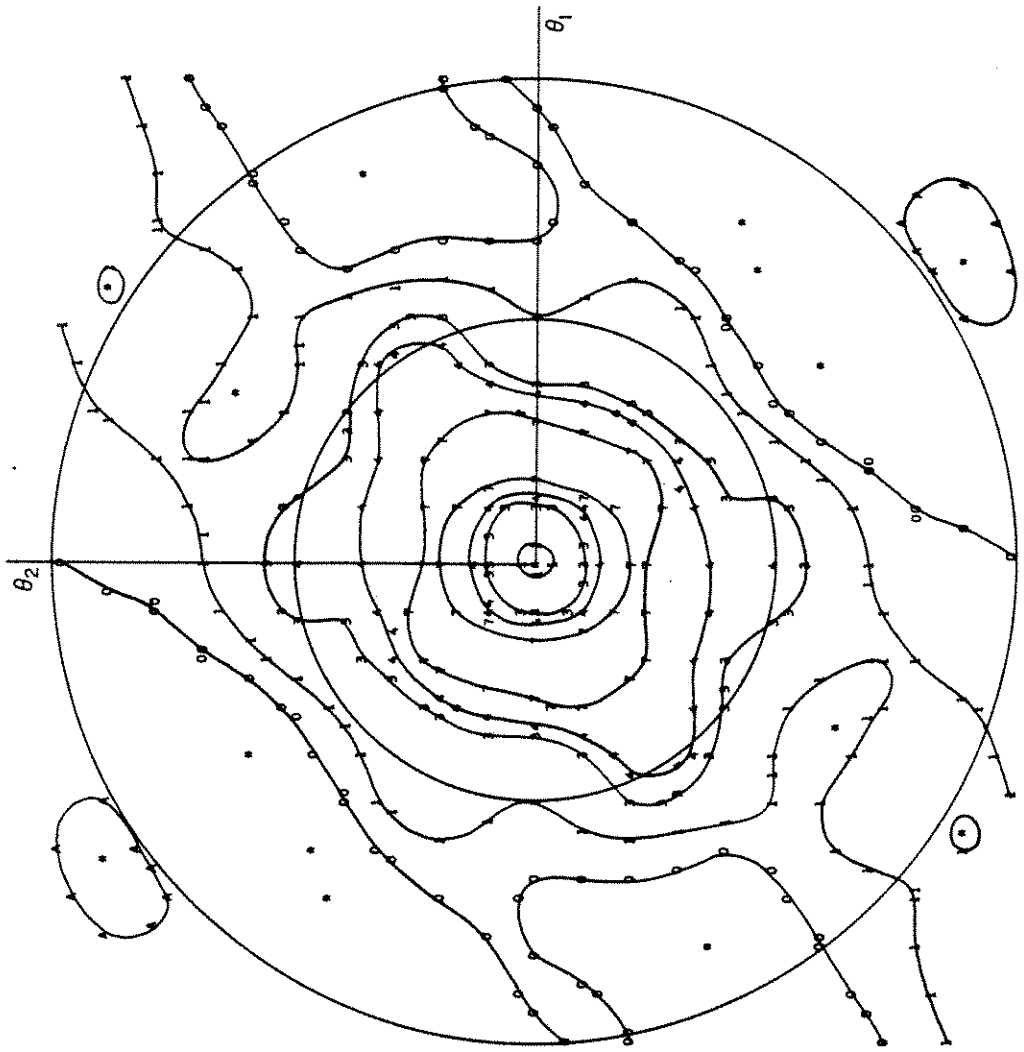

Figure 14h: $\phi = 45°$, $\delta = 2\overset{''}{.}0$, $2\overset{''}{.}5$, $3\overset{''}{.}0$, $\lambda = 5300$ Å.

Table 21. Half-maximum and half-area range corrections vs. velocity aberration. Pulse length = 0.2 nsec, $\phi = 45°$, $\lambda = 5300$ Å.

θ_1 (μrad)	θ_2 (μrad)	Centroid (m)	Δ (m)	Half-maximum (m)	Δ (m)	Half-area (m)	Δ (m)
			a: Dihedral angle = 2".0				
0	0	1.2570	-0.0099	1.3037	+0.0007	1.2873	+0.0018
0	25	1.2405	-0.0264	1.2979	-0.0051	1.2597	-0.0258
0	50	1.2698	+0.0029	1.3028	-0.0002	1.2863	+0.0008
25	0	1.2679	+0.0010	1.3021	-0.0009	1.2857	+0.0002
50	0	1.2715	+0.0046	1.3033	+0.0003	1.2893	+0.0038
50	50	1.2218	-0.0451	1.2994	-0.0036	1.2309	-0.0546
			b: Dihedral angle = 2".5				
0	0	1.2643	-0.0026	1.3028	-0.0002	1.2912	+0.0057
0	25	1.1954	-0.0715	1.2808	-0.0222	1.2104	-0.0751
0	50	1.2708	+0.0039	1.3033	+0.0003	1.2874	+0.0019
25	0	1.2320	-0.0349	1.2943	-0.0087	1.2516	-0.0339
50	0	1.2685	+0.0016	1.3033	+0.0003	1.2846	-0.0009
50	50	1.2501	-0.0168	1.3028	-0.0002	1.2683	-0.0172

The variations in the half-area range correction tend to follow those in the centroid. On the other hand, the variations in the half-maximum correction are remarkably small throughout the diffraction pattern, presumably because the strongest portion of the return comes from the closest part of the array. This is evident in Figure 12t, which shows the incoherent return pulse shape for a 0.2-nsec transmitted pulse at an incidence angle of 45° on the array.

In summary, the maximum systematic error in the range correction is probably on the order of 2 cm. The data presented in Figure 14 and Tables 15 and 21 can be used to obtain a more detailed estimate of the uncertainties that can be expected under various conditions.

11. INFRARED TRANSFER FUNCTION

This section gives the reflectivity and range correction for the infrared reflector carried by Geos 3. The dimensions and specifications of the cube corner are given in Section 2, and the position and orientation, in Table 2a and Figure 5.

Since the back faces are uncoated, the cube corner depends on total internal reflection. The minimum incidence angle ϕ_c at which total internal reflection can be lost is given by the formula

$$\phi_c = \sin^{-1} (n \sin \phi_c') \quad ,$$

where

$$\phi_c' = \tan^{-1} \sqrt{2} - \sin^{-1} \frac{1}{n} \quad .$$

The index of refraction is n = 2.19 at 10.6 μ for Irtran-2, which gives

$$\phi_c' = 27.^{\circ}57$$

and

$$\phi_c = \sin^{-1} (1.01348) \quad .$$

Since the sine of ϕ_c is greater than unity, no loss of total internal reflection occurs.

The reflectivity of the infrared reflector is plotted in Figure 15 as a function of the direction of the incident beam, where the angles θ and ϕ are as defined in Figure 6. The active reflecting area is normalized to unity at normal incidence, and the area at normal incidence is 10.6088 cm^2. The two lower curves, normalized to the center of the Airy disk, give the average reflectivity at 10.6 μ in the 25- to 50-μrad annulus of

the far-field pattern. The data used to plot the reflectivity curves are listed in Table 22. The fact that the reflectivity is not unity at normal incidence is due primarily to the phase changes resulting from total internal reflection at the back faces. The difference between the reflectivities for the two orthogonal polarizations of the incident beam is largely the result of reflection losses at the front face. The active reflecting area repeats every 60° in θ, while the reflectivity in the annulus repeats every 120° in θ. For both the active reflecting area and the reflectivity in the annulus, the value for $30° - \theta$ equals that for $30° + \theta$.

The data in Table 22 can be used to calculate signal strengths from the range equation of Section 5. The cross section $A_S G_S$ is equal to $ARG_{10.6}$, where

$A = 10.6088 \text{ cm}^2$,

R = reflectivity from Table 22 ,

and

$$G_{10.6} = \frac{A}{\lambda^2} = 9.4418 \times 10^6 \quad .$$

Since the Geos 3 spacecraft is triaxially stabilized, range measurements to the infrared reflector can be accurately related to the spacecraft center of gravity. The relationship of the spacecraft coordinate system to the orbital plane is given in Section 3. If the direction from the cube corner to the illuminating laser is given by a unit vector $\hat{u}$ in the spacecraft coordinate system and the position of the center of the front face of the infrared reflector is represented by the vector $\vec{p}$, then the range correction to the center of gravity of the satellite is

$$\text{infrared range correction} = \hat{u} \cdot \vec{p} - L \sqrt{n^2 - \sin^2 \phi} \quad ,$$

where

L = length of reflector (2.475 cm) ,

n = index of refraction (2.19) ,

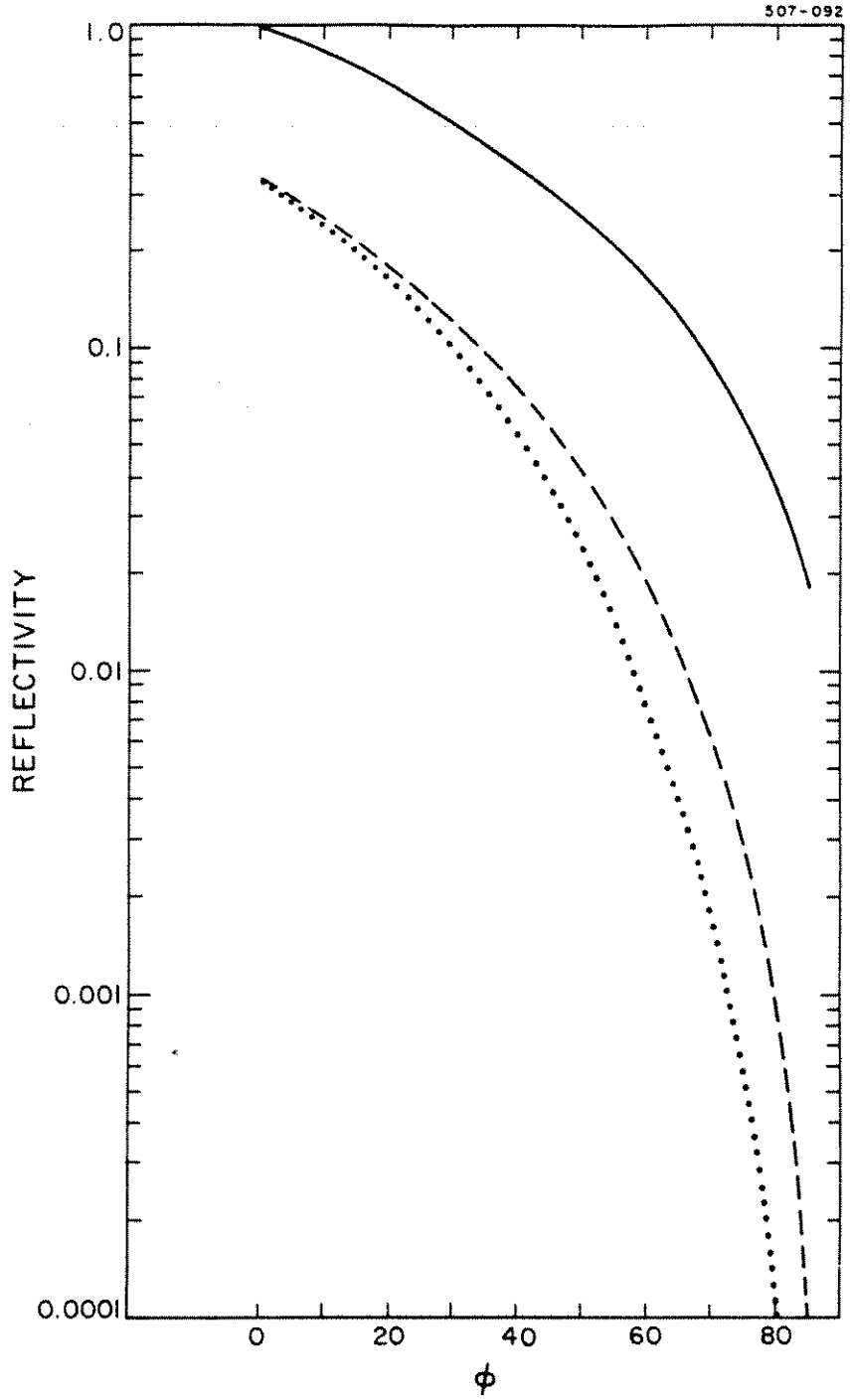

Figure 15. Active reflecting area (solid curve) and average reflectivity in the 25- to 50-μrad annulus of the far-field diffraction pattern for the Geos 3 infrared reflector. The dashed and dotted curves represent the electric field vector $\vec{E}$ parallel and perpendicular, respectively, to the plane of incidence. The incidence angles θ and ϕ are defined in Figure 6. a: $\theta = 30°$, $n = 2.19$, $\lambda = 10600$ Å.

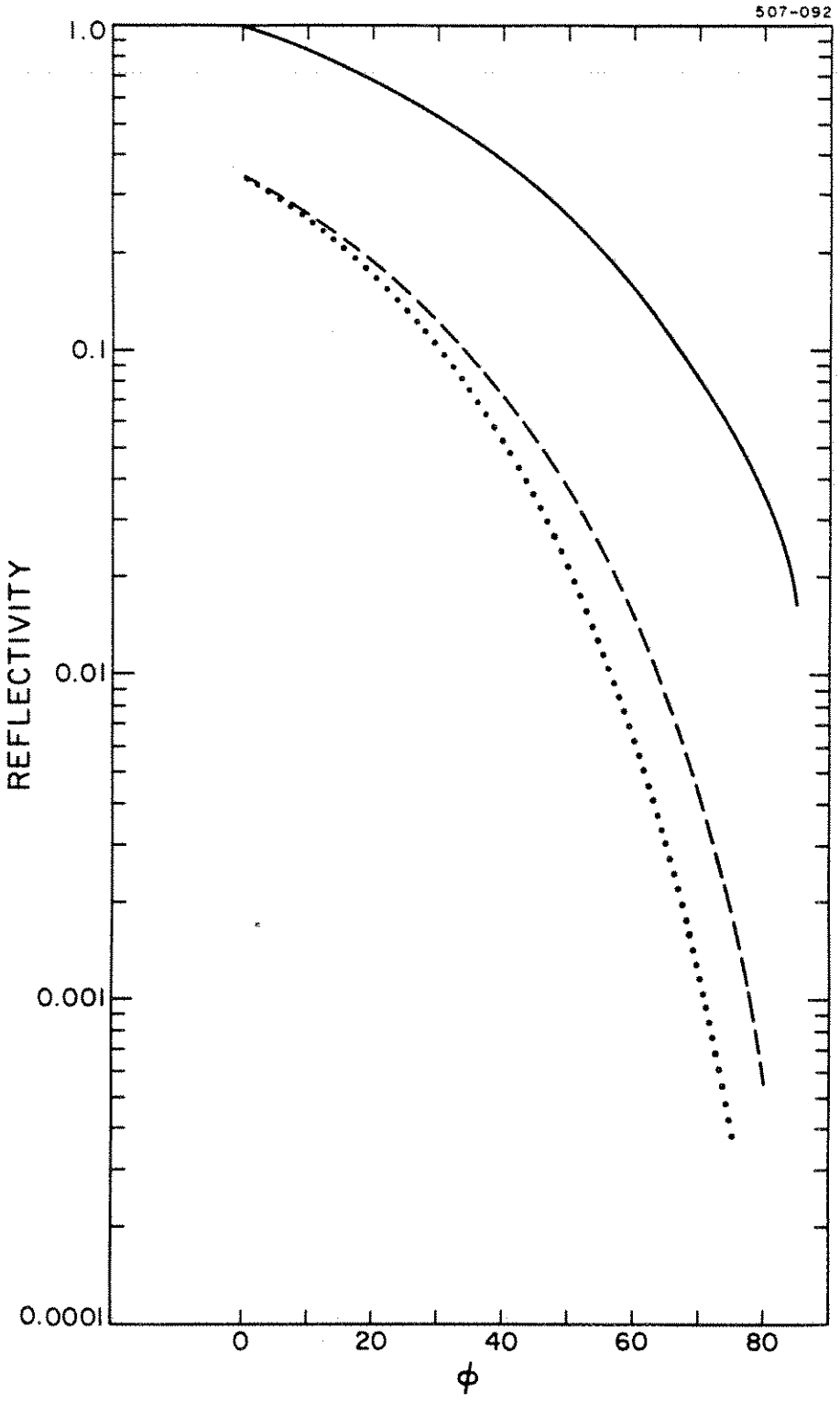

Figure 15b: $\theta = 60°$, $n = 2.19$, $\lambda = 106000$ Å.

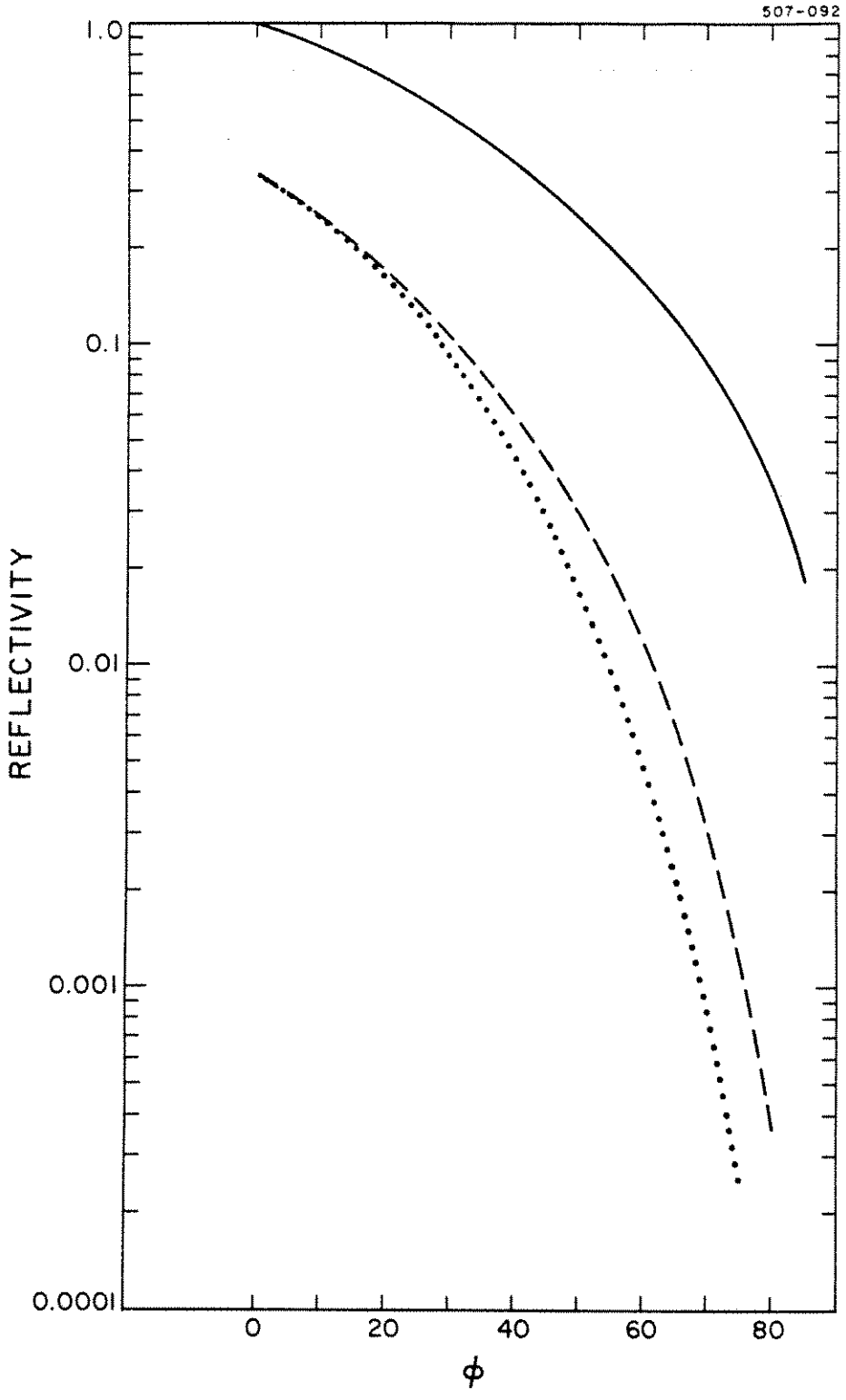

Figure 15c: $\theta = 90°$, $n = 2.19$, $\lambda = 106000$ Å.

Table 22. Average reflectivity of the infrared cube corner in the 25- to 50-μrad annulus of the far-field diffraction pattern, first with the electric field vector $\vec{E}$ parallel and then perpendicular to the plane of incidence.

a: $\vec{E}$ parallel to the plane of incidence

PHI	THETA 30	THETA 60	THETA 90
0	.340065	.340065	.340065
5	.292426	.297813	.291989
10	.249486	.257633	.247418
15	.211208	.219741	.206351
20	.177224	.184329	.168945
25	.147027	.151616	.135432
30	.120143	.121852	.106026
35	.096240	.095302	.080854
40	.075159	.072183	.059898
45	.056883	.052592	.042983
50	.041445	.036564	.029741
55	.028839	.024023	.019605
60	.018952	.014832	.012129
65	.011549	.008563	.006883
70	.006305	.004471	.003442
75	.002862	.001960	.001402
80	.000895	.000598	.000387
85	.000101	.000066	.000039

b: $\vec{E}$ perpendicular to the plane of incidence

0	.340065	.340065	.340065
5	.291112	.296475	.290676
10	.245002	.253012	.242971
15	.202676	.210896	.198016
20	.164520	.171183	.156836
25	.130607	.134787	.120308
30	.100904	.102466	.089050
35	.075390	.074786	.063341
40	.054071	.052056	.043098
45	.036916	.034256	.027902
50	.023759	.021086	.017057
55	.014245	.011985	.009691
60	.007829	.006230	.005016
65	.003849	.002930	.002298
70	.001622	.001197	.000888
75	.000538	.000390	.000265
80	.000114	.000083	.000050
85	.000008	.000006	.000003

$$\phi = \cos^{-1} (-\hat{Z} \cdot \hat{u}) \quad ,$$

$\hat{Z}$ = unit vector in the direction of the Z axis.

The second term accounts for the optical path length in the reflector.

Since there is only one infrared reflector, no coherent variation of the range or intensity will result from interference. There is also no uncertainty as to the mean point of reflection, as in the case for the optical array, which has cube corners distributed in range from the observer. Because the return pulse has the same shape as the incident pulse, no difference arises among different detection methods. The only satellite-induced range errors are those due either to uncertainties in the position of the reflector with respect to the center of gravity of the satellite or to the orientation of the spacecraft with respect to the plane of the orbit.

12. ACKNOWLEDGMENTS

The author wishes to express his appreciation to J. F. Smola of the Applied Physics Laboratory and P. O. Minott of Goddard Space Flight Center for providing data on the Geos 3 retroreflector array.

13. REFERENCES

1. Arnold, D. A., Calculation of Retroreflector Array Transfer Functions. Final Technical Report, NASA Grant NGR 09-015-196, December 1972. [This report gives results computed for satellites BE-B (6406401), BE-C (6503201), Geos 1 (6508901), D1C (6701101), D1D (6701401), Geos 2 (6800201), Peole (7010901), and Geos 3.
2. Arnold, D. A., Optical Transfer Function of NTS-1 Retroreflector Array. Technical Report RTOP 161-05-02, NASA Grant 09-015-002, Supplement No. 57, October 1974.
3. Arnold, D. A., Optical Transfer Function of Starlette Retroreflector Array. Technical Report RTOP 161-05-02, NASA Grant NGR 09-015-002, Supplement No. 57, February 1975.
4. Weiffenbach, G. C., Use of a Passive Stable Satellite for Earth Physics Applications. Final Report, NASA Grant NGR 09-015-164, April 1973.